NATIONAL COOPERATIVE HIGHWAY RESEARCH PROGRAM

Report 402

Fatigue Design of Modular Bridge Expansion Joints

R. J. DEXTER
R. J. CONNOR
M. R. KACZINSKI
ATLSS Engineering Research Center
Lehigh University
Bethlehem, PA

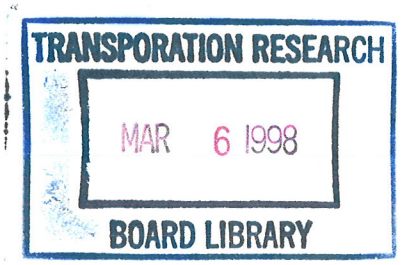

Subject Areas

Bridges, Other Structures, and Hydraulics and Hydrology

Research Sponsored by the American Association of State Highway and Transportation Officials in Cooperation with the Federal Highway Administration

TRANSPORTATION RESEARCH BOARD
NATIONAL RESEARCH COUNCIL

NATIONAL ACADEMY PRESS
Washington, D.C. 1997

NATIONAL COOPERATIVE HIGHWAY RESEARCH PROGRAM

Systematic, well-designed research provides the most effective approach to the solution of many problems facing highway administrators and engineers. Often, highway problems are of local interest and can best be studied by highway departments individually or in cooperation with their state universities and others. However, the accelerating growth of highway transportation develops increasingly complex problems of wide interest to highway authorities. These problems are best studied through a coordinated program of cooperative research.

In recognition of these needs, the highway administrators of the American Association of State Highway and Transportation Officials initiated in 1962 an objective national highway research program employing modern scientific techniques. This program is supported on a continuing basis by funds from participating member states of the Association and it receives the full cooperation and support of the Federal Highway Administration, United States Department of Transportation.

The Transportation Research Board of the National Research Council was requested by the Association to administer the research program because of the Board's recognized objectivity and understanding of modern research practices. The Board is uniquely suited for this purpose as it maintains an extensive committee structure from which authorities on any highway transportation subject may be drawn; it possesses avenues of communications and cooperation with federal, state and local governmental agencies, universities, and industry; its relationship to the National Research Council is an insurance of objectivity; it maintains a full-time research correlation staff of specialists in highway transportation matters to bring the findings of research directly to those who are in a position to use them.

The program is developed on the basis of research needs identified by chief administrators of the highway and transportation departments and by committees of AASHTO. Each year, specific areas of research needs to be included in the program are proposed to the National Research Council and the Board by the American Association of State Highway and Transportation Officials. Research projects to fulfill these needs are defined by the Board, and qualified research agencies are selected from those that have submitted proposals. Administration and surveillance of research contracts are the responsibilities of the National Research Council and the Transportation Research Board.

The needs for highway research are many, and the National Cooperative Highway Research Program can make significant contributions to the solution of highway transportation problems of mutual concern to many responsible groups. The program, however, is intended to complement rather than to substitute for or duplicate other highway research programs.

Note: The Transportation Research Board, the National Research Council, the Federal Highway Administration, the American Association of State Highway and Transportation Officials, and the individual states participating in the National Cooperative Highway Research Program do not endorse products or manufacturers. Trade or manufacturers' names appear herein solely because they are considered essential to the object of this report.

NCHRP REPORT 402

Project 12-40 FY '94

ISSN 0077-5614

ISBN 0-309-06255-1

L. C. Catalog Card No. 97-062205

Price $30.00

NOTICE

The project that is the subject of this report was a part of the National Cooperative Highway Research Program conducted by the Transportation Research Board with the approval of the Governing Board of the National Research Council. Such approval reflects the Governing Board's judgment that the program concerned is of national importance and appropriate with respect to both the purposes and resources of the National Research Council.

The members of the technical committee selected to monitor this project and to review this report were chosen for recognized scholarly competence and with due consideration for the balance of disciplines appropriate to the project. The opinions and conclusions expressed or implied are those of the research agency that performed the research, and, while they have been accepted as appropriate by the technical committee, they are not necessarily those of the Transportation Research Board, the National Research Council, the American Association of State Highway and Transportation Officials, or the Federal Highway Administration, U.S. Department of Transportation.

Each report is reviewed and accepted for publication by the technical committee according to procedures established and monitored by the Transportation Research Board Executive Committee and the Governing Board of the National Research Council.

Published reports of the

NATIONAL COOPERATIVE HIGHWAY RESEARCH PROGRAM

are available from:

Transportation Research Board
National Research Council
2101 Constitution Avenue, N.W.
Washington, D.C. 20418

and can be ordered through the Internet at:

http://www.nas.edu/trb/index.html

Printed in the United States of America

FOREWORD

By Staff
Transportation Research Board

This report contains the findings of a study undertaken to develop performance-based specifications for the fatigue design of modular bridge expansion joints. The report includes a proposed fatigue design specification and commentary, a proposed fatigue test specification and commentary, and fatigue design examples. The contents of this report will be of immediate interest to bridge designers.

Modular bridge expansion joints are designed to accommodate large longitudinal expansion and contraction movements of bridge superstructures. In addition to supporting wheel loads, a properly designed modular joint will prevent water and debris from draining onto the underlying superstructure and substructure. Many premature failures of modular bridge expansion joints can be attributed to fatigue problems. Expansion joints are subjected to more load cycles than other superstructure elements, but the load types and magnitudes and fatigue-stress ranges that are applied to these joints have not been well defined. Additionally, sufficient data have not been available on field measurements and laboratory testing of fatigue-critical joint details. Neither the AASHTO *Standard Specifications for Highway Bridges* nor the AASHTO *LRFD Bridge Design Specifications* include fatigue design criteria for these joints. Because of this lack of data and guidance, modular bridge expansion joints in the United States are designed by their suppliers using proprietary techniques.

Under NCHRP Project 12-40, Lehigh University identified critical parameters that influence fatigue performance of modular bridge expansion joints and the predominant causes for fatigue failure of in-service joints. Using field tests of modular bridge expansion joints the research team was able to assess behavior under static and dynamic truck loading and define critical stress locations. Fatigue criteria were developed through laboratory testing. These activities culminated in specific proposals to ensure the design of durable modular bridge expansion joints.

CONTENTS

AUTHOR ACKNOWLEDGMENTS

This work was sponsored by the American Association of State Highway and Transportation Officials, in cooperation with the Federal Highway Administration and was conducted through the National Cooperative Highway Research Program which is administered by the Transportation Research Board of the National Research Council. The research agency was the ATLSS Engineering Research Center at Lehigh University.

Professor John W. Fisher, Director of the ATLSS Center, provided valuable guidance in the course of this research. The authors appreciate the patience and direction of Scott Sabol and David Beal of NCHRP, and the planning, review, and suggestions of the project panel. Mr. Zuo Zhang Ma and Mr. Hugh Sutherland provided technical assistance in the field measurements. John Hoffner, Larry Heffner, Todd Anthony, Steve Leonard, Roger Moyer, Ed Tomlinson, and other ATLSS technicians provided assistance throughout the laboratory testing. The photographs in the laboratory were taken by Richard Sopko. Kevin Johns assisted with the preparation of the figures. Undergraduate research assistants included Ben Graybeal, Amy Pastore and Eric Schneider.

Akhilesh Agarwal from the Ministry of Transportation of Ontario and Professor Ferdinand Tschemmernegg from the University of Innsbruck served as consultants in this project. The authors are especially grateful to Andreas Kluibenschedl, who finished his studies for the University of Innsbruck under the direction of Prof. Tschemmernegg while visiting ATLSS in 1992. Andreas' research is a valuable resource, and Andreas continued to patiently help us understand papers written in German. The authors would also like to recognize the Connecticut, Colorado, and Washington State Departments of Transportation for their vital support in the field measurements. The authors are also grateful for the cooperation of Watson Bowman, ACME—a division of Harris Specialty Chemicals, The D.S. Brown Company, and Techstar Inc.

FATIGUE DESIGN OF MODULAR BRIDGE EXPANSION JOINTS

SUMMARY

The initial performance of typical modular bridge expansion joints (MBEJs) has been good and most MBEJs have not had durability problems. However, in some cases, MBEJs have developed fatigue cracks and other durability problems. Causes of the problems include the following: (1) the dynamic response of these systems was not fully understood; (2) poor details were specified and fabricated; and (3) some installations were poorly constructed. In addition, in today's construction process, MBEJs are typically procured by a low-bid process. This situation, combined with the fact that there are currently no nationally accepted design specifications for MBEJs, contributes to the problems.

To address these problems, experimental and analytical research was performed and performance-based specifications and commentary for the fatigue design of MBEJs were developed. To determine the static and dynamic response of different MBEJ systems subjected to truck loading and to verify proposed structural analysis models, field tests were conducted at four sites. The key findings of the field tests were as follows: (1) a MBEJ can be modeled as a two-dimensional frame by using beam elements; (2) maximum measured amplified dynamic vertical moment range was 1.63 times the corresponding static moment; (3) horizontal bending moment range measured under normal driving conditions was up to 23% of the amplified vertical bending moment; (4) horizontal moment ranges measured during emergency braking tests were almost 50% of the amplified vertical moments; and (5) the measured stress ranges from typical traffic were slightly less than the stress ranges predicted on the basis of the proposed upper-bound limit-state design loads.

The static load and strain distributions were also measured in the laboratory and were found to be similar to distributions measured in the field. A practical test procedure was developed to determine the fatigue resistance of critical details. Fatigue tests of centerbeam-to-support-bar connections indicate that the fatigue resistance of full-penetration welded connections is equivalent to AASHTO category C, and the fatigue resistance of bolted connections is equivalent to AASHTO category D. Partial-penetration welded centerbeam-to-support-bar connections have very low fatigue resistance and therefore are not feasible under the proposed design specifications.

The proposed fatigue design specifications are designed to be integrated with the current load and resistance factor design specifications for bridge design. To be consistent with these bridge specifications and allow for regional differences in the bridge fatigue design

loading or changes in the loading over time, the proposed MBEJ fatigue design specifications use the same fatigue design truck as the current AASHTO bridge specifications—i.e., the HS-15 loading (after taking into account the load factor of 0.75 for fatigue). One important modification of the AASHTO truck loading for MBEJs is explicit recognition that the rear axles of the HS truck loading in the specifications actually represent tandem axles. For the purposes of comparison, a single axle of the HS-15 tandem rear axles is equivalent to a "fatigue limit state" static axle load (i.e., an axle load that is supposed to be only rarely exceeded) of 107 kN (24 kips).

The proposed dynamic amplification factor is conservatively set as 1.75. The recommended horizontal load range, acting simultaneously with the vertical load range, is equal to either 20% or 50% of the amplified vertical load for installations either on open highways or near facilities where continuous heavy braking is expected, respectively. A simplified method is proposed to estimate the distribution factor (i.e., the fraction of the design wheel load range assigned to a single centerbeam).

CHAPTER 1

INTRODUCTION AND RESEARCH APPROACH

1.1 PROBLEM STATEMENT

On most bridges, at least one deck joint is placed in the roadway surface to accommodate the longitudinal expansion and contraction of the bridge superstructure (*1*). Historically, the finger or tooth joint has been installed on most structures with >150 mm (6 in.) of total movement. Although finger joints have generally proven to be structurally sound in a wide variety of bridge types, they have not been effective in controlling water and debris from passing through the deck joint and collecting on the underlying superstructure. Figure 1.1 is a view from under a bridge, with a finger joint showing severe corrosion of the superstructure components in the vicinity of the open joint. Deck drainage has also contributed to the deterioration of substructure units, changed the behavior of pinned connection structural systems, and contributed to fatigue cracking and even failure of a structure (*1–3*). Even in those finger joints that use a trough to collect drainage, lack of maintenance often leads to clogged drains and the same problems described above (*4,5*).

Sealed expansion joints offer corrosion protection to the underlying bridge superstructures by eliminating drainage through the deck joint. If a sealed expansion joint remains effective, this corrosion protection has a tremendous potential payoff by extending the useful life of both concrete and steel bridges and by reducing the need for coatings as well as the need for coating maintenance and replacement. One type of sealed expansion joint uses elastomeric seals that flex between edge beams, which are embedded in the haunches of the concrete deck slab. These strip-seal expansion joints are typically limited to relatively small movements with a total range of <127 mm (5 in.).

A modular bridge expansion joint (MBEJ) uses one or more transverse centerbeams to separate two or more of the elastomeric seals and therefore increases the total possible range of movement. In most MBEJ systems, the centerbeams are connected to longitudinal support bars, which slide in and out of support boxes embedded in the haunches. The support bars slide between elastomeric bearings. The most common type of MBEJ system, know as a welded multiple-support-bar system, is shown in Figure 1.2. In this system, each support bar is attached to only one centerbeam. In other types of systems, a single-support bar may support all of the centerbeams. In these joints, in addition to sliding longitudinally, the support bars also may swivel in the support box.

The greatest factor affecting the performance of any sealed expansion joint is durability (*6–10*). Most modern MBEJ systems have remained effective with little or no maintenance. However, some MBEJ installations have required significant maintenance and even replacement. There have been at least three types of problems: (1) problems that can be traced to improper installation—for example, poor consolidation of the concrete under the support boxes; (2) wear and tear of the elastomeric parts; and (3) fatigue cracking of steel parts and their connections.

Construction problems can be solved with adequate installation specifications and inspection (*9*). Any problems with the elastomeric parts are generally solved by improvements in the materials (*11*). Although this report presents what is known about these two types of durability problems and recommends some specifications to reduce their occurrence, the primary emphasis is on the fatigue performance of the steel parts and their connections.

The typical steel MBEJ with either the full-penetration welded connection or a typical bolted connection can be designed to be resistant to fatigue cracking under the most severe truck loading. However, there is currently little guidance on how to design a fatigue-resistant MBEJ. In fact, there are no general design or fatigue design provisions for MBEJs in the AASHTO bridge design specifications (*12*). Some states have recently developed fatigue-performance requirements for MBEJs that require some fatigue testing (*13,14*). However, there are no established fatigue design procedures or specifications for carrying out the required tests (*15*).

MBEJs are typically procured on a lowest-bid basis. Without any specifications, the low-bid process inevitably leads to a decreased margin of safety against fatigue as manufacturers try to make MBEJs more economical (*6*). MBEJs have traditionally been designed by manufacturers using proprietary techniques, which in some instances have not adequately addressed the dynamic load response and fatigue resistance (*16–20*). Lack of design criteria has often resulted in the use of welded details with poor fatigue resistance (*17–19*). The fatigue resistance and durability of many joint applications has been further compromised because the dynamic response of these systems was not fully understood and some installations were poorly constructed (*16,20*).

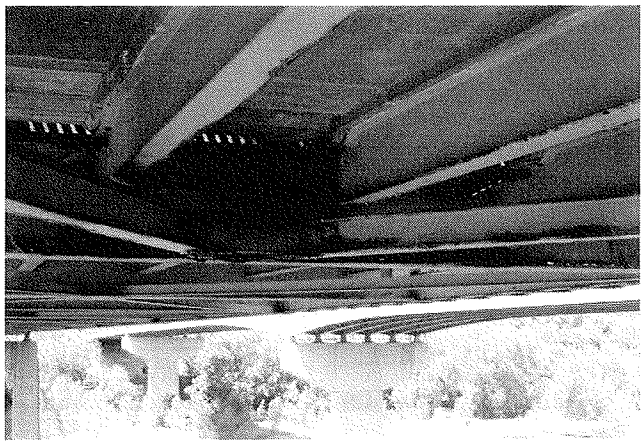

Figure 1.1. View from under a bridge deck showing extensive corrosion damage in the vicinity of an open finger joint system.

This report describes research that was conducted to support the development of performance-based specifications and commentary for the fatigue design of MBEJs. The specifications must account for the complex behavior of the MBEJ as a system, but the specifications must also be reasonably easy to use. The specifications must be general so that innovative new designs for MBEJs are not excluded.

The design specifications proposed in Appendix A of this report meet these requirements. The proposed specifications consist of a static axle load and a procedure to distribute the axle load to individual centerbeams. The load is multiplied by an impact factor to account for the dynamic response of the MBEJ. To account for dynamic response, a certain percentage of this load is applied in the horizontal direction. Structural analysis models are recommended for computing the stress range at the critical details. A test specification is proposed in Appendix B, which is intended to determine the fatigue-resistance data required for the design procedure (i.e., the S-N curve and the fatigue threshold stress range) for the critical connection details. MBEJ systems that are designed in accord with these proposed specifications should be resistant to fatigue cracking and should have an initial first cost that is only slightly greater.

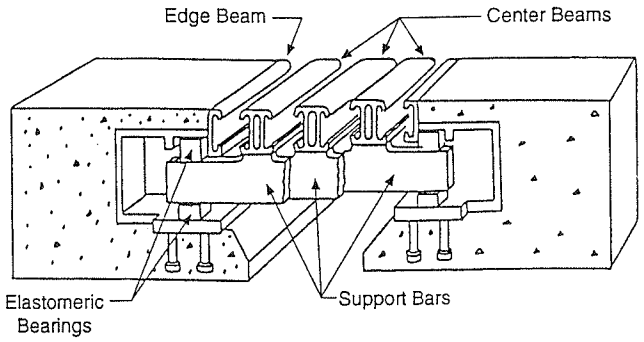

Figure 1.2. Schematic of a welded multiple-support-bar MBEJ system.

1.2 OVERVIEW OF NCHRP PROJECT 12-40

This research was sponsored by the National Cooperative Highway Research Program (NCHRP) as Project 12-40, *Fatigue Criteria for Modular Bridge Expansion Joints.*

The specific objectives of the research project are as follows:

- Identify and rate all known factors that significantly affect MBEJ durability, including (1) construction-related factors; (2) material specifications for elastomeric parts; (3) factors that affect loading and dynamic response; and (4) factors that affect the fatigue resistance of the critical details.
- Determine the static and dynamic response of several different modular expansion joint systems to truck loading.
- Develop reasonable structural analysis models to compute bending moments and combined stress ranges at critical details.
- Develop a test procedure to determine the fatigue resistance of critical connection details in the various types of MBEJ systems.
- Generate some preliminary fatigue test data for common connection details used in most modern MBEJ systems.

The approach to this research was as follows:

- A review of the international literature and a survey were conducted, which identified current design methods and practice for MBEJs and the potentially significant factors pertaining to durability and overall performance of MBEJs. The parties surveyed included current manufacturers of MBEJs, departments of transportation, turnpike authorities, and bridge commissions in the United States and Canada.
- Field tests were performed that also identified performance factors for MBEJs and determined typical static and dynamic response of MBEJs subjected to truck loading. The field tests included inspection, instrumentation, and field measurements (primarily of strain) at selected MBEJ sites.
- Laboratory static tests and fatigue tests were conducted on both complete MBEJ systems and subassemblies. The geometry and type of specimens tested in the laboratory were designed to be similar to the systems tested in the field. Static load and strain distributions measured in the laboratory were demonstrated to be similar to

those measured in the field. A practical test procedure was developed to determine the fatigue resistance of critical MBEJ details, and some preliminary test data were obtained for common details.

- Structural analysis models were refined and the overall design procedure was calibrated on the basis of field and laboratory measurements. Important aspects of the structural analysis include the following: (1) the wheel-load distribution to individual centerbeams; (2) the frame analysis to determine bending moment distributions; and (3) the method of computing the combined stress range at critical details for checking the fatigue resistance.

1.3 ORGANIZATION OF THE REPORT

Chapter 2 presents a detailed summary of the research findings, including (1) a discussion of performance factors for MBEJs and (2) descriptions and results of field tests, laboratory static tests, and fatigue tests. Chapter 3 presents the development of, and rationale for, the proposed MBEJ design specification and test specification. The proposed design specification is presented in Appendix A, the test specification is presented in Appendix B, and several design examples are presented in Appendix C. Chapter 4 presents overall conclusions from the research and recommends future research that may be valuable.

CHAPTER 2
FINDINGS

The findings of the literature review, survey, field testing, and laboratory testing are summarized in this chapter. The findings of the literature review and survey, along with knowledge gained during this project, are synthesized into the following discussion of performance factors. More detailed discussion of the literature and the survey were presented in an interim report (*20*), which also contains more details about field testing.

2.1 DISCUSSION OF FACTORS AFFECTING THE PERFORMANCE OF MBEJS

The initial functional performance of MBEJs typically has not been a problem (*7,9,10*). Therefore, the critical issue with respect to performance of MBEJs is durability. There have been at least three types of durability problems: (1) problems that can be traced to improper installation—for example, poor consolidation of the concrete under the support boxes; (2) wear and tear of the elastomeric parts such as seals; and (3) fatigue cracking of the structural members (centerbeams and support bars) and their connections. To develop an effective performance-based specification for the fatigue design of MBEJs, consideration must be given to all these potential problems and the associated performance factors. The following discussion briefly summarizes what is known about construction-related problems and problems with the elastomeric components. However, the primary emphasis in this research was dynamic loading and the fatigue performance of the structural members and their connections. The construction-related problems and problems with the elastomeric parts should be the subject of further research.

2.1.1 Construction-Related Performance Factors

Several references (*1,7,9,10,14,21*) and many of the agencies surveyed have noted MBEJ durability problems that are a result of poor detailing or poor construction techniques. Construction problems include poor consolidation of concrete under the support boxes, concrete in the support boxes, and improper placement of reinforcement steel near the joint.

Poor consolidation of the concrete around support boxes and edge beams (*21*) is a relatively common problem. An example of this condition is presented in Figure 2.1. In extreme cases, voids under a support box could lead to settlement and movement of the box. If a support box is not well supported, it is ineffective as a support and the span of the centerbeams is essentially doubled. Because the moment increases in proportion to the span, the live load stress and stress ranges are approximately doubled. The increase in stress may be large enough to cause fatigue cracking of critical details and may even cause overload failure of MBEJ components. In addition, inadequate support has negative effects on the ride quality of the MBEJs. Concrete should be placed on one side of the support-bar box and vibrated so that it appears on the opposite side before concrete is placed there.

Another relatively common problem is accidental casting of deck concrete into the support boxes. Figure 2.2 shows a support box containing concrete. Although measures are usually taken to prevent this problem, concrete was found in the support boxes at one of the MBEJ sites visited in field tests. At this location, no structural distress appeared to be caused by the concrete in the support box. However, at another location, a shear failure due to overload was documented on an MBEJ that had an entire support box filled with concrete, thus preventing the occurrence of thermal movements.

Problems with poor detail design include improper detailing of superstructure elements and reinforcement steel, reflective cracking in the concrete cover directly above support boxes, and lack of access to the underside of the MBEJ for inspection and maintenance. Figure 2.3 presents an example of reflective cracking in the concrete deck directly above support boxes. This type of cracking was observed at all bridge sites and support box locations visited during field testing. The cracking appeared to be most significant at the support boxes placed in a region of the deck with transverse negative moment causing transverse tension stress in the top of the deck—i.e., where the deck is continuous over a support in a direction transverse to the longitudinal axis of the bridge. The discontinuity in the slab thickness caused by the support box is likely to be a factor in this cracking. Another consideration is the relative flexibility of the thin plates used to construct the top of the support boxes. In either case, it appears that the solution may be to provide adequate concrete

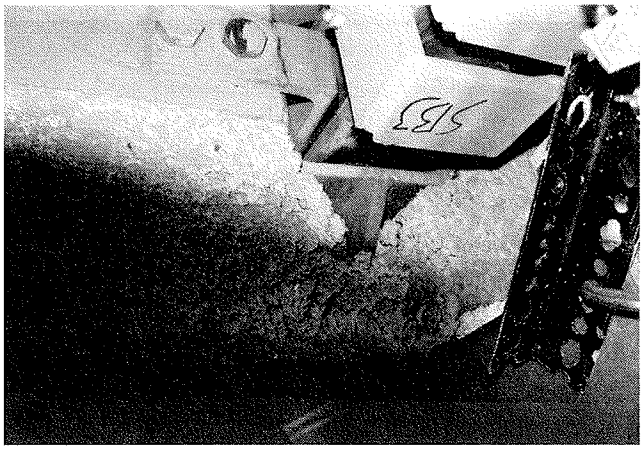

Figure 2.1. Lack of concrete consolidation under a support box.

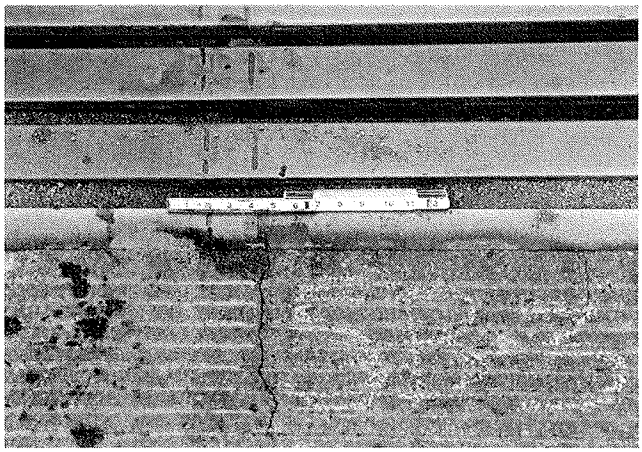

Figure 2.3. Concrete deck cracking over a support box.

cover and transverse reinforcement over the support boxes to minimize the crack widths. A minimum thickness-to-width ratio also should be considered for support box top plates.

Slump of the concrete mixture is also important because shrinkage cracks will occur if it is too moist. These cracks permit water intrusion, which causes eventual delamination of the concrete cover over the support-bar boxes.

Blockouts are used for modular joints to facilitate placement and adjustment. The blockout must be designed to support the weight of the joint, particularly on deck overhangs. Sometimes the ends of steel girders are notched to accommodate the joint. The possible fatigue problem at these notches should be considered. Careful installation of the joint and placement of blockout concrete are critical to ensure that the joint is durable.

Close cooperation among the designer, contractor, and joint manufacturer is required to ensure a quality joint installation. For example, designers should work with manufacturers when detailing blockout reinforcement. By working together, experienced designers, typically more familiar with reinforcement needs and details of the adjacent structural elements, and manufacturers, often more familiar with installation problems and factors affecting MBEJ durability, will likely have good ideas that reduce placement problems during construction. Unfortunately, it is difficult to anticipate reinforcement requirements during design because the joint system and manufacturer are not known until after the contract is awarded.

The problem of joint inaccessibility became apparent when the research team was attempting to select sites for the field visits. For example, one joint considered for field testing had a 530-mm (21-in.) movement classification, yet it provided an accessible opening from below of only about 150 mm (6 in.) at 29°C (84°F). MBEJs detailed in such a way cannot be inspected or repaired from below by any reasonable method.

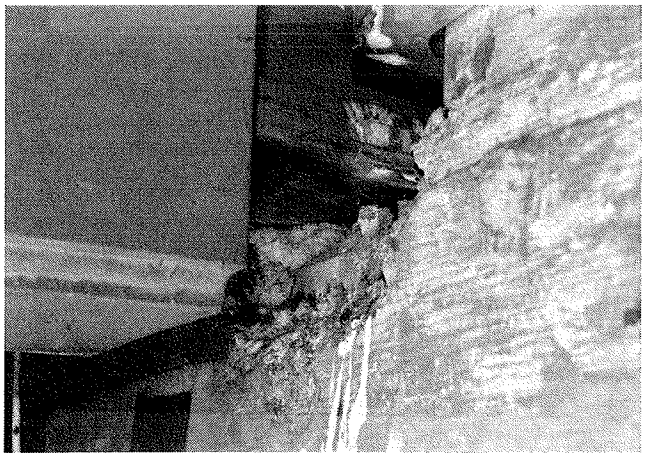

Figure 2.2. Accidental casting of deck concrete in a support box.

2.1.2 Durability of Elastomeric Components

The three main types of elastomeric MBEJ parts are seals, bearings and springs, and equidistant devices (*11*). The water tightness of the neoprene seals (often called glands) is essential for an MBEJ to act as an effective barrier between sensitive bridge details and runoff water and other road debris. Leaking joints can lead to problems such as corrosion of structural steel, frozen bearings, or concrete deterioration at the bridge seat (*1,2*). Once the MBEJ has been installed, several agencies require that the joint be tested for watertightness by flooding the joint under about 75 mm (3 in.) of water for several hours (*6*).

In addition to traffic loading, the effects of ultraviolet light or chemicals, such as deicing compounds, also contribute to seal deterioration. The ASTM specifications for the seal material are believed to be sufficient to ensure adequate durability under normal wear and tear and environmental exposure.

However, failures may occur because of detachment from the centerbeams, although recent improvements in the design and adhesive are believed to have addressed this problem.

Some agencies do not allow the seal to be installed in the field because of these problems. However, if the joint is placed in stages as it often is in rehabilitation of existing bridges, a field splice is required in the seal if it is installed in the shop. Field splices of the seals have sometimes been a problem and therefore are typically avoided. Splices may also be prohibited by individual agencies. Therefore, in the case of staged construction, it may be advantageous to have seals installed in the field to allow installation of one continuous seal without a splice after both parts of the MBEJ are installed.

Box-type seals have both advantages and disadvantages relative to typical strip seals. There may be differences in the resistance to detachment from the centerbeams. It is thought that the double seal provides a safeguard against leakage, because if the top seal becomes punctured the second seal will act as a backup system. However, some believe that this backup seal can do more harm than good. If the top seal becomes punctured, the box seal can fill with water and, during cold weather, freeze. In this situation, the seal is not capable of providing the needed movement capacity and can be pulled from the centerbeam or edge beam. There are also advantages and disadvantages of the seals with respect to splicing.

Damage to centerbeams or neoprene seals from the impact of snowplows can greatly decrease the performance of MBEJs. Often, the seal becomes slightly dislodged from the joint by a single passage of a plow truck. Subsequent plow passages damage the seal until it is torn. Many agencies recess the joint slightly, between 3 and 13 mm, to reduce the chances of damage from snowplow impacts. No particular disadvantages of this recess were noted.

Another common problem is that the seals fill with debris. Traffic passing over the joint can work the seal from its anchorage by pushing on this debris. Manufacturers claim that MBEJ systems are self-cleaning because as the joint approaches full open and closed positions, debris is expelled from the joint. However, one study (*10*) points out that many designers conservatively oversize the MBEJ, thus preventing the joint from being self-cleaning. Those joints inspected during our field studies were usually free of debris only in areas of high traffic volume.

Many skewed joints with acute angles between approximately 30 and 70 degrees have had problems with buckling of the neoprene seals (*10*). Because the movement of a skewed joint is not only perpendicular but also parallel to its seal, buckling of the seal occurs. Snowplows or even general truck traffic can easily damage the buckled seal.

Neoprene bearings and equidistant springs have had reported problems with becoming loose and falling out of position. If the bearings fall out, the span length is effectively increased because the bearings are no longer in place to support the support bar. Like the problem of support box settlement described above, increasing the span length leads to higher bending moments and a greater likelihood of fatigue.

Other potential problems with the bearings are fatigue, excessive wear, and compression set because of repeated truck loading. A fatigue test procedure for the bearings (presented in Appendix B) was developed to help ensure their durability. Although fatigue is typically assessed in terms of the stress range applied to a member, in nonlinear materials it can be shown that the strain range, rather than the stress range, is actually the parameter that determines fatigue life. In addition, for nonlinear, viscoelastic materials such as elastomers, the stiffness of the component varies with the strain rate. Therefore, the fatigue life is determined by the displacement range applied to the specimen and does not vary significantly if the strain rate (and hence the load range) is varied.

Dynamic test results indicate that the MBEJ spring, like most elastomeric materials, exhibits a dynamic stiffness versus frequency relationship, which can be approximated by a power law. Therefore, the dynamic stiffness/load frequency data are linear when plotted on a log-log scale (Figure 2.4).

Fatigue tests were conducted on a limited number of springs and bearings. Throughout the fatigue test, load and displacement measurements as well as maximum surface temperatures were monitored. Although the load range remained constant for each of the tests, creep in the elastomeric material gradually reduced the thickness of the spring or bearing. This reduction in thickness leads to a reduction in precompression in an actual support box. Loss of precompression can result in bearings falling out of the support box.

Based on the limited number of tests conducted, a guideline for durability testing of these components was developed and is included as an appendix to the fatigue-testing acceptance criteria for MBEJs that are included as Appendix B. It must be emphasized that the attached guidelines for the testing of springs and bearings are a minimum for these components and that additional research is required to provide a more comprehensive test specification. Furthermore, the MBEJ manufacturers have learned which materials give

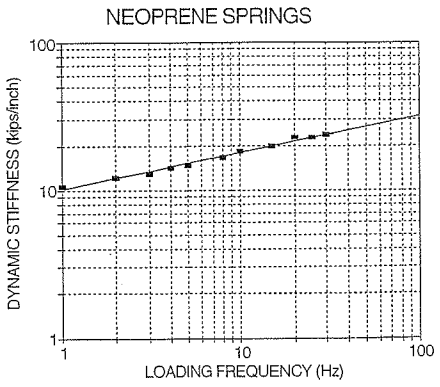

Figure 2.4. Dynamic stiffness vs. load for a bearing.

good durability. Thus, the in-service performance of the bearings and springs in most recent MBEJs is excellent. Therefore, it is not clear whether it is necessary to test the bearings and springs.

Based on the information obtained through the survey and the literature review, equidistant devices have not been a significant problem in MBEJs. This is likely because equidistant devices do not take significant loads from the truck loading. The biggest demand on these devices comes from maximum joint movements, which occur relatively infrequently.

2.1.3 Fatigue Resistance of the Structural Components

The MBEJ structural components are typically fabricated from ordinary structural steel with welded or bolted details. The fatigue strength of these details is very nearly independent of the strength level or type of structural steel. The material properties (strength and fracture toughness) and weld quality have not been noted as particular problems. Therefore, there is no need for additional material or welding specifications that are specific to MBEJs.

The fatigue strength of particular details in aluminum are approximately one-third the fatigue strength of the same details in steel. None of the specifications that were obtained through the agency survey permitted the use of aluminum members in MBEJ systems. According to the surveys and several reports (*21–23*), joints manufactured from aluminum have had significantly more problems than joints fabricated from steel. For example, aluminum joints have been particularly susceptible to damage from steel snowplows. Also, because the coefficients of thermal expansion of aluminum and concrete are quite different, problems such as spalling and cracking often arise at the interface of the two materials. This problem is less pronounced in steel joints because steel and concrete have very similar coefficients of thermal expansion.

The magnitude of the applied stress ranges is the most critical performance factor relevant to fatigue of MBEJs. For a given design load, the nominal applied stress range is determined primarily by the section modulus and span of the centerbeam or support bar. Most manufacturers have developed a large centerbeam bar shape that maximizes the section modulus that will fit within typical height and width restrictions. The same large sections are used in most MBEJs when there is a fatigue requirement in the specifications. Because the section is typically the same, the most important variable affecting fatigue resistance is the centerbeam span [for a given centerbeam/support-bar (CB/SB) connection type]. Manufacturers typically prefer larger centerbeam spans to reduce the cost of the MBEJ system (by reducing the number of support boxes). However, the moment and associated stress range increase in proportion to the span. Larger centerbeam sections have been used in special large-movement MBEJs, including tubes and members built up from two shapes.

In addition to the increase in static moment, centerbeam spans greater than 1220 mm (about 4.0 ft) are reported to have greater dynamic amplification (impact factor) (*15*). This is discussed in greater detail in the next section. Because of the adverse effects of large spans, prescriptive specifications have been written in Europe (*24*) that limit the centerbeam span to 1220 mm (about 4.0 ft).

In most fatigue design specifications for structures (*12, 25*), the fatigue resistance of details is reflected in the detail category, which is the primary performance factor for fatigue. Each detail category (Category A through E') corresponds to a particular S-N curve (stress range versus number of cycles) from the AASHTO bridge design specifications (*12*) as shown in Figure 2.5. The detail category is determined from the lower bound of large numbers of full-scale test data (*26*) and can be thought of as a relative ranking of the severity of the stress concentration associated with the detail geometry.

The dashed lines in Figure 2.5 indicate the stress range for each S-N curve corresponding to the constant-amplitude fatigue limits (CAFL). The CAFL is the stress range below which the constant-amplitude fatigue tests do not exhibit cracking after millions of cycles. These tests and the data obtained from such tests are often called runouts.

As explained in the next section, an MBEJ typically experiences more than 10 million cycles over the expected life of the deck. The fatigue design procedure for such long-life variable-amplitude loading in the current bridge design specifications in the United States (*12*) is based on the CAFL, which is called the fatigue threshold. The upper part of the S-N curve is needed only for situations in which the expected number of cycles is less than the number of cycles associated with the CAFL and is referred to as being in the finite-life region or regime.

For economic reasons, most full-scale fatigue testing is carried out at high stress ranges, resulting in lives of less than a million cycles. Therefore, the finite-life part of the S-N curve is well-defined for most details (*26*). However, for most details, few tests have been conducted with the stress range near the CAFL. Some tests have indicated that details that share a common S-N curve in the finite-life regime often have a unique CAFL—e.g., transverse stiffeners have a different CAFL than other Category C details (*12*). Consequently there is much greater uncertainty in the CAFL than in the finite-life part of the S-N curve. For MBEJs and other deck elements subjected to long-life loading, the emphasis in fatigue testing of details should be on defining the CAFL, which requires more expensive long-term testing at stress ranges close to service stress ranges.

Fatigue-critical MBEJ details include (1) the CB/SB connection; (2) connection of any attachments to the centerbeams (e.g., horizontal stabilizers or outriggers); and (3) shop or field splices in the centerbeams. In many cases, MBEJ details can be clearly associated with analogous details in the bridge design specifications (*12*). In some cases,

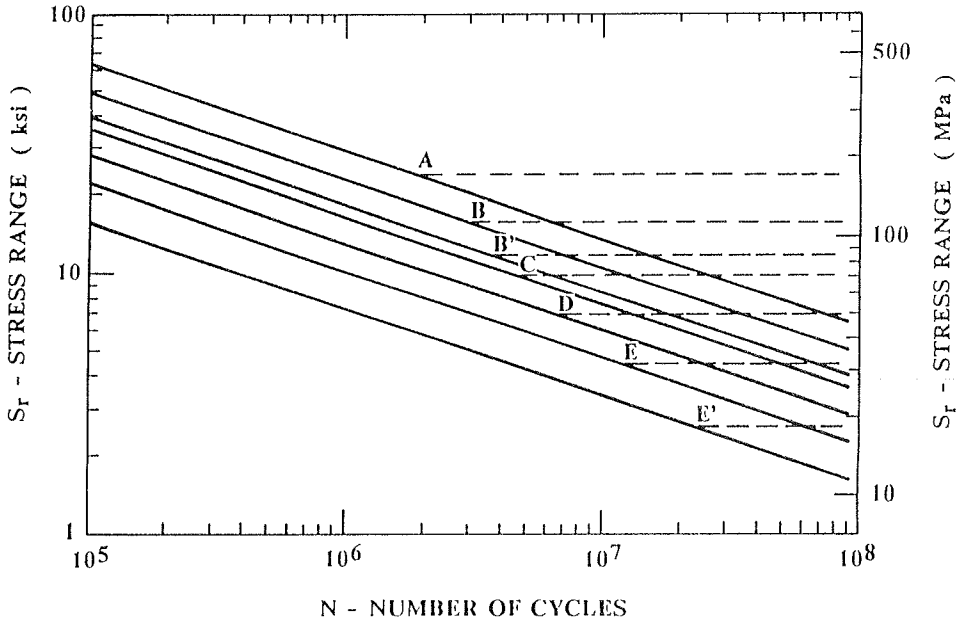

Figure 2.5. AASHTO S-N curves.

the association is not clear and must be demonstrated through full-scale fatigue testing.

The detail of primary concern is the CB/SB connection. Fatigue problems have been reported by several agencies in both welded and bolted details (*17–19*). A typical full-penetration welded connection can be associated with Category C. Fillet-welded connections have very poor fatigue resistance and should not be allowed.

Bolted connection details, such as the detail shown in Figure 2.6, have been used for single-support-bar MBEJs. According to AASHTO bridge specifications, these connections should be classified as a Category D detail with respect to the bending stress range in the centerbeam. As in any construction, more than one bolt must be used in bolted connections. Numerous failures were reported with an MBEJ that relied on a single bolt for the CB/SB connection (*19*). This is an extremely poor fatigue detail (because of high prying forces on the single fastener).

The bolted connections in single-support-bar MBEJs usually involve a yoke or stirrup through which the support bar slides or swivels, as shown in Figure 2.6. It is difficult to determine what fraction of the vertical reaction force range at the support bar is carried by the stirrup and what fraction passes directly through the bearing, but it is clear that the stirrup must take part of the load range, especially the uplift portion. However, there have been no particular problems noted with these stirrups.

Field-welded splices of the centerbeams and edgebeams are also prone to fatigue. In new construction, it may be possible to make a full-penetration welded splice in the field before the joint is lowered into the blockout. However, in reconstruction work, the joint is often installed in several sections at a time so that traffic flow can be maintained. In these cases, the splice must be made after the joint is installed. Because of the difficulty in access and position, it may be impossible to obtain a full-penetration butt weld in the field after the joint is installed, especially if there is more than one centerbeam. For this reason, partial-penetration joints with inherently poor fatigue resistance are often used.

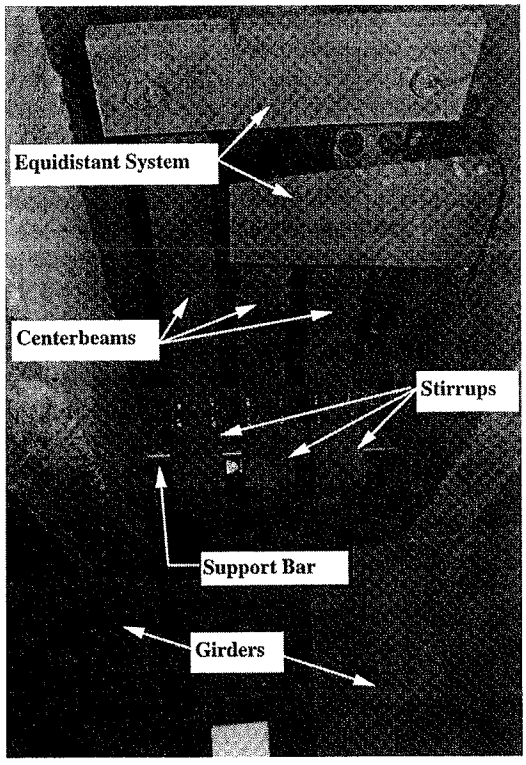

Figure 2.6. Typical bolted single-support-bar MBEJ.

Other splice details have been proposed that add attachments to increase the moment of inertia of the centerbeam in the location of the splice in an attempt to reduce the stress range at this detail. An example is shown in Figure 2.7. The ends of these attachments, if welded, are often a very severe detail and therefore may create a worse condition than the field splice itself.

There are several variations of bolted splices, one of which is shown in Figure 2.8. These and other bolted splices have been used successfully, and no cracking of the bolted splice details has been reported. The bolted splice detail shown in Figure 2.8 was tested as part of the laboratory fatigue tests reported later. The bolted splice plates behave like a hinge—i.e., they do not take bending moments. As a result, such details are subjected only to small shear stress ranges and need not be explicitly designed for fatigue. However, the hinge in the span creates greater bending moments at the support-bar connection; therefore, to reduce the applied stress ranges at the support-bar connection, the span with the field splice must be much smaller than the typical spans.

Thin stainless steel slider plates are often welded like cover plates on the support bars, as shown in Figure 2.9. In the AASHTO bridge design specifications, the fatigue strength of the ends of cover plates is Category E. However, there have not been any reports of fatigue cracks at these slider plate details in MBEJs. The lack of problems may be because the support-bar bending stress range is much lower at the location of the slider plate ends than at the centerbeam connection, which is the detail that typically governs the

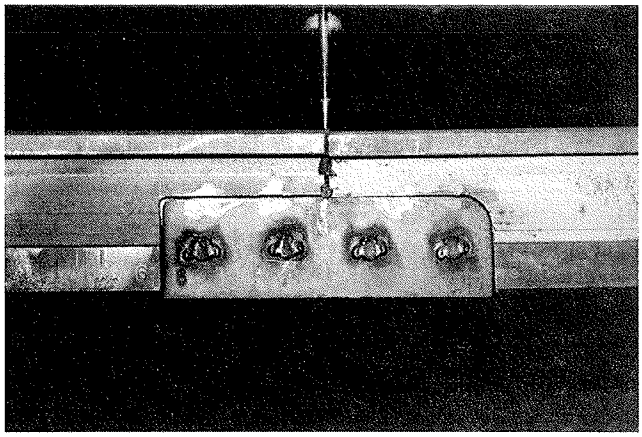

Figure 2.8. Hinge-type centerbeam field splice.

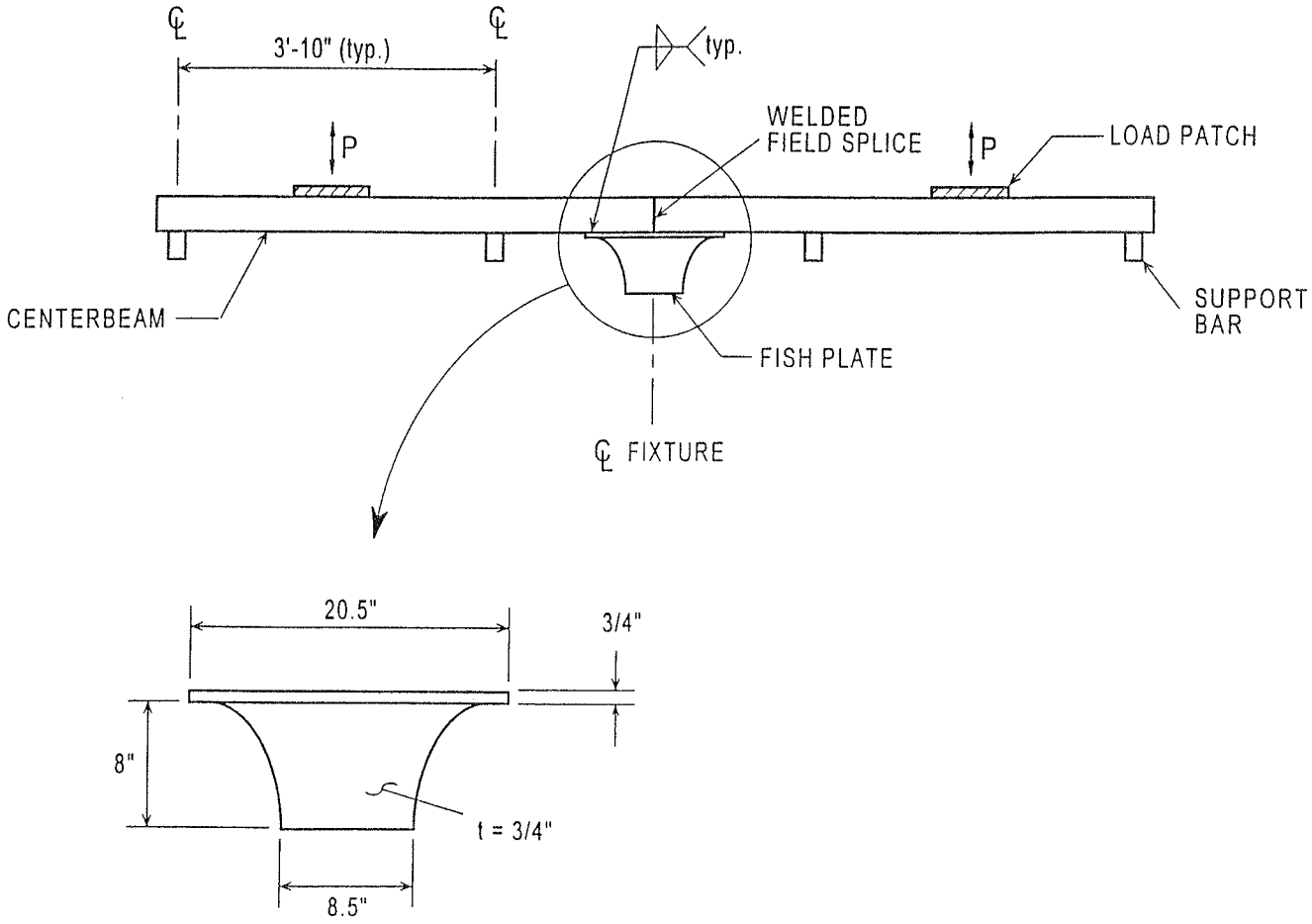

Figure 2.7. Detail of fish-plate-type centerbeam field splice.

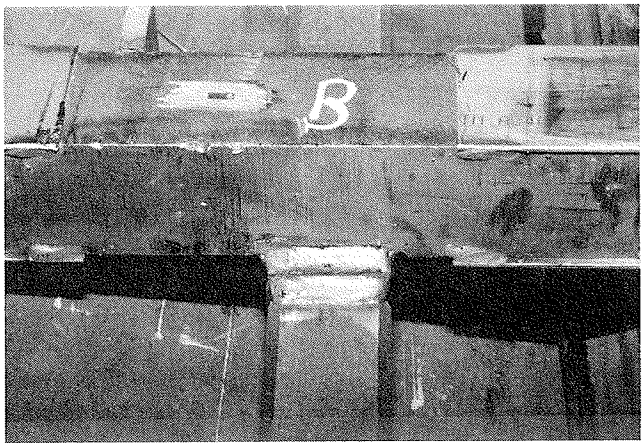

Figure 2.9. Typical stainless steel slider plates.

fatigue design of the support bar. Also, it is possible that the fatigue strength is greater than that of conventional cover plates, perhaps because of the thinness of the slider plate. For economic reasons, some manufacturers have proposed bonding the slider plates with adhesives. The adhesive joint would not affect the fatigue strength of the support bar and therefore potentially could be better than a welded detail. However, at least one manufacturer has had problems with the long-term performance of the adhesives. As a result, many agencies require these stainless steel plates to be welded to the support bar.

Figure 2.10 shows that a typical welded attachment on the sides of a support bar reacts against the horizontal equidistant springs. Like the slider plate ends, these attachments are of little concern with respect to the bending stress range in the support bar because the stress range at these details is very small. In addition to checking the equidistant spring attachments with respect to the stress range in the support bar, there is also some bending load in the attachment itself. The equidistant springs take part of the horizontal load, especially in single-support-bar systems. The horizontal load is also transferred through friction in the bearings and springs of the centerbeam connection. However, because this transfer is influenced by the dynamic behavior of the MBEJ, it is very difficult to quantify the load in the attachments. Because there have been no reported problems with cracking of these equidistant attachments or wear of the springs, it is recommended that they need not be explicitly designed as a loaded attachment for fatigue.

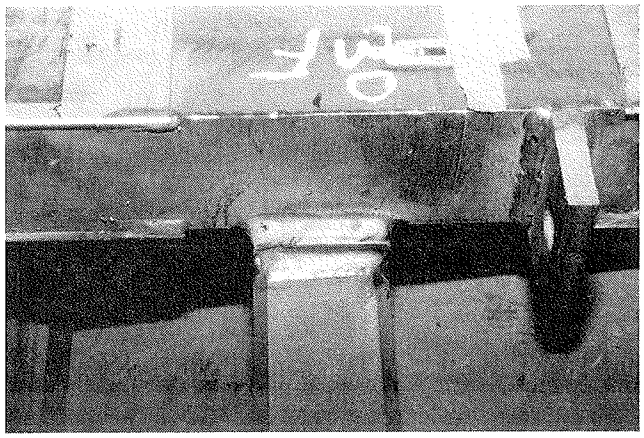

Figure 2.10. Typical attachment welded to a support bar.

Finally, welding of temporary attachments to the centerbeams or support bars for erection purposes can create hot spots that are sensitive to fatigue cracking. As a result, some agencies do not permit these temporary weldments. However, this prohibition is not warranted because there is no residual effect on fatigue life if these details are removed and the surface is ground smooth.

Residual stresses are an important factor in the fatigue resistance of MBEJs. The presence of tensile residual stress means that even compressive applied cyclic loads can cause fatigue cracking by creating a local fluctuation in the tensile residual stress. In addition to the initial residual stress in the component bars from the manufacturing processes, welding creates high residual stresses. Initial misalignment or out-of-straightness of the centerbeams can result in locked-in residual forces and moments if the centerbeams are forced into place during fabrication or installation. In some incidents of MBEJ failure, it has been reported that the centerbeam sprang up into the path of traffic after the connection failed, which indicates that there were significant locked-in forces in the centerbeams.

2.1.4 Performance Factors Related to Loads and Dynamic Response

The fatigue lives of MBEJ details are governed by local stress ranges, which are related to truck-axle loads. The axle loads are amplified as a result of the dynamic action of the truck and the response of the MBEJ system (*27*). The dynamic response of an MBEJ (or any other deck component) to a variable series of trucks is very difficult to estimate without field measurements. The stress ranges are variable in amplitude and difficult to characterize. Therefore, the truck-axle loads and the dynamic response of the MBEJ to these loads are the performance factors with the greatest uncertainty.

It is explained in this section that, in the range of typical axle loads and because of the way these axle loads are distributed in patches that increase in size with increasing load, the maximum load in a centerbeam of an MBEJ is not sensitive to the maximum axle load. Therefore, although there is great uncertainty in the maximum truck-axle load (which is a problem for all bridge elements), the effect of this uncertainty is not that significant for MBEJs.

The factors related to load and dynamic response that are most significant with respect to the durability of MBEJs are

those that affect the fatigue behavior and fatigue design of the structural members and connections. Therefore, it is necessary to briefly review the fatigue design philosophy and the loading data required for the fatigue design of MBEJs.

Each individual axle causes one load cycle in bridge deck elements. When the entire truck spectrum is considered, this results in approximately 4.5 axles or cycles of loading on average for every truck (*28*). Clearly, most structures that require a modular expansion joint carry enough truck traffic to justify an infinite-life fatigue design approach. Bridges with even moderate traffic quickly experience millions of load cycles. For example, assuming an MBEJ with a 25-year life and a Category C CB/SB connection (the CAFL is 70 MPa or 10 ksi), it can be shown that the maximum permissible average daily truck traffic (ADTT) is about 100 trucks per day if the CAFL is just slightly exceeded. With such a low limit on ADTT, a finite-life calculation is not of much use. Furthermore, uncertainty about the number of axles per truck and the number of fatigue cycles per axle makes a finite-life design approach difficult. In addition, little cost is added to the MBEJ by designing for infinite fatigue life. Therefore, the fatigue design procedure recommended here for MBEJ is based primarily on the infinite-life approach. (The proposed fatigue design procedure allows a finite-life calculation to be carried out to design MBEJs for bridges with very low volumes of traffic.)

Figure 2.11 shows the lower part of an S-N curve with assorted possible variable stress-range distributions superposed. The AASHTO load and resistance factor design (LRFD) code and the Eurocode (*25*) both use an effective stress range to characterize variable-amplitude loading. The effective stress range, shown as S_{re} in Figure 2.11, is the cube root of the mean cube of the stress ranges (called the root mean cube [rmc]). The effective stress range is defined by Miner's rule together with the fact that the exponent of the power law describing the S-N curves is 3.0. The effective stress range is used the same way as a constant-amplitude stress range with the S-N curves in the finite-life regime (Case 1 and Case 2 in Figure 2.11).

The infinite-life fatigue design philosophy requires that essentially all the stress ranges are less than the CAFL. This situation is shown in Figure 2.11 as Case 3. This philosophy is based on variable-amplitude fatigue tests on full-scale girders with welded details, which show that if <1/10,000 cycles exceed the CAFL, then essentially infinite life is obtained (*29*). This infinite-life approach is the basis of provisions in the AASHTO LRFD specifications (*12*) and has also recently been applied in developing AASHTO fatigue design specifications for wind-loaded sign, signal, and luminaire support structures (*30*).

One advantage of this approach for structures with complex stress histories is that it is not necessary to accurately predict the entire distribution of future stress range. The fatigue design procedure simply requires a knowledge of the stress range with an exceedence level of 1/10,000, which is called the fatigue-limit-state stress range (S_{rmax} in Figure 2.11). As indicated in the previous section, the infinite-life approach relies on the CAFL as the parameter that determines the fatigue resistance. The emphasis in fatigue testing of details therefore should be on defining the CAFL.

Significant previous research on the fatigue of MBEJ was conducted in Europe (*31*); consequently the fatigue of critical details has been evaluated with the Eurocode (*25*). Therefore, it is useful to compare the Eurocode and AASHTO provisions for fatigue. There are large differences between the Eurocode and the AASHTO LRFD code in the specified procedures regarding long-life variable-amplitude fatigue. However, both procedures produce essentially the same design for a given set of loads. For example, there is a big difference between the Eurocode and AASHTO in the way the CAFL is defined and used. In development of codes in the United States, the CAFL has been defined from full-scale test data

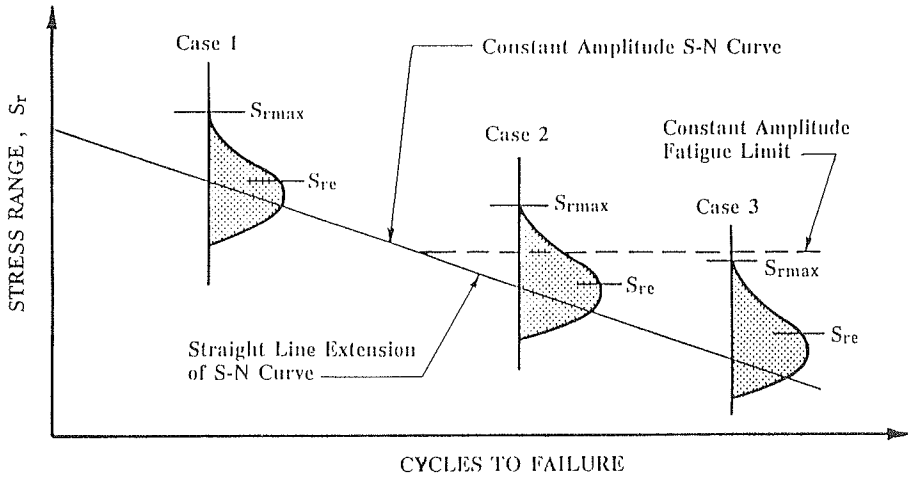

Figure 2.11. Possible cases of S_{re} and S_{rmax} in relation to the CAFL.

in combination with fracture mechanics analysis in some cases. The CAFL is the largest stress range for which all fatigue tests are terminated with no observed cracking. The number of cycles associated with the CAFL is whatever number of cycles corresponds to that stress range on the S-N curve for that category or class of detail. The CAFL occurs at an increasing number of cycles for lower fatigue categories or classes. Sometimes different details that share a common S-N curve (or category) in the finite-life regime have different CAFL.

In the Eurocode, S-N curves have CAFL at 5 million cycles regardless of the category (categories are called classes in the Eurocode). The Eurocode S-N curves have a change in slope below the CAFL with a cutoff at 100 million cycles.

However, because both approaches are based on experimental data, it is not surprising that both result in approximately the same design for given fatigue loads (*32*). For example, with the Eurocode and considering a class 90 detail (AASHTO Category C), the effective stress range should be just below the fatigue strength at 100 million cycles, which is about 40 MPa. The LRFD fatigue design specifications, discussed further below, compare the effective stress range with one-half the CAFL. The CAFL for AASHTO Category C is 70 MPa, so the effective stress range must be <35 MPa. Therefore, there is approximate agreement between the two approaches and the AASHTO infinite-life approach is slightly more conservative (*32*). Because there are no significant advantages of the Eurocode approach and because the MBEJ specifications should be compatible with the current AASHTO LRFD specifications, the Eurocode approach is not discussed further.

Since 1974, the basic fatigue design loads in the AASHTO LRFD bridge design specifications do not differ significantly from previous bridge design specifications. The procedure simply involves assuring that the calculated nominal stress range produced by a specified fatigue truck is below the appropriate allowable stress range for the detail under consideration. In reality, bridges carry many different types of trucks with considerable variations in gross weight and axle spacing.

As discussed above, a variable-amplitude stress-range spectrum can be represented by an effective constant-amplitude stress range equal to the rmc of all stress ranges. This rmc concept has been applied to the variable-amplitude load spectrum obtained from weigh-in-motion (WIM) data to determine an equivalent truck capable of producing the same cumulative fatigue damage as the variable series of trucks. The resulting truck is referred to as the fatigue truck in design and considerably simplifies fatigue evaluation by representing the variety of trucks of different weights and types found in actual traffic. Through examination of extensive WIM data, a fatigue truck equal to the HS-15 vehicle with a 9.14-m (30-ft) axle spacing was recommended in *NCHRP Report 299* (see Figure 2.12) (*33*). A constant axle spacing of 9.14 m (30 ft) was found to best approximate the axle spacing of typical four- and five-axle trucks responsible for most fatigue damage to bridges.

The philosophy behind the AASHTO LRFD specifications is not clearly stated. The effect of the specifications is that the HS-15 truck represents the effective fatigue truck, which approximately represents the rmc of all gross vehicle weights (GVWs). Actually, the HS-20 truck is used in the LRFD specifications with a fatigue load factor of 0.75 (i.e., 0.75 times the HS-20 is the same as HS-15). Rather than introduce another possibly confusing design truck in the code, it was decided to use the HS-20 truck with a factor to achieve, in effect, an HS-15 truck.

In the LRFD bridge fatigue design specifications, the stress range produced by the fatigue truck (S_{re}) is compared with one-half the CAFL. This implies that the actual fatigue-limit-state truck weighs twice the gross weight of the HS-15 truck. The ratio of the effective GVW to the GVW of the fatigue-limit-state truck in the measured spectrum is referred to in the literature as the α factor (*28*). The LRFD specifications imply that α equals 0.5 and that the fatigue-limit-state truck is about HS-30.

The α factor of 0.5 implied by the LRFD specifications is not consistent with the findings of *NCHRP Report 299* and the *Guide Specification for Fatigue Design of Steel Bridges*

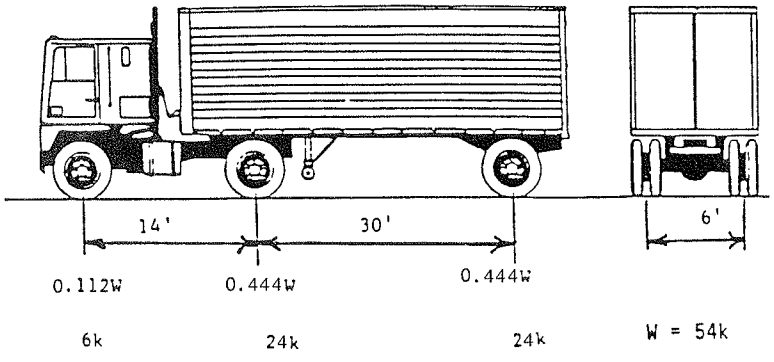

Figure 2.12. Fatigue truck as specified in NCHRP Report 299 and AASHTO LRFD.

(*34*), which imply that the α factor should be closer to 0.33. With α factor of 0.33, the fatigue-limit-state truck is about 3 times heavier than the effective fatigue truck, or about HS-45. This finding was based on a reliability analysis, comparison with the original AASHTO fatigue-limit check, review of nationwide WIM data, and a study of peak ratio (peak/effective) measured stress spectra. According to the statistics of the GVW spectra (33), this HS-45 fatigue-limit-state truck has only a 0.023% probability (about 1 in 5000) of exceedence, which is almost consistent with the recommendation from *NCHRP Report 354* (*29*) that the fatigue-limit-state stress range has an exceedence of <1/10,000. If the α factor of 0.33 is correct, the stress range produced by the fatigue truck should be compared with one-third instead of one-half the CAFL. The HS-30 fatigue-limit-state truck implied by the AASHTO LRFD provisions clearly has a much higher probability of exceedence.

Researchers have investigated the apparent inconsistency in the exceedence level of the fatigue-limit-state truck weight with individuals who were involved in the development of the LRFD bridge specifications (J. W. Fisher and D. Mertz, personal communication about the rationale behind the fatigue design provisions contained in the AASHTO LRFD bridge design specification). The theoretically low exceedence level of the fatigue-limit-state truck weight implied by the LRFD code has been defended because it is believed that other aspects of the design process are overconservative, such as the assumptions in the structural analysis. The *Guide Specifications for Fatigue Design of Steel Bridges* (*34*) apparently resulted in overly conservative estimates of fatigue life compared with behavior observed in the field. As a result, the LRFD specification was calibrated to match existing field experience. It is not clear whether the same factors apply in consideration of load models for MBEJs—e.g., the overconservative structural analysis techniques used for bridge member design are not used for analysis of MBEJs.

For the design of deck elements, it is the axle weights and not just the GVW that are required for fatigue evaluation. It is very important to note that the single rear axles of the HS-15 fatigue truck are actually intended to represent a tandem axle as shown in Figure 2.13 (*33,35*). Representation as a single axle is reasonable for design of bridge main members because the close spacing of tandem axles [about 1.2 m (4 ft)] effectively generates only one stress cycle. This simplification also eases design of main members by decreasing the number of axles (loads) that must be considered and leads to more conservative, yet reasonable, designs of typical bridge members. However, this simplification is not appropriate for the design of MBEJs. As shown in the field test data discussed below, each axle of the tandem axle groups creates a unique stress cycle in a MBEJ.

Incidentally, the simplification of the HS rear axles as single axles is probably also not appropriate for other deck elements. Grid deck elements, the transverse diaphragms in orthotropic decks, and even floor beams may be subjected to each axle load of a tandem axle. However, the LRFD code does not clearly indicate that this should be taken into account in the fatigue design of these elements.

If the HS-15 tandem axle load is split, the effective axle load is 53 kN (12 kips) for each axle. With the α factor of 0.5 implied by the AASHTO LRFD specification, the fatigue-limit-state axle load is 107 kN (24 kips). To be in agreement with the AASHTO LRFD code, this is the design axle load recommended in the MBEJ specifications discussed in Section 3.

As expected, measured axle load data (*35,36*) show axle loads that substantially exceed the 107-kN fatigue-limit-state

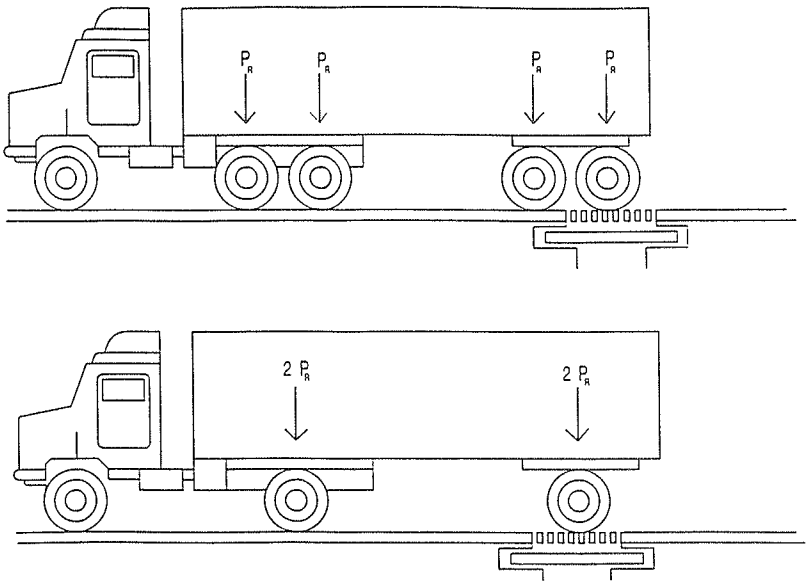

Figure 2.13. Five-axle truck idealized as an equivalent three-axle truck.

axle load implied by the AASHTO LRFD specifications. The shape of the axle-load spectra are essentially the same as the GVW spectra—i.e., the α factor is about 0.33. This α factor suggests that the fatigue-limit-state axle load with an exceedence level of about 1/10,000 is approximately 160 kN (36 kips). In fact, measured axle-load data (*36*) show axle loads exceeding 160 kN (36 kips) in some cases. The appropriate axle load to use in general design specifications is very uncertain, however, because the measured axle-load spectra are very site specific in this extreme tail of the distributions and the data are very sparse.

Aside from the fatigue-limit-state axle load, the rest of the loading spectrum does not matter when the infinite-life approach is used. Also, the precise number of cycles does not have to be forecast. Rather, it is necessary only to establish that the total number of cycles exceeds the number of cycles associated with the CAFL. Therefore, it is not necessary to know precisely the expected life of the deck and future traffic volumes. Thus, despite the uncertainty in the appropriate value for the fatigue-limit-state axle load, it is considerably simpler to use the infinite-life approach than to try to account for the cumulative damage of the whole distribution of future axle loads, which is even more uncertain.

In the fatigue design of bridge deck elements in the AASHTO LRFD code, the fatigue design stress range is obtained from a static analysis where the wheel loads (one-half the axle loads) are applied in patches. The load patches in the LRFD code are calculated in a manner that differs from the calculation in the standard specifications. However, in both methods, the patches increase in size as the load increases, which results in an applied pressure on continuous deck surfaces approximately the same as typical truck tire pressures (700 kPa [100 lbf/in.^{2}]). In the AASHTO LRFD code, the patch has a fixed width of 508 mm (20 in.) and a tire pressure of 860 kPa (125 lbf/in.^{2}). The patch increases in length as the load increases. In this case, the area of a centerbeam that can be covered by the tire patch area is fixed as the centerbeam width times the tire patch width.

In the ideal case where the tire pressure on the load patch is constant, the load in a centerbeam is equal to the tire pressure times the area of the centerbeam under the tire. Because the area of the centerbeam under the tire patch does not change, the total load on the centerbeam does not increase with increasing axle load, above some minimum magnitude. In this ideal case, the centerbeam load would not depend at all on the magnitude of the axle load.

However, the actual distribution of the tire load is not as simple as the constant pressure idealization, because there are gaps in the contact surface with the tire between the centerbeams of the MBEJ. The load patch sizes and distribution of load among centerbeams were studied experimentally, as summarized in Section 2.3 of this report. The results of the load patch studies are discussed in even greater detail elsewhere (*37*). As explained in Section 2.3, a variety of assumptions have been made about how the tire patch load is distributed to the centerbeams. For now, the important point is that the tire pressure distribution is close to being constant pressure. This phenomenon means that the load in one centerbeam does not increase significantly after the design axle load reaches a minimum magnitude. Fortunately, this phenomenon mitigates the uncertainty in the fatigue-limit-state axle load.

When vehicles pass over the MBEJ, there is an apparent amplification of the vertical response of the centerbeam of the MBEJ compared with the response when a truck slowly rolls over the MBEJ. Several researchers have measured this dynamic amplification of the response of MBEJs in the field (*20,31,32,38–42*). The increase in dynamic response relative to static response results in an increase in stress range at a given detail, which must be accounted for in design. In the AASHTO LRFD specifications, an impact factor of 1.75 is recommended for deck elements. This value of the impact factor specified in the LRFD code came from a study of MBEJs by Tschemmernegg (*31*) and includes the effect of rebound, as explained later. The impact factor of 1.75 is also consistent with the magnitude of impact measured in the field tests, as explained in Section 2.2. However, this impact factor is probably not applicable to other deck elements, because it is primarily due to the dynamic response of the MBEJ rather than an actual increase in the applied load.

When vehicles traverse the MBEJ at constant speed, a horizontal dynamic response is also excited that causes a horizontal bending moment range, again leading to an increase in stress range at details (*20,31,38*). Large horizontal forces can be applied by vehicles at MBEJs located near traffic metering devices such as stop lights or toll facilities (*19,20*). Special consideration should be given to MBEJs installed near such devices. Other than the general requirement that all bridge elements should be designed for a horizontal force equal to 5% of the vertical load, there are no specific recommended horizontal loads due to wheel load impact in the AASHTO code.

The degree of dynamic amplification in both the vertical and horizontal directions depends on damping and matching the load impulse period and the resonant period. Resonant frequencies and damping ratios for MBEJs have been estimated from the time histories of MBEJ responses. For example, measurements explained in Section 2.2 indicated that the MBEJ on the Charter Oak Bridge in Hartford, Connecticut, has an apparent resonant frequency of about 130 Hz in the vertical direction and 60 Hz in the horizontal direction and an apparent damping of about 7% of critical damping in both directions. These observations compare very well with values reported by Tschemmernegg (*10*) for a welded multiple-support-bar MBEJ—i.e., 132 Hz vertically with 7.2% damping and 54 Hz horizontally with 14% damping.

Tschemmernegg (*43*) provides a graph that shows the frequency as a function of span length for several types of expansion joints, including welded multiple-support-bar systems and swivel-type single-support-bar systems. The graphs

do not provide frequency data for bolted single-support-bar systems. The estimates from these graphs are in reasonable agreement with the observed frequencies from the field tests.

Roeder (*17*) provides a formula for the period of the loading impulse, which was attributed by Roeder to Tschemmernegg. The formula states that the period is approximately equal to two bar spacings divided by vehicle speed. This formula was derived by assuming that the tire patch length covers three centerbeams simultaneously. Although this formula appears to be arbitrary, it gives good agreement with the loading period that was measured from the time histories. The measured impulse periods were typically within 20% of the calculated values.

This period of the loading impulse was also calculated based on a more rational approach presented by Ostermann (*39*), where impact time is equal to the sum of the tire contact length and width of a centerbeam flange divided by vehicle speed. The results produced by this method were consistently higher than the measured duration and not in as good as agreement as the previous method. It is believed that this discrepancy may be caused by uncertainty in the actual tire contact lengths. Therefore, calculated loading periods based on the Tschemmernegg method are considered more reliable and consistent with the test data.

The dynamic amplification factor (ratio of peak dynamic moment to static moment) for a generic undamped elastic system subjected to a symmetric triangular impulse load peaks at about 1.5 as the ratio of the impulse period to resonant period approaches 1. As explained in Section 2.2.3, the loading period for the Charter Oak Bridge was about 8 msec for a vehicle speed of 96 km/h (60 mph). This period is very close to the resonant period and the measured peak response from the time histories was about 1.3 times the static bending moment at this location. Other tests, where the ratio of the loading period to the resonant period was >1.5, exhibited dynamic amplification factors less than 1.1.

The strategy for avoiding excessive vertical amplification that has been discussed by Tschemmernegg (*10*) is to keep the frequency higher—i.e., keep the ratio of the impulse period to the resonant period much larger than 1.0. Tschemmernegg has stated that this objective can be achieved for welded multiple-support-bar systems by keeping the centerbeam span between support bars less than 1220 mm (48 in.). It is clear from his graphs of the resonant frequencies for MBEJs that for spans smaller than 1220 mm the vertical frequency is larger than 140 Hz, or the period is shorter than 7 msec. This lower-bound loading impulse period of 7 msec is consistent with the measured loading periods, the smallest of which was 8 msec (125 Hz) for the Charter Oak Bridge, where the truck was traveling at 96 km/h (60 mph), which is near the legal speed limit.

Although limiting the span outright is not appropriate for a performance-based specification, Tschemmernegg's suggestion is mentioned in the commentary. It is a good idea to avoid MBEJ designs that are susceptible to dynamic amplification for vehicles that travel at or below the speed limit. However, the occasional speeding vehicle (probably more frequent than 1/10,000) may cause loading impulse periods of 7 msec or less. Therefore, Tschemmernegg's suggestion to keep the centerbeam span between support bars less than 1220 mm (48 in.) is probably not sufficient to avoid amplification entirely. Therefore, the specifications still should anticipate the worst-case vertical dynamic amplification.

The horizontal bending moment response and the vertical response are completely different phenomena. The typical horizontal response is relatively small at steady speeds, on the order of $\pm 5\%$ of the static vertical bending moment or a total range of $<10\%$. However, the horizontal bending is critically important because the section modulus for bending in the horizontal direction is quite often about one-fourth the section modulus in the vertical direction. Therefore, a horizontal bending moment equal to 20% of the vertical bending moment, as recommended by Tschemmernegg, corresponds to a horizontal bending stress range as large or larger than the vertical bending stress range. These stress ranges are then summed to check the fatigue strength.

The resonant period for horizontal response is typically about twice the loading period, indicating that resonance in the horizontal direction is difficult to avoid. This is in contrast to the vertical response period, which is generally smaller than the loading period and can be controlled by keeping the centerbeam span below 1220 mm (nominally 48 in.). In fact, according to the analytical predictions of the response, if the period of the response could be made larger than 3 times the loading period, the response could be minimized. In this case, it could help to make the MBEJ less stiff in the horizontal direction, and some designs have clearly attempted to accomplish this. Fortunately, the damping is higher in the horizontal direction and therefore this horizontal amplification is mitigated to a significant extent. Tschemmernegg has presented data showing that the horizontal response is about one-half what would be computed without damping.

In some cases, the peak horizontal response is slightly out of phase with the peak vertical response. In these cases, the two peak responses would not be additive. However, careful examination of the time histories reveals that in about one-half the cases the peaks occur nearly in phase so the responses would be additive. Because the fatigue design strategy is based on the largest stress ranges, the assumption should be made that the peaks occur in phase.

Although skew has not been identified by any of the agencies responding to the survey as a factor affecting loading of the joint, MBEJs installed on skewed structures may require special attention in the design process. Skew, as defined in the AASHTO LRFD bridge design specification, is the angle between the centerline of a support and a line normal to the roadway centerline; therefore, a joint transverse to the longitudinal axis is considered to have a 0-degree skew. On structures with joint skews greater than 14 degrees, it can be

shown that the wheels at either end of an axle do not roll over a particular centerbeam simultaneously. This asymmetric loading could significantly affect the stress range at fatigue-sensitive details, either favorably or adversely. Nevertheless, a skewed centerbeam span is subjected to a range of moments that includes the negative moment from the wheel in the adjoining span followed or preceded by the positive moment from the wheel in the span. In addition, this asymmetric loading increases the number of fatigue cycles applied to the CB/SB connection, although the magnitude of the reaction force will be lower.

A joint located on a structure with significant settlement or deterioration of the approach roadway may be exposed to higher than expected impact forces because of dynamic excitation of the vehicle. The approach slab roughness is another potential factor. In fact, results of measurements (*41*) from an instrumented axle on a test truck indicated that deviations of −48% to +96% are possible between dynamic and static axle loads. Quantifying these effects for a specification is very difficult. Because field measurements were taken at a variety of locations, typical truck excitations should be reflected in the design loads derived from the field measurements.

It has been shown that the approach roadway alignment at the joint can have a significant effect on the dynamic amplification of wheel loads applied to the MBEJ. Problems have also been reported with MBEJs that were attributed in part to the roadway grade (*19*). The grade adds a component of horizontal force because of inclination of the weight vector.

As indicated in Section 2.1.1, poorly consolidated concrete under support boxes increases the effective span length of the centerbeams and affects the vertical dynamic amplification as described above.

2.2 FIELD TESTS

The primary objectives of the field test program were to determine the static and dynamic response of various modular expansion joint systems when subjected to truck loading and to develop a rational equivalent static load model for inclusion in the proposed specification. This equivalent static load model is based on measurements of wheel load distribution, horizontal and vertical dynamic impact factors, and the relationship of horizontal and vertical wheel loads with respect to their relative magnitude, number of cycles, and coincidence of peaks. At each field test location, approximately 3 m (10 ft) of the MBEJ was instrumented with strain gages and displacement transducers to measure the response of the joint when subjected to a series of controlled static and dynamic loads and several hours of uncontrolled dynamic loads. The controlled static and dynamic tests were conducted by using a test truck with known axle loads approximately equal to the legal load limit. A brief summary of findings from each component of the field test program is described below. First, a review of previous field test techniques and results is presented.

2.2.1 Review of Previous Field Testing

There are few published data obtained from field testing of MBEJs. Previous field testing is limited to work conducted by Tschemmernegg (*31,38,40*) and, more recently, work by Roeder (*43*) on a large MBEJ installed on the Third Lake Washington Bridge in the state of Washington and work by Agarwal (41) on the Burlington Skyway Bridge in Ontario. The field testing conducted by each of the above researchers is briefly discussed below.

The most significant source of data on MBEJs acquired through field studies has been generated by Professor Ferdinand Tschemmernegg of the University of Innsbruck in Austria. He has field tested MBEJs on several highway bridges located in Europe (*31,38,40*) and has reported the dynamic response of MBEJs from strain gages for relatively long-term samples (one-half day or more) of uncontrolled traffic. Tschemmernegg noted that the α factors for the spectrum of measured centerbeam stress ranges ranged from 0.4 to 0.5. His α factors are more consistent with the value of 0.5 implied by the AASHTO LRFD specifications than α factors based on GVW or axle-load spectra (typically 0.33). This could be because of the effect described in Section 2.1.4 that increasing axle load does not cause a proportional increase in centerbeam response. This effect would flatten out the spectra of stress ranges in the centerbeam relative to the shape of the spectra of axle loads—i.e., increase the α factor.

As a result of his most recent measurements, Tschemmernegg has recommended a static fatigue-limit-state axle load of 130 kN (29 kips). He has usually defined this fatigue-limit-state axle load as the largest measured response in a long-term sample. His fatigue-limit-state axle load has an exceedence level of approximately 1/5000.

The load recommended by Tschemmernegg is larger than the corresponding load recommended in this report (i.e., 107 kN [24 kips]), which is based on the AASHTO LRFD bridge specifications. As explained in Section 2.1.4, it is known that the AASHTO fatigue-limit-state axle load is smaller than the axle load with a 1/10,000 exceedence level determined from WIM studies. However, because the load on a particular centerbeam tends to level off with increasing axle loads above 100 kN, the discrepancy between the axle load recommended by Tschemmernegg and that recommended here is not that significant.

Tschemmernegg recommended a dynamic impact factor of 1.4 that was applied to this static vertical load to obtain the maximum downward amplitude of the response. He proposed that 30% of the vertical dynamic (amplified) load be applied as an upward rebound force. The stresses generated by these vertical upward and downward forces are added to determine the fatigue stress range. Therefore, the total amplification of static vertical load due to impact and rebound is 1.82. The recommended amplified vertical axle load range is 236 kN (52 kips) and includes the effect of downward impact and rebound.

Tschemmernegg reported a maximum horizontal response amplitude due to normal traffic, which was 20% of the amplified downward part of the vertical load range. Based on this 20% ratio, a ratio of total horizontal to total vertical load of 20% has subsequently been used in most fatigue testing of MBEJs. However, because the rebound part of the total vertical amplified load is smaller than the downward part of the amplified vertical load, Tschemmernegg's recommended horizontal load is ±15% of the total vertical load range. Therefore, the total amplified horizontal fatigue-limit-state axle load range was 71 kN (16 kips), which is 30% of the total amplified vertical fatigue-limit-state load range. Therefore, the horizontal load ratio in Tschemmernegg's design loads is inconsistent with the horizontal load ratio that has been used in testing (*13,43,44*).

Tschemmernegg matched the largest horizontal response in one direction from the long-term samples with the largest horizontal response in the other direction to obtain his total recommended horizontal load. It is likely that these two responses were not from the same vehicle; in fact, they could be hours apart. This approach is regarded as too conservative because it essentially implies that every vehicle causes the maximum response in both directions. Tschemmernegg also reported that the maximum horizontal response due to braking was about 2.5 times greater than his recommended horizontal load, but this was not recommended for use in fatigue design.

For the purpose of comparison, the horizontal load recommended here is either 20% or 50%, respectively, of the amplified vertical load for installations on open highways or near facilities where continuous heavy braking is expected. The basis for these recommended horizontal loads is discussed in Section 2.2.2.

Field tests were conducted by Roeder as a result of significant fatigue cracking on a large swivel-type MBEJ on the Third Lake Washington Bridge in the state of Washington in 1991 (*41*). He recommended a vertical fatigue-limit-state axle load range of 310 kN (70 kips), which includes impact and rebound. Roeder's proposed axle load is about 30% higher than that proposed by Tschemmernegg. The horizontal fatigue-limit-state axle load range proposed by Roeder is only 13% of the total vertical load range or 40 kN (9 kips), which is about 56% of the horizontal load range proposed by Tschemmernegg.

Agarwal (*41*) conducted field tests on MBEJs installed on the Burlington Skyway in Ontario. Recommendations of loads to be used for strength or fatigue-limit states were not made, although an impact factor of 1.8 was recommended for fatigue (accounting for downward and rebound forces). Agarwal reported that no large horizontal response was measured, even under extreme braking and acceleration tests. This finding is inconsistent with all other field tests. It is possible that Agarwal's instrumentation on the centerbeam was unable to detect horizontal bending strains.

2.2.2 Description of Field Test Sites and MBEJs

Selection of candidate MBEJ sites for field tests were made according to the type of MBEJ system as well as several other factors. Two basic types of MBEJ systems are commonly used: (1) the multiple-support-bar systems, where each centerbeam is fixed to a separate support bar at each support location, and (2) the single-support-bar systems where all the centerbeams slide along on a single support bar. Agencies that owned the type of MBEJs of interest were then contacted and asked if they could provide the support necessary for field testing. Accessibility for instrumentation and inspection was investigated by review of drawings and photographs provided by the department of transportation or the MBEJ manufacturer.

Four sites were selected for the field tests, as shown in Table 2.1. These four MBEJs were located in three states

TABLE 2.1 Summary of MBEJs in field tests

MBEJ Location	MBEJ Size, Type & (Installation Date)	Maximum Support Bar Spacing	Vertical Grade	Comments
Charter Oak Bridge I-5 Over CT River Hartford, CT	240 mm W.M.S.B. (1992)	1525 mm (5'-0")	-1.2 %	Horizontal Curve (660 m Radius)
Lacey V. Murrow Bridge Seattle, WA	960 mm W.S.S.B. (1993)	2030 mm (6'-8")	+5.1 %	----
I-90/5 HOV Bridge Seattle, WA	460 mm W.M.S.B. (1991)	1435 mm (4'-8 1/2")	-5.4 %	----
I-70/I-25 Flyover Ramp Denver, CO	305 mm B.S.S.B. (1992)	1675 mm (5'-6")	-5.0 %	Horizontal Curve (150 m Radius) (8 % Superelevation)

Notes: W.M.S.B. - welded multiple-support-bar
W.S.S.B. - welded single-support-bar
B.S.S.B. - bolted single-support-bar

(Connecticut, Colorado, and Washington) and represented a range of field conditions.

2.2.2.1 *Charter Oak Bridge*

The MBEJ on the Charter Oak Bridge, which was instrumented and tested during the week of July 25, 1994, is shown in Figure 2.14. The structure is a multispan, continuous plate girder bridge that carries I-5 and CT-15 over the Connecticut River near Hartford, Connecticut. Several welded multiple-support-bar MBEJs are installed on the structure to accommodate movements of approximately 160 mm (nominally 6 in.), 240 mm (nominally 9 in.), and 320 mm (nominally 12 in.). The MBEJ with 240 mm of movement, which is located on the northbound structure at Pier 12, was selected for testing. A plan and cross section of the joint is shown in Figure 2.15. Instrumentation was placed along a 3-m (10-ft) section of the MBEJ in the exit ramp between Support Boxes 3, 4, and 5. Both centerbeams (CB-1 and CB-2) and the six support bars at these three support-box locations were instrumented.

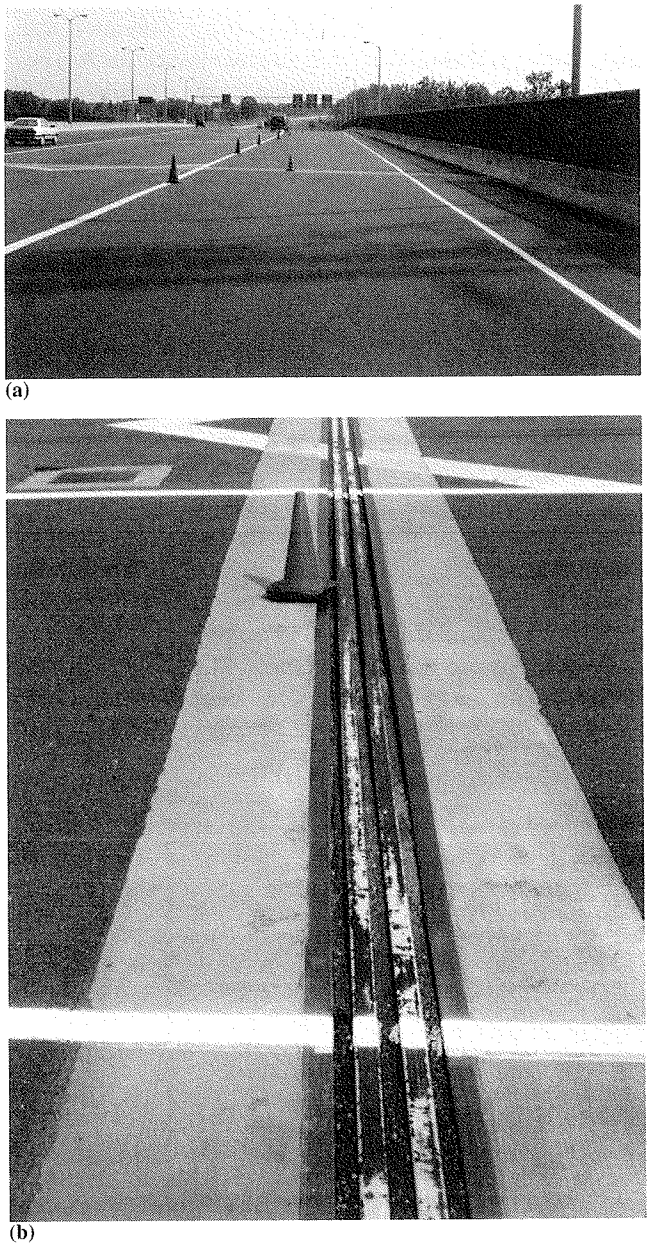

Figure 2.14. MBEJ tested on the Charter Oak Bridge: (a) view of joint in exit ramp looking east; (b) view looking northwest across joint.

Controlled dynamic tests were conducted with a single-axle dump truck loaded with sand in the two positions noted in Figure 2.15. Tests were conducted at truck speeds of 2 km/h (1 mph), 48 km/h (30 mph), and 96 km/h (60 mph). Uncontrolled dynamic tests were also conducted, but the instrumented section of the MBEJ was located in a lightly traveled position of the roadway. Therefore, data obtained from the uncontrolled dynamic test did not indicate the presence of very high stresses due to normal traffic and are not discussed further.

2.2.2.2 *Lacey V. Murrow Bridge*

The MBEJ on the Lacey V. Murrow Bridge, shown in Figure 2.16, was instrumented and tested from August 15 to 18, 1994. The structure is a 2-km (1.2-mi) floating bridge that carries I-90 (eastbound) over Lake Washington near Seattle, Washington. A plan and section of the welded single-support-bar system with 960 mm (nominally 36 in.) of movement, which was selected for testing, is shown in Figure 2.17. This MBEJ was selected for study because it is one of the largest in the world. The installed cost of the joints was $884,112 (U.S.) or about 1% of the $87.8 million (U.S.) bridge cost (*32*).

The joint is located at Pontoon T on the east side of the structure in a 5.1% positive (uphill) grade. Centerbeams 10 and 11 were instrumented along a 4.6-m (15-ft) section of the MBEJ in the shoulder and first traffic lane. The instrumentation extended between, and was included on, Support Bars 3, 4, 5, and 6.

This MBEJ is a special type of single-support-bar system called a swivel-joint or swivel-joist system because the support bars swivel as well as slide longitudinally. This MBEJ is designed to take a variety of movements including lateral translation, changes in lake elevation, and racking as well as longitudinal movement. These movements are a special requirement of the floating bridge (*45*). A similar but older MBEJ on the Third Lake Washington Bridge, parallel to the Lacey V. Murrow Bridge, had been studied previously because of fatigue problems at certain welded connections (*18,42,44*). The connection details on the Lacey V. Murrow MBEJ appeared to be significantly improved relative to this earlier design. For example, the stirrup connection attachment to the centerbeam is fabricated with large radii to improve the fatigue resistance of this detail.

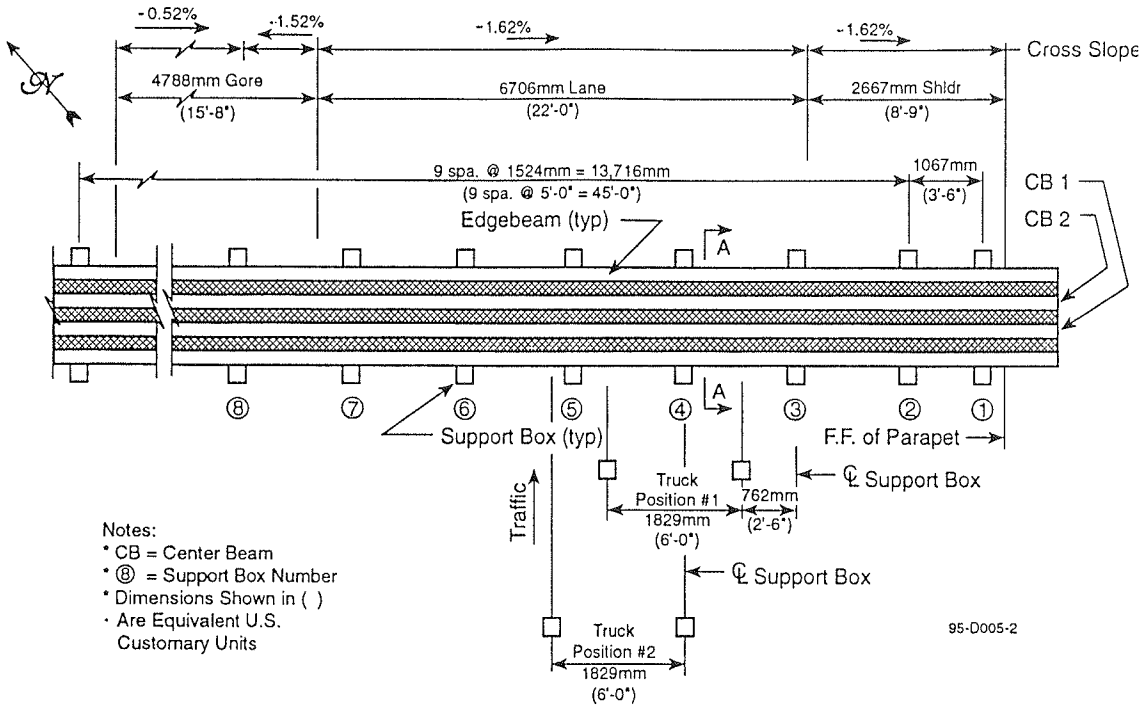

PLAN - CHARTER OAK BRIDGE MBEJ

(no scale)

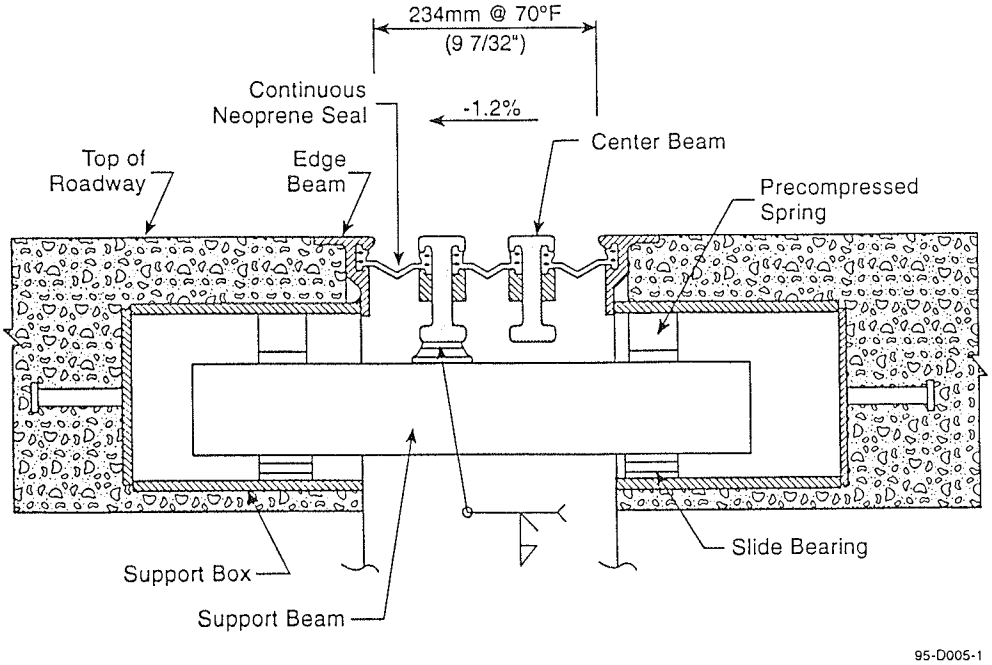

Section A - A

(no scale)

Figure 2.15. Plan and section of Charter Oak Bridge MBEJ.

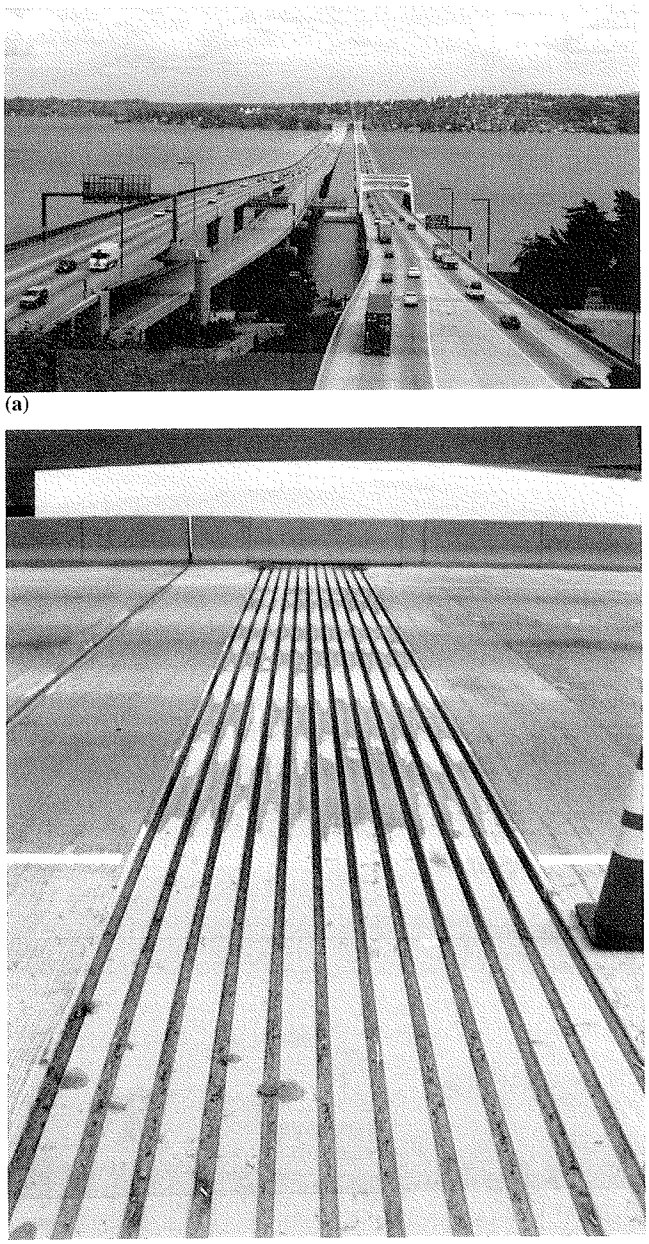

Figure 2.16. MBEJ tested on Lacey V. Murrow Bridge: (a) view of Lacey V. Murrow Bridge, looking east (bridge is on right); (b) view looking north across joint.

Controlled static and dynamic tests were conducted with both single- and tandem-rear-axle dump trucks at various speeds up to 80 km/h (50 mph). The controlled braking tests were conducted at speeds of 48 and 80 km/h.

2.2.2.3 I-90/I-5 High-Occupancy-Vehicle (HOV) Structure

Another MBEJ in the Seattle area was instrumented and tested from August 17 to 22, 1994. The bridge is a steel box girder structure that carries HOV and Metro buses on I-90 and I-5 in and out of downtown Seattle. The welded multiple-support-bar MBEJ system, which is located at the west abutment (Pier 21) in this HOV structure, was tested. This MBEJ, shown in Figure 2.18, has nominally 460 mm (18 in.) of movement. A plan and section of the joint is shown in Figure 2.19. Instrumentation was placed along 3 m (10 ft) of the MBEJ in the outbound traffic lane between Support Boxes 2 and 4. Centerbeams 4 and 5 as well as the support bars carrying these centerbeams at Support Boxes 2, 3, and 4 were instrumented.

Controlled static and dynamic tests were conducted with both single- and tandem-rear-axle dump trucks during the evening/early morning of August 21/22, 1994, at the two positions shown in Figure 2.19. The controlled dynamic tests were run at various speeds up to 72 km/h (45 mph) in the outbound direction, which has a vertical grade of −5.4%. Because of the roadway geometry, maximum test speed was limited to 75 km/h (45 mph). Braking tests were conducted at 48 and 72 km/h with both the single- and tandem-axle trucks.

To investigate the effects of roadway grade on horizontal force, the test truck was also run in the opposite direction over the joint. This was possible because the structure was closed to all traffic during testing. Controlled dynamic tests were run at speeds up to 72 km/h (45 mph). Braking tests at 48 and 72 km/h as well as acceleration tests were conducted with the truck traveling in this direction.

2.2.2.4 I-70/I-25 Flyover Ramp Interchange

From September 16 to 19, 1994, an MBEJ in Denver was instrumented and tested. The MBEJ, shown in Figure 2.20, was located on the I-70/I-25 flyover ramp, which carries traffic from I-70 eastbound to I-25 northbound in Denver, Colorado. It is a multispan, continuous twin box girder bridge on horizontal and vertical curves. Figure 2.21 is a plan and section of the bolted single-support-bar MBEJ located at Pier 9 of the structure. This MBEJ is designed to accommodate approximately 305 mm (12 in.) of movement. Approximately 3.4 m (11 ft) of the MBEJ was instrumented along the inside shoulder of the roadway between Support Boxes 2 and 4. Instrumentation was placed on all three centerbeams in this two-span region of the joint. Unfortunately, tight clearances did not allow strain gages to be attached to the support bars on this MBEJ system.

Controlled dynamic tests were conducted at the two positions shown in Figure 2.21. A single-axle dump truck was used for the tests at speeds up to 72 km/h (45 mph). On this bridge, the maximum speed was limited by roadway geometry; maximum test speeds were 72 km/h at Position 1 and 64 km/h at Position 2. The braking tests were conducted at 32 and 64 km/h.

2.2.3 Field Test Instrumentation

At each field test location, approximately 3.0 to 4.6 m (10 to 15 ft) of the MBEJ was instrumented with up to 32 channels

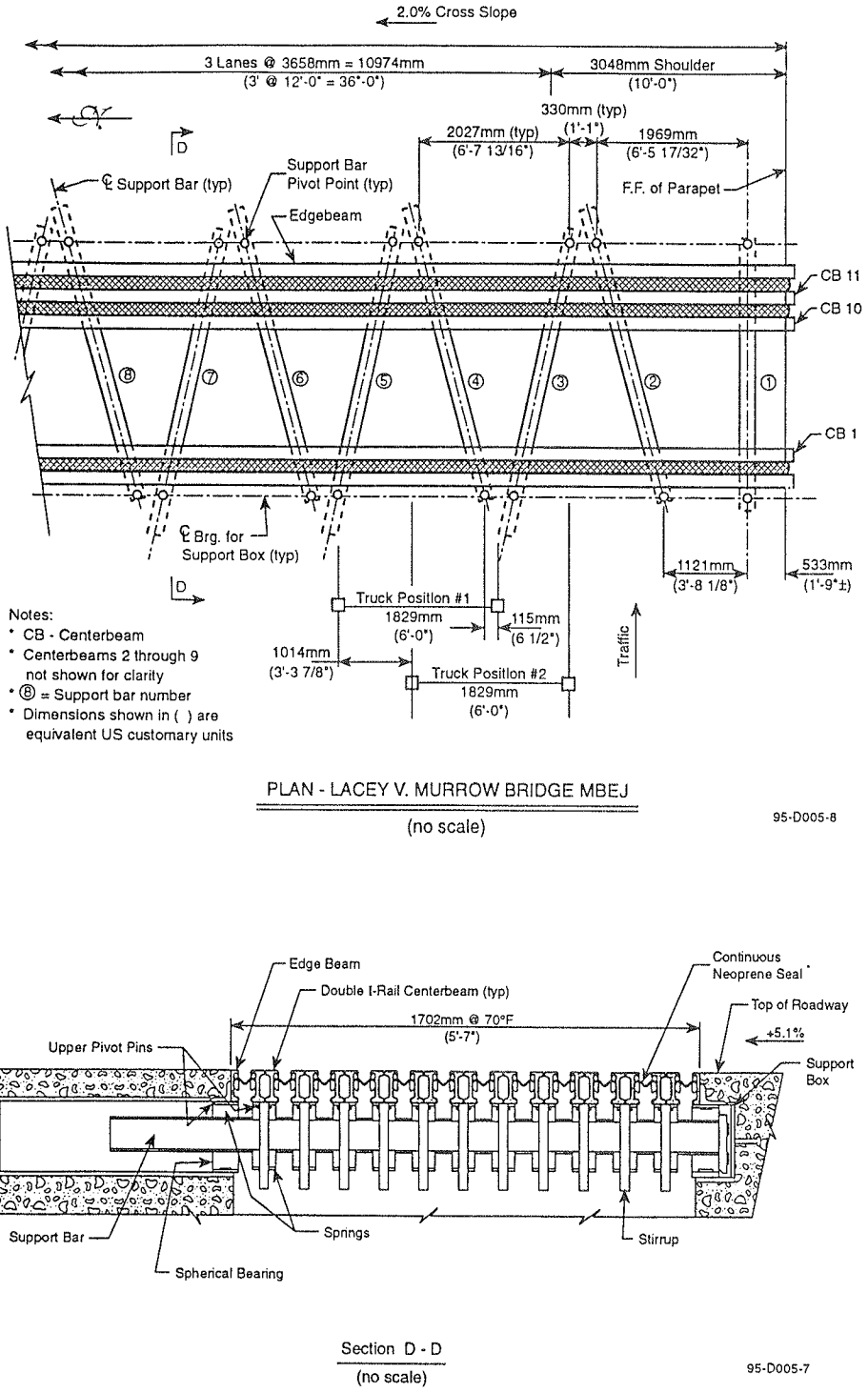

Figure 2.17. Plan and section of Lacey V. Murrow Bridge MBEJ.

of strain gages and displacement transducers to measure the response of the MBEJ when subject to a series of static and dynamic loads. An example of the typical instrumentation plan is presented in Figure 2.22 and photographs of typical instrumentation installations are shown in Figure 2.23. The MBEJs were typically instrumented along two span lengths of the centerbeam in both the positive and negative bending moment regions. Five sets of strain gages were usually installed along the instrumented section of each centerbeam. At each location, two strain gages were positioned on the bottom flange of the centerbeam in an orientation that allowed both vertical and horizontal bending moments to be calculated. The vertical

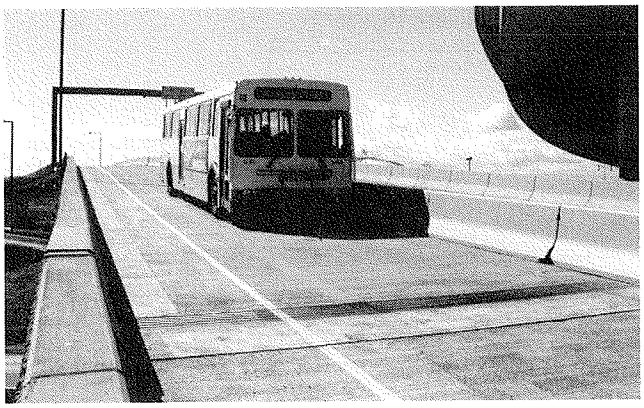

(a)

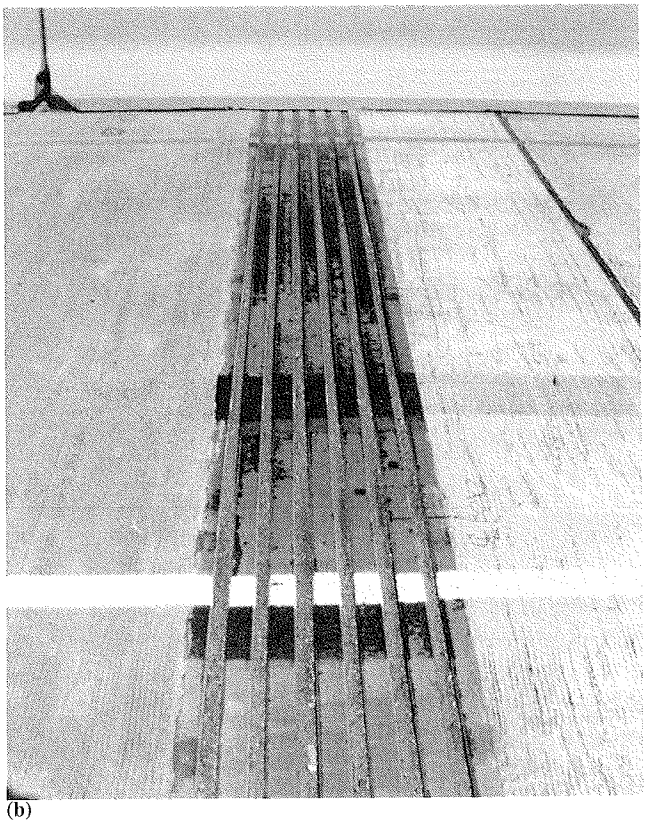

(b)

Figure 2.18. MBEJ tested on the I-90/I-5 HOV bridge: (a) view of joint in outbound HOV lane; (b) view looking northwest across joint.

bending moment is calculated by averaging the two gage readings and the horizontal moment is calculated by taking the difference of the two measurements. Strain gages were also placed on each of the support bars that would carry load from the instrumented centerbeams.

Vertical displacements of the last centerbeam on the MBEJ (i.e., Centerbeam 3 on the I-70/I-25 flyover ramp) were measured at both midspan positions between the three support boxes. The horizontal displacement of this centerbeam was also measured on the underside of the MBEJ adjacent to the interior support bar (i.e., Support Box 3 on the I-70/I-25 flyover ramp). In addition, the vertical deflection of this support bar was also measured as close to the support box as possible. All data were recorded on the Kyowa analog data recording system shown in Figure 2.24.

2.2.4 Procedures and Results of the Field Tests

The field tests included inspection, instrumentation, and measuring strains and displacements of selected members. A thorough inspection was made of each MBEJ that was field tested. This visual inspection of the MBEJ did not reveal any structural distress, fatigue cracking, or excessive water leakage. However, several minor problems were observed and included cracking of the concrete bridge deck at support box locations, lack of concrete consolidation around support boxes, concrete placement into the support boxes, and uneven elevations along the top of the centerbeams (i.e., recesses up to 3 mm [0.125 in.]). General measurements of the ambient temperature, overall joint opening or support-bar span, and centerbeam spacing were recorded at each site.

The primary objective of the field measurements was to collect enough data to understand the static and dynamic response of several different MBEJ systems to truck loading. To obtain these data, more than 450 tests were conducted at the four MBEJ sites. Field tests included (1) static tests where the MBEJ was loaded vertically and horizontally and small hydraulic jacks were used to verify the instrumentation and analysis models by using a known load directly on a centerbeam; (2) static tests where the test truck was parked on the MBEJ to evaluate the portion of the wheel load imparted to a particular centerbeam (i.e., the distribution factor); (3) controlled dynamic tests where the test truck rolled over the MBEJ at steady speeds while braking and while accelerating to compare with the static truck loads to obtain a dynamic amplification; and (4) uncontrolled dynamic tests in regular traffic to examine the spectrum of typical loads.

The data collected were used to (1) verify proposed structural analysis models and (2) develop design axle loads including appropriate amplification and horizontal loads. To interpret the data, it was useful to convert the measured strains to measured bending moments and compare them with bending moments computed by using structural analysis models. The structural analysis model used to compare with the measurements was a general purpose linear three-dimensional frame-analysis computer program. The model consists of only the centerbeam, which is assumed to be continuous over supports. Both rigid supports and supports with specific vertical and horizontal spring constants were used in the analyses.

The apparent measured dynamic response of the MBEJ system to truck loading was compared with a static response computed by using calibrated structural analysis models. The effect of dynamic amplification, rebound, and horizontal component of the load has been characterized in terms of amplification factors or ratios of the apparent dynamic response to the static response.

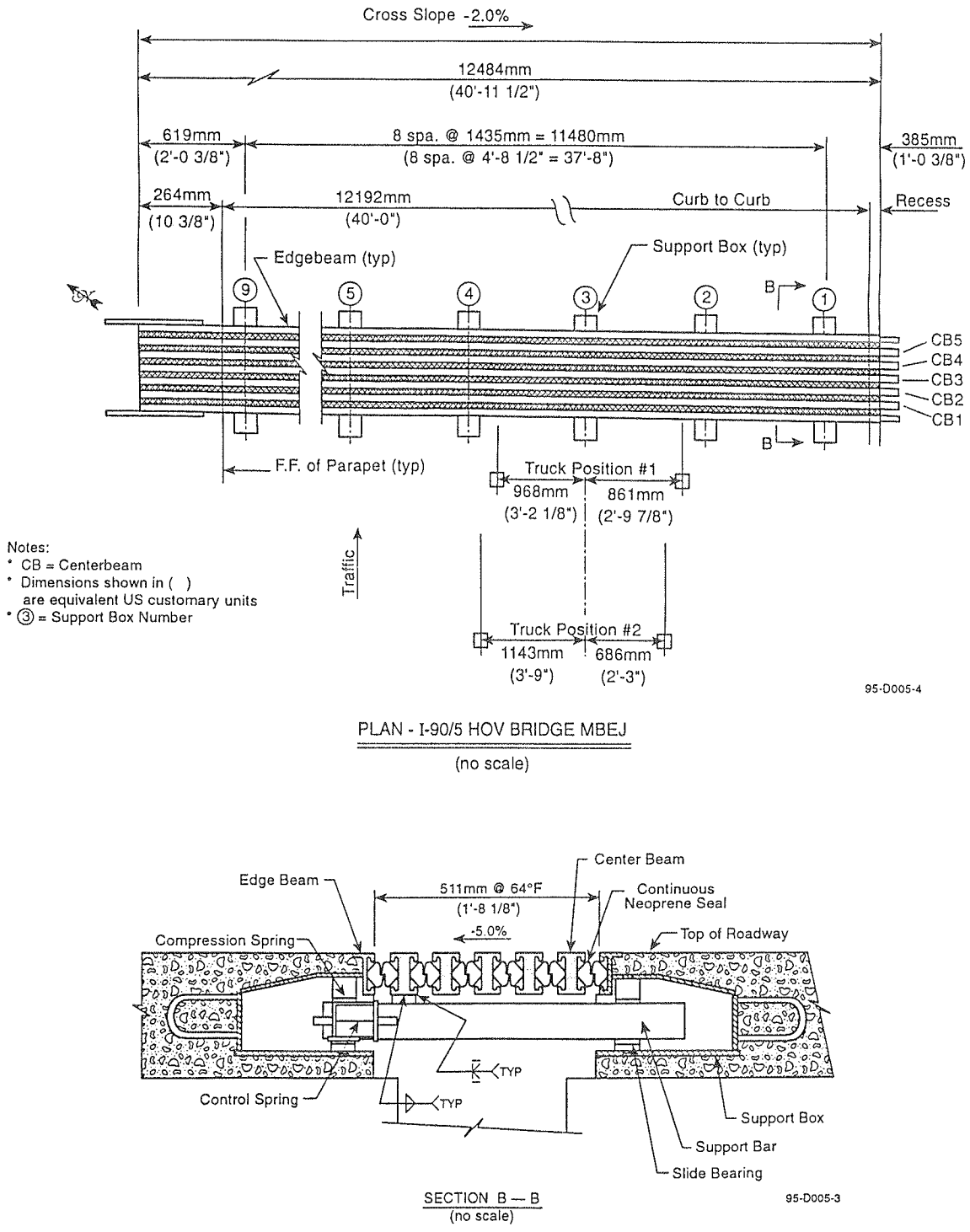

Figure 2.19. Plan and section of I-90/I-5 HOV bridge MBEJ.

2.2.4.1 Static Calibration Tests Using Hydraulic Jacks

Static calibration tests were conducted by applying horizontal and vertical loads up to 90 kN (20 kips) to the centerbeams of the joint with a hand-held hydraulic jack. The purpose of the static calibration tests was to verify operation of instrumentation and calibrate the structural analyses with a known load.

Vertical calibrations were carried out with a 10-ton hydraulic cylinder, which was placed at selected positions (i.e., over a support bar and midspan between support bars) along instrumented centerbeams. The jack reacted against the frame of the loaded test truck, and a calibrated pressure

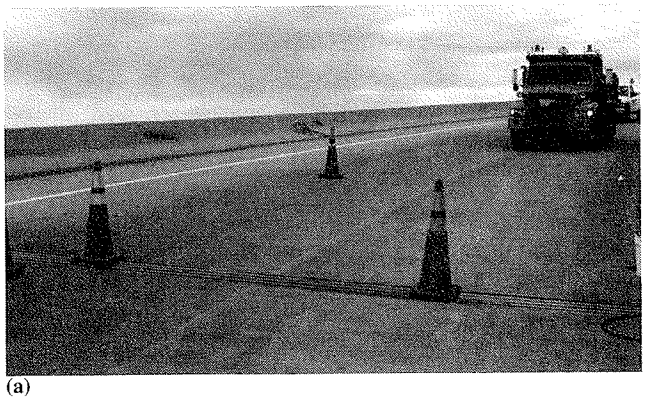

(a)

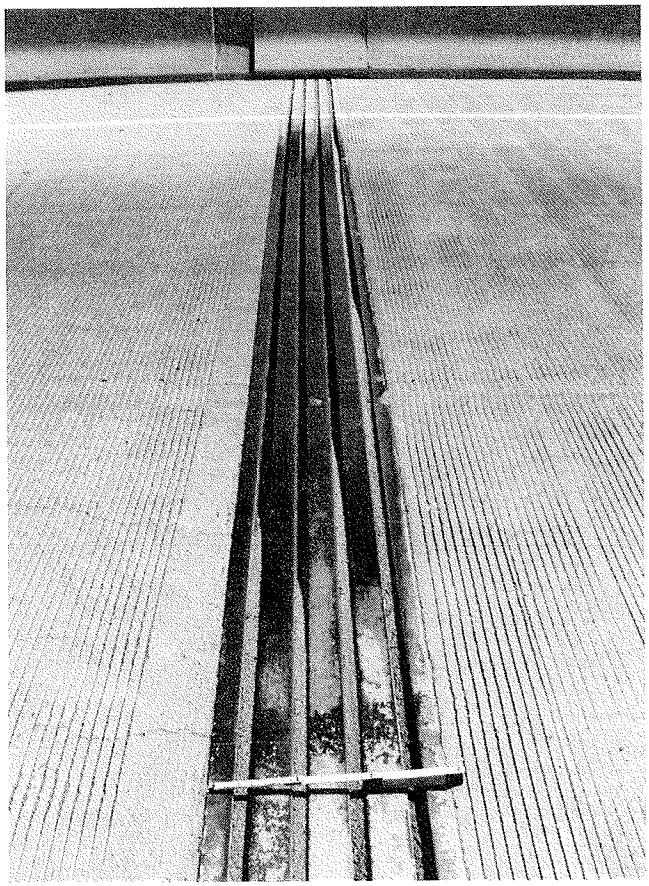

(b)

Figure 2.20. MBEJ tested on the I-70/I-25 flyover ramp structure: (a) joint with traffic control and test truck in position; (b) view looking east across joint.

gage attached to the pump was used to measure the applied load as shown in Figure 2.25. Load was increased monotonically and strains and displacements were recorded continuously by the data acquisition system.

Results of the vertical calibration tests in which the jack was placed between support boxes indicate that the centerbeams of all four MBEJs behave as multispan continuous beams (i.e., the support bars act as vertically rigid roller supports commonly assumed for continuous spans). Behavior of the support bars can be modeled as simply supported beams with an applied load (the reaction from the centerbeam) at the location of the connection to the centerbeam. Support-bar stresses calculated by this method were also in good agreement with the measured stresses resulting from vertical jacking loads.

Tests conducted with the jack placed directly over a support box indicate that the elastomeric bearings have a significant influence on the measured strains in the centerbeam. Figure 2.26 shows the measured vertical bending moments at points along a centerbeam in the Charter Oak Bridge MBEJ when the jacking load was placed directly over a support bar. If the supports were vertically rigid, the force would be transferred directly into the support and there would be no bending strains in the centerbeam. Obviously, any bending strains measured result from compression of the elastomeric springs. It can be shown that the deflection due to bending of the support bar is very small compared with the compression of the elastomeric springs.

In the structural analysis of the centerbeam for this case (jacking directly over a support bar), it is necessary to idealize the supports as springs. The vertical deflections measured during static jack calibration (as well as the static truck tests discussed later) were used to estimate vertical spring stiffness. The estimated values were in the range 9 to 90 kN/mm (50 to 500 kN/in.) for all MBEJs tested. Results from structural analyses to determine the vertical bending moment due to this jacking load with various spring stiffnesses are also shown in Figure 2.26. The figure shows that when a vertical spring with a stiffness of 87 kN/mm is used to represent the support bar and elastomeric bearings, the analysis compares favorably with the measured results for this MBEJ. This spring stiffness is reasonable but toward the upper bound compared with measured spring stiffnesses.

The horizontal calibration tests were conducted with a 1-ton duckbill-type hydraulic cylinder, which was placed between centerbeams at selected locations along the top of the joint as shown in Figure 2.27. A calibrated pressure gage mounted on the pump was used to measure applied loads.

In some of these tests the support bars or centerbeams (for single-support-bar systems) did not slip and the centerbeam developed negative bending moment at the support almost as large as the maximum positive bending moment. In other words, the centerbeam was behaving like a continuous beam supported on rigid supports much like the case of vertical bending. Presumably the resistance to sliding is from friction of the bearings and the stiffness of the equidistant springs.

In other tests, it was clear that the support bars or centerbeams slipped significantly and that several spans of the centerbeam were bending outward as if they were one large span. There was no negative bending moment at the supports in this case; rather there was a positive bending moment in the adjacent spans with a magnitude slightly less than the maximum positive moment at the location of the jack. Simi-

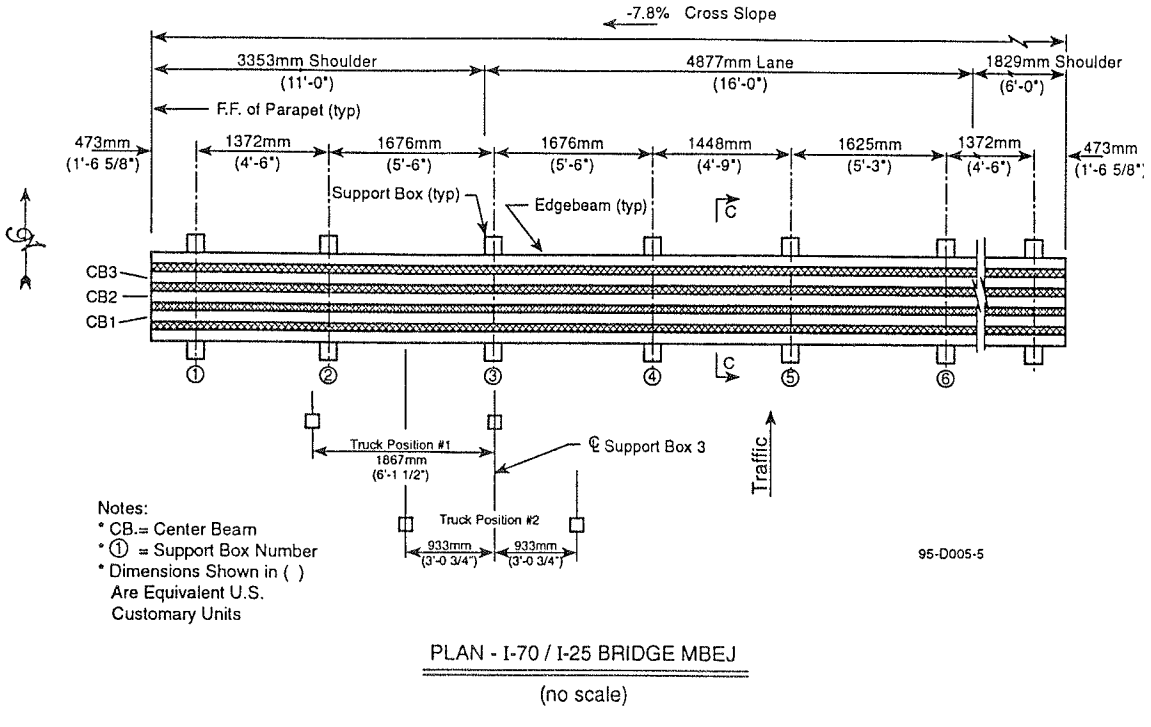

PLAN - I-70 / I-25 BRIDGE MBEJ

(no scale)

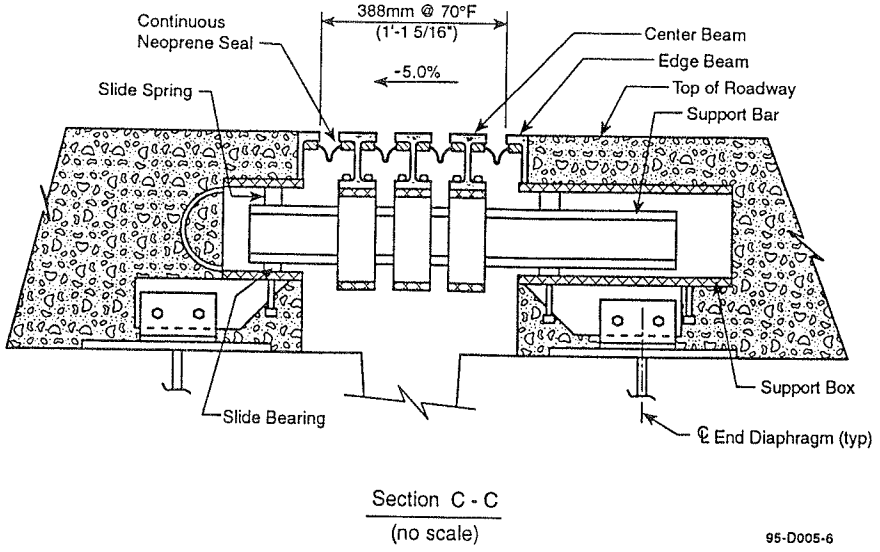

Section C - C

(no scale)

Figure 2.21. Plan and section of I-70/I-25 flyover ramp structure MBEJ.

lar stick-and-slip behavior was observed in the braking and accelerating dynamic tests.

Another type of horizontal jacking test was conducted with steel shims placed between the bottom flanges of the centerbeams at instrumented support box locations (or as close as physically permitted). A photograph of a joint with these shims installed is presented in Figure 2.28. When the joint was shimmed, it behaved as a continuous beam on rigid supports with respect to horizontal bending. These shims were also installed during selected dynamic tests to evaluate the effect of support-bar sliding stiffness on the horizontal MBEJ response.

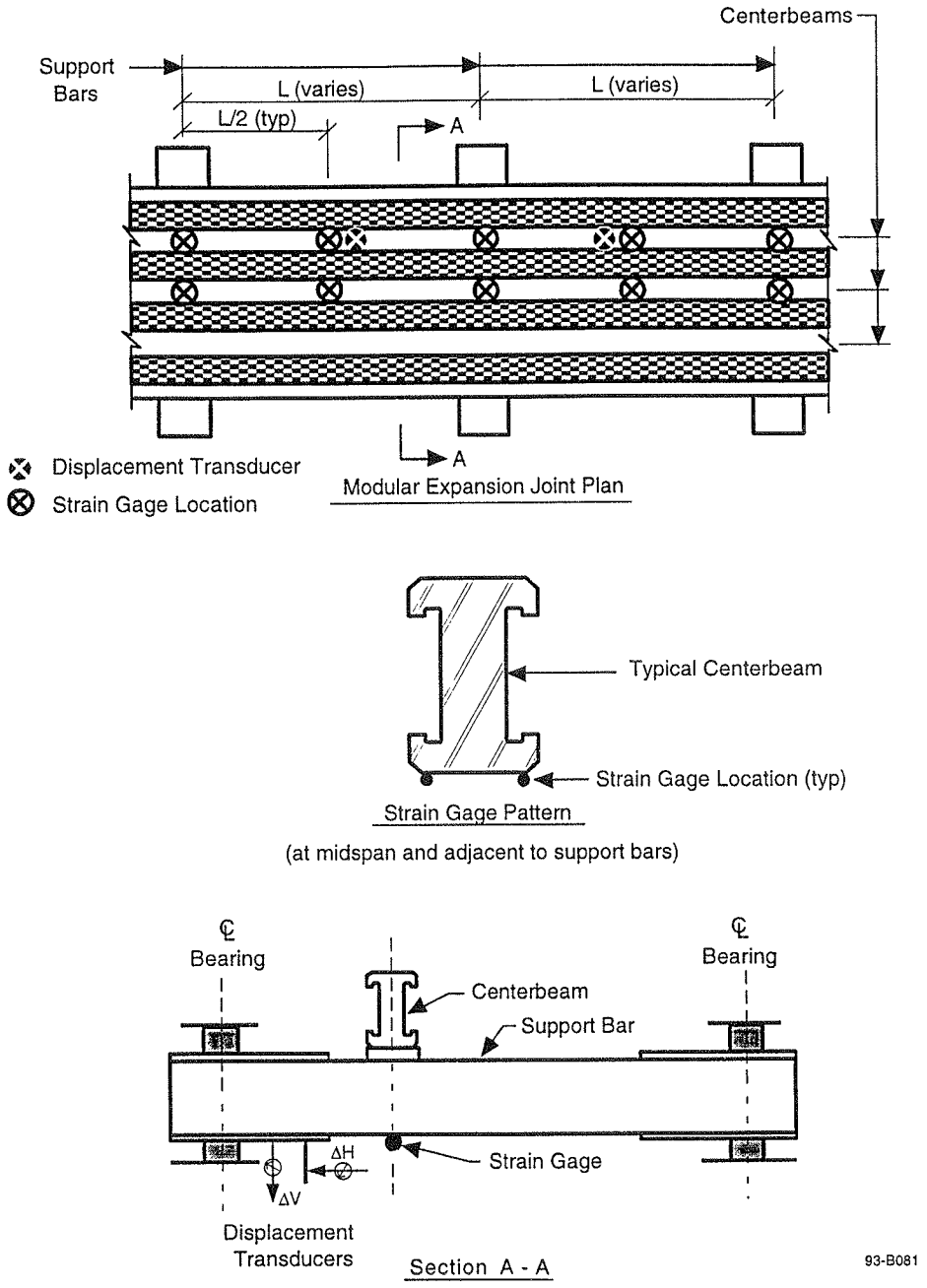

Figure 2.22. Typical instrumentation plan.

2.2.4.2 *Controlled Static Truck Tests*

Controlled static and dynamic tests were conducted by using a loaded test truck with axle loads near the legal load limit. A single-rear-axle dump truck was used at each site and a tandem-rear-axle dump truck was also provided for tests at both MBEJ locations in Washington. Individual axle weights for each truck are given in Table 2.2.

Note that all the single-axle trucks except the truck used for the I-70/I-25 flyover in Denver had an axle load of almost 100 kN. These loads are about as high as a single axle of the HS-30 tandem-rear-axles, which are the fatigue-limit-state-axle load based on AASHTO bridge specifications and the axle loads recommended for fatigue design of MBEJs in this report. Wheel spacing and individual tire footprint dimensions are given in Table 2.3.

Static tests were conducted by parking the truck on the joint and also by making several slow-speed [2 to 4 km/h (1 to 2 mph)] "crawl" runs over the joint with the test truck at various positions along the MBEJ. The test truck positions

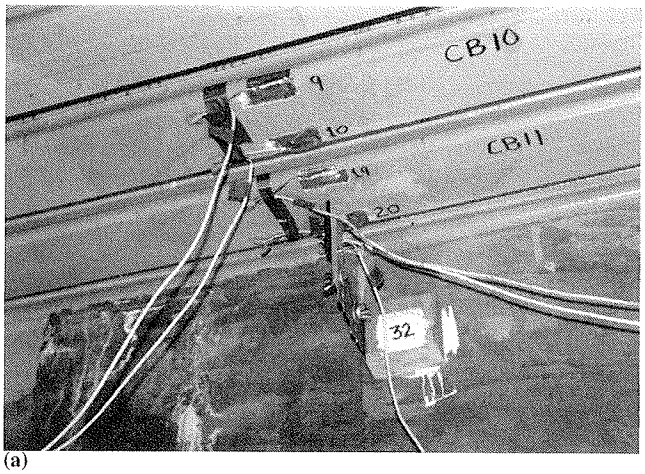

(a)

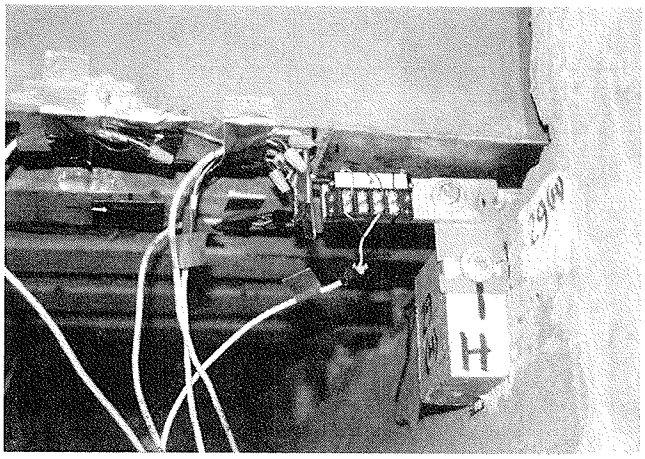

(b)

Figure 2.23. Typical installations of instrumentation: (a) strain gages and displacement transducer on the Lacey V. Murrow MBEJ; (b) horizontal displacement transducer on the support bar of the I-90/I-5 HOV MBEJ.

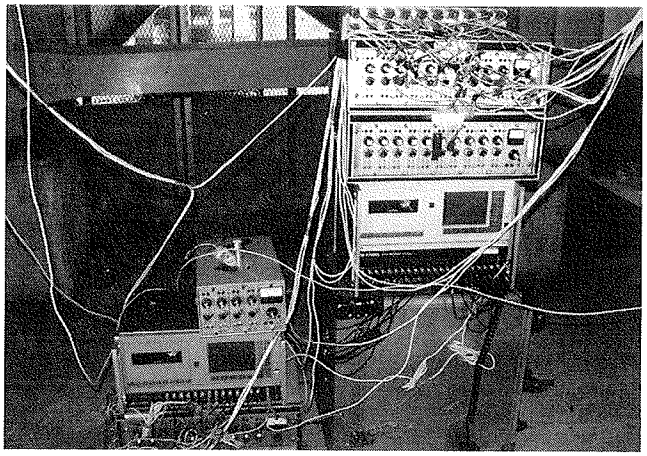

Figure 2.24. Data recording system.

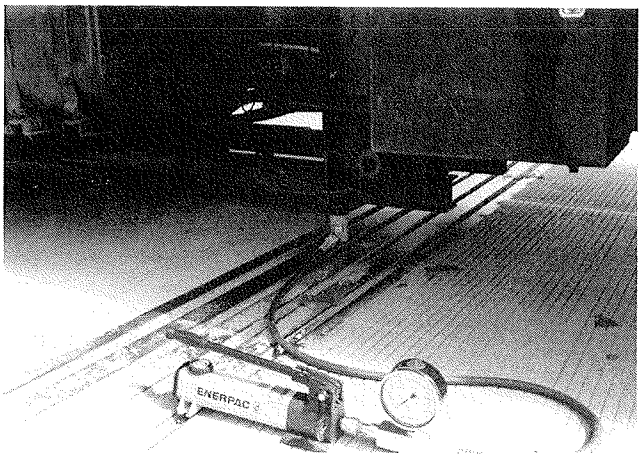

Figure 2.25. View of static vertical calibration test with a hydraulic jack.

along the joint included (1) one wheel at midspan of an instrumented centerbeam span to produce maximum bending moment in the centerbeam and (2) one wheel directly over an instrumented support bar to produce maximum bending moment in the support bar. Because the maximum support-bar spacing was between 1.5 and 1.8 m (5 to 6 ft) on most joints, quite often the wheel positions that produced maximum positive bending in the centerbeam also produced large (nearly maximum) negative bending moments.

These static truck tests provide a baseline for comparison with the dynamic tests to determine the effect of speed on dynamic amplification. Extensive comparison was made of the measured displacements and strains to structural analysis to ensure that the data were consistent and that a static response could be predicted from structural analysis.

The primary result of the static tests is determination of a ratio of apparent vertical load on a centerbeam to the total applied wheel load. In the literature, this ratio has been called a distribution factor. The distribution factor is used in design to determine the fraction of the design wheel load applied to the centerbeam under consideration. For example, a distribution factor of 0.4 indicates that a maximum of 40% of each wheel load is applied to any one particular centerbeam.

The apparent load on a centerbeam was found by performing structural analysis and comparing the measured bending moments with the calculated bending moments. The optimal apparent load magnitude was found (1) by calculating an average value from all the measurement locations for all applicable tests, and (2) by using a graphical trial-and-error procedure to obtain the best agreement with the measured data at all the measurement locations along a centerbeam. The results from both methods were in good agreement.

Wheel Patch Length. The AASHTO codes give various ways to calculate patch areas for the design of decks.

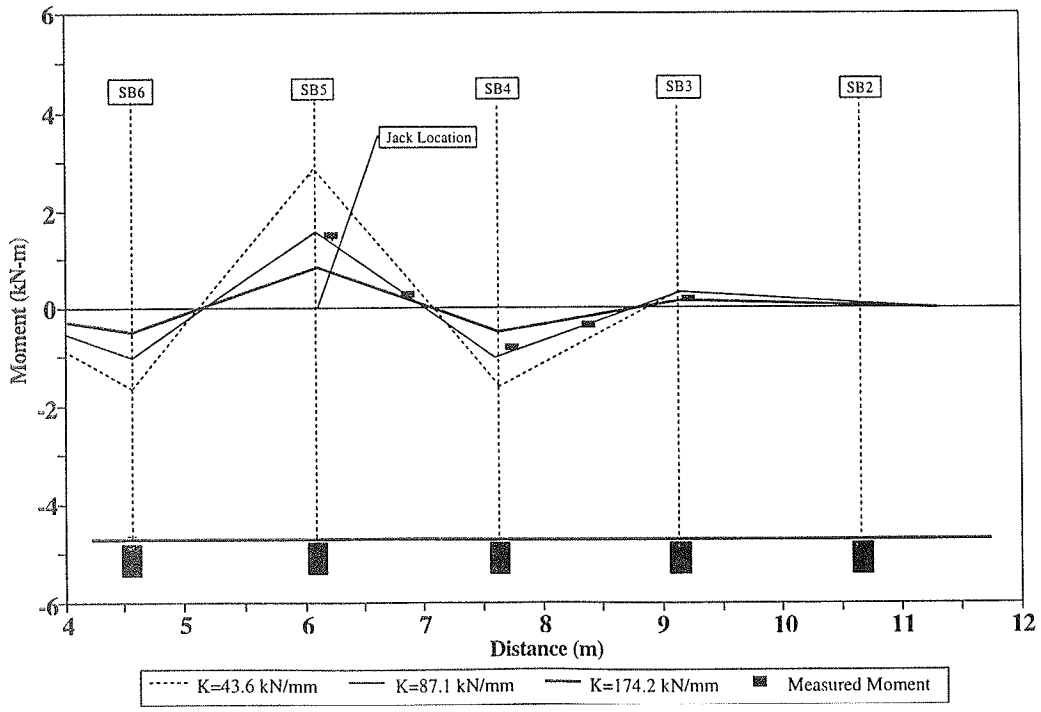

Figure 2.26. Moment diagram due to a static vertical calibration over a support box.

Wheel load patch lengths were determined by using both the 1994 LRFD AASHTO bridge specification and 1992 ASD/LFD AASHTO bridge specification. These code calculations were performed with the code-recommended axle loads. Table 2.4 provides a summary of MBEJ centerbeam and gap dimensions and also compares the measured tire patch lengths for the test trucks with tire patch lengths calculated by various methods. It is clear from the table that none of these calculations are consistent and none agree well with the measured patch length.

In the method outlined in the 1992 ASD/LFD AASHTO standard specification, the width of the patch varies as well as the length. (The change in width is not consistent with the observed behavior of tires, which have relatively rigid sidewalls and do not bulge laterally with increases in load.) Therefore, this method is not discussed further.

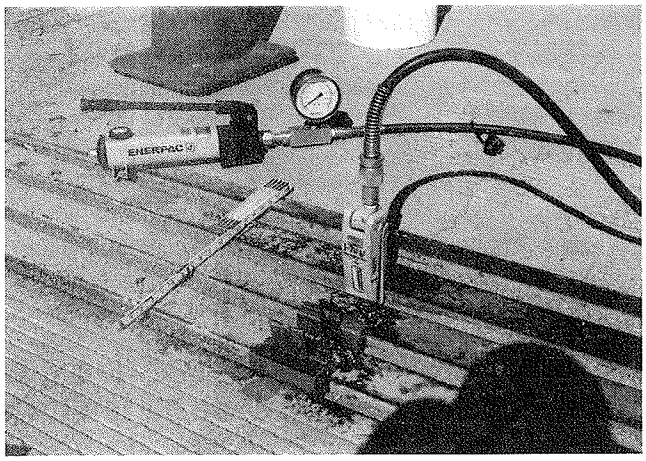

Figure 2.27. View of static horizontal calibration test with a hydraulic jack.

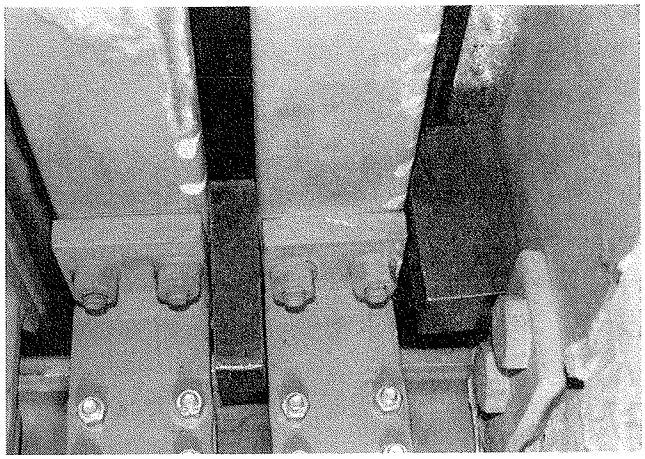

Figure 2.28. Installation of steel blocks to provide horizontal support.

TABLE 2.2 Test truck axle load data

MBEJ Location	Type of Rear Axle	Front Axle Load kN (kip)	First Rear Axle Load kN (kip)	Second Rear Axle Load kN (kip)
Charter Oak Bridge	Single	42.5 (9.6)	100.0 (22.7)	----
Lacey V. Murrow Bridge	Single	51.8 (11.7)	100.9 (22.8)	----
	Tandem	57.0 (13.0)	85.0 (19.2)	85.0 (19.2)
I-90/5 HOV Bridge	Single	51.6 (11.7)	96.7 (21.9)	----
	Tandem	64.6 (14.6)	84.0 (19.0)	84.0 (19.0)
I-70/I-25 Flyover Ramp	Single	45 (10.2)	78 (17.6)	----

A 56-kN (12.5-kip) wheel load is specified in the 1994 AASHTO LRFD (using the 220-kN [50-kip] tandem axle). The LRFD method to estimate wheel patch length is based on a constant width of 508 mm (20 in.) and a tire pressure of 860 kPa (125 lbf/in.^{2}). An impact factor of 75% is specified for deck components, a load factor of 1.75 is used for strength design, and a load factor of 0.75 is used for fatigue design. Although it appears more logical to calculate a patch size based on actual service loads, according to the LRFD code these factors are supposed to be included in the patch size calculation. Calculations using both load factors are shown in the table. The measured results are bounded by the

TABLE 2.3 Test truck geometry

MBEJ Location	Type of rear axle	L1 mm (in.)	L2 mm (in.)	Sf mm (in.)	Sr mm (in.)	A mm (in.)	B mm (in.)	C mm (in.)	D mm (in.)	E mm (in.)
Charter Oak Bridge	Single	4164 (164)	----	2019 (79.5)	1848 (72.75)	216 (8.5)	222 (8.75)	248 (9.75)	546 (21.5)	203 (8)
Lacey V. Murrow Bridge	Single	4470 (176)	----	2083 (82)	1829 (72)	203 (8)	267 (10.5)	260 (10.25)	546 (21.5)	203 (8)
	Tandem	4572 (180)	1346 (53)	2057 (81)	1829 (72)	216 (8.5)	267 (10)	241 (9.5)	559 (22)	216 (8.5)
I-90/5 HOV Bridge	Single	4470 (176)	----	2083 (82)	1829 (72)	203 (8)	267 (10.5)	260 (10.25)	546 (21.5)	203 (8)
	Tandem	4572 (180)	1346 (53)	2057 (81)	1829 (72)	216 (8.5)	267 (10.5)	241 (9.5)	559 (22)	216 (8.5)
I-70/I-25 Flyover Ramp	Single	3835 (151)	----	2032 (80)	1867 (73.5)	229 (9)	229 (9)	267 (10.5)	533 (21)	203 (8)

TABLE 2.4 Comparison of measured and calculated rear wheel patch lengths for single-axle dump trucks

MBEJ Location	Centerbeam Width "B" mm (in.)	Gap Width "G" mm (in.)	Measured Tire Contact Width[2] "W" mm (in.)	Measured Tire Pressure kPa (psi)	Measured Patch Length "L" mm (in.)	AASHTO ASD/LFD "L"[3] mm (in.)	AASHTO LRFD (Strength)[4] "L" mm (in.)	AASHTO LRFD (Fatigue)[4] "L" mm (in.)
Charter Oak Bridge	57 (2.2)	51.1 (2.0)	406 (16)	703 (102)	248 (9.8)	203 (8)	389 (15)	167 (6.6)
Lacey V. Murrow Bridge	114 (4.5)	38.3 (1.5)	406 (16)	772 (112)	260 (10.3)	203 (8)	389 (15)	167 (6.6)
I-90/5 HOV Bridge	64 (2.5)	35 (1.4)	406 (16)	772 (112)	260 (10.3)	203 (8)	389 (15)	167 (6.6)
I-70/I-25 Flyover Ramp	80 (3.1)	32 (1.3)	406 (16)	724[1] (105)	267 (10.5)	203 (8)	389 (15)	167 (6.6)

Notes: 1. Tire pressure not measured at this location - value shown is estimated.
2. Dimension is 2 times "E" value shown in Table 2.3.
3. Values shown are based on a 142 kN (32 kip) single axle.
4. Values shown are based on a 220 kN (50 kip) tandem axle.

AASHTO LRFD results by using either strength or fatigue load factors.

Centerbeam Distribution Factors. As previously defined, the distribution factor is the ratio of apparent vertical load on a centerbeam to the total applied wheel load. The distribution factor is used in design to determine the fraction of the design wheel load applied to the centerbeam under consideration. Table 2.5 compares the measured static distribution factor with distribution factors calculated by various methods described below. The measured distribution factors were found by performing structural analysis and obtaining the best agreement with the measured data at all the measurement locations.

Many of the methods are based on the idea that the load is uniformly distributed over a patch length and that if there are gaps each centerbeam picks up load from a tributary area. The tributary area method is analogous to the method used to distribute uniform loads on a concrete deck slab to individual beams. In several publications, variations on this tribu-

TABLE 2.5 Summary of measured and calculated distribution factors (rear-axle loads of single-axle trucks)

MBEJ Location	Measured Static	Tschemmernegg Method	1994 AASHTO LRFD[1]	FDL Method Using Measured "L"
Charter Oak Bridge	0.37	0.49	0.5	0.54
Lacey V. Murrow Bridge	0.69	0.62	0.82	0.65
I-90/5 HOV Bridge	0.34	0.37	0.5	0.45
I-70/I-25 Flyover Ramp	0.51	0.48	0.41	0.48

Notes:
1. Values Shown are Based on a 220 kN (50 kip) Tandem Axle with Fatigue Load Factors

tary area method are referred to as the FDL method (it is not known what FDL stands for). These methods require the assumption that the distributed load that is actually over gaps between the bars finds a way to get into the adjacent centerbeams. Presumably, the tire wall acts like a bridge over the gaps. One possible FDL scheme is to apply the load from one-half the gap on either side to the centerbeam. The distribution factor in this case is $(B + G)/L$, where B is the centerbeam width, G is the gap width, and L is the length of the wheel patch. In several publications (*16,41*), a more conservative version of the FDL method has been used that is based on the situation where the tire patch extends out over one gap but does not touch the neighboring bar. In this situation, the entire gap on one side is applied to the centerbeam and the distribution factor is therefore $(B + 1.5G)/L$. Table 2.5 shows the FDL method with the measured patch lengths, which gave reasonable results.

The AASHTO LRFD code also has a method of calculating the distribution of tire pressure on interrupted surfaces. This method is presented elsewhere (*16*) as the PDL method (it is not known what PDL stands for). As explained in the AASHTO LRFD code, the actual contact area on the centerbeam is used with the pressure increased in proportion to the ratio of the specified contact area (or total patch area) to actual contact area. In other words, the total load is distributed uniformly to the reduced contact area. In terms of a distribution factor, the PDL method reduces to the centerbeam width B divided by the sum of the lengths in the actual contact area.

Table 2.5 also shows the results of the PDL method as implemented in the 1994 AASHTO LRFD code, using the 220-kN (50-kip) and 56-kN (12.5-kip) wheel load for the tandem axles. Results with the fatigue load factor give the best agreement with the measured static distribution factors, although the results for the I-70/I-25 flyover ramp are about 20% nonconservative. When the strength load factor was used in these calculations, the result was much smaller and hence more nonconservative for this case.

The method presented in graphical form by Tschemmernegg (Figure 2.29) gives distribution factor as a function of centerbeam width and gap between centerbeams. This method is a variation on the PDL method and appears to be based on a tire with a minimum 235-mm (9.25-in.) patch length that is adjusted as a function of centerbeam gap width. A length equal to 30% of all the gaps covered by the patch is added to the 235 mm (9.25 in.)—i.e., $L = 235$ mm $+ 0.3SG$. This implies that the patch length increases when the tire is over an interrupted surface but not as large an increase as would have to occur if the pressure were to remain constant. The wheel appears to be placed so that the patch extends out over one gap but does not touch the neighboring bar. Then the distribution factor can be found by the ratio of the centerbeam width B to the sum of the lengths in the actual contact area, as in the PDL method. As shown in Table 2.5, this method compares reasonably with the results measured in the field.

Wheel patch lengths and distribution factors based on the field test data were discussed in detail in the interim report (*20*). Subsequently, laboratory tests have been performed that also provided data on patch lengths and distribution factors. Therefore, further discussion of these topics is deferred to Section 2.3.

Moment diagrams generated from structural analysis assuming rigid supports are in very good agreement with the

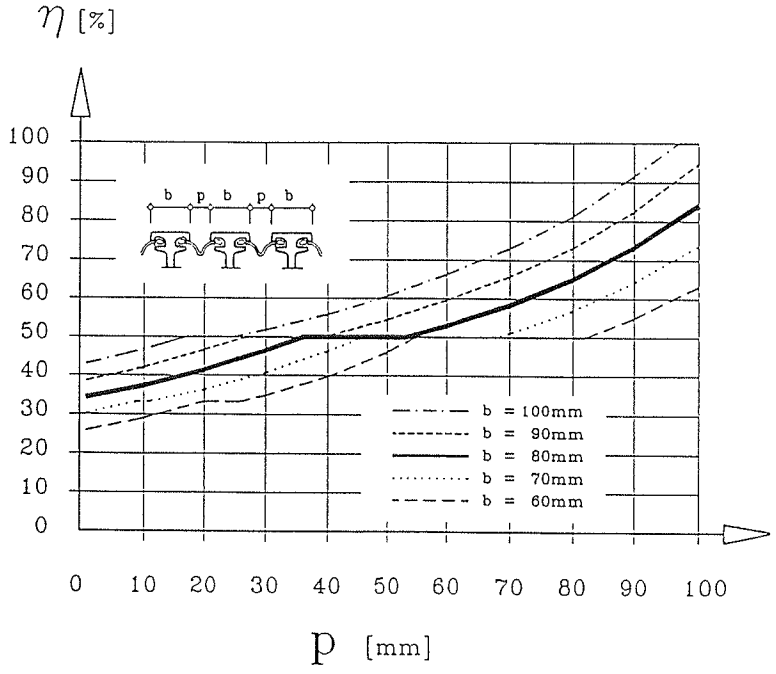

Figure 2.29. Graph of distribution factors recommended by Tschemmernegg.

measured data when the truck is centered over a support box. For tests in which the truck is centered over a support box (i.e., the wheels are near the middle of the centerbeam spans), the effect of the elastic bearings is rather small and the system can be analyzed with rigid supports. Static truck tests in which one wheel of the truck is positioned over a support bar indicate that system behavior is similar to that observed while jacking over a support bar. As discussed above, effects of elastomeric springs on the moment diagram are more pronounced for cases in which the load is directly over a support bar. However, the stress in the centerbeam is always highest when the wheel is near the middle of the span. Therefore, the continuous beam model, which is commonly assumed, is adequate for design.

2.2.4.3 Controlled Dynamic Truck Tests and Dynamic Amplification

Controlled dynamic tests were conducted with the same trucks as described for the static tests in Tables 2.2 and 2.3. Controlled dynamic tests were performed with the trucks in the same positions as in the static tests: (1) one wheel at midspan of an instrumented centerbeam with the other wheel nearly in the middle of the adjacent span to produce maximum bending moment in the centerbeam; and (2) one wheel directly over an instrumented support bar (with the other wheel close to the adjacent support bar) to produce maximum bending moment in the support bar. Trucks traversed the joint at steady speeds from 16 to 96 km/h (10 to 60 mph).

The purpose of these tests is to determine the relationship between vehicle speed and dynamic response in terms of strain and displacement. Because design of bridges and bridge components is typically performed by static analysis, it is convenient to express the dynamic response in terms of an amplification relative to the static loading. A static load is multiplied by a dynamic load amplification factor (impact factor) to obtain an equivalent static load. When the bridge component is analyzed statically by using the equivalent static load, the result is presumed to be equivalent to the actual dynamic response. The amplification factor must account for dynamic effects of the vehicle, bridge superstructure, and the MBEJ. The vehicle dynamics are affected by the approach roadway.

This equivalent-static-force approach requires that the distribution and relative magnitude of the actual dynamic deflections and bending moments are proportional to the static deflections and bending moments. The field measurements presented below indicate that this requirement is approximately satisfied. However, in the case of MBEJs, the magnitude of the load affects the wheel load patch length and its distribution. Therefore, for MBEJs, the amplification factor (or any other load factor) must be applied to the centerbeam load (i.e., after distribution) or the computed static response and not to the wheel load directly.

Both strain and displacement measurements were analyzed for each MBEJ site and in general were in good agreement with analytical predictions. However, the strain-gage data appeared to be more repeatable and sensitive to the effects of dynamic truck loads. Therefore, the following discussion is focused on the strain measurements.

Vertical Moment. Figures 2.30 to 2.33 show typical time histories for the four MBEJs with the single-rear-axle test trucks run at the highest steady speed possible. The time histories show vertical and horizontal bending moment at midspan of a selected centerbeam. These bending moments were derived from a pair of strain gages at midspan where the vertical bending moment was calculated from the average of the two strain gages and the horizontal bending moment was calculated from the difference between the two strain gages. It can be seen that the response to the front axle is typically 70% to 80% of the response to the rear axle. This ratio of the response is consistent with the ratio of front-to-rear apparent static centerbeam loads (Table 2.6), which range from 55% to 86%. The ratios of apparent static centerbeam loads for the front and rear axles are greater than the corresponding ratios for the total axle loads, which range from 42% to 58%. The centerbeam loads are closer because of a higher distribution factor for the front axle. This is a good illustration of the phenomenon discussed in Section 2.1.4; the response of the centerbeam does not increase nearly as much as the increase in total axle load.

Figures 2.30 to 2.33 show a range of behavior. For example, the MBEJ on the Charter Oak Bridge (Figure 2.30) clearly has the most dynamic amplification and the most rebound. Figure 2.34 shows a bending moment diagram of a centerbeam for the truck in this position on the MBEJ. To take this source of uncertainty out of the comparisons, the diagram is calculated for the static case with the measured distribution factor.

Note the very good fit to the crawl run measured bending moments at all measurement locations as illustrated in Figure 2.34. This agreement reinforces the conclusion that the data are very consistent and that the continuous beam model on rigid supports is adequate for design. The measured dynamic bending moments are also shown on Figure 2.34. It was also observed that in the positive bending moment regions, the measured bending moment increases significantly with speed. This increase can be seen by comparing the maximum response, shown in Figure 2.30, with the response at 48 km/h, which is shown in Figure 2.35.

There does not appear to be as much of an increase in the negative bending moment response near the supports. This phenomenon was observed in every MBEJ—i.e., if there was significant amplification, it occurred primarily at the midspan locations. Subsequent discussion focuses on the midspan bending moment, because it is the largest response and apparently the most sensitive to dynamic effects. Because there is amplification at the midspan locations, the proposed

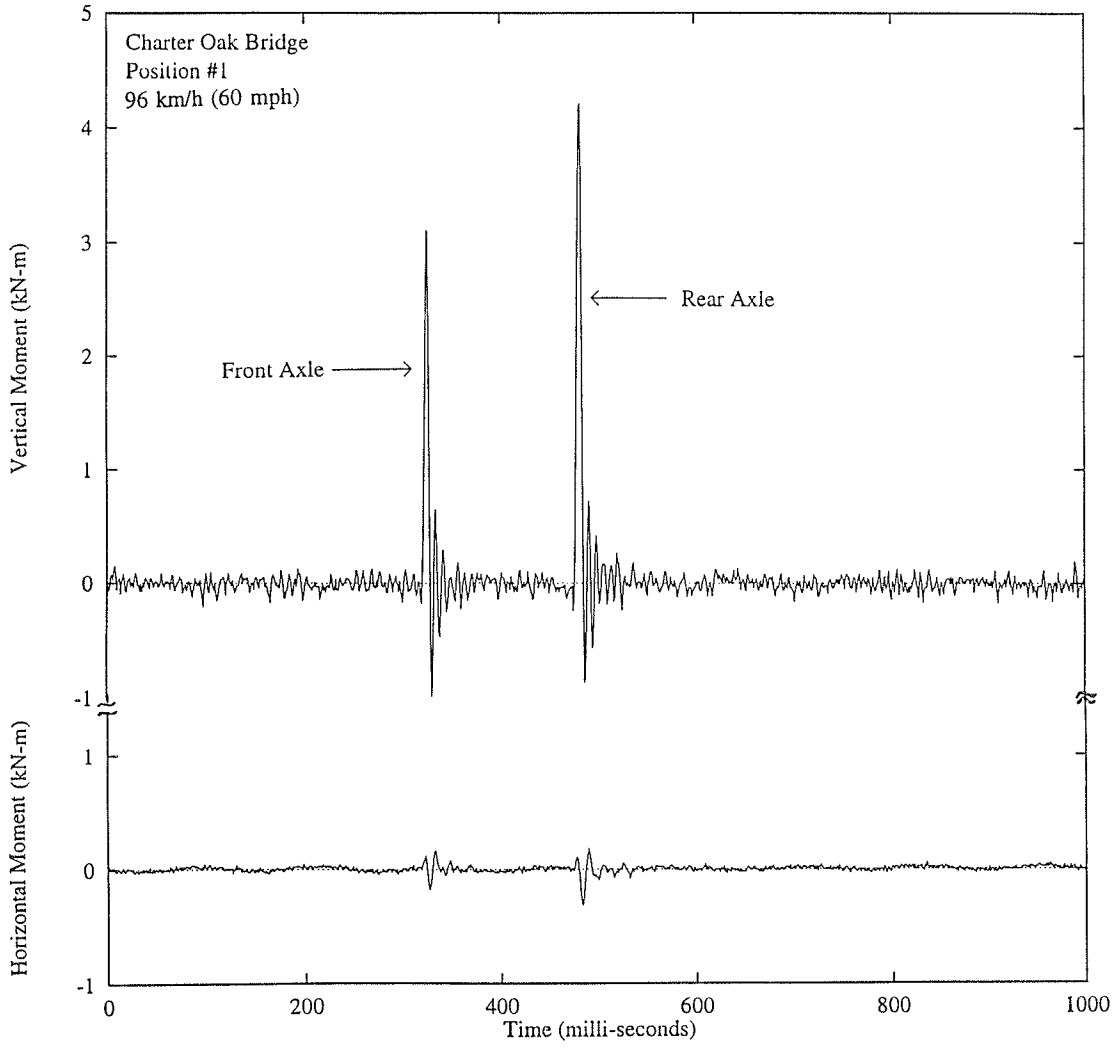

Figure 2.30. Dynamic time history for the Charter Oak Bridge MBEJ (single-axle truck at 96 km/h).

design specification uses the worst-case amplification and applies this in an equivalent static load analysis. Note that this tends to overstate the stress range at the negative moment regions, which is the location of the fatigue-sensitive details.

Table 2.7 shows estimated frequencies and damping ratios for the MBEJs tested. These estimates were made directly from the time histories and should be considered an approximation, especially with regard to estimated damping. The Charter Oak Bridge has an apparent resonant frequency of about 130 Hz in the vertical direction and 60 Hz in the horizontal direction and an apparent damping of about 7% of critical damping in both directions.

The measured frequencies and damping compare very well with values reported by Tschemmernegg (*15*) for a welded multiple-support-bar MBEJ—i.e., 132 Hz vertically with 7.2% damping and 54 Hz horizontally with 14% damping. Table 2.7 also shows the resonant frequency, which was estimated by using a graph from Tschemmernegg (*43*) that shows the frequency as a function of span length for several types of expansion joints, including welded multiple-support-bar systems and swivel-type single-support-bar systems. The graphs do not provide frequency data for bolted single-support-bar systems and therefore no estimate was made for the I-70/I-25 flyover ramp MBEJ. In general, the estimates from these graphs are well within the confidence bands for the observed frequencies.

Table 2.7 also shows the period of the loading impulse, which was estimated by using a formula attributed by Roeder (*17*) to Tschemmernegg that is two bar spacings divided by the vehicle speed. The formula assumes a tire patch length that covers three centerbeams simultaneously. Although this formula appears arbitrary, it gives good agreement with the loading period measured from the time histories. The calculated impulse periods were generally within 20% of the measured values shown in Table 2.7 except for the I-90/I-5 HOV bridge MBEJ. As discussed in Section 2.1.4, an approach by

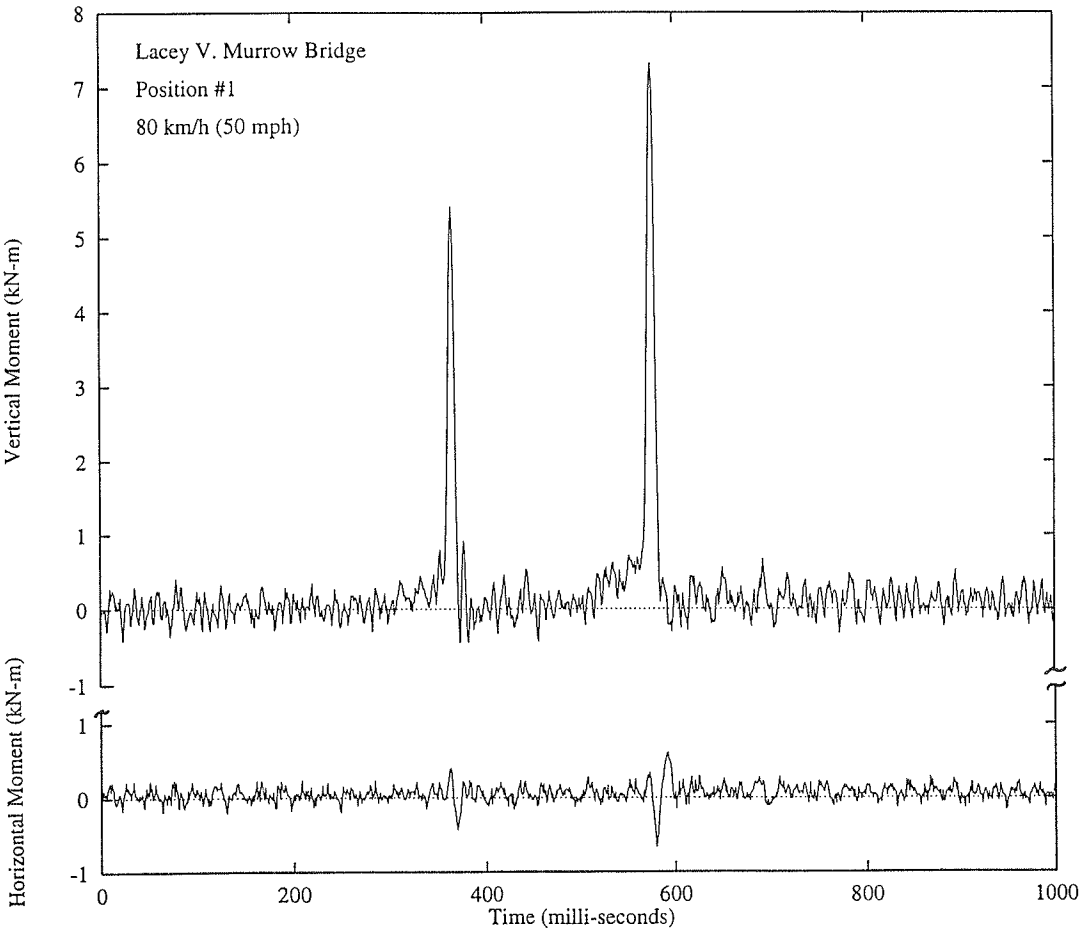

Figure 2.31. Dynamic time history for the Lacey V. Murrow Bridge MBEJ (single-axle truck at 80 km/h).

Ostermann (*39*) to calculating the impact time did not compare as well.

As discussed in Section 2.1.4, the dynamic amplification factor (ratio of peak dynamic moment to static moment) for a generic undamped elastic system subjected to an impulse load peaks at about 1.5 as the ratio of the impulse period to resonant period approaches 1. In the last column of Table 2.7, this predicted dynamic amplification factor is presented along with the maximum value from examination of the time histories.

The maximum dynamic amplification factor from the time histories is defined as the peak dynamic bending moment (in the positive moment region) divided by the static bending moment. The static bending moment is determined from a continuous beam model by using the apparent static center-beam loads in Table 2.6.

Because the loading period was within 3% of the resonant period for the Charter Oak Bridge, the maximum dynamic amplification factor of 1.5 is predicted. The measured peak response from the time histories was 4.2 kN-m, which is about 1.3 times the static bending moment at this location. Therefore, the response was significantly amplified but not as much as predicted.

The dynamic amplification with the vehicle at 96 km/h (60 mph) is in contrast to the lack of amplification on this same MBEJ when the vehicle was traveling at one-half the speed, as shown in Figure 2.31. The lack of amplification at one-half the speed is expected, considering that the loading period is twice as large as the resonant period in this case. These results show that vehicle speed is a very important factor in the dynamic response.

As shown in Table 2.7, the maximum vehicle speed was lower in the other MBEJ field tests. This was due to a variety of factors noted in Table 2.1, such as significant uphill grade or tight horizontal curve. Therefore, the loading period at the maximum test speed was longer than the resonant period; accordingly, the dynamic response was lower.

The loading period for the I-70/I-25 flyover ramp and the I-90/I-5 HOV bridge was still within 15% of the vertical resonant period. Theoretically, these MBEJs should still have

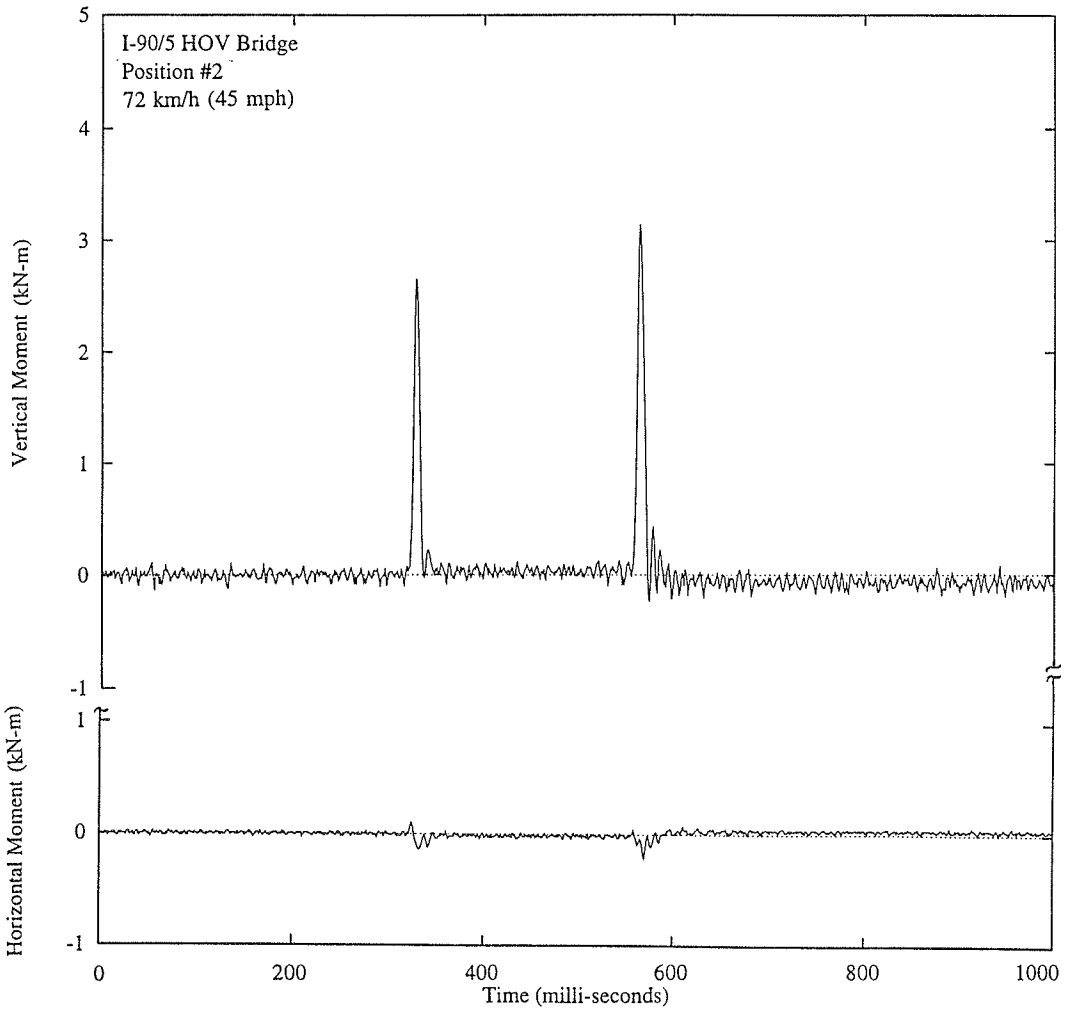

Figure 2.32. Dynamic time history for the I-90/I-5 HOV bridge MBEJ (single-axle truck at 72 km/h).

exhibited a dynamic amplification factor of about 1.4. However, the experimental data for these bridges do not show large amplifications. The measured resonant frequency for the I-90/I-5 HOV bridge may be too small. The frequency estimated from Tschemmernegg's frequency graphs is 33% higher. This could explain the apparent lack of amplification in this bridge. However, in general, the measured response appears to be about 20% lower than the theoretical response. This reduction is probably due to the effect of damping, which is not included in the theoretical predictions.

The strategy put forth by Tschemmernegg (*10*) for avoiding excessive vertical amplification was discussed in Section 2.1.4. The strategy is to keep the frequency higher—i.e., keep the ratio of the impulse period to the resonant period larger than 1.0. Tschemmernegg has stated that this objective can be achieved for welded multiple-support-bar systems by keeping the centerbeam span between support bars less than 1220 mm (48 in.). It is clear from his graphs of the resonant frequencies for MBEJs that for spans smaller than 1220 mm the vertical frequency will be larger than 140 Hz or the period will be shorter than 7 msec. This lower-bound loading period of 7 msec is consistent with all the measured loading periods, the closest of which is the Charter Oak Bridge where the test truck was traveling near the speed limit and had a loading impulse period of approximately 8 msec (125 Hz).

As discussed in Section 2.1.4, the occasional speeding truck may cause loading impulse periods of 7 msec or less. Tschemmernegg's suggestion to keep the centerbeam span between support bars less than 1220 mm (48 in.) is probably not sufficient to avoid amplification entirely. Therefore, the specifications should anticipate the worst-case vertical dynamic amplification, regardless of the span.

Numerous time histories were examined for each test (truck speed and location) and the peak values of centerbeam midspan bending moment from among any of the instrumented spans was recorded. A summary of the apparent peak moments is presented in tables in the interim report (*20*). These peak moments are the worst-case responses from a

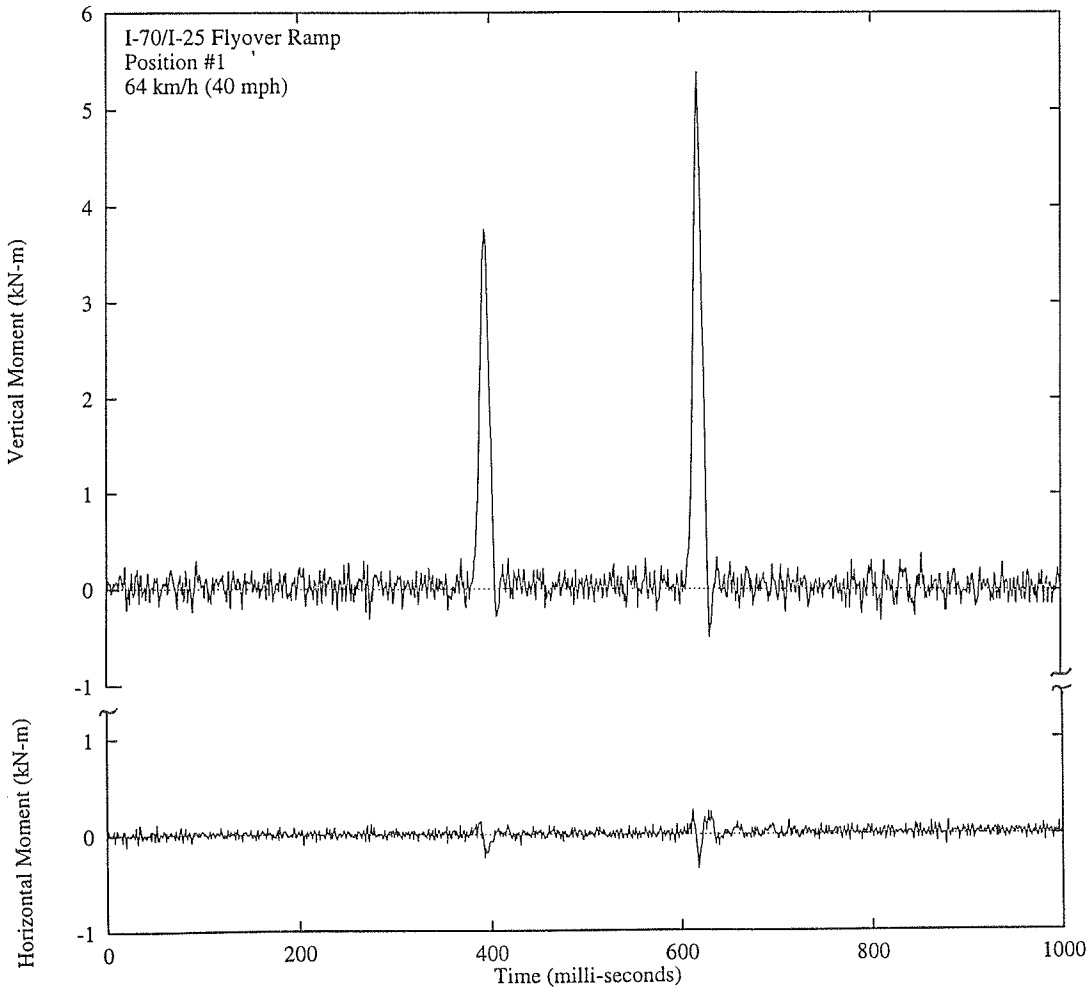

Figure 2.33. Dynamic time history for the I-70/I-25 flyover ramp structure MBEJ (single-axle truck at 64 km/h).

TABLE 2.6 Measured static centerbeam (CB) loads

MBEJ Location	Type of Rear Axle	Front Wheel CB Load kN (kip)	First Rear Wheel CB Load kN (kip)	Second Rear Wheel CB Load kN (kip)
Charter Oak Bridge	Single	10.2 (2.3)	18.7 (4.2)	----------
Lacey V. Murrow Bridge	Single	21.8 (4.9)	35.1 (7.9)	----------
	Tandem	22.3 (5.0)	32.5 (7.3)	32.5 (7.3)
I-90/5 HOV Bridge	Single	14.2 (3.2)	16.5 (3.7)	----------
	Tandem	12.6 (2.9)	18.7 (4.2)	18.7 (4.2)
I-70/I-25 Flyover Ramp	Single	16.5 (3.7)	20.0 (4.5)	----------

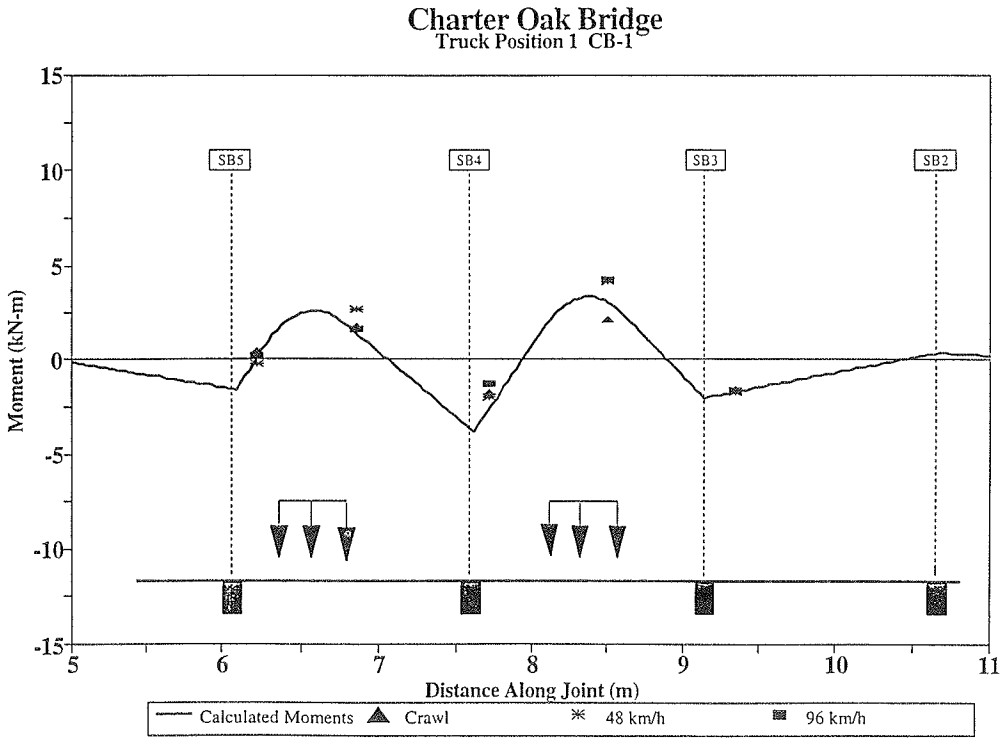

Figure 2.34. Moment diagram of Charter Oak Bridge MBEJ (dynamic truck loads).

number of different centerbeam spans. The peak moments were divided by the static bending moments (based on the loads in Table 2.6) and the results are expressed as a percentage.

The peak dynamic amplification factor for any test was 1.32 for the Charter Oak Bridge. The maximum uplift was 31% of the static load, so a total load range of 1.63 times the static value is derived from these tests. (Another way to characterize the uplift would be as 23% of the amplified downward part of the vertical load or 19% of the total amplified vertical load range.)

These test results from the Charter Oak Bridge MBEJ represent a worst case for vertical dynamic amplification. The total dynamic amplification of 1.63 is in reasonable agreement with the total dynamic amplification of 1.82 measured by Tschemmernegg, as explained in Section 2.2.1. The current 1994 AASHTO LRFD impact factor of 1.75 appears to be a reasonable worst case.

The tight horizontal curve of the I-70/I-25 flyover ramp [150-m (490-ft) radius, 8% superelevation] caused increased vertical moments at midspan of the centerbeam under the wheel closest to the outside of the curve. As shown in Table 2.8, the moment in the outer span increased by 40% as speed increased to 64 km/h (40 mph). The response at this higher speed is shown in Figure 2.33. The increased vertical moments could be due to lateral traction forces (resisting centrifugal force) or there could be a larger downward force resisting a lateral overturning moment of the vehicle. The fact that such a large dynamic amplification could not be due to conventional resonant amplification alone is supported by the appearance of the time history shown in Figure 2.33, which shows little ringing and little rebound. It is presumed that about one-half of the apparent 40% moment increase in the outside span is due to conventional dynamic amplification—i.e., about 20%—and a similar amplification is due to centrifugal force. This explanation is consistent with the elastic rebound, which at 14% is almost one-half that observed in the Charter Oak Bridge MBEJ.

A factor to increase the apparent load for cases where there is a tight horizontal curve was considered. However, the maximum speed is limited at these locations, and therefore the dynamic amplification is typically much lower than the worst case that will be applied in the proposed specification. The lower dynamic amplification is apparent in the data from the MBEJ in the I-70/I-25 flyover ramp. The decreased dynamic amplification approximately offsets the increased vertical load because of the horizontal curve. Therefore, in the interest of keeping the specification simple, the effect of horizontal curvature can safely be ignored.

Horizontal Moment. Horizontal bending is critically important because the section modulus for bending in the horizontal direction is quite often about one-fifth the section modulus in the vertical direction. Therefore, a horizontal bending moment range equal to 20% of the vertical bending moment range corresponds to a horizontal bending stress

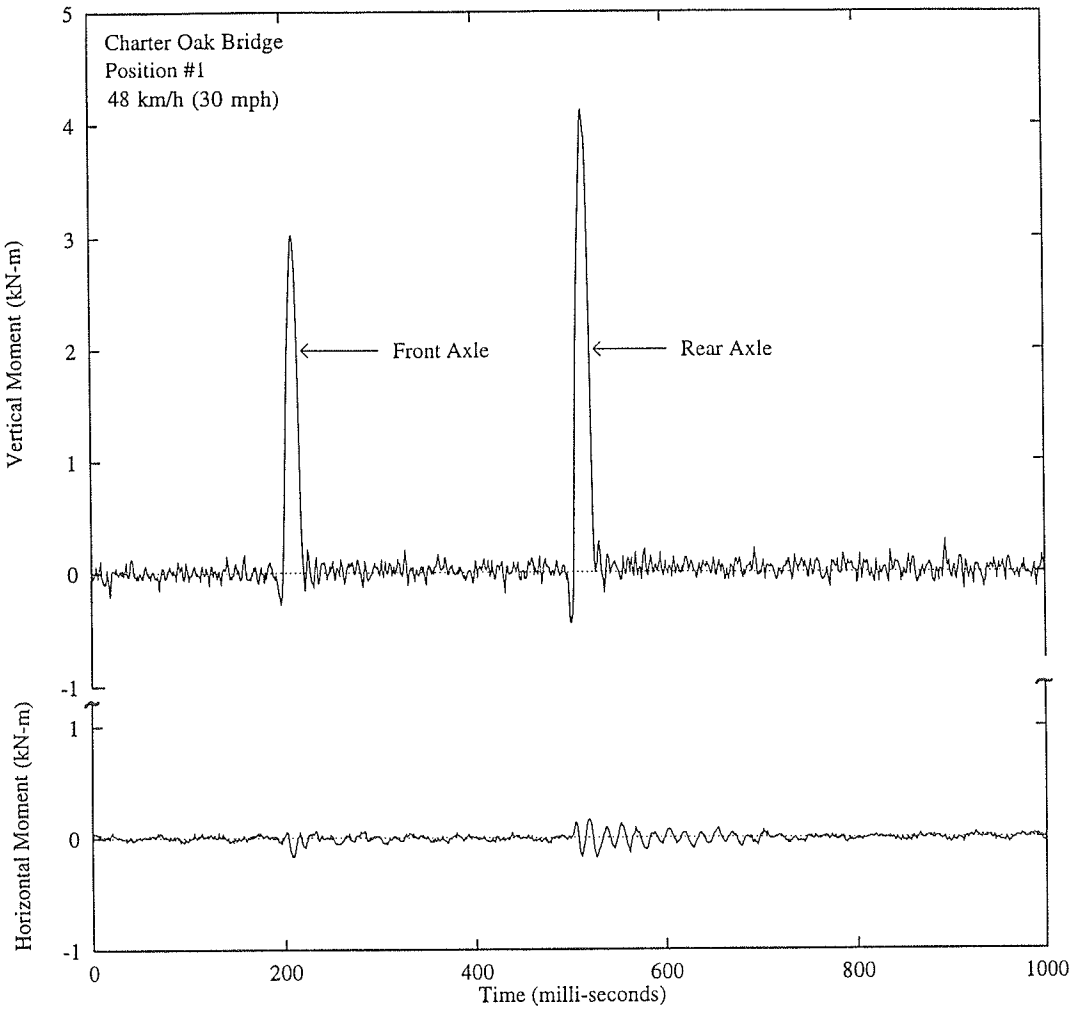

Figure 2.35. Dynamic time history for Charter Oak Bridge MBEJ (single-axle truck at 48 km/h).

TABLE 2.7 Dynamic response data for instrumented MBEJs

MBEJ Location and Test Truck Speed (km/h)	Vertical			Horizontal			Loading Period (millisec)	Ratio of Loading Period to Vertical Resonant Period	Observed (Theoretical) Dynamic Amplification Factor
	f (Hz) and T(millisec) Observed	f (Hz) from Graph	% Damping	f (Hz) and T(millisec) Observed	f (Hz) from Graph	% Damping			
Charter Oak Bridge (96)	130 (7.7)	140	7	60 (16.7)	50	7	7.9	1.03	1.3 (1.5)
Lacey V. Murrow (80)	118 (8.5)	90	8	30 (33.3)	70	7	14.9	1.75	1.1 (1.1)
I-90/5 HOV Bridge (72)	120 (8.3)	160	7	60 (16.7)	55	10	9.5	1.14	1.1 (1.4)
I-70/I-25 Flyover Ramp (64)	91 (11.0)	-----	7	50 (20.0)	-----	15	12.4	1.13	1.2 (1.4)

TABLE 2.8 Effect of horizontal curve on vertical moments

Effect of Horizontal Curve		
Test Speed	Moment Ratio (Inner Span)	Moment Ratio (Outer Span)
16 km/h	1.06	1.04
32 km/h	1.02	1.19
48 km/h	0.96	1.25
64 km/h	0.83	1.45

Notes: 1. Moment ratio is defined as the ratio of the dynamic run moment to the crawl (2 km/h) run moment.
2. Inner span moments were measured between support boxes 2 and 3 on centerbeam 3.
3. Outer span moments were measured between support boxes 3 and 4 on centerbeam 3.

range as large as the vertical bending stress range. These stress ranges are then summed to obtain the maximum nominal biaxial bending stress range, which is then used to check the fatigue strength.

The horizontal bending moment response is a completely different mode than the vertical response. The typical horizontal response is relatively small at steady speeds; in every case except one the horizontal moment was less than $\pm 7\%$ of the amplified vertical bending moment—i.e., the total horizontal load range was less than 14% of the amplified vertical bending moment range.

The exception was the response from a dual-axle truck crossing the I-90/I-5 HOV bridge MBEJ at 64 km/h (40 mph). The time history for this test is shown in Figure 2.36. In this test, the horizontal bending was forward 13% and backward 9% for a total range of 22% of the total amplified vertical bending moment. The response in this test was unusually high compared with all the other tests at steady speed, including the tests at slightly lower speed on this MBEJ with this truck and the tests with the single-axle truck at even higher speeds. Examination of the time history for this test, shown in Figure 2.36, reveals that the front axle gives a much higher horizontal response than the rear axles. This is a characteristic of all the braking tests—i.e., the truck pitches forward and places extra force on the front axle. Although it was supposed to be a steady-speed test, it is believed that the driver was braking. This test gives an indication of the magnitude of the response to mild braking, whereas the braking tests described below were rather extreme.

As explained in Section 2.2.1, Tschemmernegg reported a maximum total amplified horizontal fatigue-limit-state axle load that is 30% of the total amplified vertical fatigue-limit-state load range. However, Tschemmernegg matched up the largest horizontal response in one direction from the long-term samples with the largest horizontal response in the other direction to obtain his total recommended horizontal load. It is likely that these two responses were not from the same vehicle; in fact they could be hours apart. This can explain why his horizontal load is a greater percentage of the vertical load than the 22% reported here. Tschemmernegg's approach is regarded as too conservative, because it essentially implies that every vehicle causes the maximum response in both directions.

In addition to single-axle trucks, tandem-axle trucks were also used on the Lacey V. Murrow and I-90/I-5 HOV structures located in Seattle. No significant variations in MBEJ behavior were observed in tests conducted with single- and tandem-axle trucks. The time scale of the damped vibrations is on the order of tens of milliseconds, whereas the time between the impacts of the first and second rear axles are on the order of 50 msec or more. Therefore, the response from the impact of the first rear axle is almost completely damped out by the time the second rear axle impact occurs, as shown in Figure 2.36. This finding indicates that there is probably also very little interaction between vehicles, even in heavy traffic.

Table 2.7 shows that the resonant period for horizontal response is typically about twice the loading period, indicating that resonance in the horizontal direction is difficult to avoid. This is in contrast to the vertical response period, which is generally smaller than the loading period and can be mitigated by keeping the centerbeam span below 1220 mm (nominally 48 in.). In fact, according to the analytical predictions of the response, if the period of the response could be made larger than 3 times the loading period, the response could be minimized. In this case, it could help to make the MBEJ less stiff in the horizontal direction, and some designs have clearly attempted to accomplish this. Fortunately, the damping is higher in the horizontal direction and therefore this horizontal amplification is mitigated to a significant extent. Tschemmernegg has presented data that show that the horizontal response is about one-half what would be computed without damping.

In some cases, the peak horizontal response is slightly out of phase with the peak vertical response. In these cases, the two peak responses are not additive. However, careful examination of the time histories reveals that in about one-half the cases, the peaks occur nearly in phase so that the responses are additive. Because the fatigue design strategy will likely

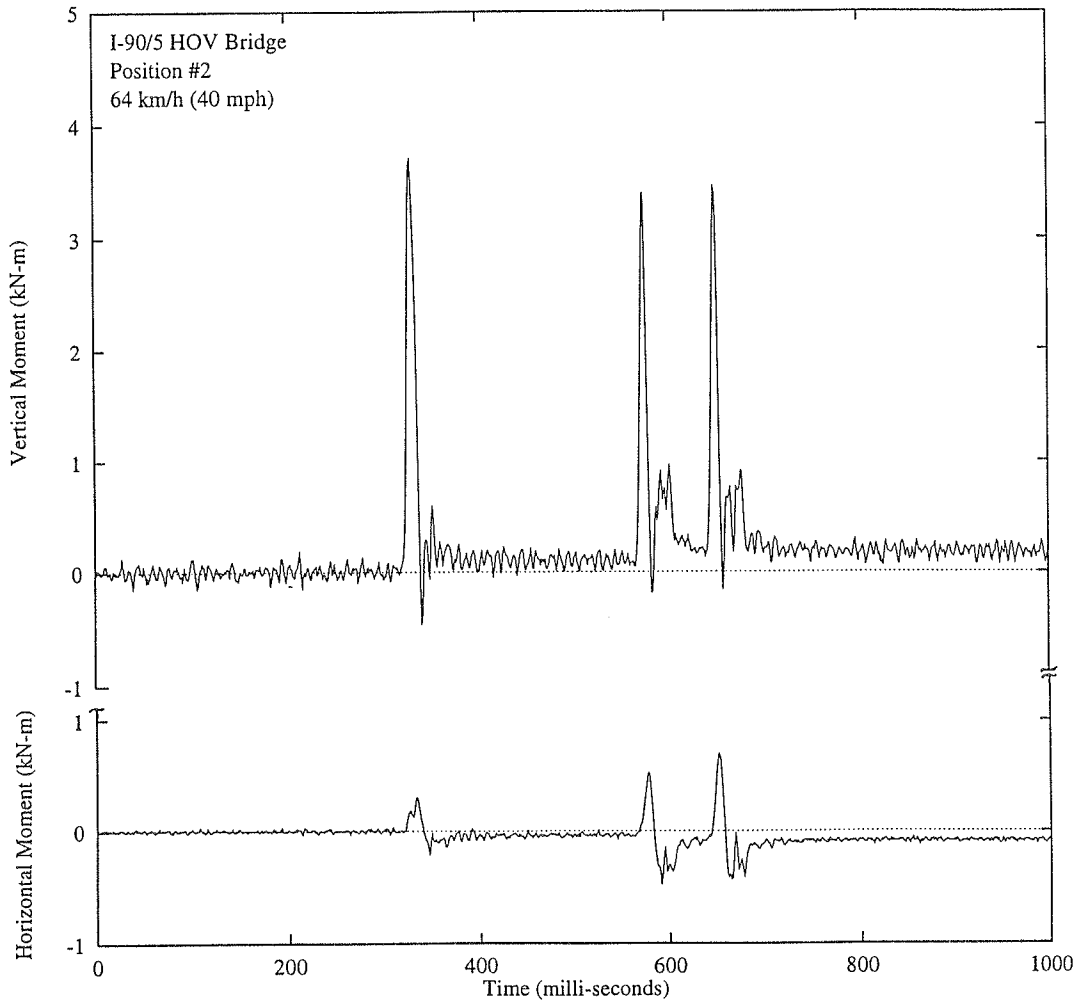

Figure 2.36. Dynamic time history for I-90/I-5 HOV bridge MBEJ (dual-axle truck at 64-km/h suspected braking condition).

be based on the largest stress ranges, it should be assumed that the peaks occur in phase.

The effects of steel blocks placed between centerbeams as described above were examined in the dynamic tests as well. There appears to be only a slight influence to MBEJ behavior from the addition of these blocks. This observation indicates that, during the impact loading, MBEJs behave as if they were supported horizontally in a rigid manner. This phenomenon was previously reported by Tschemmernegg.

Finally, the effect of grade on horizontal bending moment was also evaluated. A series of controlled dynamic tests at the I-90/I-5 HOV structure were conducted with the test truck traveling in both the downhill and uphill direction over the MBEJ. A maximum horizontal response would be expected for vehicles traveling downhill where the horizontal component of the axle load and horizontal dynamic force would be in the same direction. For vehicles traveling uphill, the axle load component and dynamic force would be in opposite directions. Unfortunately, the small magnitude of bending moment caused by the horizontal component of axle load is indistinguishable from horizontal dynamic effects.

Braking and Acceleration Tests. Braking and acceleration tests were performed with the test truck to study the response of the joint to these worst-case horizontal load conditions. The braking tests were performed at several initial speeds. The driver was instructed to brake as hard as possible. In many cases, the driver caused the wheels to lock up and skid across the MBEJ. In the acceleration tests, the truck began from a stop just behind the MBEJ and accelerated as fast as possible in low gear. At all locations except the I-90/I-5 HOV structure in Seattle, Washington, these tests were repeated with the joint blocked from below at the support box locations (as described above for the horizontal calibration).

Horizontal force effects resulting from braking and acceleration tests were typically much greater than measured during the steady-speed tests. For example, Table 2.9 shows some displacement data for two of the MBEJs. The displacements

TABLE 2.9 Measured displacement data for steady-speed tests compared with braking tests

MBEJ Location	Crawl Run			48 km/h (30 mph)			48 km/h (30 mph) with Braking		
	Vertical Support Bar Defl.[1] mm (in.)	Vertical Center Beam Defl. mm (in.)	Horiz. Defl.[2] mm (in.)	Vertical Support Bar Defl.[1] mm (in.)	Vertical Center Beam Defl. mm (in.)	Horiz. Defl.[2] mm (in.)	Vertical Support Bar Defl.[1] mm (in.)	Vertical Center Beam Defl. mm (in.)	Horiz. Defl.[2] mm (in.)
I-90/5 HOV Bridge	0.91 (0.04)	1.68 (0.66)	0.53 (0.021)	1.02 (0.04)	1.8 (0.07)	0.48 (0.019)	0.51 (0.02)	0.89 (0.35)	2.79 (0.11)
I-70/I-25 Flyover Ramp	----	1.19 (0.047)	0.2 (0.008)	----	1.27 (0.05)	0.38 (0.015)	----	0.74 (0.029)	3.81 (0.15)

Notes: 1. Measured at Face of Support Box
2. Horizontal Centerbeam Deflection at a Support Bar.

increase with speed relative to the crawl run, as expected. Note that the horizontal displacements are 6 to 10 times greater for the braking test than for the steady-speed test.

Figure 2.37 shows the time history of the vertical and horizontal bending moment response of the Charter Oak Bridge MBEJ subjected to braking from 48 km/h. The response can be compared with the response in Figure 2.35, which was a test at a steady speed of 48 km/h. Note that the vertical response is relatively unaffected by the braking, although the horizontal response is clearly different. The front wheel as well as the rear wheel produces a large horizontal response. The horizontal response at 48 km/h was greater than the horizontal response at 96 km/h. The loading impulse period at 96 km/h, shown in Table 2.7, is about one-half the horizontal resonant period. Therefore the amplification should be a maximum at 48 km/h, where the loading impulse period would be almost equal to the resonant period.

The horizontal response of the MBEJ in the Lacey V. Murrow Bridge was significantly greater than the response in the other MBEJs. The extremely large horizontal forces on this MBEJ from braking and accelerating may be due to the large width of the centerbeam, which gives a larger surface for traction. The maximum horizontal moment range (forward plus backward moment) is a total of 65% of the total amplified vertical moment range. The maximum horizontal moment range due to acceleration is 30% of the total amplified vertical bending moment.

Other than the Lacey V. Murrow Bridge MBEJ, which appears to be a special case, the MBEJ in the I-90/I-5 HOV bridge exhibited the next greatest horizontal response due to braking. The total range of the maximum horizontal response due to braking is equal to 47% of the total amplified vertical moment range. This range compares with a maximum horizontal moment range of 14% of total amplified vertical moment under steady speeds and a total horizontal moment range of 22% of the total amplified vertical moment at the I-90/I-5 HOV bridge MBEJ under slight braking (as shown in Figure 2.36).

Tschemmernegg also reported that the maximum horizontal response due to braking was about 75% of the total amplified vertical moment range, which is consistent with the measurements in this report. Tschemmernegg did not recommend that the larger braking forces be used in fatigue design.

Other than the Lacey V. Murrow Bridge MBEJ, the greatest total range of the horizontal bending moment response due to acceleration is 13% of the total amplified vertical moment range, which is not as severe as the effect of braking.

Obviously, the large swivel-type single-support-bar MBEJ on the Lacey V. Murrow Bridge is a special case with respect to horizontal response from braking or accelerating. It may be recommended that special attention be given to the potential response that may occur for braking and accelerating on these types of large MBEJs. This particular MBEJ has a centerbeam with a rather high horizontal section modulus about as large as the vertical section modulus (S_h is 61% of S_v), so it may be designed to withstand these high horizontal loads. However, the horizontal bending section modulus is typically about 5 times smaller than the vertical section modulus, so forces on the same order as the vertical forces would cause extremely large stresses. In any case, the design specification applicable to ordinary MBEJs should not be based on the unusual response that occurs for this special type of MBEJ.

It is debatable whether a fatigue design specification should include the special effects of braking and accelerating in the design forces. The fatigue design approach is based on keeping almost all the loading cycles (except the largest 0.01% of occurrences) lower than the CAFL. If these braking or accelerating forces occur more frequently than 0.01% of the occurrences, then they should be included. However, it is difficult to imagine that under normal circumstances 0.01% of the vehicles will be braking as violently as was

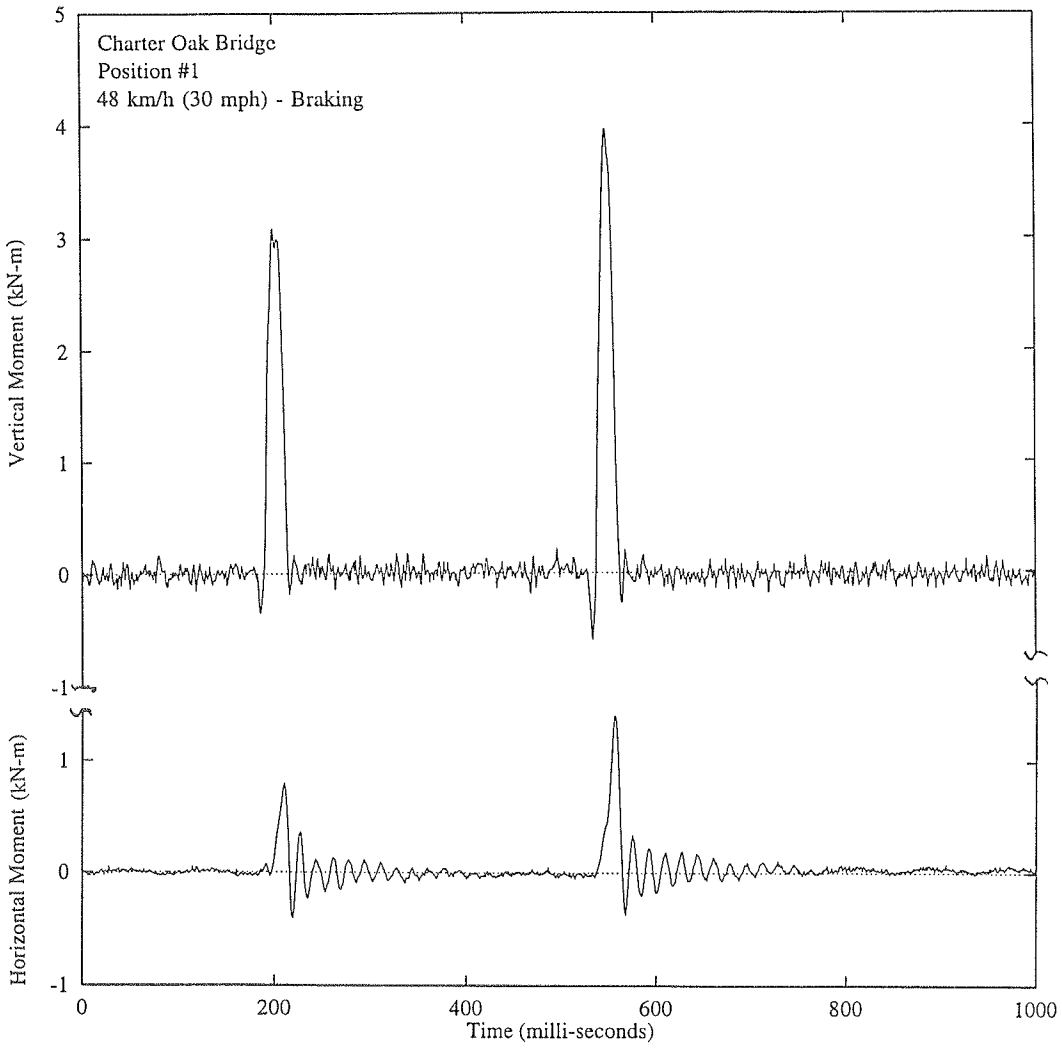

Figure 2.37. Dynamic time history for Charter Oak Bridge MBEJ (single-axle truck braking from 48 km/h).

done during these braking tests. On the other hand, more routine braking, such as occurred inadvertently during the test shown in Figure 2.36, can lead to a horizontal bending moment as large as 22% of the total amplified vertical bending moment range.

Braking or acceleration forces can occur if the MBEJ is located near a traffic light or stop sign, and this might be treated as a special case in the proposed specification. Large bridge structures that typically utilize MBEJs also experience high traffic volume. As a result, these highways are frequently susceptible to congested traffic in which all vehicles are constantly stopping and starting while crossing the MBEJ. For example, almost every day during the field work on the Lacey V. Murrow Bridge, rush-hour traffic was at a crawl (braking or accelerating) over the joint. It is highly likely then that large simultaneous vertical and horizontal loads would exceed 0.01% of the occurrences and possible fatigue problems could arise.

If the effect of routine braking is taken as 22% of the total amplified vertical moment range, this is larger than the accelerating moment range for all bridges except the Lacey V. Murrow Bridge. Thus, a design horizontal force of this magnitude would cover any circumstances except braking and accelerating on large swivel-type single-support-bar systems and violent braking on any MBEJs. These situations could be covered by special provisions.

2.2.4.4 Uncontrolled Dynamic Tests

The uncontrolled dynamic load tests consisted of monitoring the instrumented modular expansion joint while the

structure was open to normal traffic conditions. These measurements were used to qualitatively evaluate the differences between traffic loading and controlled dynamic test loads. A minimum of 3 hr of uncontrolled dynamic load monitoring was obtained from each bridge during midday traffic. Stress ranges less than 7 MPa (1 ksi) were not counted. Generally, this excluded all cars and most light trucks. In the uncontrolled tests, both of the bottom strain gages were monitored individually where each gage shows a combined vertical and horizontal response. Large differences in strain in these gages were not observed, indicating that the horizontal stress ranges were not very large.

Restrictions on lane closures required that the section of the MBEJ instrumented be as close to the curbline as possible. Instrumentation was located very close to the shoulder on the Charter Oak and I-70/I-25 bridges and subsequently measured stresses were rather low and do not properly reflect conditions in the actual travel lanes. The stresses measured at the Lacey V. Murrow and I-90/I-5 HOV MBEJs best represent the actual traffic conditions on their respective structures. However, the instrumentation was not optimally placed with respect to the heaviest truck traffic on these structures either.

Uncontrolled dynamic testing was conducted on the Lacey V. Murrow Bridge during a weekday evening rush hour. A stress-range histogram generated from strain gages located in a positive moment region of a centerbeam is presented in Figure 2.38. The maximum vertical stress during the uncontrolled tests on the Lacey V. Murrow Bridge was 36.5 MPa, which is only slightly greater than the maximum measured vertical stress range during the controlled tests (35 MPa). The design stress range for vertical bending only is 1.63 times the static moment, or about 46 MPa. Considering that the design horizontal stress range would be added on top of that, the proposed design loads appear to be conservative.

A segment of the time history from this uncontrolled test, which contains some of the most significant stress cycles, is presented in Figure 2.39. The peaks correspond to a typical tractor-trailer truck followed closely by a triaxle dump truck. Also shown is a portion of the uncontrolled tests in which no trucks were crossing the MBEJ. The small peaks represent the effect of either trucks located in other lanes or passenger cars directly over the joint. The large stress range of 31 MPa indicated on the time history is close to one of the maximum stress ranges and is slightly less than the maximum stress range from the test trucks. The rebound from this loading is about 25% of the downward stress, which is slightly greater than the maximum 23% rebound in the controlled tests (23% rebound corresponds to 31% of the static vertical load). The rebound in the uncontrolled tests could be larger because of different characteristics of the trucks. However, the difference is small enough to ignore.

Instrumentation installed on the I-90/I-5 HOV structure was located within a traffic lane. The structure carries no commercial traffic and is open only to commuter buses and

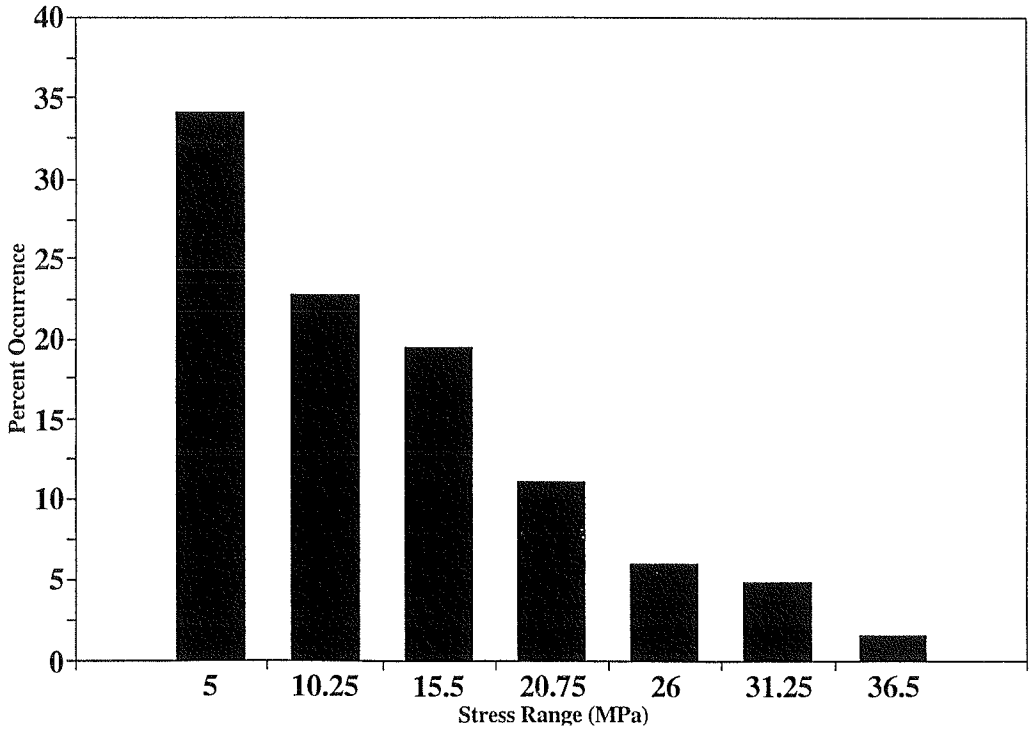

Figure 2.38. Stress-range histogram for Lacey V. Murrow Bridge MBEJ.

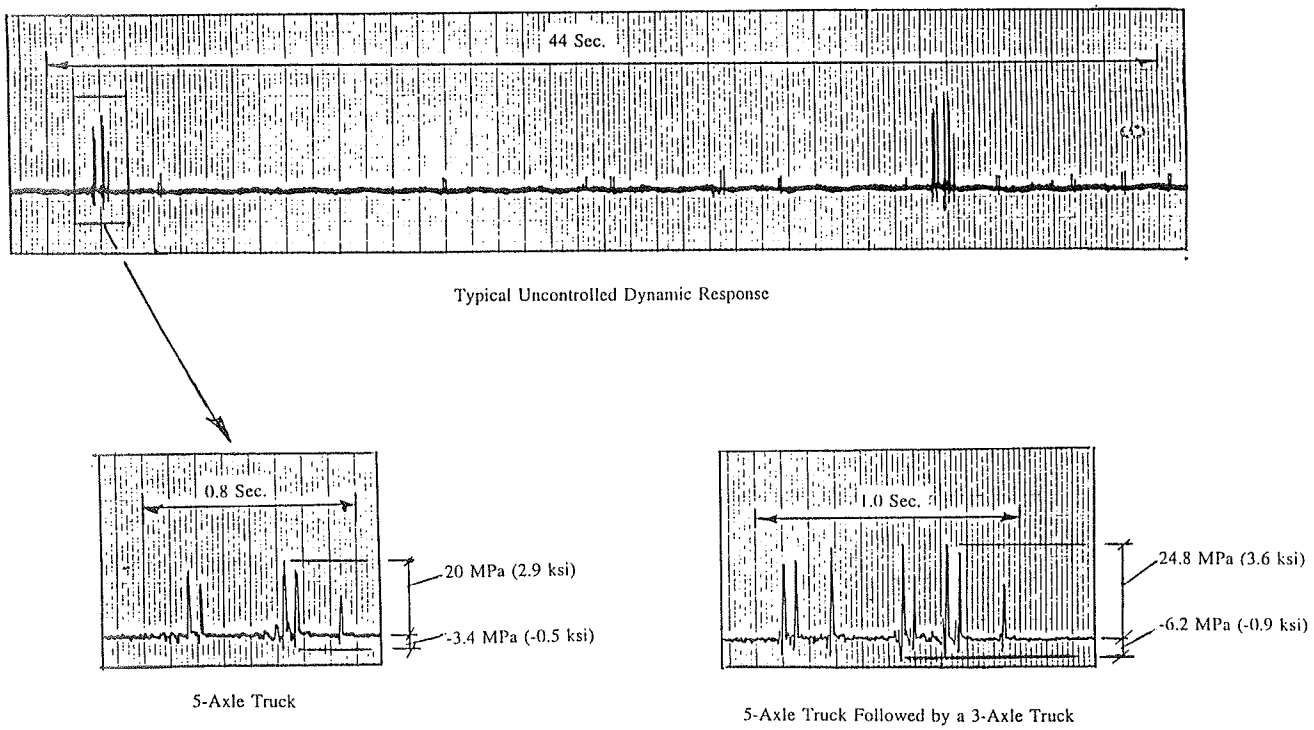

Figure 2.39. Representative time history from an uncontrolled dynamic test (Lacey V. Murrow Bridge MBEJ).

passenger cars. A stress-range histogram for this structure is presented in Figure 2.40. Uncontrolled testing was conducted for approximately 3 hr during peak evening traffic when approximately 30 fully loaded buses crossed the joint. The bimodal shape of the loading spectrum was produced by triaxle buses, which have a middle axle that is much heavier than the other two axles. This middle axle is responsible for the peak on the histogram at about 42 MPa.

The maximum vertical stress range from the uncontrolled test was 49 MPa. The largest vertical stress range in the controlled tests was slightly greater—i.e., 50 MPa. The design stress range would be about 163% of the static vertical

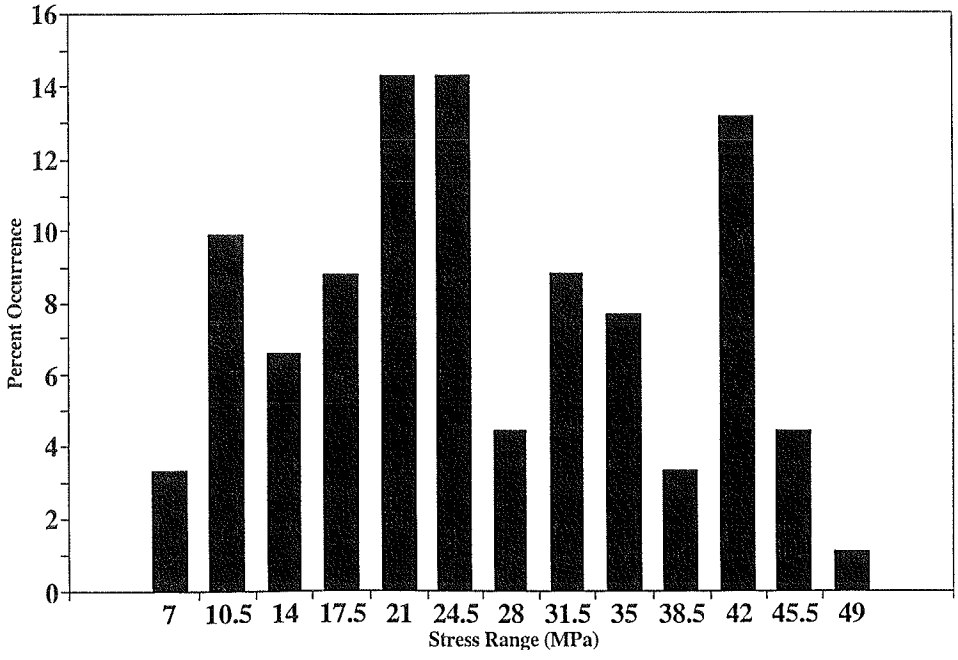

Figure 2.40. Stress-range histogram for I-90/I-5 HOV bridge MBEJ.

response, which is approximately 60 MPa. If a horizontal stress range of about equal magnitude is added to this, the proposed design loads would be conservative.

In all cases, the controlled tests gave a response typical of the highest responses measured during the uncontrolled tests. The use of a controlled dynamic and static test program to study the behavior of MBEJs was justified by the fact that little, if any, interaction was observed among vehicles during the uncontrolled dynamic tests. The uncontrolled test results also indicate that the preliminary proposed design loads give a very conservative margin above the typical measured stress ranges.

Because of the position of instrumentation along the joint, and the limited length of time available to monitor the joint, the uncontrolled dynamic test data are not considered good enough to directly estimate fatigue loads, as was done by Tschemmernegg, for example (see Section 2.2.1). However, if the design loads were extracted from the uncontrolled test data in this manner, it is clear that these design loads would be lower than the design loads recommended in Section 3. Therefore, the approach taken here is slightly more conservative.

2.2.5 Summary of Field Test Findings

The significant findings of the field studies were as follows:

1. Maximum dynamic amplification up to 1.63 times the static response was measured. This dynamic amplification includes both downward and upward (rebound) components. Large vertical amplifications are more common in MBEJs with longer centerbeam spans [>1220 mm (4.0 ft)] and at MBEJ sites with high-speed traffic.
2. MBEJs were observed to behave as continuous beams on rigid supports when subjected to vertical wheel loads.
3. Measured horizontal moment ranges (as a percentage of amplified static vertical moment; 1.63 times the static vertical moment) were up to 12% for steady speeds, up to 23% for routine braking and maximum acceleration, and up to 48% for extreme emergency braking.
4. Horizontal response of the Lacey V. Murrow Bridge MBEJ to extreme braking and acceleration was much greater than the response of other MBEJs tested. Horizontal moment ranges in the Lacey V. Murrow Bridge MBEJ were measured (as a percentage of the amplified static vertical moment) up to 64% for extreme braking and up to 29% for acceleration. However, there was very little vertical amplification of this MBEJ during controlled dynamic tests. The unique response of this MBEJ is attributed to the type and size of the MBEJ and not to other site conditions.
5. Typical measured stresses were well below the CAFL of good (i.e., Category C) MBEJ details. MBEJs possessing details with a lower fatigue life (Category D or less) may be expected to experience fatigue cracking during service.

2.3 LABORATORY STATIC TESTS

The objectives of the laboratory static tests include (1) comparing the static load and strain distributions with those measured in the field; (2) investigating tire patch lengths and the fraction of wheel load carried by individual centerbeams (distribution factors); and (3) comparing the static load response of complete-assembly MBEJs with the response of subassembly specimens consisting of a single centerbeam supported on three or four support bars. The results show that the subassembly has similar behavior and therefore can be used as a simplified specimen for fatigue testing.

As shown in Table 2.10, five full-scale complete-assembly MBEJs were tested by applying loads with a truck axle and tires filled with air (see Figures 2.41 and 2.42). The complete-assembly specimens tested are essentially identical to those instrumented in the field. Static tests were also conducted on nine full-scale MBEJ subassembly specimens with loads applied through a steel fixture (see Figure 2.43).

Full-penetration welded multiple- and single-support-bar connection details and bolted single-support-bar connection details were included in the test program. Different center-

TABLE 2.10 Summary of complete-assembly specimens

Specimen	Type	Centerbeam Width mm (in)	Centerbeam Span mm (in)	Number of Centerbeams
AF-1	W.M.S.B.	57 (2.23)	1524 (60)	2
AF-2	W.S.S.B.	114 (4.46)	1278 (50.3) min 1753 (69) max	3
BF-1	W.M.S.B.	64 (2.5)	1435 (56.5)	5
CF-1	B.S.S.B.	80 (3.125)	1524 (60)	3
CF-2	B.S.S.B.	80 (3.125)	1524 (60)	3

Notes: W.M.S.B. - welded multiple-support-bar
W.S.S.B. - welded single-support-bar
B.S.S.B. - bolted single-support-bar

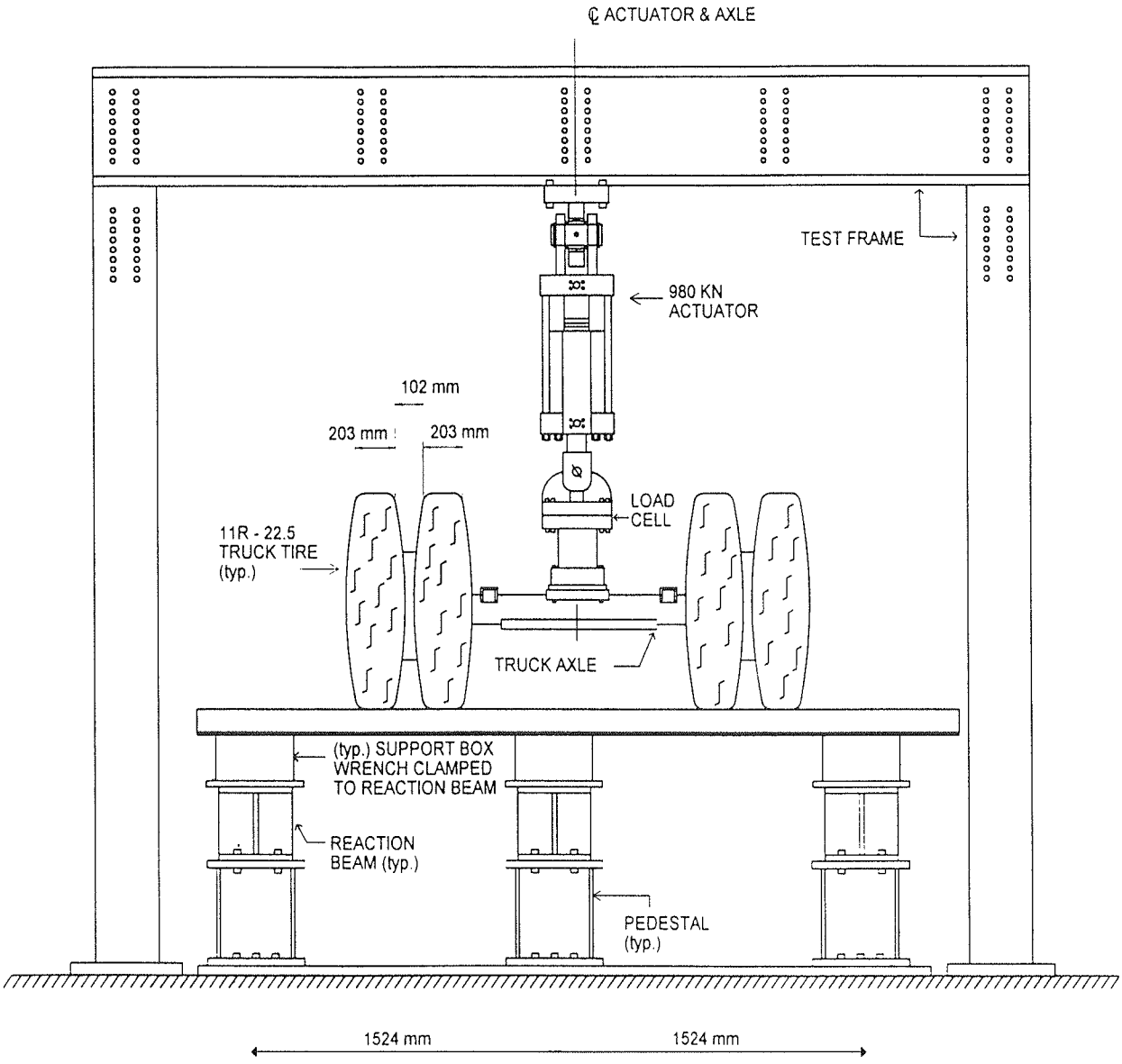

Figure 2.41. Detail of typical complete-assembly test setup.

beam field splice details were also included on selected specimens.

2.3.1 Static Test Procedures

2.3.1.1 Description of Complete-Assembly Static Tests

Load was applied to the complete-assembly MBEJ through air-filled tires mounted on an actual truck axle attached to the hydraulic actuator, as shown in Figures 2.41 and 2.42. The support boxes of the MBEJ were securely fastened to a fixture attached to the reaction floor. To study the effects on overall MBEJ behavior during the static tests, particularly the distribution of the applied axle load among centerbeams, the location of the MBEJ, axle load, centerbeam gap, and tire pressure were varied separately.

Axle loads from 0 to 156 kN (35 kips) were applied in 22-kN (5-kip) increments for each gap width, and tire pressure and strains were recorded. Tests were repeated at least twice and the results were reproducible. Tires were inflated to a maximum of 655 MPa (95 lbf/in.^{2}), near the maximum recommended by the manufacturer. Tire pressure was varied on only one specimen (specimen TSF-1). Tests were conducted with tires inflated to pressures of 448 MPa (65 lbf/in.^{2}), 517 MPa (75 lbf/in.^{2}), and 655 MPa (95 lbf/in.^{2}).

The MBEJ specimen was horizontal—i.e., no horizontal force was applied. Subjecting the MBEJ exclusively to vertical loading eliminates the influence of horizontal load on the response of the system. Previously, similar tests were

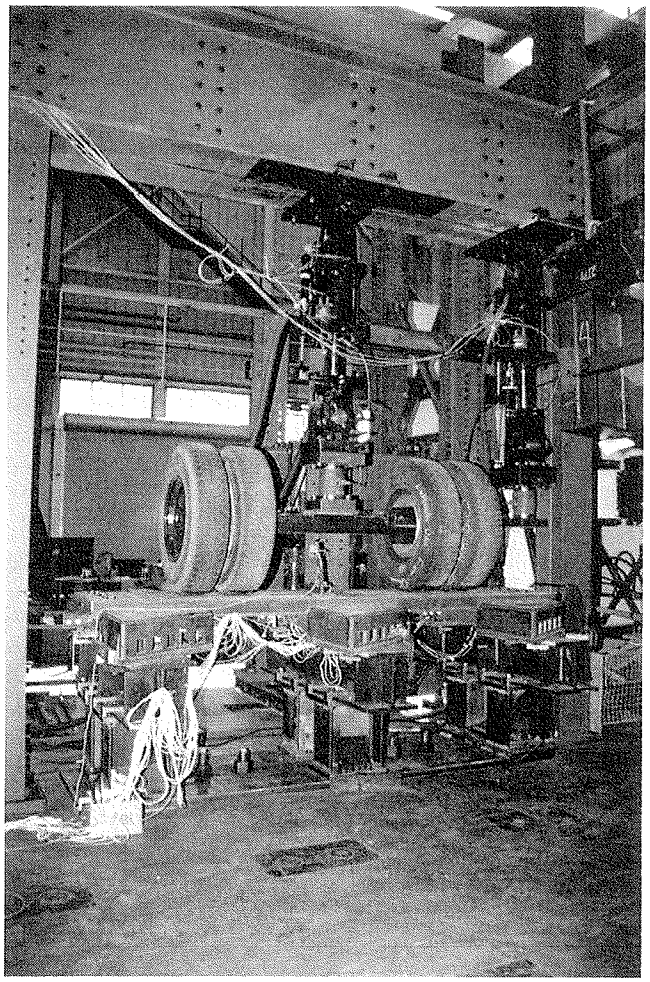

Figure 2.42. Typical complete-assembly test setup.

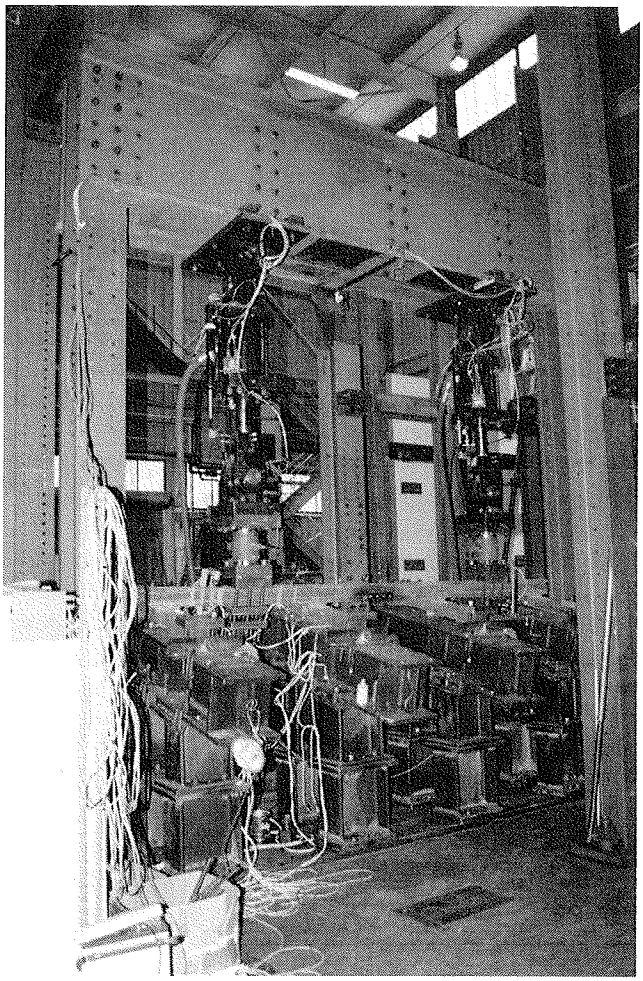

Figure 2.43. Typical subassembly test setup.

conducted at Lehigh University with complete-assembly specimens inclined about 11 degrees to create a horizontal load component (*44*). The tests were difficult to analyze because horizontal load effect confounded the effects of other variables. The in situ dynamic horizontal response is markedly different than the static response measured in the laboratory; therefore, the effects of horizontal load on response may best be described with data obtained from field studies.

2.3.1.2 Description of Subassembly Static Tests

In the subassembly tests, the specimens were inclined so that horizontal loads equal to 20% of the vertical load were applied. This was accomplished by inclining the specimen approximately 11 degrees off the horizontal plane (see Figure 2.43). The proportion of horizontal load applied is about the same as the maximum horizontal bending moment measured during the field studies, which was up to 23% of the total amplified vertical bending moment for mild braking, as discussed in Section 2.2.4. The field test data also show that the horizontal and vertical force effects often occur simultaneously; thus, applying these forces in phase in the laboratory is appropriate.

Although the horizontal load is only 20% of the vertical load, the horizontal section modulus of a typical centerbeam can be as little as one-fourth the vertical section modulus. As a result, horizontal bending stresses almost equal to the vertical stresses can be expected. Also, this horizontal load is applied at the top of the centerbeam, which creates a moment in the CB/SB connection.

Typical elastomeric-type bearings installed in complete MBEJ systems were replaced with steel bearings for the subassembly tests. Replacement of the standard bearings with steel is required because applied loads are considerably higher than actual service loads during fatigue tests. These high loads are applied so that a fatigue test can be completed in a reasonable amount of time. Based on individual static and fatigue tests of standard elastomeric bearings conducted at the ATLSS center, it has been shown these materials are not capable of withstanding the high loads and number of

cycles delivered during the fatigue tests (*43*). The behavior of the elastomeric bearings, as explained in Section 2.1.2, is strain-rate dependent. Therefore, the behavior in the laboratory at about 3 Hz is not even close to the behavior of the bearings in the field at 100 Hz or more. For the most part, these bearings are durable in service. A separate test procedure for bearing was developed for bearings and is given in Appendix B. Fortunately, results obtained in field and laboratory tests conducted on complete-assembly specimens have shown that MBEJs can be modeled quite reasonably, assuming there are rigid supports. Therefore, use of the steel bearings should not have changed the load or strain distributions significantly, although overall displacement would be expected to be different.

Load was applied through two computer-controlled 982-kN (220-kip)-capacity hydraulic actuators as shown in Figure 2.43. The actuators were controlled by computer using load control. For the static tests, both tensile and compressive loads of −89 to +89 kN (−20 to +20 kip) were applied to a given specimen over 22-kN (5-kip) intervals. To shake down the specimen in the fixture, each test was repeated several times. As in service, loads were applied at the centerline of the centerbeam top flange.

As discussed below, both upward and downward loads were applied during the fatigue tests. Thus, the specimen needed to be securely restrained from "walking" off the bearings. The system used to hold the support bar is shown in Figure 2.44. Once the specimen was located in the fixture as required, the anchor bolts were fully tightened by the turn-of-the-nut method with an air impact wrench. This ensured that sufficient preload was developed and maintained to secure the specimen in the proper position throughout the test.

2.3.1.3 Laboratory Test Instrumentation

Each specimen was instrumented with strain gages in a layout similar to that used in the field studies. Figures 2.45 and 2.46 present typical strain gage layouts for a complete-assembly and subassembly specimen, respectively. Strains were recorded with a Huttinger Baldwin data acquisition system capable of sampling 60 channels.

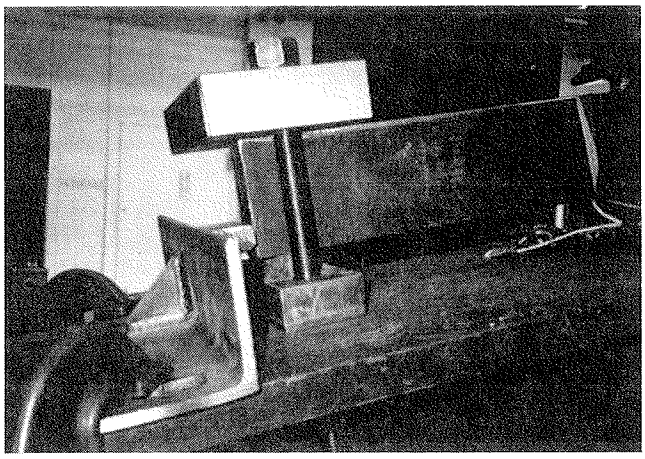

Figure 2.44. Subassembly support bar bearing detail.

Global behavior of individual specimens was evaluated by instrumenting each specimen with several strain gages in an identical pattern. These data were then used to compare overall behavior among like specimens. Measured strains in specimens of similar type were found to be very consistent. Static tests were repeated several times for a given specimen, and test results were found to be reproducible. To obtain more detailed information about specimen behavior (i.e., moment transfer at the CB/SB bar connection), additional strain gages were placed at selected locations on some specimens. Both the global and local data were then compared with the analytical models.

2.3.2 Complete-Assembly Static Test Results

As noted above, the position of the MBEJ, gap width, and tire pressure were varied during the complete-assembly static tests. The primary objective of these complete-assembly static tests was to investigate the influence of each of these parameters on the portion of load carried by each centerbeam (i.e., distribution factor). The findings of the static tests are discussed below. Details pertaining to the complete-assembly specimens are summarized in Table 2.10.

2.3.2.1 Effect of Axle Load

Axle loads up to 155 kN (35.0 kips) were applied in 22-kN (5.0-kip) increments at each gap width, and strains were recorded. The measured distribution factor was calculated by taking the ratio of the measured vertical moment on a centerbeam to the calculated vertical moment that would result from the entire axle load being applied to that centerbeam. The calculated theoretical moments were obtained by modeling individual centerbeams and respective support bars as beam elements in a three-dimensional frame. A commercially available software package was used for analysis.

Figure 2.47 presents the distribution factor as a function of the total applied axle load for each of the three centerbeams in specimen BF-1. The results show a decrease in distribution factor of the primarily loaded centerbeam with increasing load. The rate of decrease of the distribution factor decreases at higher axle loads. Figure 2.48 presents the portion of the axle load carried by each centerbeam versus total applied axle load in specimen BF-1. This load is obtained by multiplying the measured distribution factor by the total axle load. All specimens exhibited trends similar to those shown in Figures 2.47 and 2.48 regardless of centerbeam width, gap, or tire pressure.

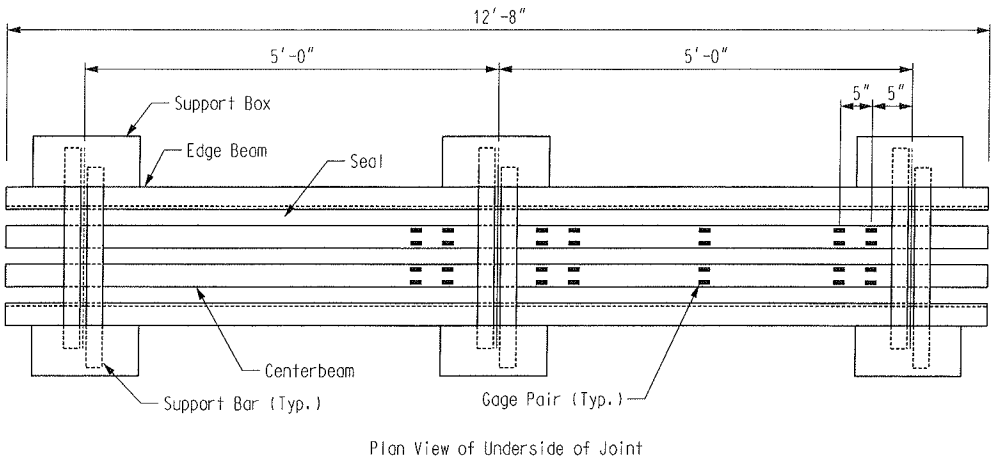

Figure 2.45. Typical complete-assembly strain gage plan.

Figure 2.48 illustrates the phenomenon that was explained in Section 2.1.4—i.e., that the increase in the response of the centerbeam is not proportional to the increase in the total axle load. For example, the appropriate value of the fatigue-limit-state axle load is uncertain, and estimates range from 100 to 160 kN. Figure 2.48 shows that as the total axle load increases from 100 to 160 kN, an increase of 60%, the load on the centerbeam increases from 55 to only 65 kN, an increase of only 18%. All but 10 kN of the additional 60 kN was transmitted to the other centerbeams as the load increased. This effect mitigates the uncertainty in the total axle load.

2.3.2.2 *Effect of Centerbeam Gap*

Gap between centerbeams was varied from 12.7 to 76.2 mm (0.5 to 3.0 in.), typically in 0.5-in. increments. Figures 2.49 and 2.50 present distribution factor versus gap width for various axle loads along with Tschemmernegg's recom-

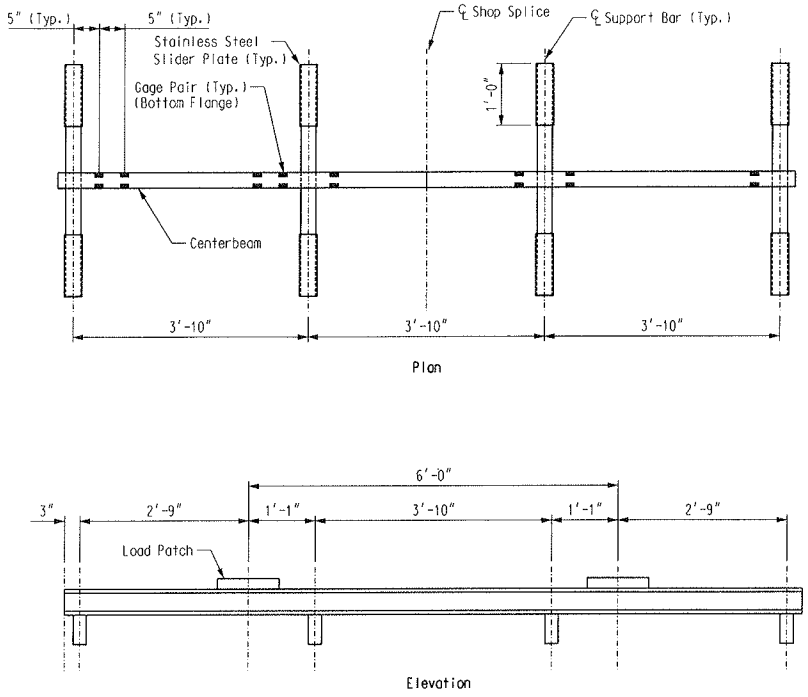

Figure 2.46. Typical subassembly strain gage plan.

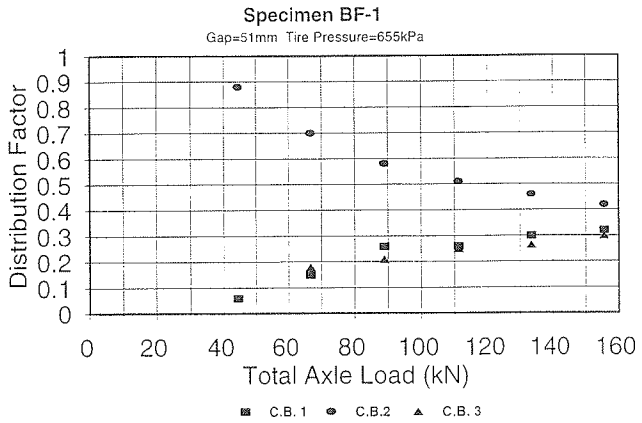

Figure 2.47. Measured centerbeam distribution factor in specimen BF-1.

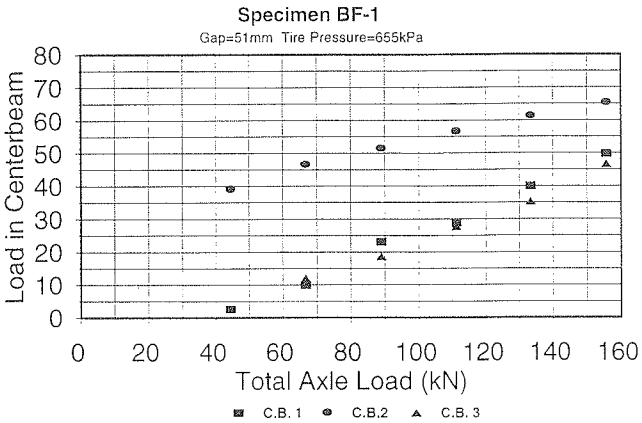

Figure 2.48. Apparent share of axle load carried by each centerbeam in specimen BF-1.

mended distribution factor (given in Figure 2.29), which is shown for comparison. The widths of the centerbeam are 79.4 mm (3.125 in.) and 63.5 mm (2.5 in.) for Figures 2.49 and 2.50, respectively. At load levels of >100 kN, which are the load levels associated with design, Tschemmernegg's method appears to overpredict the share of the load carried by a centerbeam for the MBEJ shown in Figure 2.49. However, in Figure 2.50 the agreement at high load levels is good.

To study the effect of axle position, tests were conducted in which the MBEJ was repositioned with the axle located between two centerbeams and with the axle located directly above a centerbeam for one specimen. The measured distribution factor for the latter case (i.e., the axle positioned directly over the centerbeam) consistently resulted in a higher distribution factor than the former.

2.3.2.3 Effect of Tire Pressure

The influence of tire pressure on distribution factor is shown in Figure 2.51. Pressures of 448 kPa (65 lbf/in.^{2}), 517 kPa (75 lbf/in.^{2}), and 655 kPa (95 lbf/in.^{2}) were used. At low axle loads, the distribution factor increases in proportion to the tire pressure. However, in the range of axle loads greater than 100 kN, tire pressure is no longer a significant variable.

Individual tire footprint lengths were also measured at two different pressures (551 kPa [80 lbf/in.^{2}] and 655 kPa [95 lbf/in.^{2}]). This was accomplished by coating the bottom of the tires with paint, placing a piece of paper on a rigid steel plate beneath the tire, and applying a load. The axle was then lifted, the paper was removed, and the process was repeated at a different load.

Figure 2.52 shows the average tire footprint length for the two different pressures. Tire width was observed to remain

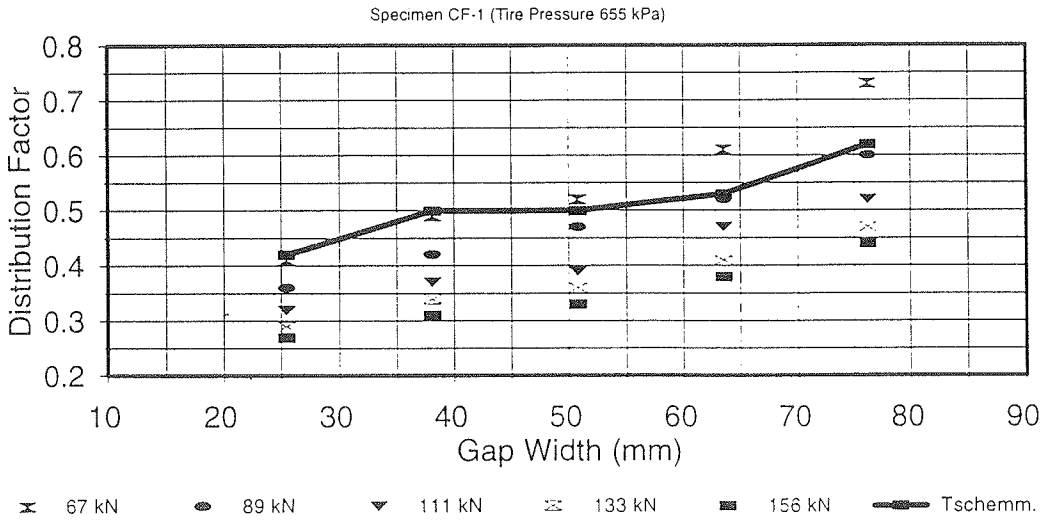

Figure 2.49. Distribution factor vs. gap for a 79.4-mm-wide centerbeam subjected to different axle loads.

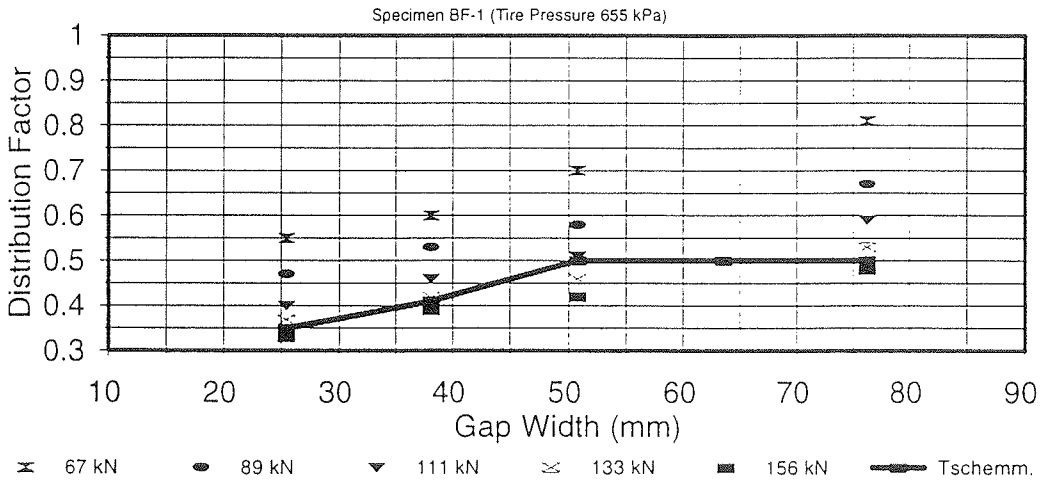

Figure 2.50. Distribution factor vs. gap for a 63.5-mm-wide centerbeam subjected to different axle loads.

essentially constant as load increased. At loads above 25 kN, the change in the tire patch length is approximately inversely proportional to the change in tire pressure. However, the tire patch area is about 30% larger than would be calculated for a uniform pressure on the order of 655 kPa. This means that there are areas of the tire footprint, in the gaps between centerbeams and near the edges of the patch, where the rubber is in contact with the surface but significant pressure is not exerted on the surface.

Figure 2.53 compares the measured average footprint length for the case of 655-kPa tire pressure and the footprint length calculated according to the 1994 AASHTO LRFD bridge design specification for both the strength and fatigue limit states. Figure 2.53 also shows the six tire patch lengths of the rear axles measured during the field tests, which ranged from 248 to 267 mm for 50-kN wheel loads. The laboratory data and the field data are in good agreement.

According to the specification, patch length can be estimated as follows:

$$L = \gamma\,(1 + IF/100)P/(0.438\ \text{kN/mm}) \qquad (2.1)$$

where

L = patch length (mm);
γ = load factor (1.75 for strength I, 0.75 for fatigue);
P = wheel load (71 kN for design truck, 56 kN for design tandem); and
IF = impact factor (%).

This equation is based on a patch width of 508 mm (20 in.) and a tire pressure of 861 kPa (125 lbf/in.^{2}). Hence, the denominator is the product of (508 mm) $\times$ (0.861 N/mm^2) = 0.438 kN/mm. The assumed tire pressure of 861 kPa (125 lbf/in.^{2}) is on the high end of typical truck tires (T. R. Con-

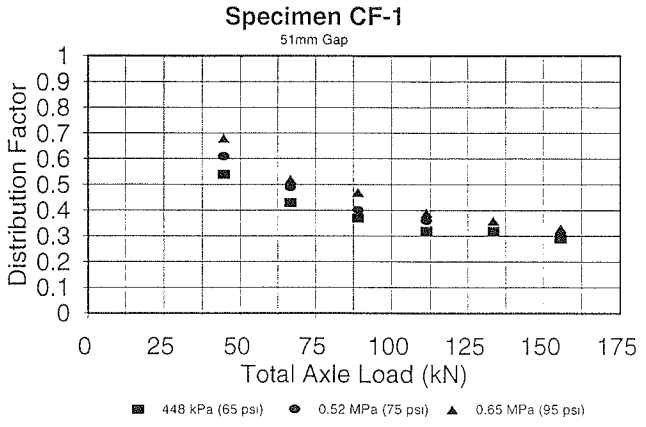

Figure 2.51. Effect of tire pressure on distribution factor.

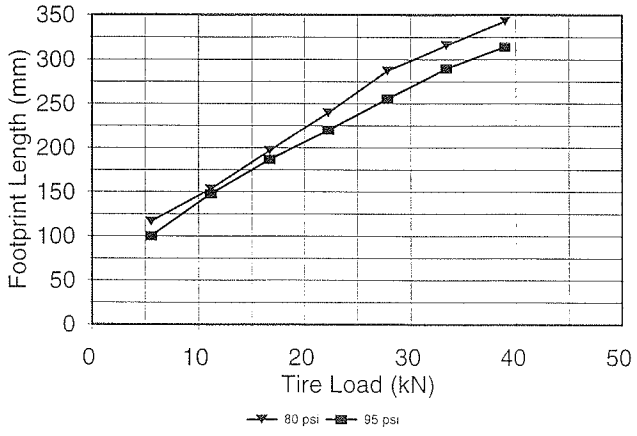

Figure 2.52. Patch length vs. wheel load for pressures of 551 and 655 kPa.

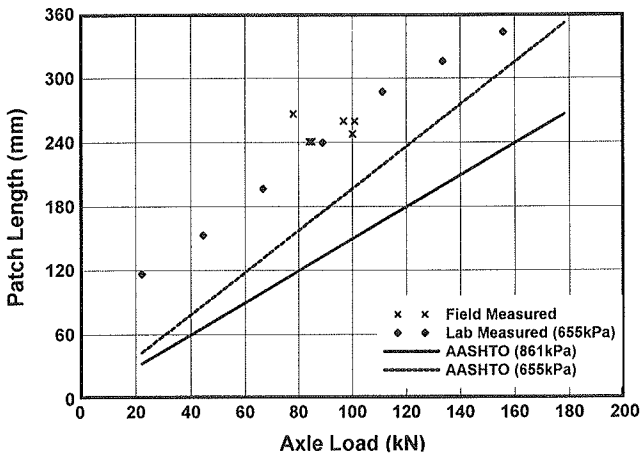

Figure 2.53. Comparison of AASHTO calculated patch length with measured patch length.

nor, personal communication [Connor is former manager of Kost Tire and Muffler in Forest City, Pennsylvania, and has over 20 years of experience in sales of car and heavy truck tires]) but results in a conservative (shorter) estimate of the patch length. The AASHTO code specifies the 71-kN (16-kip) wheel load of the design truck as a design case. For this case, Equation 2.1 gives a patch length of 213 mm (8.4 in.) with the fatigue load factor (which is slightly smaller than measured values), and 490 mm (19 in.) with the strength load factor (which is much larger than measured values). Recall that this wheel load actually represents a tandem and therefore should be divided by 2 to find a realistic footprint for dual wheels. If only one-half the wheel load were used in Equation 2.1, one-half the patch length would be calculated.

Figure 2.53 also shows the footprint length calculated according to Equation 2.1, with the tire pressure assumed to be 655 instead of 861 kPa. In this case, the agreement with the measured data is not as bad. However, some inconsistencies with Equation 2.1 must be addressed.

As shown in Equation 2.1, load and impact factors are applied to the load when the patch length is determined. For strength design, increasing the wheel load with a load factor increases the patch length and subsequently spreads the load out over a greater area. The larger patch length decreases the calculated local forces and stresses. In terms of the load on a particular centerbeam, application of impact factors decreases the share of load and results in an unconservative and unintended effect.

Also, the impact factor accounts for both downward amplification and upward rebound. However, application of the full impact factor to the wheel load implies that patch length increases with upward rebound. With the equation above, modifying the load also modifies the patch length and subsequently the wheel load distribution factor.

The patch length should reflect the best estimate of the actual patch length in service, so that reasonable load distributions are obtained locally. Then the force effects—e.g., the moment ranges in the centerbeams—should be multiplied by the load factors and impact factors.

2.3.2.4 *Effect of Centerbeam Height Mismatch*

The effect of vertical misalignment between adjacent centerbeams was investigated by placing thin shims on selected centerbeams, applying load, and measuring strains. Results indicate that vertical misalignment of centerbeams greatly influences the share of load carried by a given centerbeam. For example, in a three-centerbeam complete-assembly specimen, the axle was centered over the middle centerbeam, and steel shims were placed on the two adjacent centerbeams. The share of the load carried by a centerbeam that is next to one 3 mm (0.125 in.) below the surface may increase 24%. If the adjacent centerbeam is 6 mm below the surface, the share of the load carried by the higher centerbeam may increase 33%. The effect of misalignment is more pronounced at smaller gap widths (less than 38 mm or 1.5 in.).

2.3.3 Subassembly Static Test Results

Static tests were conducted on all nine subassembly specimens. During these tests, load was applied monotonically in 22-kN (5-kip) increments from −89 to +89 kN (−20 to +20 kips). The specimens included in the matrix exhibited a broad range of welded details found on multiple-support-bar MBEJs currently manufactured in the United States. The matrix also included two centerbeam and two support-bar span lengths. Support-bar width also ranged from 38.1 to 127 mm (1.5 to 5 in.); however, support-bar depth varied only slightly. Geometry of the centerbeams also varied only slightly. This is because centerbeams used in multiple-support-bar MBEJs produced by domestic manufacturers are quite similar.

Strains were recorded and subsequently used to calculate moments at strain gage locations. These moments were then compared with those obtained through structural analysis to investigate the effects of the fixture on boundary conditions. A commercially available frame analysis package was used for analysis. Each subassembly was modeled as a three-dimensional frame on pinned supports with beam elements. The translational stiffness of the supports was fixed in all directions. This assumption is reasonable, as the specimen was supported on steel bearings during the test. Measured vertical and horizontal moments were found to be in very good agreement with those determined analytically under proper boundary conditions. Specific details about results obtained through the static tests are discussed below.

The method of anchoring the support bars to the fixture discussed above was found to provide some restraint to the support bars. Specifically, small but measurable fixed-end moments were developed at support bar ends because of the clamping force of the anchor plates. These end moments tend to decrease the maximum midspan stress developed in the

support bar. Rotational restraint to strong axis bending of the centerbeam was also measured. These restraining forces are also a result of anchoring the support bar and tend to increase the stresses in the weld throat. To investigate the effect of restraint, several static tests were conducted with only compressive loads applied with the anchor bolts both loose and fully tightened.

Previous fatigue testing of full-scale subassembly specimens has been conducted on similar specimens at Lehigh University. During these tests, only compressive loads were applied and a different fixture, not capable of developing the restraining forces discussed above, was used. Observed cracks found in both test programs were identical, indicating that the fixture used in this program had little if any effect on the relative proportions of the stress components and the mode of fatigue cracking. It should be noted that the effect of these restraints was taken into account when the applied stress ranges for the S-N data were calculated.

The effects of support-bar stiffness on vertical centerbeam moments was investigated by varying support-bar stiffness in the model; the extreme case was a rigid support (i.e., a two-dimensional model). It was observed that support-bar stiffness has little effect on centerbeam moments, indicating that a two-dimensional model with pinned supports is sufficient as long as proper rotational restraints, if present, are considered.

Calculated and measured horizontal moments for a typical subassembly specimen were compared. The calculated moments were obtained from a three-dimensional frame analysis with beam elements. Measured moments were found to be in generally good agreement with those obtained analytically. However, calculated moments obtained with a two-dimensional model overestimate the horizontal moments.

Additional moment arising from horizontal forces was also measured in the support bars. These moments result from the horizontal component of the load applied at the top of the centerbeam. Figure 2.54 shows a typical moment diagram for a support bar. The additional moment from the horizontal load is the difference between the moments on either side of the centerline. Measured horizontal support-bar moments were not as consistent as vertical support-bar moments. Nevertheless, for most specimens the measured horizontal moment component was in reasonable agreement with predicted moments.

The additional moment in the support bar due to horizontal loads depends on the moment arm of the applied horizontal force at the top of the centerbeam. In the past, the assumption has been made that the moment arm was the distance from the top of the centerbeam to the middepth of the support bar. An attempt to estimate the length of this moment arm was made by using the measured support-bar moments. The results indicate that a moment arm equal to the distance form the top of the centerbeam to the middepth of the support bar yields very reasonable, slightly conservative results.

In summary, the following are the most important findings from the static tests of subassemblies:

1. Vertical moments in MBEJ subassemblies can be reasonably modeled by two-dimensional frame analysis with beam elements provided that proper boundary conditions are considered.

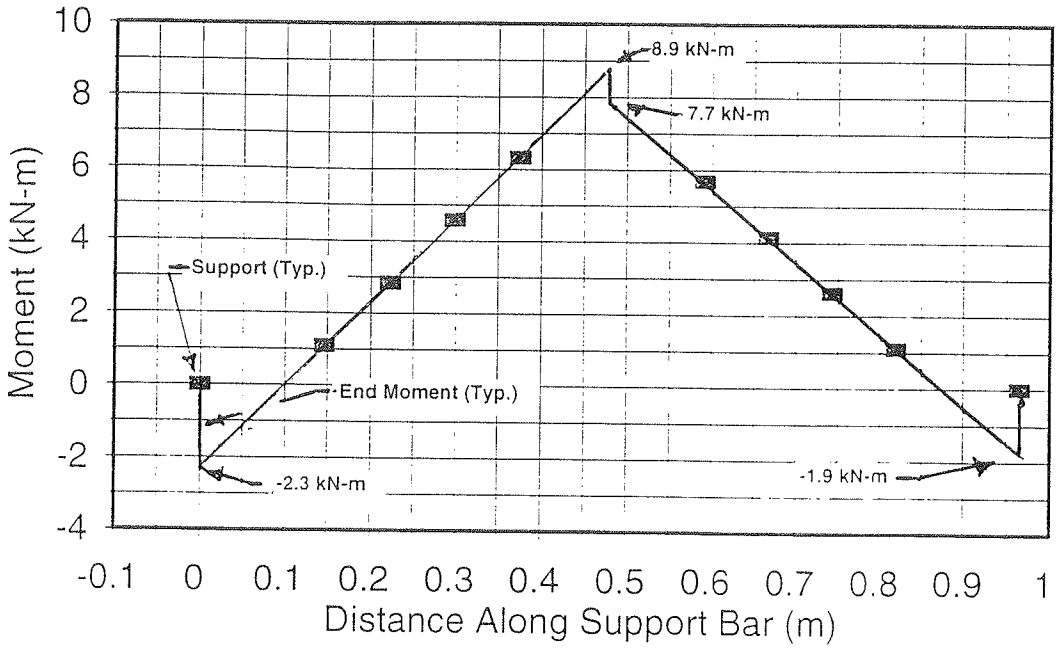

Figure 2.54. Moment diagram for a support bar in which significant end moments were measured.

2. Horizontal moments in MBEJ subassemblies can be reasonably modeled with a three-dimensional frame analysis with beam elements provided that proper boundary conditions are considered. A two-dimensional frame analysis is acceptable but will overestimate the horizontal moments.
3. The depth of the moment arm used to estimate the increase in support-bar moment resulting from horizontal loads can be conservatively taken as the distance from the top of the centerbeam to middepth of the support bar.
4. MBEJ subassemblies can be effectively used to characterize and represent the behavior of complete-assembly MBEJs provided that the proportions of the applied loads reasonably reflect actual loads applied in the field as best as possible.

2.4 LABORATORY FATIGUE TESTS

Fatigue testing was conducted on a variety of specimens including complete MBEJ assemblies and subassemblies consisting of individual centerbeams and the associated support bars. A summary of the test specimens, loads, and cycles to failure is shown in Table 2.11. The first six tests are actually two complete bolted single-support-bar MBEJ assemblies. Each of these assemblies had three centerbeams, which were tested sequentially for a total of six tests.

Specimens included at least two centerbeam spans (three support bars), and nine of the subassemblies included three spans. The CB/SB connections included bolted single-support-bar connections as well as full-penetration and fillet-welded multiple-support-bar connections. Many of these specimens also included various splice details. Load ranges are shown instead of stress ranges because the stresses are a function of the connection location (interior versus exterior), crack initiation location, and connection geometry. Most of the specimens exhibited at least two cracks, and some specimens exhibited as many as four cracks. Thus, multiple data were obtained from each test.

2.4.1 Fatigue Test Procedures

Figure 2.43 showed a typical test setup for a three-span subassembly specimen. Loads were applied to each fatigue test specimen by two computer-controlled actuators that simulated the two wheel loads of an axle. The specimens were inclined at an angle of 11 degrees so that the nominal horizontal load range was 20% of the vertical load range. The loads varied as sine waves at frequencies of 2 to 3Hz, which were in phase for the two actuators.

The actuators were centered in the spans of the two-span specimens. In the three-span specimens, the actuators were centered in the outer two spans, which created a constant bending moment over the interior span. This arrangement of the two actuators gave the maximum bending moment in the centerbeams and resulted in spacings that were reasonably close to the theoretical 1800-mm spacing of the wheels of the AASHTO standard HS truck.

The actuators were operated in load control; thus, the load range was maintained even as fatigue crack growth occurred. Increases in displacement that occurred as a result of crack growth were monitored and the tests were automatically

TABLE 2.11 Summary data for fatigue tests (all dimensions in mm)

Specimen	CB/SB Connection	SB Width	# Spans @Length	Splice Detail	Load Range kN	Number of Cycles(10^3)
C-1	Bolted	80	2@1524	F.P.[1]	+21.4 to -72.1	5806
C-2	Bolted	80	2@1524	F.P.[1]	+44.5 to -133.5	34
C-3	Bolted	80	2@1524	F.P.[1]	+32.9 to -102.8	149
C-4	Bolted	80	2@1524	none	-13.4 to -78.3	545
C-5	Bolted	80	2@1524	none	-13.4 to -78.3	257
C-6	Bolted	80	2@1524	none	-13.4 to -75.7	797
B-1	Fillet	63	3@1168	fish plate	+23.3 to -76.7	1388
B-2	Fillet	63	3@1168	hinge	+23.3 to -76.7	1003
B-3	Fillet	127	3@1168	fish plate	+23.3 to -76.7	1658
B-4	Fillet	127	3@1168	fish plate	+29.4 to -96.1	1069
B-5	F.P.	127	3@1168	hinge	+29.4 to -96.1	2149
B-6	F.P.	127	3@1168	hinge	+29.4 to -96.1	2326
A-1	F.P.	38	3@1270	none	+15.5 to -51.1	3374
A-2	Thin F.P.[2]	38	3@1270	none	+23.3 to -76.7	1262
A-3	Thin F.P.[2]	38	3@1270	none	+23.3 to -76.7	1525
A-4	Thin F. P.[2]	38	2@1524	none	+22.3 to +77.0	276
A-5	Thin F. P.[2]	38	2@1524	none	+22.3 to +57.9	839

F.P. is full-penetration

[1] Full-penetration shop splice

[2] The thin full-penetration weld has a narrow hourglass shape.

stopped if the displacement increased out of the original range by ±2.5 mm (0.1 in.). This increase in displacement range occurred before complete fracture of the specimen but not until after the crack had become at least 50 mm in length along the surface of the specimen.

Load ranges for the tests were selected so that fatigue cracking was anticipated within 3 million cycles. A test typically lasted 5 to 7 days and ran 24 hr a day. The tests were terminated either when the specimen fractured, when the crack had grown to a significant length, or when the crack growth appeared to stop. Defining failure in terms of significant crack size is obviously somewhat subjective. Cracks had typically penetrated at least 51 mm (2 in.) into the weld when a test was stopped. Note that this depth of cracking represents a larger percentage of the cross-sectional area of the weld for the narrow full-penetration welds compared with the very large (63.5 × 127 mm) full-penetration welds.

Most of the specimens exhibited more than one crack. When one connection fractured before the others, the actuator loading that particular span of the specimen was shut down. The other actuator was then run alone until failure was achieved for either or both of the other two connections in the respective span. The loads on the remaining actuator were adjusted so that the nominal stress ranges in the remaining connections were essentially equal to those measured at the start of the test.

Previous fatigue tests conducted on similar MBEJ subassemblies at the ATLSS Center (*44*) were conducted with downward forces only. These previous tests revealed a potential problem with downward-only loading on the full-penetration welded details. Fatigue cracking initiated in a region where there are compressive applied stresses. The fatigue cracking is possible at these locations because of the tensile residual stress associated with the weld (i.e., the sum of the applied and residual stresses were at least partially in tension during the load cycle). However, the crack growth in these previous tests essentially ceased once the crack left the tensile residual stress field.

To attempt to avoid this problem, most of these tests were conducted with the loads at least partly in uplift. Most of the tests were conducted with 23% of the total load range upward. This percentage of uplift is similar to but slightly greater than the 19% maximum uplift that was observed in the field studies (see Section 2.2.4.3). These rebound forces generate tensile stresses that promote continued propagation of the cracks that would arrest under downward loading only. It turns out that the problem of slow crack growth still occurs even with 23% uplift. It is believed that in service the crack growth would be more rapid because of variation of the location of the wheel loads. The wheel loads in the test are located to maximize the potential for crack initiation. However, this is not the optimum location for maximum propagation of long cracks. Therefore, in service the MBEJ may be subjected to wheel loads that cause more rapid crack propagation. Because it is not considered practical to vary the location of the wheel loads in the tests, the load ratio was altered to achieve the same effect. As explained later, the last two tests in Table 2.11 (A-4 and A-5) were conducted with the load range entirely in tension, and this eliminated the problem of slow crack growth.

For the reversal loading, a fixture was required that was capable of delivering both compressive and tensile forces directly to the specimen without any slip. It was also essential that this fixture be robust enough to survive the entire test program and yet not influence the behavior of the specimen. Figure 2.55 presents a photograph and Figure 2.56 presents a detailed drawing of the fixture. The fixture was placed on the centerbeam at the required transverse location, leveled, and clamped onto the centerbeam by the lock bolts. Each actuator was then carefully positioned on the respective beveled plate and attached with bolts. Measured strains, compared with measurements with load applied through tires, showed that this fixture had no significant influence on centerbeam behavior near the connections to the support bar.

Previous fatigue testing of MBEJ at the ATLSS Center (*44*) included complete-assembly and subassembly multiple-support-bar MBEJ specimens. These tests indicated that subassembly testing of multiple-support-bar MBEJs was valid. This conclusion was reconfirmed in the static testing described in Section 2.3, which showed that the stress distribution in the subassemblies was essentially the same as in the complete assemblies.

However, for single-support-bar systems, individual CB/SB subassemblies had not been previously tested. An MBEJ subassembly specimen typically consisted of an individual centerbeam and four equally spaced support bars. The geometry of the subassembly was of dimensions typically found in service so that appropriate shear and moment ratios were maintained. There were concerns that the effects of overall system behavior—e.g., equidistant devices—on the stresses and fatigue life would not be included. Therefore,

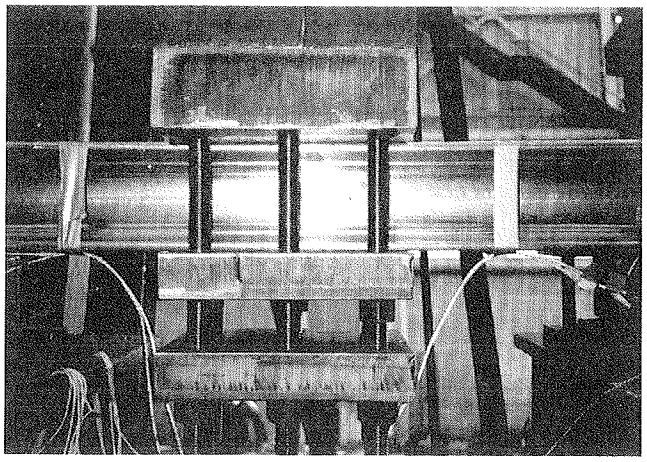

Figure 2.55. Fixture used to apply load to centerbeam.

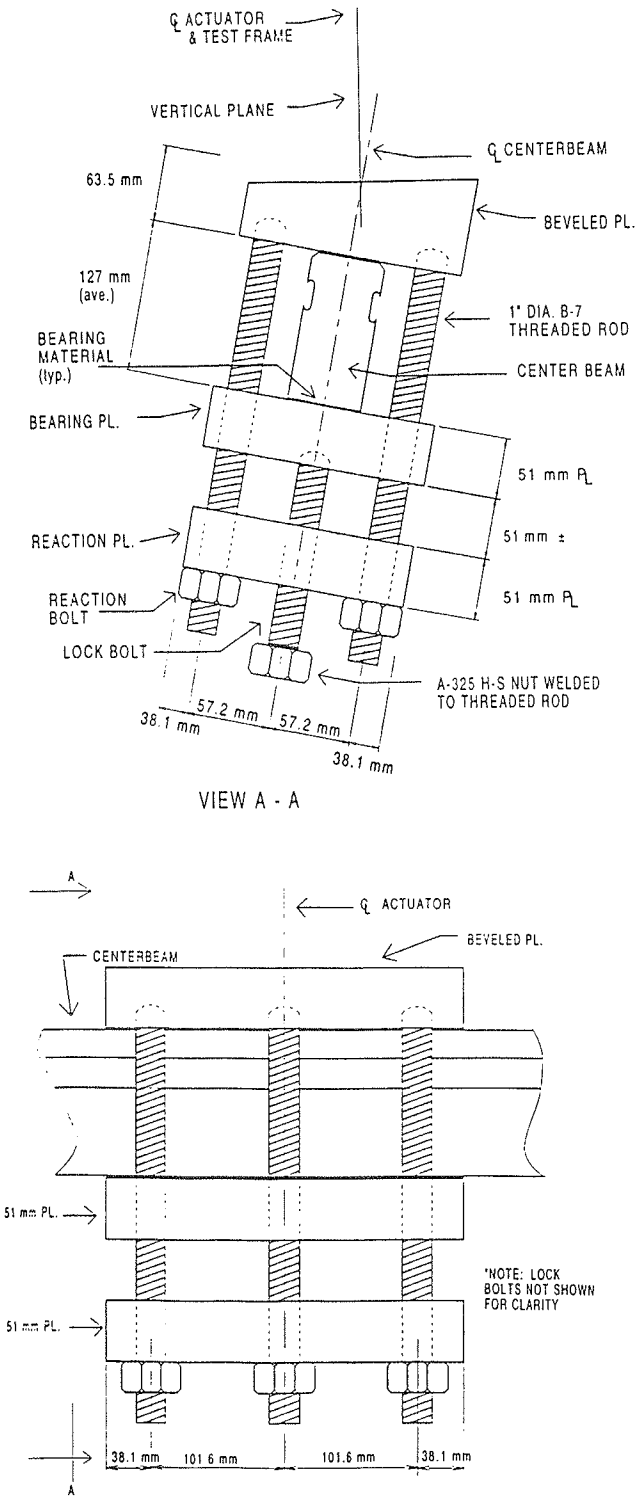

Figure 2.56. Detail of fixture used to apply load to centerbeam.

complete assemblies of the single-support-bar MBEJ systems were tested. It was concluded that the system behavior has only a relatively small effect and can be ignored. Therefore, in the recommended test procedure, subassembly tests are permitted for single-support-bar as well as multiple-support-bar systems.

The same fixture was used to grip each centerbeam separately in the complete-assembly tests. To avoid interference with the fixture, the strip seals between the centerbeams were not installed. Also, the bearings and equidistant springs in the complete-assembly tests were replaced with steel discs of about the same size. As explained previously, these elastomeric parts are incapable of taking the elevated loads at the low frequencies in these tests. A separate fatigue test procedure was developed for the elastomeric bearings, which attempts to account for the strain-rate-dependent behavior. This procedure is presented in Appendix B.

The field studies revealed that elastomeric components, when subjected to the high-frequency loading applied in the field, essentially behave as rigid supports. Loading frequencies applied in the laboratory (2 to 3Hz) are considerably lower than those measured during the field studies. Thus, replacing the elastomeric components with steel results in behavior closer to that observed in the field. Static and dynamic strain measurements were made and compared with measurements made before the elastomeric components were replaced. The steel bearings were found to have only a modest effect on measured strains.

The centerbeams C-4, C-5, and C-6 were in a complete-assembly single-support-bar MBEJ that had special attachments for equidistant control at midspan. These attachments resemble outriggers because they bear against the neighboring centerbeams. These outrigger attachments made it impossible to connect the fixture to the centerbeam for application of upward loads. A fixture capable of applying downward loads only was fabricated, and the fatigue tests on these specimens were conducted with downward loads only. During this test, the downward loads resulted in tensile stress ranges at the outrigger attachment details beneath the actuator. These were the details that cracked in these tests and not the CB/SB connection details.

When failure occurred in the complete-assembly tests and the test on one centerbeam was terminated, the specimen was repositioned and another centerbeam was fatigue tested. The support bar is actually tested three times in this procedure. However, the support bars in the single-support bar systems do not crack because there are no fatigue-critical details.

2.4.2 Fatigue Test Results

2.4.2.1 Single-Support-Bar Fatigue Tests

Fatigue tests were conducted on complete assemblies of bolted single-support-bar MBEJ systems consisting of three centerbeams. All specimens contained two continuous centerbeam spans over three equally spaced support bars (see Figure 2.57). The total load ranges applied to specimens C-1, C-2, and C-3 were such that 23% of the load range was upward and 77% of the load range was downward. Cracking occurred in the centerbeam at the location of bolt holes where stirrups for the CB/SB connection were attached. The stress

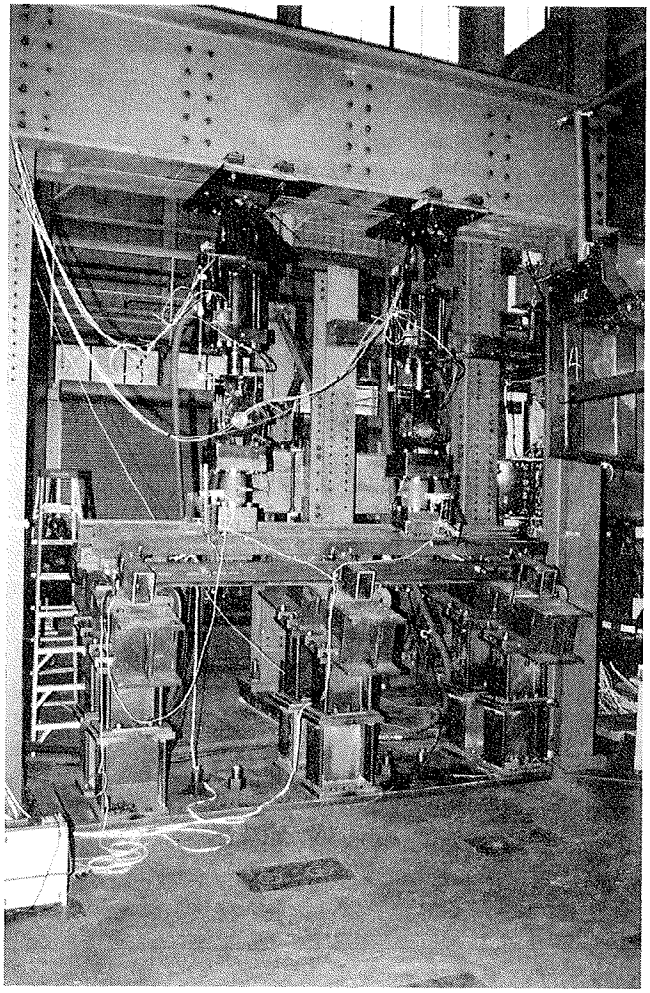

Figure 2.57. Complete-assembly fatigue test.

range is calculated for the bottom corner of the centerbeam as the sum of the net-section bending stress range in the vertical direction and the net-section bending stress range in the horizontal direction due to the centerbeam end moments at the CB/SB connection.

The centerbeams in specimens C-4, C-5, and C-6 were loaded only in compression (i.e., no uplift was applied) because of outrigger attachments as explained previously. Cracking occurred in the centerbeam at the location of bolt holes where the outrigger attachments were connected. The stress range is calculated for the bottom corner of the centerbeam from the sum of the net section vertical and horizontal bending as explained above. The bending moments in this case are the midspan moments at the location of the outrigger detail.

The results from the bolted joint tests are shown in Figure 2.58. The data associated with the outrigger details in the positive moment part of the span are shown separately from the data associated with the bolted stirrup detail in the negative moment region (at the CB/SB connection). These data show that there is no significant difference in the two bolted details. The lower bound to the fatigue strength appears to be Category D, which was expected because most types of mechanically fastened connections are also Category D details as shown in the AASHTO bridge design specifications.

Testing should be done at some later time to determine the CAFL (called the fatigue threshold stress range in the AASHTO LRFD code) for bolted CB/SB connection details for MBEJs. The fatigue threshold for Category D is 49 MPa. However, during the test the research team noticed difficulty obtaining cracks at stress ranges as high as 70 MPa. This may

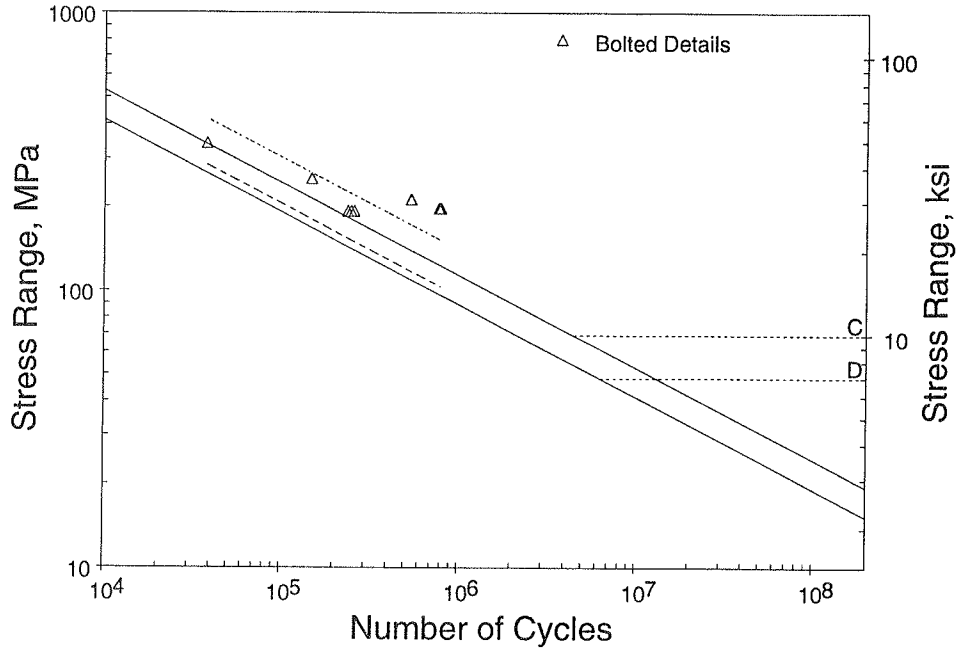

Figure 2.58. S-N plot: bolted single-support-bar CB/SB connections.

indicate that although at the relatively high stress ranges the bolted detail is a Category D detail, the bolted detail may have a threshold that is higher than the threshold for other Category D details. There are many precedents of details within a common category having unique fatigue thresholds.

Full-penetration centerbeam shop splices were included in specimens C-1, C-2, and C-3. No observed fatigue cracks developed at these splice details. However, the stress ranges at the locations of the splices were smaller than the stress ranges at the bolted details that cracked.

Only the bolted details at the outrigger and the stirrup caused cracking. No other details of the single-support-bar systems appear to be any more vulnerable to fatigue cracking than these details. Therefore, it is not necessary to duplicate all the various details in the complete-assembly tests.

The stress ranges at the critical outrigger and stirrup details were very easy to calculate and were in good agreement with the strain measurements. There was no apparent effect on the cracking from stress ranges in the outrigger or the stirrup itself but only from the stress range in the centerbeam. Therefore, it is not necessary to reproduce the complex stress ranges in the outrigger or the stirrup—i.e., it would be sufficient to have these details as passive attachments in subassembly tests. Finally, the stress ranges at the critical outrigger and stirrup details were not significantly affected when the bearings and equidistant springs were replaced with steel blocks. Therefore, it is concluded that it would be adequate to perform subassembly tests for single-support-bar MBEJs.

2.4.2.2 Multiple-Support-Bar Subassembly Fatigue Tests

All welded subassemblies except A-4 and A-5 contained a three-span continuous centerbeam over four equally spaced support bars (see Figures 2.43 and 2.46).

Full-Penetration Connections Table 2.11 summarizes specimen data and test results for the three wide full-penetration weld details and the four narrow full-penetration weld details. There were three possible cracking modes in these welded CB/SB connections, which are defined below as Types A, B, and C. In design, all three possible cracking modes must be checked, and each cracking mode requires a unique nominal stress calculation.

Type A cracking originated at the centerbeam weld toe, propagated up into the centerbeam at approximately a 45-degree angle, and grew back over the connection. This type of cracking is shown in Figure 2.59. It is well known that fatigue cracks grow perpendicularly to the plane of principal stress. Thus, a crack is an excellent indicator of the orientation of the principal stress field. Clearly the crack is driven by a combination of horizontal bending stress in the centerbeam and vertical stresses in the weld throat at this location. The vertical component is generated by the following three forces: (1) the vertical reaction at the support, (2) the overturning moment resulting form horizontal force, and (3) the end moment in the centerbeam due to support-bar restraint. The third force component is a result of the clamping forces developed in the fixture (as discussed in Section 2.3) and is

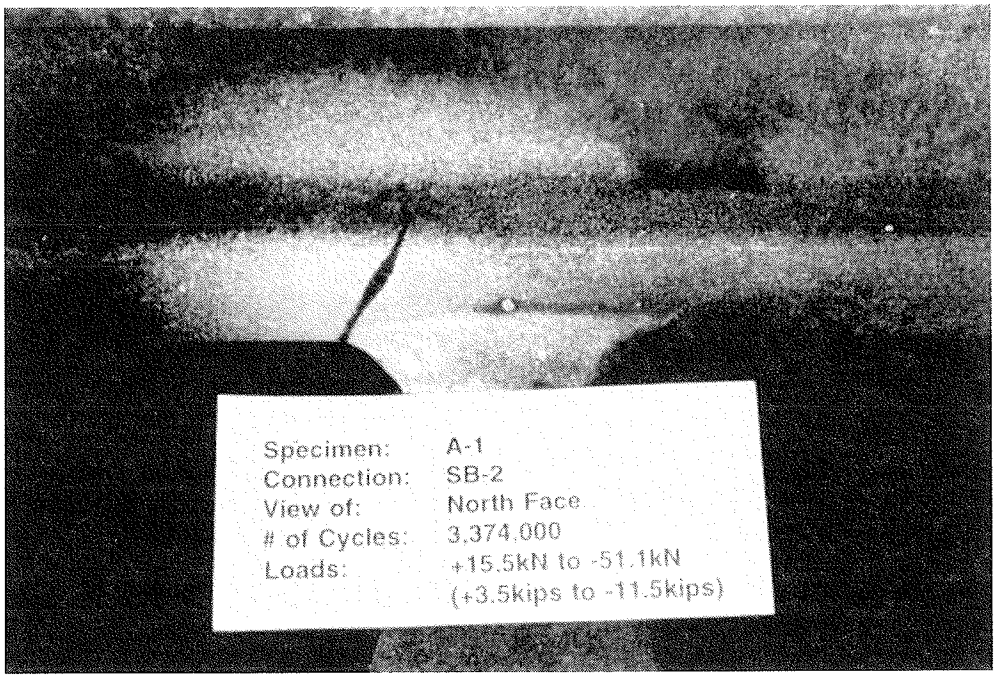

Figure 2.59. Detail of Type A crack.

not present in actual complete-assembly MBEJs. This deviation from the service loading is acceptable as long as the actual stress range at the connection detail is taken into account.

The principal stress range was obtained by taking the square root of the sum of the squares of the horizontal and vertical stress ranges (i.e., the vector sum). This estimate of the principal stress range is used because the magnitude of the shear stress ranges at the critical locations is not known. The results of this estimate are approximately correct for the range of stress combinations appropriate for MBEJs. The examples in Appendix C show the specific calculations required to determine Type A stress ranges as well as the location and orientation of the force components leading to Type A cracks.

Type B cracking originated at the support-bar weld toe, propagated down into the support bar at approximately a 45-degree angle, and grew back under the connection. This type of cracking is shown in Figure 2.60. The fatigue crack indicates the orientation of the principal stress field. As in the

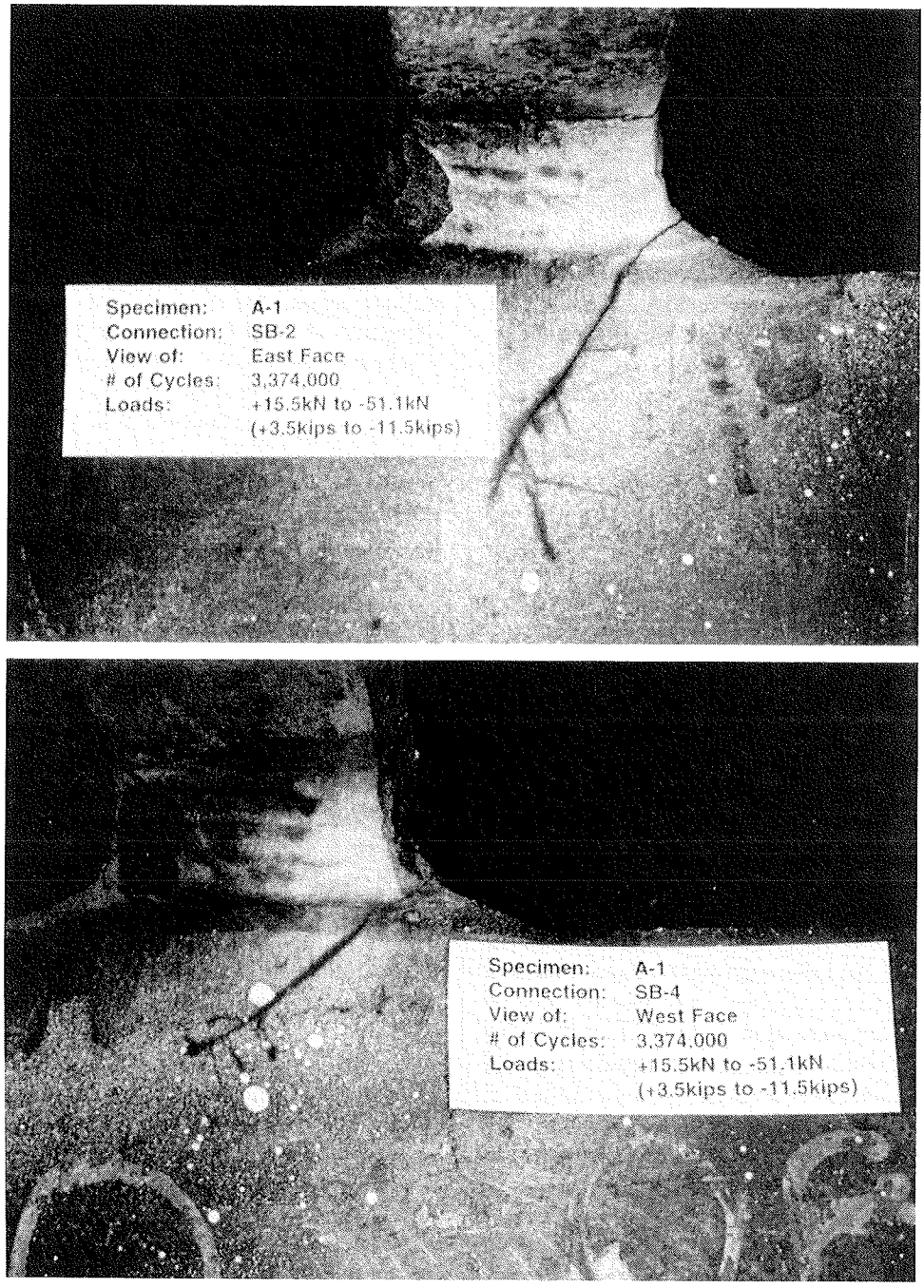

Figure 2.60. Detail of Type B crack.

case of Type A cracking, the crack is driven by a combination of horizontal and vertical stresses in this location. The vertical component is generated by the same three forces discussed for Type A cracking. In the case of Type B cracking, however, the horizontal component is a result of longitudinal support-bar bending stress. The support-bar bending moment is the sum of the moment created by the applied centerbeam reaction and the additional bending moment developed by the horizontal force applied at the top of the centerbeam. The principal stress is calculated from a vector sum of these two stress ranges. The examples in Appendix C show the specific calculations required to determine Type B stress ranges as well as the location and orientation of the force components leading to Type B cracks.

Type C cracking originated in the weld throat and typically grew in a plane parallel to the longitudinal axis of the support bar at about middepth of the weld throat (see Figure 2.61). The stress range driving Type C cracking is the vertical stress range in the throat of the weld generated by the following three components: (1) the vertical reaction at the support, (2) the overturning moment resulting from horizontal force, and (3) the end moment in the centerbeam due to end restraint. Appendix C presents the specific calculations required to determine Type C stress ranges as well as the location and orientation of the force components leading to Type C cracks as part of a detailed design example.

Type C cracking does not occur unless the magnitude of the vertical stress range in the throat of the weld exceeds the stress ranges at the weld toes for Type A and B cracking. Therefore, Type C cracking occurred only in the narrow full-penetration welds. Wider full-penetration welded details experienced Type A or B cracking only, presumably because the relative magnitude of the vertical stress range is small as a result of the much greater weld cross sections compared with the horizontal bending stress range in either the centerbeam or the support bar. The load range capacity of the narrow welds is limited by Type C cracking. For the same centerbeam and support bar, larger load range capacity generally can be obtained with the wider welds. The optimum weld width would be large enough so that Type A or B instead of Type C cracking is expected.

Occasionally, Type C cracks were observed to turn down into the support bar but only after significant growth had occurred; the crack then grew at approximately a 45-degree angle. This change in propagation direction is attributed to the changing orientation of the plane of principal stress with crack growth.

Figure 2.62 shows the stress range and cycles data for the full-penetration weld details in S-N curve format along with the AASHTO fatigue Categories C and D for reference. The mean of the data is also plotted as well as the mean − 2 standard deviations (the lower bound). The line corresponding to the mean − 2 standard deviations of the data provides a 97.5% survival probability. As indicated, the mean − 2 standard deviations is in best agreement with the S-N curve for Category D.

However, it is believed that Category D is too conservative. The lower bound is unusually low in this case because of the high standard deviation. Ironically, the high standard deviation is due primarily to the very-long-lasting test results. (These long-lasting test results do not occur when the proposed tension-only test method is used.) Thus, these good test results in effect put a penalty on the lower bound.

Most of the data fall above the Category C line. In fact the three test data that fall slightly below the Category C line were from tests that were terminated prematurely and could have run for more cycles.

The wide full-penetration weld test data are differentiated in Figure 2.62. The rate of crack growth was very slow in these wide welds. Because of limited time, these tests had to be terminated before crack extension to a depth of about 51 mm (2 in.) was attained. If these tests were continued, the data probably would have had substantially more cycles associated with failure.

As previously mentioned, the fatigue cracks in welded multiple-support-bar systems slow down when no longer affected by residual stress, even with the 23% uplift load. It is believed that this slow crack growth would not occur in service. One reason is that the position of trucks over the joint is more variable than it is in the tests. Some of the wheel loads will be in adjacent spans, where they can cause a reversal of the moment in the span with the crack. Although these reversal moments are smaller than the primary moments required for crack initiation, they are large enough to continue to propagate a crack. Therefore, it is believed that once a long crack is initiated in service, it would propagate quickly to failure because of the loads in adjacent spans in combination with the rebound loads.

Another possible reason that slow growth may not be exhibited in service is that there may be locked-in residual bending moments in the centerbeam that can keep a crack in tension. Reports from the field indicate that, after cracking the connection, centerbeams have in some cases risen up into traffic. This displacement of the centerbeam indicates that it was forced into place during construction and that these forces were locked in place when the connection was made.

The solution to the problem of slow crack growth is to conduct the tests in such a way that the applied stress range is entirely in tension at the welded detail of interest. For the typical MBEJ systems, the detail of primary interest is the CB/SB connection. To keep these details on the underside of the centerbeam in tension, the load should be entirely uplift. Tension-only loading is required in the proposed test specification. Tension-only loading simulates the possibility of a locked-in bending moment. The proposed test method would also cause cracks to propagate quickly to failure without significantly influencing the initiation and growth of small cracks.

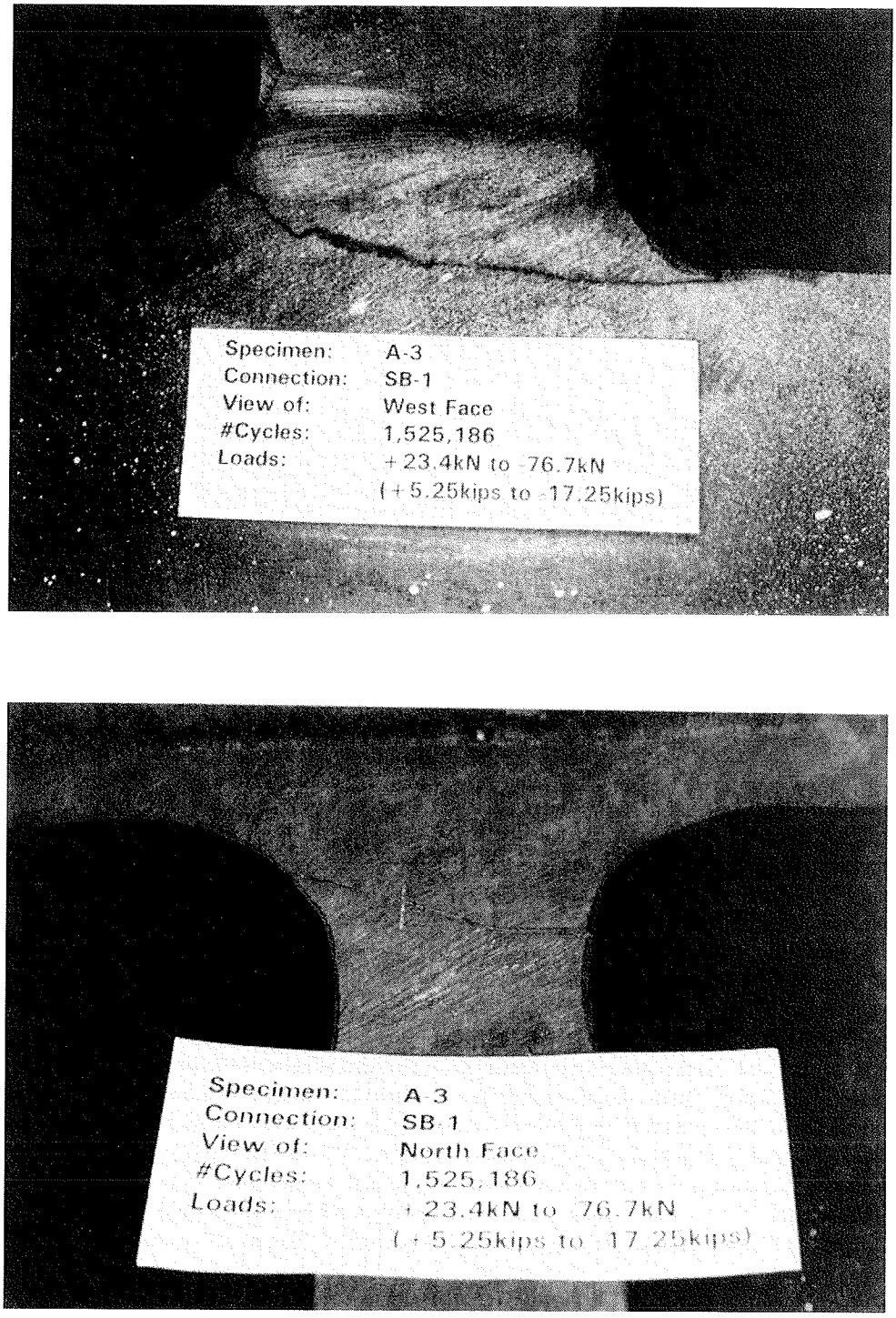

Figure 2.61. Detail of Type C crack.

One way to cause the applied stress range at the CB/SB connection to be entirely in tension is to test the subassemblies inclined as in the tests described below, but upside down, with loads in compression only. This was the technique used for the last two tests (A-4 and A-5 in Table 2.11); the data are presented in Figure 2.62. The data obtained during these tension-only tests fall within the scatter of data obtained in the tests with load reversals. Note that the fixtures for a test with the load in one direction only can be much simpler than the fixtures required for reversing load. Thus, this change also has the advantage of considerably simplifying the testing.

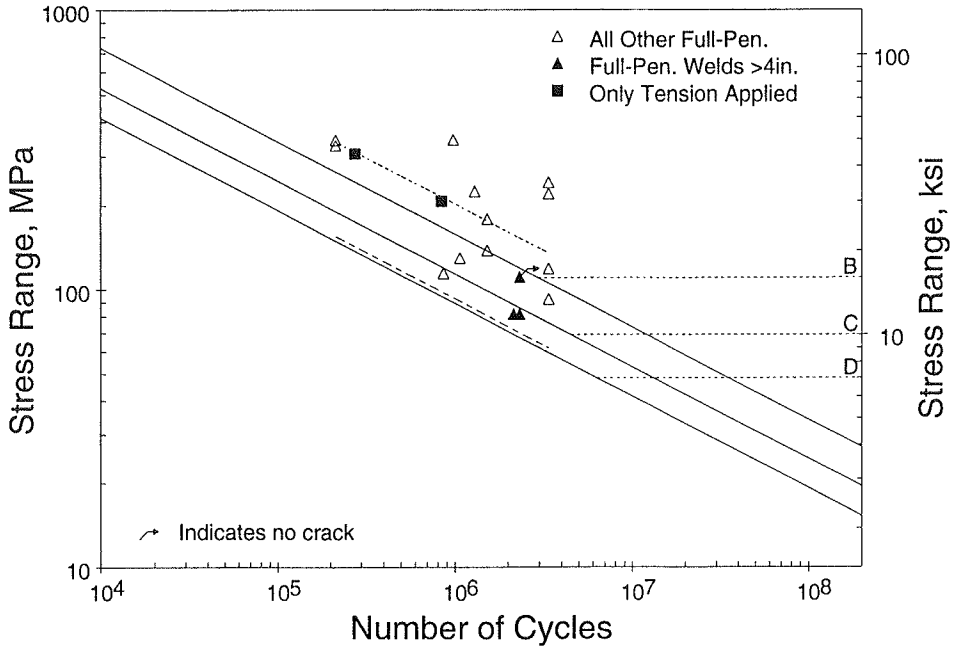

Figure 2.62. S-N plot: full-penetration CB/SB connections.

Tension-only loading could be a problem for the stirrup details in single-support-bar systems. If these systems are tested with the loads entirely in uplift, all the load will be transmitted through the stirrups. It is believed that in service at least two-thirds of the reaction force at the CB/SB connection is transferred directly in bearing through the bearing between the centerbeam and the support bar. This was confirmed in field tests where a strain gage was placed on the stirrups and very low strain ranges were observed. If the unrealistically high demand of the tension-only loading causes the stirrup detail to crack, an exception to the tension-only test requirement is allowed. These single-support-bar systems may be tested with 30% uplift and 70% downward. However, it is believed that most of the stirrup details could actually meet the more stringent tension-only test, so the reversal loading test may not be necessary at all.

There were no observed fatigue cracks in base metal away from the welded CB/SB connections. In a previous test program (*44*), it was found that Category A applied for the base metal of the centerbeam shapes, and this rarely governs the fatigue design of the MBEJ.

Fillet-Welded Connections Four specimens featured fillet-welded CB/SB connections. Figure 2.63 presents a schematic of a typical fillet-welded detail. The fill plate is inserted to provide a nominal clearance between a centerbeam and adjacent support bars. There is a large lack of fusion zone on each surface of the fill plate that effectively acts as a large built-in crack. Figure 2.64 is a photograph of a fillet-welded connection that has completely fractured. The large lack-of-fusion zone is clearly visible at the center of the connection.

Figure 2.65 presents an S-N plot of the data obtained from the fatigue tests conducted on the fillet-welded connections. The mean − 2 standard deviations falls below Category E'. The stress range for these data is calculated in terms of the entire area of the connection, including the unfused areas. This calculation is the same as the calculation that would be used for Type C cracks in full-penetration welds. In this manner, the fillet-welded connections can be compared directly with the full-penetration welded connections.

The fillet-welded connections offer a fatigue strength less than 25% of the fatigue strength of the full-penetration-welded connections. For connections of comparable size with a given set of fatigue-design loads, the fillet-welded connection would allow centerbeam spans only 25% of the length allowed by full-penetration welds. The examples in Appendix C show that the full-penetration weld details typically allow a centerbeam span up to about 1220 mm. The fillet-welded connections would allow a span of up to only 300 mm, which clearly is not feasible. Therefore, the low fatigue strength of the fillet-welded connections means that they will in effect be excluded from use once this specification is adopted. Therefore, these fillet-welded connection details are not discussed further.

Centerbeam Field Splices. As mentioned in Section 2.1.3, the centerbeam splices, especially the field splices, are

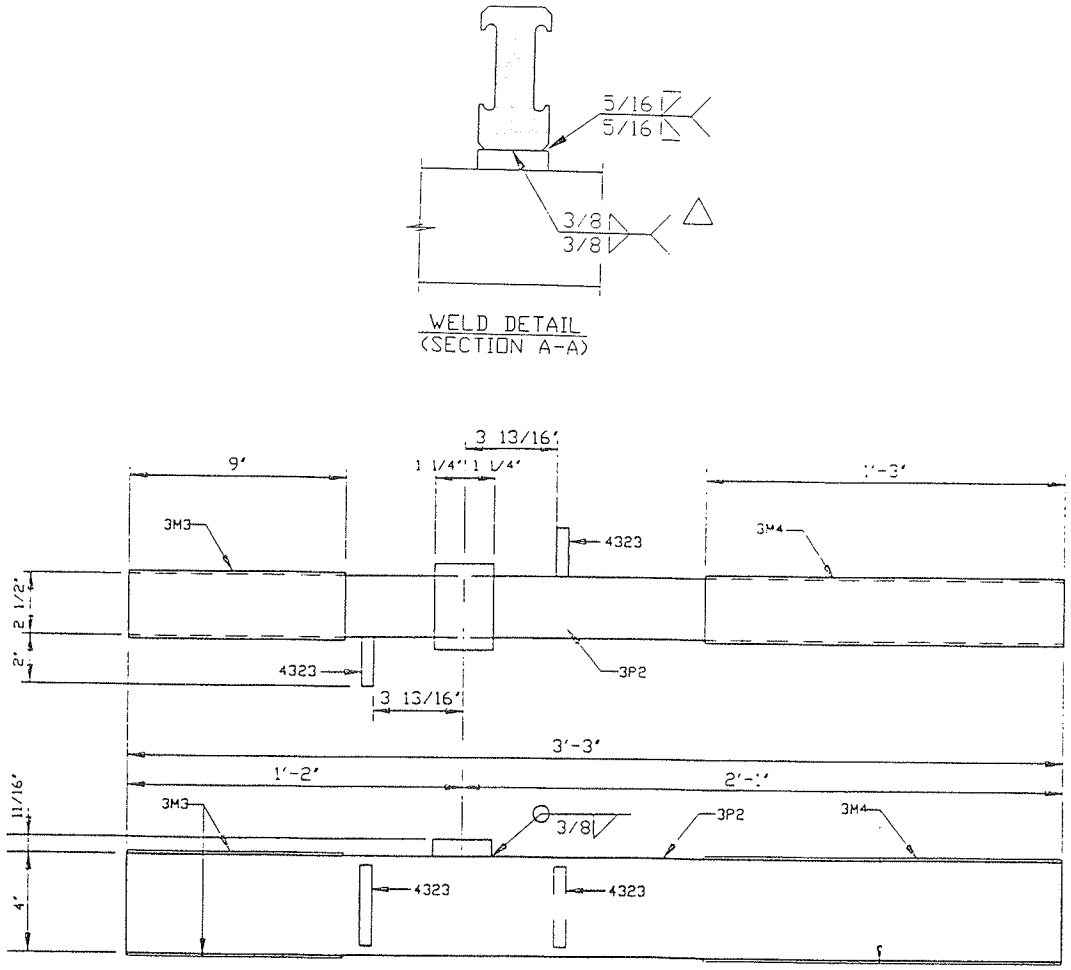

Figure 2.63. Detail of fillet-welded CB/SB connection.

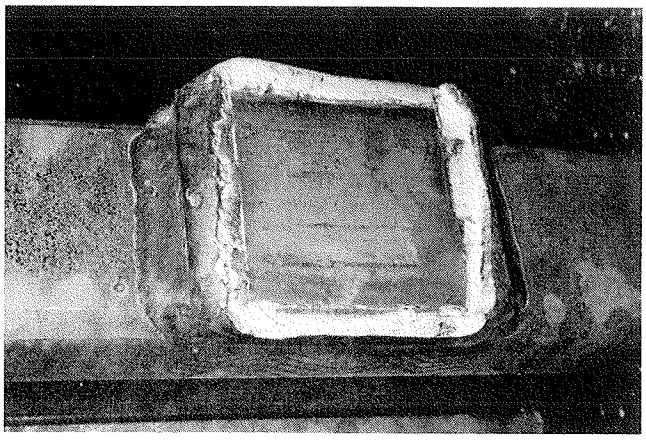

Figure 2.64. Failed fillet-welded CB/SB connection (note: support bar has completely fractured off).

one of the MBEJ details of greatest concern. Full-penetration weld splices perform well and can be expected to have a fatigue strength of Category B if the surfaces of the centerbeam are ground smooth. These full-penetration splices ordinarily should not govern the fatigue design of the MBEJ. However, a full-penetration weld can be made in the field only in the case of an MBEJ with only one centerbeam.

Full-penetration splice welds are typically made from two sides. After the root passes are placed in the first side, this root should be back-gouged to good weld metal before a weld is made from the second side. Figure 2.66 shows two typical cross sections of centerbeams with attempted full-penetration weld splices. Obviously, these welds were not back-gouged to good weld metal before a weld was made from the second side. The large unfused areas evident in the root of these welds essentially act like initial cracks. Cracks can propagate easily to failure from these unfused areas. Therefore, full-penetration welds must be back-gouged.

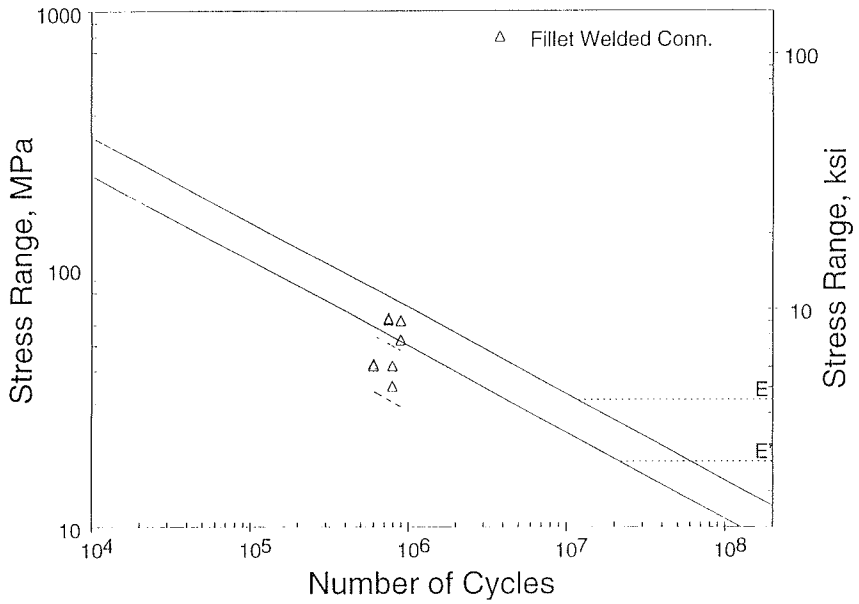

Figure 2.65. S-N plot of fillet-welded CB/SB connection.

Partial-penetration splice weld details have even larger unfused areas and should never be used.

Two other types of centerbeam splice details were included on selected subassembly specimens—the hinge detail and the fish-plate detail. The hinge detail is illustrated in Figure 2.67. One option that has been considered is to have no splice at all; instead, there are short sections of centerbeam cantilevered from two support boxes that butt together but are not joined. The problem with this arrangement is that the centerbeam ends may not be aligned. The hinge detail was then conceived to maintain alignment but still allow rotation to occur and therefore minimize the stress range in the area of the splice.

The bolt plates carry shear only (no moment). There were no observed fatigue cracks at any of the hinge details with the actuators located in Spans 1 and 3. However, the demands on the splice in the center span were not that severe with the actuators in the other spans. One test was conducted in which an actuator was positioned in Span 2 as close as possible to the hinge and a load range of +26.7 kN (+6 kips) to −89 kN (−20 kips) was applied. The percentage of vertical uplift (rebound) is consistent with the proportions measured during

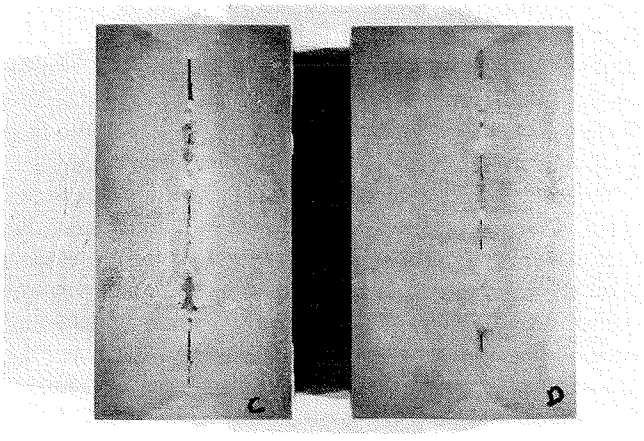

Figure 2.66. Typical cross sections of centerbeams with attempted full-penetration weld splices.

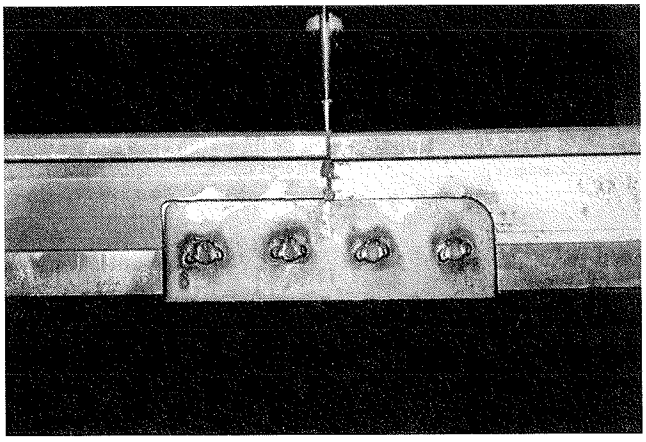

Figure 2.67. Hinge-type centerbeam field splice.

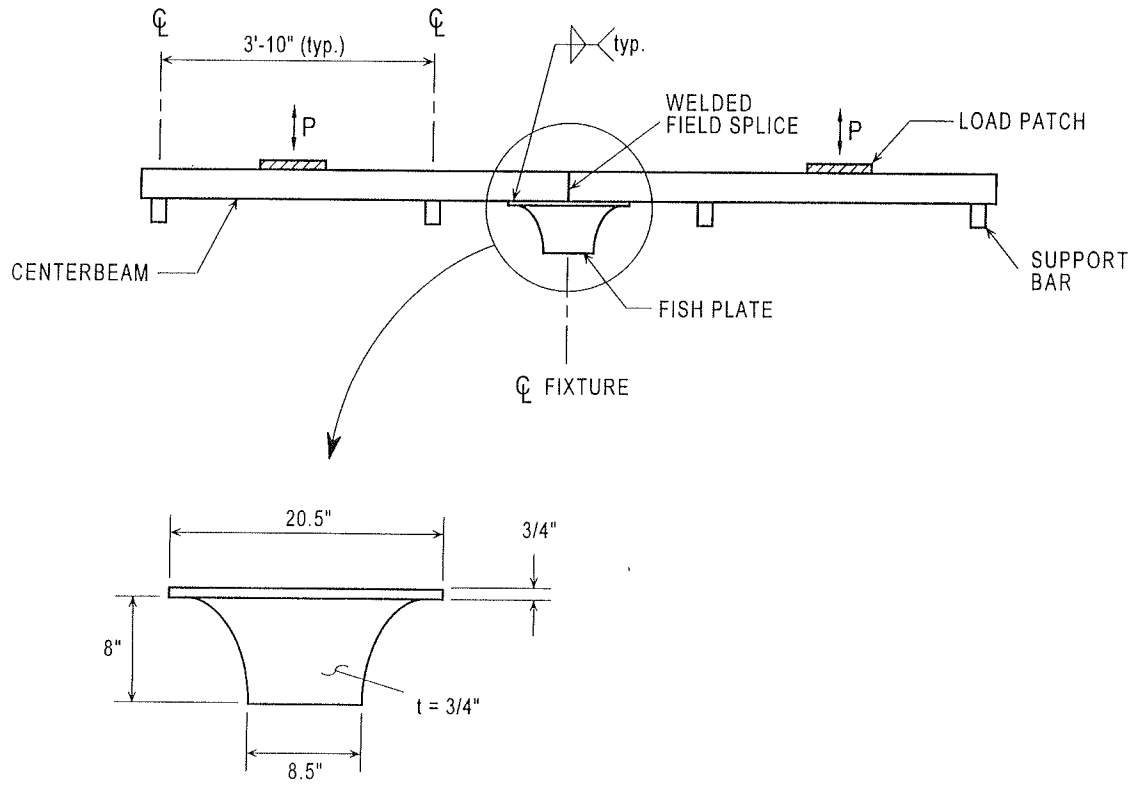

Figure 2.68. Detail of fish-plate-type centerbeam field splice.

the field studies. Because of limited time, the test was terminated at 192,000 cycles. However, because the loads were so large, this is equivalent to millions of cycles of service loads. At the end of the test, a very shallow crack was observed at a weld toe of one of the welded nuts on the south side of the connection. This crack did not appear to have any adverse affects on the performance of the connection.

Because the connection performed quite well throughout the test, it appears that such a splice is an effective way to join centerbeams in the field. Also, such a connection eliminates the possibility of fabricating a welded splice of poor quality that is susceptible to fatigue cracking. The hinge splice does not have to be explicitly designed for fatigue, because it takes no bending moment. (The shear stresses are minimal and could not govern the fatigue design.) More testing of splice details is recommended. The effects of such a connection on the joint seal and water tightness are also unknown and should be investigated.

The fish-plate-type detail illustrated in Figure 2.68 carries both moment and shear. The plate extending below the centerbeam is intended to decrease the nominal stress range in the actual centerbeam connection by increasing the section modulus. To verify this, a fish-plate connection was heavily instrumented on one specimen. The data indicate that because of shear lag through the connection, the increase in moment of inertia of the cross section is not as effective in reducing bending stresses as would be theoretically calculated.

The fish-plate details did not crack in these tests; however, the applied stress ranges in the center span were not of sufficient magnitude to cause fatigue cracking. The longitudinal splice plate is analogous to a partial-length cover plate on a beam. Because of the splice-plate geometry, it would be classified as a Category E or possibly Category E' detail. Thus, the decrease in stress range at the splice that is realized by strengthening the centerbeam is more than offset by the low fatigue strength of the cover plate detail added. Minimizing the length of the centerbeam span in which this type of splice is located could reduce the stress range and possibly allow the use of this detail. However, the hinge-type splice is considered preferable. Neither of these splice details has any significant effect on the performance of the seal.

One fish-plate splice detail has been known to fail in Washington State after 11 years of service. It was reported that the fish-plate splice broke off of the centerbeams, resulting in misalignment of the centerbeam. The cause of the failure is unclear, but it was suspected that the splice detail was not welded to one of the centerbeams.

CHAPTER 3
INTERPRETATION, APPRAISAL, AND APPLICATIONS

The literature review and the survey revealed at least three types of problems with MBEJs: (1) problems that can be traced to improper installation, (2) wear and tear of the elastomeric parts, and (3) fatigue cracking of steel parts and their connections. It is believed that construction problems have been solved by greater awareness of the potential problems, adequate installation specifications, and inspection (*9*). Currently, most of the standard job specifications have adequate installation specifications. Also, because of the use of more durable materials, wear and tear of the elastomeric parts has not been as significant a problem as it was in the past. Therefore, the focus of this research was on development of performance-based specifications and commentary for the fatigue design of the steel parts and their connections.

MBEJs have traditionally been designed by the manufacturers using proprietary techniques. Also, MBEJs are typically procured on a lowest-bid basis. Without any specifications, the low-bid process could lead to a decreased margin of safety against fatigue (*6*). Currently, there are no general design or fatigue design provisions for MBEJs in the AASHTO bridge design specifications (*12*). There are some state specifications, most of which were developed in the past few years. Many of the state specifications are derived from a specification for the state of Washington (*13,14*), which was based on work by Tschemmernegg. The state of Washington specification has fatigue design loads and performance requirements for MBEJs and requires fatigue testing. However, there are no established fatigue design procedures or specifications for carrying out the required tests (*15*).

This chapter presents the development of, and rationale for, the proposed MBEJ design specification and test specification. The requirements for this specification include the following: (1) the specifications must account for the complex dynamic behavior of the MBEJ as a system; (2) the specifications must be reasonably easy to use; and (3) the specifications must be general so that innovative new designs for MBEJs are not excluded. These requirements are often in conflict and a balance must be struck between accuracy and simplicity. A pure performance-based specification would not present a method for demonstrating adequate fatigue resistance. Therefore, a balance also must be struck between being a general performance-based specification and being sufficiently clear that the specification is interpreted in a uniform way.

The design specification proposed in Appendix A and the test specification proposed in Appendix B optimally meet these requirements. The proposed specifications are based on the findings of the literature review, survey, field testing, and laboratory testing, which were summarized in the previous chapter. The test specification is intended to determine the fatigue-resistance data required for the design procedure (i.e., the fatigue threshold stress range) for the critical connection details. Several design examples using the specification are presented in Appendix C.

The impact of the proposed specifications is discussed in Section 3.2. A typical steel MBEJ with either the full-penetration welded connection or a typical bolted connection can be designed to be resistant to fatigue cracking by using the proposed specification. MBEJ systems designed in accord with these proposed specifications should have only a slightly greater initial first cost.

3.1 DEVELOPMENT OF THE PROPOSED SPECIFICATION

The proposed specifications were designed to be integrated with the 1994 AASHTO standard specification for highway bridges—LRFD. There are aspects of the loads, fatigue performance requirements, and commentary that may be useful for a wide variety of expansion joints and other deck elements, although the details of the proposed specification apply primarily to the fatigue design and strength design of multiple-support-bar and single-support-bar MBEJs. These were the only types of MBEJ used at the time of the report. Every attempt was made to make the specification as general as possible so that it would be applicable to any new innovative types of MBEJ.

The functional design of MBEJs (e.g., what movement range to design for, how the equidistant springs work, etc.) is not addressed in this specification. There have been few reported problems of inadequate functional design, so this is not regarded as requiring additional AASHTO specifications beyond what is currently included in most state bridge specifications. The specification is also limited to the steel load-carrying components, connections, and attachments of the MBEJ. The design of the elastomeric components for strength and durability is not addressed. However, a test pro-

cedure for elastomeric bearings was developed and is included in Appendix C.

3.1.1 Fatigue-Limit State Axle Load

The fatigue lives of MBEJ details are governed by the local stress ranges, which are related to the portion of the truck axle loads carried by the individual centerbeams. As discussed in Section 2.1.4, a variable-amplitude stress-range spectrum can be represented by an effective constant-amplitude stress range equal to the rmc of all stress ranges. This rmc concept has been applied to the variable-amplitude load spectrum obtained from WIM data to determine an equivalent truck capable of producing the same cumulative fatigue damage as the variable series of trucks. The resulting truck is referred to as the fatigue truck in design and considerably simplifies fatigue evaluation by representing the variety of trucks of different weights and types found in actual traffic. Through examination of extensive WIM data, a fatigue truck equal to the HS-15 vehicle with a 9.14-m (30-ft) axle spacing was recommended in *NCHRP Report 299* (*33*). The AASHTO LRFD specifications use the HS-20 truck with a fatigue load factor of 0.75 to achieve, in effect, an HS-15 truck rather than introduce another possibly confusing design truck in the code.

The effective fatigue truck is a useful concept for the finite-life fatigue design approach—i.e., design for a specific number of cycles (typically <2 million) by using the S-N curve. The infinite-life fatigue design approach (as discussed in Section 2.1.4) was used in this proposed specification because the number of load cycles applied to MBEJs exceeds the number of cycles associated with the CAFL. In the infinite-life approach, it is postulated that fatigue cracking will never initiate if fewer than 1/10,000 cycles exceed the CAFL. The stress range with an estimated exceedence level of 1/10,000 is the important fatigue design parameter, which is called the fatigue-limit-state stress range.

Ideally, for infinite-life design of MBEJs, it is necessary to estimate the truck axle load with a 1/10,000 exceedence level. This axle load is referred to as the fatigue-limit-state axle load. There are some measured axle load spectra from WIM studies (*35,36*). Some measured spectra show many axle loads exceeding 160 kN (36 kips). However, the data in that range of the distributions (the extreme tail) are very sparse. Although the lower part of the distributions are relatively consistent from site to site, the extreme tail of the distributions from the measured axle load spectra are very site specific. Therefore, there is significant uncertainty in the appropriate value for the fatigue-limit-state axle load.

The identification of the fatigue-limit-state load was previously considered in *NCHRP Report 299* (*33*). In this case, the axle loads were not of particular interest and the spectra of GVW were studied. One term that is used in the discussion of load spectra is the α factor, which is the ratio of the effective rmc load to the fatigue-limit-state load. In *NCHRP Report 299* (*33*), it was found that the α factor for the GVW spectra was close to 0.33. With an α factor of 0.33, the fatigue-limit-state truck is about 3 times heavier than the effective fatigue truck, or about HS-45. (Actually, according to the statistics of the GVW spectra [*33*], this HS-45 fatigue-limit-state truck has an exceedence level slightly greater than the target 1/10,000 level, more like 1/5000, but this is considered close enough.)

As explained in Section 2.1.4, the AASHTO LRFD specifications imply the use of an α factor of 0.5. Therefore, the use of the HS-15 fatigue truck implies that the fatigue-limit-state truck is only HS-30. The AASHTO code was calibrated to give reasonable designs, because it was believed that the findings of *NCHRP Report 299* (*33*), which were incorporated in the *Guide Specification for Fatigue Design of Steel Bridges* (*34*), resulted in overly conservative estimates of fatigue life compared with observed service behavior.

According to the AASHTO LRFD specification, the axle load corresponding to the HS-30 truck is the fatigue-limit-state axle load. For the design of deck elements, it is the axle weights and not just the GVW that is required for fatigue evaluation. Although it is not so important for the design of most bridge elements, it is very important for the design of MBEJs to recognize that the single rear axles of the HS fatigue truck are actually an idealization of a tandem axle (*33,35*). The field test data (see, for example, Figure 2.36) clearly show each axle of the tandem-axle groups creates a unique stress cycle in an MBEJ. (As noted previously, simplification of the HS rear axles as single axles is probably not appropriate for other deck elements as well. The nature of this axle load is an issue that should be clarified in the LRFD code.) Therefore, the HS-30 tandem-axle load should be split, and in this case each axle load is 107 kN (24 kips). Therefore, the fatigue-limit-state axle load implied by the AASHTO specifications is 107 kN (24 kips).

If the recommendations of *NCHRP Report 299* (*33*) (α factor of 0.33) were followed, the fatigue-limit-state truck would be HS-45, and the corresponding split-axle load would be 160 kN (36 kips), which is in basic agreement with the measured axle load data. Thus, there is a basic discrepancy between the axle load of 107 kN (24 kips) implied by the AASHTO LRFD specifications, which has an exceedence level much more frequent than 1/10,000, and the measured axle load and GVW data, which indicate that the axle load with a 1/10,000 exceedence level is more like 160 kN (36 kips). This discrepancy presents a dilemma for development of this specification for MBEJs. On the one hand, the theoretical design axle load should correspond to the 1/10,000 exceedence level; on the other hand, it would not make sense to design MBEJs to a higher load than other deck elements. There is already a higher impact factor to account for the dynamic effects.

One point of reference is Tschemmernegg's recommended design axle load, which is incorporated in the state of Washington specifications. Tschemmernegg's recommended design load includes impact; if the impact factor of 1.82 is divided out, the static design load is 130 kN

(29 kips). No reported fatigue cracks have occurred on MBEJs that have been designed in accordance with the state of Washington specification, which has been in effect in Washington since 1993 and in other states for several years. Although time will tell, it may be concluded for now that the 130-kN static axle load is sufficient to prevent fatigue cracking. Therefore, the 160-kN (36-kip) axle load—i.e., the theoretical 1:10/000 exceedence level axle load—appears to be too conservative.

There are several advantages associated with using the load model already specified in the LRFD specification for design of MBEJs. For example, the axle loads prescribed for fatigue and strength design were rationally developed from extensive WIM data and have been found to reasonably represent the actual truck-load spectrum. More importantly, use of these loads also permits the application of load and resistance factors already prescribed in the specification. A different load for MBEJs may be confusing and would require another truck to be defined in Article 3.6.1.2.2. It would appear irrational to have a different truck for the MBEJs than for other deck elements. Therefore, the proposed specification uses the standard HS-20 fatigue design truck in the LRFD specification. In addition, if the AASHTO fatigue design truck is altered in the future, or if individual departments of transportation prescribe a greater load, there is no need to update the proposed MBEJ specifications.

After careful consideration, a compromise solution was crafted in the proposed specification. (Many compromises and tradeoffs were made in developing the proposed specifications, and these are summarized in Section 3.1.10.) The proposed specification uses the tandem axle of the standard HS-20 fatigue design truck with a load factor of 0.75, as in the LRFD specification. To compensate for any perceived lack of conservatism in the loads, a very conservative assumption is made about the distribution factors. (Distribution factors determine the share of the axle load transmitted to an individual centerbeam.) As explained in Section 3.1.2, the conservative assumption in the distribution factors results in values that are on average about 21% above the distribution factors that would correspond to the more typical assumptions that have been made in the past. The distribution factors are about 21% greater than those recommended in the state of Washington specification, for example. The effect of this conservative assumption is that the loads on a centerbeam are 21% larger than they would be if the more typical assumptions had been made.

This 21% margin can be thought of as a 21% increase in the fatigue-limit-state axle load if the more typical (smaller) distribution factors were to be used. In other words, the effect on the centerbeam is the same as if the real fatigue-limit-state axle load is 130 kN (29 kips) and the real (smaller) distribution factors were used. The real fatigue-limit-state axle load is approximately in agreement with the static axle load implied by the current state of Washington specification.

As discussed in Section 3.2, the design axle load, the distribution factors, and the other provisions of the proposed specification yield typical MBEJ designs with maximum span lengths of about 1220 mm (48 in.). As discussed in Sections 2.1.4 and 2.2, 1220 mm is the recommended maximum span length to control excessive dynamic effects in the MBEJ. MBEJ manufacturers have been able to design MBEJs to the state of Washington specification without a substantial premium in first cost. Therefore, the design axle load and the distribution factors in the proposed specification are believed to be calibrated about right.

The data obtained from field tests confirm that these proposed loads and distribution factors are conservative. The largest stress ranges measured in field tests, including the test trucks at the legal limit and the uncontrolled truck and commuter bus traffic, were <50 MPa, which is $<70\%$ of the fatigue-limit-state stress ranges calculated for these MBEJs with the fatigue-limit-state axle load and the proposed distribution factors (which were >70 MPa). In fact, most of these MBEJs would not quite meet the proposed specifications. Because these MBEJs are not cracked and the measured stress ranges are well below the fatigue threshold or CAFL for the typical details, it is concluded that these particular MBEJs are not being exposed to loads as large as those in the proposed specifications.

As explained in Section 2.1.4, wheel loads are distributed in patches of constant width that increase in length with increasing load. The area that the centerbeam has in contact with the wheel load patch is fixed, so the fraction of the load carried by one centerbeam (the distribution factor) decreases as the load increases. This interesting phenomenon of MBEJs has the fortunate effect that the increase in the centerbeam load is not proportional to the increase in the design axle load. The laboratory static tests discussed in Section 2.3 showed this phenomenon. Figure 2.48 showed that as the total axle load increases from 107 to 160 kN, an increase of 50%, the load on the centerbeam increases from 56 to 65 kN, an increase of only 16%. All except 8 kN of the additional 53 kN is transmitted to the other centerbeams as the load is increased. The percentage increase in the centerbeam is much less because the actual distribution factor decreased as the load increased. This effect mitigates the uncertainty in the total axle load.

As explained in Section 3.1.2, fixed distribution factors were chosen for the proposed specification. The proposed distribution factors were calibrated to agree with measured values for axle loads of about 130 kN. Because the distribution factors are fixed, the phenomenon described above is not apparent—i.e., the fixed distribution factors give the incorrect impression that the centerbeam loads and stress ranges increase in direct proportion to the axle load.

Aside from the fatigue-limit-state axle load, the rest of the loading spectrum does not matter when the infinite-life approach is used. Also, the total number of cycles is not required; the only requirement is that the number of cycles is large enough to exceed the number of cycles associated with the CAFL, which is almost always going to be true. Therefore, it is not necessary to know precisely the expected life of the deck and future traffic volumes. Thus, despite the uncertainty

in the appropriate value for the fatigue-limit-state axle load, it is considerably simpler to use the infinite-life approach than to try to account for the cumulative damage of the whole distribution of future axle loads, which is even more uncertain.

For strength design, two load combinations may be considered. In addition to the HS-20 truck, the 222-kN (50-kip) tandem axle [each axle is 111 kN (25 kips)] is also a possible load case. (This 222-kN tandem axle is not used for fatigue design in the AASHTO LRFD code, presumably because it is perceived to occur rarely.) Each main axle of the HS-20 vehicle (142 kN [32 kips] total) actually represents tandem axles of 71 kN (16 kips). Therefore, if the HS-20 axles are treated as tandems, it is clear the 222-kN tandem axle will govern for strength design.

3.1.2 Distribution of the Load to Centerbeams (Distribution Factor)

The distribution of load to the centerbeams was discussed in Sections 2.1.4 and 2.3.2. One way to find the load in a centerbeam is to calculate a wheel load patch size and then use one of several procedures for portioning the load to the centerbeams. However, as explained in Section 2.3.2, the patch size models are not very accurate. Furthermore, there is confusion about what factors should be applied to the wheel load before the patch size is calculated.

An alternative method for calculating the load in a centerbeam is the distribution factor, which does not require calculation of a load patch size. As explained in Section 2.3, the distribution factor is the fraction of the design wheel load range assigned to a single centerbeam. Distribution factors were determined in the field and laboratory tests from the apparent load in centerbeams on the basis of strain measurements. The distribution factor was found to be dependent on applied load, tire pressure, centerbeam width, gap width, and centerbeam height mismatch.

Unfortunately, many of the factors affecting the distribution factor are difficult to quantify individually and even more difficult to incorporate in an equation or graph. Existing methods to estimate the distribution factor, such as Tschemmernegg's graph, do not incorporate all of these variables and consequently are susceptible to error when they are used outside the originally intended range.

The measured distribution factors that are relevant to the fatigue-limit-state axle load are those corresponding to tire pressures above 650 kPa (95 lbf/in.^{2}) and relatively high loads greater than 130 kN (29 kips). The centerbeam height mismatch was within tolerance (<3 mm) in these tests. The relevant measured distribution factors are shown in Figures 3.1 and 3.2 as a function of centerbeam width for the 38-mm (1.5-in.) gap opening (about midrange) and the 76-mm (3-in.) gap opening (about maximum gap opening), respec-

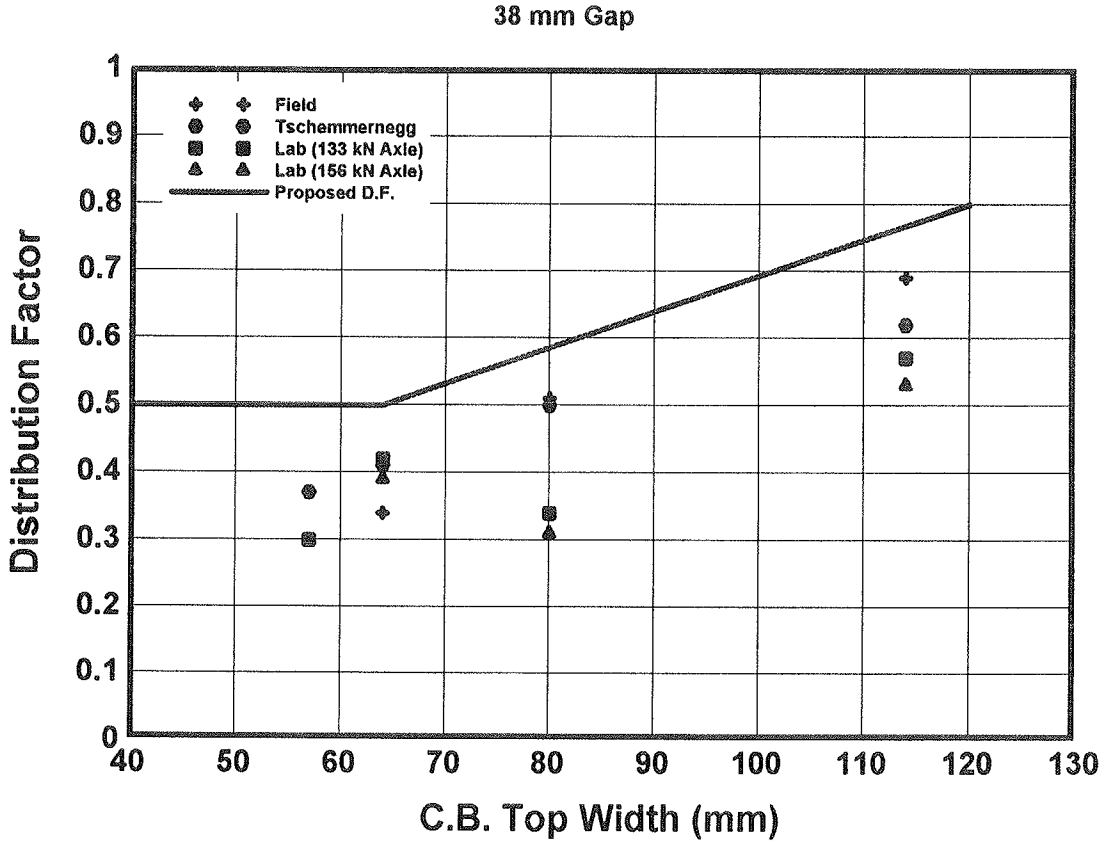

Figure 3.1. Comparison of measured distribution factors with those recommended by Tschemmernegg for a gap width of 38 mm. (Proposed distribution factor [D.F.] is also shown.)

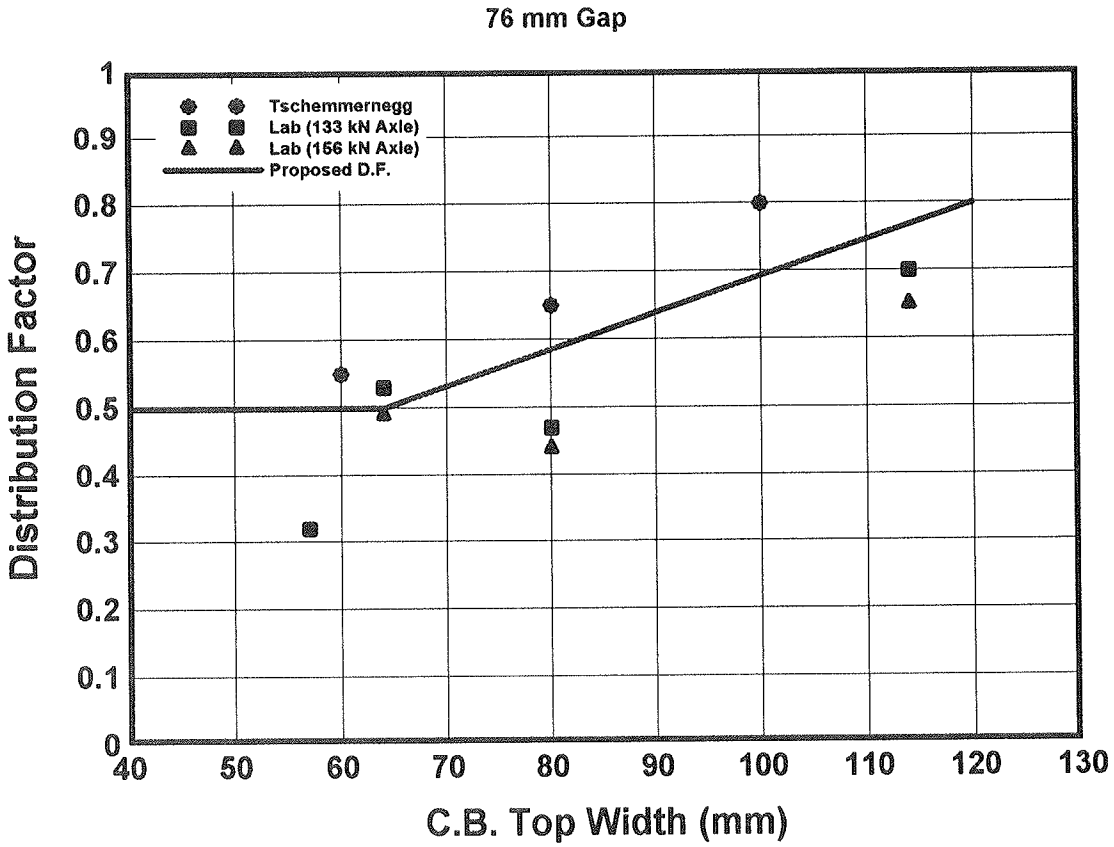

Figure 3.2. Comparison of measured distribution factors with those recommended by Tschemmernegg for a gap width of 76 mm. (Proposed distribution factor [D.F.] is also shown.)

tively. These figures also show the distribution factors from Tschemmernegg's graph. As discussed in Section 2.1.4, among the various existing schemes for distribution of loads among centerbeams, Tschemmernegg's graph gives results that agree most consistently with relevant measured data. In comparison, calculating a patch width according to current AASHTO LRFD specifications and using the distribution method for grid decks discussed in the LRFD code produced very poor agreement with experimental data and should not be used for MBEJs.

Figure 3.1 shows that the values from Tschemmernegg's graph provide a reasonable upper bound to the measured data for a gap opening of 38 mm. There is a clear trend toward increasing the distribution factor with centerbeam width, as expected. However, the measured distribution factors for the MBEJ with the 64-mm (2.5-in.)-wide centerbeams appear inconsistent with the measured distribution factors for the MBEJ with 80-mm (3.125-in.)-wide centerbeams. This inconsistency could be due to variation in centerbeam height mismatch or to a variety of other factors. The distribution factors measured in the field (the gaps were close to 38 mm) are also presented in Figure 3.1. The data from the field tests are consistent with the lower of the values from the laboratory.

Figure 3.2 indicates that, for a gap opening of 76 mm, the values from Tschemmernegg's graph are clearly too large relative to all the measured data. As was also the case in Figure 3.1, Figure 3.2 indicates that the results for the centerbeam width of 64 mm appear high relative to the trend line among the other data. Fifty percent is a reasonable upper bound value of the distribution factor for centerbeam widths up to 64 mm at the maximum gap opening. Also, no measured values of the distribution factor exceeded 70%, even for the very wide centerbeams [112 mm (4.4 in.)].

In view of the uncertainty in the distribution factor and the variation with gap opening, a simplified method is proposed to estimate the distribution factor. The simple approach was modeled after the state of Washington specification, where the distribution factor is specified for typical centerbeam widths in a table. The distribution factors in the state of Washington specification are presented in Table 3.1. These distribution factors were obtained from the graph developed by Tschemmernegg with the gap width of 38 mm—i.e., midrange.

The 38-mm gap (at midrange) is a common assumption in the fatigue design of MBEJs. The rationale for choosing the midrange of the gap (typically 38 mm) is that it is close to the mean or average opening. Although part of the time the gap and the distribution factors are larger, part of the time they are smaller. However, this argument is inconsistent with the infinite-life approach, which requires that the upper bound stress range be less than the CAFL. The largest stress ranges occur with the gap at maximum opening.

TABLE 3.1 Distribution factors (%) for 38-mm gap and 76-mm gap and proposed distribution factors

Width of Centerbeam Top Flange (mm)	Washington State (Tschemmernegg) (gap of 38 mm)	Tschemmernegg (gap of 76 mm)	Proposed Distribution Factors
60 (or less)	**40**	**50**	**50**
80	**50**	**65**	**60**
100	**60**	**80**	**70**
120			**80**

However, calculating the stress ranges at maximum gap opening is perceived as being overly conservative for fatigue. For one reason, the MBEJs are typically overdesigned for movement range, meaning that the maximum gap opening is never attained. Even though maximum gap opening occurs rarely (if at all), and there is some question about the appropriate gap opening to choose for fatigue design, maximum gap opening is clearly an appropriate assumption for checking the Strength-I limit state.

For the proposed specifications, it was decided to use the most conservative assumption with regard to gap opening in determining the distribution factors. As discussed in the previous section, this decision was made in part to compensate for a perceived lack of conservatism in the AASHTO fatigue design truck. This has the added advantage that only a single set of distribution factors are required for both the fatigue and strength limit states.

The proposed distribution factors are presented in Table 3.1 and in Figure 3.2. The proposed distribution factors are in good agreement with the measured values for a centerbeam width of 64 mm (one of the most common centerbeam sections). Figure 3.2 shows that the line of the proposed distribution factors as a function of centerbeam width has a slope that is similar to both the slope of the lower bound trend line of the measured data and the slope of the values from Tschemmernegg's graph. For centerbeam widths of 80 mm and wider, the proposed distribution factors are approximately in between the measured values and the values from Tschemmernegg's graph.

The proposed distribution factors for the maximum joint opening are about 21% above (on average) the upper-bound distribution factors (from Tschemmernegg's graph) for the joint opening at midrange. As discussed in the previous section, this ratio was shown to be about the same as the ratio between the fatigue-limit-state axle load implied by the state of Washington specifications and the AASHTO LRFD specifications. Thus, the conservative aspects of the distribution factors approximately compensate for the unconservative aspects of the AASHTO fatigue truck.

One modification of the proposed values in Table 3.1 that appears in the table in the proposed specification in Appendix A is that the centerbeam width for the minimum value of the distribution factor was increased from 60 to 64 mm. This change was made for convenience to facilitate use of the table for the most common size centerbeam, which is 63.5 mm. Otherwise, it would be necessary to interpolate for this centerbeam width without making a large difference in the resulting distribution factor.

Another advantage of using the higher distribution factor is that it may compensate for ignoring the effect of centerbeam height mismatch. Laboratory studies described in Section 2.3 indicate that a height mismatch of 3 mm resulted in a 24% increase in the measured distribution factor. The proposed distribution factors agreed with the largest of the experimental data, which may represent a typical worst case for centerbeam height mismatch within a tolerance of 3 mm.

3.1.3 Impact Factor for Vertical Load

As described in Section 2.2, the peak dynamic amplification factor measured in the field tests was 1.32. The maximum uplift was 31% of the static load, so a total load range of 1.63 times the static value is derived from these tests. (Another way to characterize the uplift would be as 23% of the amplified downward part of the vertical load or 19% of the total amplified vertical load range.) The total dynamic amplification of 1.63 is in reasonable agreement with the total dynamic amplification of 1.82 measured by Tschemmernegg, as explained in Section 2.2.1. The current 1994 AASHTO LRFD impact factor of 1.75 for expansion joints in general appears to be a reasonable worst case. (This is not surprising, because the AASHTO impact factor for expansion joints was based on Tschemmernegg's measurements on MBEJs.) Therefore, it was decided not to change the current AASHTO LRFD impact factor for MBEJs.

A joint located on a structure with significant settlement or deterioration of the approach roadway may be exposed to higher-than-expected impact forces because of dynamic excitation of the vehicle. The approach slab roughness is another potential factor. In fact, results of measurements (*41*) from an instrumented axle on a test truck indicated that deviations of −48% to +96% are possible between dynamic and

static axle loads. It would be very difficult to quantify these effects for a specification. Because field measurements were taken at a variety of locations, typical truck excitations should be reflected in the impact factor that was derived from the field measurements. The commentary to the proposed specification will mention the potential of these conditions to increase the impact factor.

At one test site with a tight horizontal curve [150-m (490-ft) radius and 8% superelevation] the vertical moments were about 20% higher than would be expected in one span and lower in another span, presumably because of centrifugal force. A factor to increase the apparent load for cases where there is a tight horizontal curve was considered. However, the maximum speed attainable for a truck on this curve was 64 km/h (40 mph). Therefore, the dynamic amplification is typically much lower than the proposed impact factor of 1.75. The decreased dynamic amplification will approximately offset the increased vertical load because of the horizontal curve. Therefore, in the interest of keeping the specification simple, the effect of horizontal curvature can safely be ignored.

The same impact factor is used for strength design, although this implies that the downward part only is amplified by the factor 1.75, because strength design deals with the peak load and not the load range. This is very conservative, because the peak downward vertical moment was 1.32 times the static moment.

3.1.4 Horizontal Load Component

When vehicles traverse an MBEJ at constant speed, a horizontal dynamic response is also excited that causes a horizontal bending moment range, again leading to an increase in stress range at details (*20,31,38*). Large horizontal forces can be applied by vehicles at MBEJs located near traffic metering devices such as stop lights or toll facilities (*19,20*). Other than the general requirement that all bridge elements should be designed for a horizontal force equal to 5% of the vertical load, there are no specific recommended horizontal loads due to wheel load impact in the AASHTO code.

The horizontal bending is critically important because the section modulus for bending in the horizontal direction may be one-fourth or even less of the section modulus in the vertical direction. The typical horizontal bending moment measured in the field was relatively small at steady speeds; the total horizontal moment response (back and forth) was $<14\%$ of the vertical moment response. In one case, a truck was presumably braking slightly and the total horizontal response was 22% of the vertical response.

Tschemmernegg reported a maximum total horizontal fatigue-limit-state load range that is 30% of the total amplified vertical fatigue-limit-state load range. However, he matched up the largest horizontal response in one direction from the long-term samples with the largest horizontal response in the other direction to obtain his total recommended horizontal load. It is likely that these two responses were not from the same vehicle; in fact they could be hours apart. This can explain why his horizontal load is a greater percentage of the vertical load than the 22% measured in the field tests (see Section 2.2). Tschemmernegg's approach is regarded as too conservative, because it essentially implies that every vehicle causes the maximum response in both directions.

Horizontal force effects resulting from braking and acceleration tests were typically much greater than measured during the steady-speed tests. In the field tests, the maximum braking effects were measured as the driver locked up the wheels and skidded across the MBEJ. The maximum horizontal moment response under these conditions was 47% of the vertical moment response at all but one site. The braking response was much greater than the response to acceleration, which was $<14\%$ of the vertical moment in all cases except one.

The exception was the Lacey V. Murrow Bridge, where the maximum horizontal moment response due to braking was 65% of the vertical moment response, and the maximum horizontal moment response due to acceleration was 29% of the vertical moment response. The extremely large horizontal forces on this MBEJ due to braking and accelerating may be a result of the large width of the centerbeam, which gives a larger surface for traction.

It is debatable whether a fatigue design specification should include the special effects of braking and accelerating in the design forces. The fatigue design approach is based on keeping almost all the loading cycles (except the largest 0.01% of occurrences) lower than the CAFL. If these braking or accelerating forces occur more frequently than 0.01% of the occurrences, then they should be included. However, it is difficult to imagine that under normal circumstances 0.01% of the vehicles will be braking as violently as was done during the field braking tests. On the other hand, more routine braking, such as occurred inadvertently during the field tests, can lead to a horizontal bending moment range as large as 22% of the total amplified vertical bending moment range.

A compromise was made in the proposed specifications. It is required that the horizontal load be 20% of the vertical load. The 20% is almost as large as the typical response due to routine braking, and therefore it is believed to be representative of typical upper-bound horizontal response. There is also a precedent for the 20% ratio; it has been used in the state of Washington specification and much of the previous testing of MBEJs was performed with a horizontal load range equal to 20% of the vertical load range.

Larger braking or acceleration forces can occur if the MBEJ is located near a traffic light, stop sign, or toll facility. Large bridge structures, which typically use MBEJs, also experience high traffic volume. As a result, these highways are frequently susceptible to congested traffic in which all vehicles are constantly stopping and starting while crossing the MBEJ. A special requirement of 50% horizontal load is

required in these cases. This special provision covers worst-case braking at most locations.

However, it is known that at least the large swivel-type single-support-bar MBEJ on the Lacey V. Murrow Bridge can have a maximum horizontal response due to braking of 65% of the vertical response. Obviously, the large swivel-type single-support-bar MBEJ on the Lacey V. Murrow Bridge is a special case with respect to horizontal response from braking or accelerating. It was decided that it would be unreasonable to increase the horizontal force requirement for ordinary MBEJs just to account for these unusual MBEJs. In the proposed commentary, it is recommended that special attention be given to the potential response that may occur for braking and accelerating on these types of large MBEJs.

Tschemmernegg reported that the maximum horizontal response due to braking was even higher—about 75% of the vertical moment response. However, he did not recommend that the larger braking forces be used in fatigue design.

In some cases, the peak horizontal response is slightly out of phase with the peak vertical response. In these cases, the two peak responses would not be additive. However, careful examination of the time histories reveals that in about one-half of cases, the peaks occur nearly in phase so that the responses would be additive. Because the infinite-life approach is used, which is based on the largest stress ranges, the assumption should be made that the peaks occur in phase. The specification will require that the effect of grade be taken into account for a grade greater than 5%. At these small angles, the increase in the horizontal load (in terms of a percentage of the vertical load) is about equal to the grade. The effect of grade was undetectable in field tests on a bridge with a grade exceeding 5% (even driving uphill and downhill over the same instrumented centerbeam span), as explained in Section 2.2.

Although horizontal loads of 20% of the amplified vertical load are specified for both fatigue and strength design, the percentages represent different types of loading for each limit state. For fatigue design, the 20% horizontal load represents a load range (i.e., 10% forward and 10% backward) and subsequently a stress range. However, for strength design, peak loads, not load ranges, are of interest. Thus, when strength is considered, the 20% horizontal component produces a peak load (not a load range) and must be applied in the direction of the braking direction. Note that this 20% peak for strength design is almost as large as peak resulting from maximum braking (one-half of 48%, or 24%). Considering that the strength vertical load is much higher with a greater load factor, this horizontal peak of 20% for strength is large enough to cover the worst possible braking or acceleration.

3.1.5 Guidance on Structural Analysis

Because of the complexity of the analysis of an MBEJ and the wide variety of assumptions that can be reasonably made, it was decided to be relatively prescriptive in the specification on how the design stress range is calculated. First, it was noted that the pair of wheel loads spaced at 1830 mm (6 ft) must be positioned to give the worst-case stress range for each particular detail. Several examples are given in the commentary. It is stated that the loads on centerbeams are to be treated as line loads along the centerline of the centerbeam—i.e., the effect of eccentricity is ignored. This is appropriate because the field test data were interpreted in the same way; therefore, any effect of eccentricity is actually built into the impact factor.

The specification allows the analysis to be conducted for the MBEJ in the midrange configuration. Because the distribution factors are already based on the worst-case gap opening, the only other effect of conducting the analysis at midrange is that the support bar span will be slightly less than if full gap opening were assumed. This minor unconservative factor is allowed because analyzing the MBEJ at midrange has been the usual procedure in the past.

Equations are provided for estimating the stress range at critical details. The equations include the following: (1) a formula for the principal stress range that governs the typical cracking in full-penetration CB/SB connection welds, and (2) a formula for the stress range in the stirrup of single-support-bar connections.

It is not known what proportion of the vertical load is carried by the stirrup as opposed to being carried directly through the bearing in a typical single-support-bar connection. It is known that very small strain fluctuations on these stirrups were measured in the field. There have been no reports of cracking due to stress ranges in the stirrup, so the possibility of no fatigue design check at all for the stress range in the stirrup was considered. However, it was believed that some fatigue strength requirement was necessary to guard against future innovative designs with inadequate stirrups. Therefore, it was decided that the stirrup should be designed for at least 30% of the total vertical load—i.e., about equal to the uplift part of the load. Horizontal load is disregarded in the analysis of stirrup details. The example problems in Appendix C verify that current typical single-support-bar connections can easily meet this requirement.

In the commentary, it is stated that the MBEJ can be accurately modeled as continuous beams on rigid supports when subjected to vertical wheel loads. For horizontal loads, it is stated that the continuous beam model is conservative but that more accurate results can be obtained from a frame analysis.

Skew is also discussed in the commentary, although skew has not been identified by any of the agencies responding as a factor that affects loading of the joint. Highly skewed MBEJs are subjected to a range of moments that includes the negative moment from the wheel in the adjoining span followed or preceded by the positive moment from the wheel in the span.

3.1.6 Guidance on Detailing

The proposed MBEJ specifications state some general requirements for the design and detailing of the bridge to accommodate MBEJ systems. Specifically, the following are required:

- Providing access to the underside of the joint system to ensure that inspection and maintenance activities are possible;
- Providing adequate concrete cover, providing adequate stiffness of the support box top plate, and installing reinforcement in the deck slab to minimize concrete cracking above support boxes; and
- Careful detailing of the joint system and deck reinforcement to ensure that proper concrete consolidation can be achieved under the support boxes.

Reference to the AASHTO LRFD bridge construction specifications is made to include additional fabrication and installation considerations and requirements.

3.1.7 Guidance on Fatigue Resistance

The fatigue design check in the specification is the same as the infinite-life provisions in the 1994 AASHTO LRFD code. The design stress range is compared with one-half of the fatigue threshold. As explained in Section 2.1.4, this is done because the fatigue design truck (and the calculated stress range) represents an effective design load, whereas the fatigue-limit-state stress range (which should be compared with the fatigue threshold) is assumed to be twice as large (α factor = 0.5).

Provisions are not included in the proposed specification for a finite-life fatigue design. Almost all structures that require a modular expansion joint carry enough truck traffic to justify an infinite-life fatigue design approach. For example, assuming an MBEJ with a 25-year life, it can be shown that with an ADTT per lane of more than 100 trucks per day, the number of cycles will exceed the number of cycles associated with the CAFL for a typical full-penetration welded CB/SB connection. A finite-life calculation would be useful only for bridges with lower ADTT. Furthermore, little cost is added to the MBEJ by designing for infinite fatigue life.

A test specification is provided in Appendix B to evaluate the fatigue resistance of the most important connection details in MBEJs. However, numerous details on the MBEJ, for which there are no test data, should be checked for fatigue. Among these details are the attachments for equidistant springs and the stainless steel slider plates, which typically do not crack in fatigue tests or in service. Because these details have no history of cracking, it was decided that, to obtain fatigue strength data, it should not be necessary to specially design a test to get them to crack.

Because it cannot be anticipated what type of details will be used in the future, the specifications state that "In cases where the details do not clearly resemble the structural details illustrated in Figure 6.6.1.2.3-1, fatigue testing shall be conducted to establish the appropriate fatigue threshold." This statement leaves up to the designer the judgment of the appropriateness of the fatigue categories in the AASHTO code and the need for testing. This judgment is routinely exercised for ordinary structural details on bridges.

As discussed in the next section, it is currently believed that the fatigue strengths of the standard welded and bolted connections are sufficiently characterized. Furthermore, the fatigue strength of these details corresponds to the expected fatigue strength for full-penetration groove welds and bolted joints based on the AASHTO fatigue design provisions for bridge structural details. As previously noted, it is suspected that the CAFL for bolted connections may be larger than currently assumed. Although it may be worthwhile to conduct additional tests to establish this greater CAFL, the current CAFL for bolted connections is conservative. Therefore, the research team believes that it should not be necessary to perform additional fatigue testing of these details or minor variations on these details.

3.1.8 Development of the Fatigue Test Procedure

The fatigue test procedure is presented in Appendix B. The objective of the fatigue testing procedure is to characterize the fatigue strength of the details. Once the fatigue strength of the details is known, the design procedure in Appendix A may be used to evaluate and design a range of MBEJ configurations by using details that are similar to those that were tested. For each configuration, the design stress range is determined by analysis, and the result is checked against the fatigue strength of the details. The tests are not intended to qualify a particular type or model of MBEJ. Each MBEJ configuration must be analyzed to determine whether it meets the specifications.

Fatigue resistance, in terms of fatigue threshold (CAFL) and the standard lower-bound S-N curves, can be established through this standard. Typically, the CB/SB connection is the critical detail or weak link with respect to the fatigue resistance of the system. Therefore, the CB/SB connection is the primary focus of the test specification. However, if there are any other details that are also susceptible to fatigue, this procedure will yield data for the fatigue resistance of these details as well.

The test procedure is based on the nominal-stress S-N curve approach and is consistent with current AASHTO fatigue design provisions. The data collected are used to establish the appropriate AASHTO fatigue category for the MBEJ details. The procedure can also be used to establish the fatigue resistance in terms of any other nominal-stress-based S-N curves, such as those included in Eurocode 3.

The specimens must be full-scale CB/SB subassemblies representative of those to be used in the field applications. Each specimen shall consist of three continuous centerbeam spans over four equally spaced support bars. Smaller subassemblies that do not consist of several continuous spans do not adequately represent the complex combined stress ranges at the critical details. Comparison of previous test data generated on smaller subassemblies with the data generated from several continuous spans indicates that the smaller subassemblies give an apparently greater fatigue strength, which is unconservative.

Some reasonable bounds on the centerbeam span length (between centerlines of support bars) and support-bar span (between centerline of bearings) are presented. Any welded or bolted attachments used to secure equidistant springs to a support bar, centerbeam, or stirrup shall be included on the specimen. A rigid load path (support fixed to the test frame or floor) shall be provided to resist any horizontal forces or displacements that are normally resisted through these attachments. In addition, any miscellaneous welded or bolted attachments shall also be included on the subassembly specimens. For example, welded attachments used to secure the elastomeric seals to the centerbeam shall be included on the specimen.

The test method requires calculating the nominal stress range at the detail of interest. The nominal stress is calculated with traditional bending and axial load equations that are used in strength design. The nominal stress does not include the effect of the local stress concentration due to the weld or bolt hole.

The number of cycles to failure typically has an order of magnitude of scatter. Therefore, a statistically significant number of data must be acquired. The test specification requires a minimum of 10 S-N curve data points. Typically, three or four cracks (data points) are obtained from each three-span specimen. Therefore, three specimens are typically required to qualify a new type of detail. Sometimes, a large number of cycles without a crack—i.e., a runout—are also a valuable data point.

Each specimen must be instrumented to measure static nominal strain ranges in the specimen, and recommendations for minimum instrumentation are made. The measured static strain ranges obtained during a calibration test shall be used to estimate the nominal moment and strain distribution in the specimen and used to verify structural analysis models. The structural analysis model is considered verified when predicted strain ranges are within ±25% of the measured strain ranges. Upon verification, the results from the structural analysis model are used in preference to the measurements to determine the nominal stress ranges at the details of interest for reporting results.

The test method describes fixtures that can be used. Typical elastomeric springs and bearings used to transfer vertical loads from the support bar to the support box must be replaced with steel bearings in the test fixture. This allows the fatigue test to be conducted at load ranges greater than those found in service.

The fatigue tests should be conducted as described in Section 2.4. The 20% ratio of horizontal-to-vertical load ranges may be obtained by inclining the specimen 11.3 degrees from the horizontal plane. To avoid problems with cracks slowing down because of applied compression stress ranges, the tests must be conducted so that the detail of interest is entirely in tension. In the normal configuration, this loading is considered uplift. However, the desired loading may also be achieved by testing the MBEJ upside down and applying the loads in compression.

The tension-only test procedure puts an unrealistic demand on the stirrup of single-support-bar MBEJs. Therefore, in the event this test procedure produces failures of the stirrup, single-support-bar systems may be tested by load reversal. The tension-only test procedure makes the stirrup take all the load range. In service, it is estimated that <30% of the load range is actually transmitted through the stirrup.

Failure criteria are specifically spelled out in the proposed test specification for a variety of types of cracks. A test may also be terminated when, for a given stress range, the specimen has survived the number of cycles required to plot the data above a particular fatigue-resistance curve. For example, if the applied stress range is 117 MPa (17 ksi) and the desired fatigue-resistance curve is Category C, then the test may be terminated after application of about 900,000 cycles. As in the design specification, specific calculations are presented for the stress ranges at various details.

Because of the large scatter inherent in fatigue tests, it is necessary to guard against the possibility of overoptimistic conclusions being drawn from a limited set of test results. Based on the results of previous fatigue testing, the upper bound of the fatigue strength for many typical details has been well characterized in the finite-life regime. Therefore, for tests at stress ranges above the CAFL (the finite-life regime), the maximum fatigue resistance (detail category) of any detail is not allowed to exceed that prescribed in Table 3.2. However, the fatigue threshold (CAFL) for these details

TABLE 3.2 Maximum permitted fatigue category for MBEJ details

Type of Detail	Maximum Permitted Category
Welded Multiple CB/SB Connections	C
Welded Stirrup Attachments for SSB Systems	B
Bolted Stirrup Attachments for SSB Systems	D
Groove-Welded Centerbeam Splices	C
Miscellaneous Welded Connections	C
Miscellaneous Bolted Connections	D

Notes:

Miscellaneous connections include attachments for equidistant devices.

Groove-welded full-penetration splices may be increased to category B if weld soundness is established by NDT.

The maximum permitted category applies only to the S-N curve at stress ranges above the threshold. A threshold that is higher than the threshold associated with these categories may be used if the threshold is established with a minimum of ten test data.

is not as well characterized. Therefore, if the testing is conducted to determine the CAFL of the detail, the test may result in a higher fatigue threshold for the detail under investigation. In such a case, all 10 data must be used to establish the fatigue threshold. The CAFL must be selected from among the CAFL for the seven AASHTO fatigue categories, corresponding to the CAFL that is just below the lowest stress range that resulted in crack.

Procedures are presented in the test specification for dealing with outliers. For example, in the event that all but one data point fall above a given desired fatigue curve, that one data point may be discarded and replaced by three new data points obtained through additional testing.

Data reporting requirements include the following:

- Nominal stress range at detail of interest (S_r);
- Applied load range for each patch;
- Number of cycles at first observation of a crack (for report purposes only, not to be used in the S-N data);
- Number of cycles at failure or termination of the test (N) and the reason for stopping the test (i.e., failure or termination);
- Type of crack;
- Joint type and manufacturer;
- A drawing showing shape, size, and dimensions of the specimen;
- Section properties and detail dimensions of the centerbeam and support bars;
- Welding procedure specifications; and
- Bolt size, bolt material specification, and method of tightening.

It is currently believed that the fatigue strength of the standard welded and bolted connections are well characterized. Furthermore, the fatigue strength of these details corresponds to the expected fatigue strength for full-penetration groove welds and bolted joints based on the AASHTO fatigue design provisions for bridge structural details. Therefore, the research team believes that it should not be necessary to perform additional fatigue testing for these details or for minor variations on these details. However, the fatigue testing provisions are useful for evaluating innovative new connections. For example, the test procedures and the performance requirements in the design specification would prevent the use of the single-bolt connection detail and the fillet-welded details that have experienced fatigue cracking in service.

3.1.9 Proposed Requirements for Elastomeric Parts

The three main types of elastomeric MBEJ parts are the seals, bearings and springs, and equidistant devices. The watertightness of the neoprene seals is essential for an MBEJ to act as an effective barrier. Several agencies require that the joint be tested for watertightness by flooding the joint under about 75 mm (3 in.) of water for several hours. This is not mentioned in the commentary because it is not known whether it is really necessary.

In addition to traffic loading, the effects of ultraviolet light or chemicals, such as deicing compounds, also contribute to seal deterioration. In general, the ASTM specifications for the seal material are sufficient to ensure adequate durability under normal wear and tear and environmental exposure. However, failures may occur because of detachment from the centerbeams, although improvements in the seal design and improved adhesive are believed to have addressed this problem. Because of these problems, some agencies do not allow the seal to be installed in the field.

The commentary does have a discussion of the problems associated with splices in the seals. If the joint is placed in stages, as in rehabilitation of existing bridges, a field splice is required in the seal if it is installed in the shop. Field splices of the seals have been a problem and therefore are typically avoided. In some cases, splices may also be prohibited by individual agencies. Therefore, in the case of staged construction, it may be advantageous to allow field-installed seals after both parts of the MBEJ are installed and spliced, so that one continuous seal can be installed without a splice.

Problems have been reported with neoprene bearings and equidistant springs becoming loose and falling out of position. Another potential problem with the bearings is fatigue or excessive wear or compression because of repeated truck loading. In addition to the fatigue test for the steel components and connections, a test procedure is also presented in Appendix B that was developed for MBEJ bearings. A displacement range is determined that corresponds to the design loads at high frequencies characteristic of service loading. To facilitate heat dissipation, the tests are conducted at lower frequencies. The test is considered successful if the load does not drop off more than 25% from the original load range after 2 million cycles. This test procedure was not the primary emphasis of this research and is considered only a preliminary requirement. However, it is known that the bearings currently in use by most manufacturers can pass the test.

It is not clear whether the problems with bearings are significant enough to warrant additional testing by this procedure. Nevertheless, the procedure is established in case it is deemed necessary. The test requirements for bearings may not be sufficient to ensure durability. Additional specifications for environmental durability should also be specified to ensure the longevity of the elastomeric components.

The equidistant devices and springs have not been a significant problem. The equidistant devices do not take significant loads from the truck loading. The largest demand on these devices comes from maximum joint movements, which occur relatively infrequently. They have been designed for adequate functionality by the manufacturers, and it is not believed that additional specifications are required.

TABLE 3.3 Significant factors affecting conservatism of specification

Conservative Factors	Unconservative Factors
Distribution factors set too high	Axle load less than 1:10,000 exceedence level
Worst-case dynamic amplification used for all MBEJ, even those with little amplification	Amplification could possibly be greater for speeding trucks
Max. amplification occurs at midspan and there is little amplification of negative bending at support	HS-20 rear axles treated as pair of axle loads
Horizontal load not always in phase	20% increase due to horizontal curve ignored
Testing is performed in all tension	Category C used for fatigue strength of F.P. welds
Use of 2-D model for horizontal loading	Possible 33% increase due to CB height mismatch ignored
Impact factor in code is greater than measured	Possible 50% horizontal component due to braking ignored in most cases
Maximum horizontal response assumed on every cycle	

Note: F.P. = full penetration

3.1.10 Summary of the Tradeoffs in the Proposed Specification

As explained in the previous sections of this chapter, compromises must be made to simultaneously meet the objectives, including simplicity, accuracy, openness, generality, and practicality. In addition, several very uncertain variables significantly affect the durability of MBEJs. Therefore, several important assumptions or simplifications have been made, the most important of which are summarized in Table 3.3.

If every assumption that was made was conservative, the resulting specification would be too conservative, costly, and impractical. Therefore, it is appropriate to make tradeoffs, so that about one-half of the assumptions will be conservative and one-half will be nonconservative. As explained in the next section, it is believed that the proposed specification is balanced and calibrated to achieve a fatigue-resistant MBEJ at only a small premium relative to current MBEJs.

3.2 IMPACT OF THE PROPOSED SPECIFICATION

The proposed specification, if followed correctly, should essentially eliminate the occurrence of fatigue cracking. The target reliability level for fatigue is 97.5% probability of no fatigue cracks over the lifetime of the MBEJ. A first attempt was also made to develop a performance test for the elastomeric bearings. The specification commentary provides a discussion of elastomeric bearings and construction-related issues that should also help reduce the occurrence of these problems. Therefore, the impact of this proposed specification should be to reduce the maintenance problems with MBEJs significantly.

The proposed specification solves a long-standing problem with MBEJs being procured on a lowest-bid basis. The specification will create a level playing field where the manufacturers can compete with products of approximately equal reliability. The proposed specification provides an established fatigue design procedure and a procedure for carrying out the required fatigue tests. The proposed specifications are reasonably easy to use but are sophisticated enough to account for the complex dynamic behavior of the MBEJ as a system. Finally, the specifications are sufficiently general so that innovative new designs for MBEJs are not excluded from consideration.

Several design examples using the specification are presented in Appendix C. A typical steel MBEJ with either the full-penetration welded connection or a typical bolted connection can be designed to be resistant to fatigue cracking by using the proposed specification. The only significant effect of the specification, besides eliminating the use of poor fatigue details such as the fillet-welded connection, is to limit the maximum centerbeam span to about 1220 mm (48 in.) for common centerbeam sections. This may cause an additional one or two support boxes to be required in a typical multilane bridge MBEJ. Therefore, MBEJ systems that are designed in accord with these proposed specifications should have only a slightly greater initial first cost. This small increase in cost will be offset by a higher level of confidence in long-term joint performance and possible decreased life-cycle costs.

The design of the MBEJ will typically be governed by the stress range at critical details for fatigue. Static strength must also be checked but will not typically govern the design. Alternative design methods and criteria may be used if such methods can be shown (through testing and analysis) to yield fatigue-resistant and safe designs.

CHAPTER 4
CONCLUSIONS AND SUGGESTED RESEARCH

4.1 CONCLUSIONS

Experimental and analytical research was carried out to develop performance-based specifications and commentary for the fatigue design of MBEJs. The following main conclusions were reached:

- Although most modern MBEJ systems have remained effective with little or no maintenance, there have been at least three types of problems: (1) problems that can be traced to improper installation, (2) wear and tear of the elastomeric parts, and (3) fatigue cracking of steel parts and their connections.
- Causes of the fatigue cracking problems include (1) the dynamic response of these systems was underestimated; (2) poor details were specified and fabricated; and (3) installation was poor.
- Field tests conducted at four different locations showed (1) MBEJ can be modeled with beam elements; (2) maximum measured dynamic vertical moment range was 1.63 times the corresponding static moment range; (3) horizontal bending moment range measured under normal driving conditions was up to 22% of the vertical bending moment range; (4) horizontal moment ranges measured during emergency braking tests were almost 50% of the total vertical moment range; and (5) the maximum measured stress ranges from typical traffic were <50 MPa, which is $<70\%$ of the stress ranges predicted based on the proposed design specification.
- Static load and strain distributions measured in the laboratory were found to be similar to the distributions measured in the field. An equivalent static load and structural analysis method were developed that produce stress ranges in the MBEJ components and connections approximately equal to the dynamic stress ranges that were measured in the field.
- A practical fatigue test procedure was developed. The fatigue resistance of full-penetration welded connections is equivalent to AASHTO Category C, and the fatigue resistance of bolted connections is equivalent to AASHTO Category D. Partial-penetration or fillet-welded CB/SB connections have very low fatigue resistance and therefore are not feasible under the proposed design specifications.
- MBEJ designed in accord with the proposed specifications should be resistant to fatigue cracking. The additional material and improved details that will be required to comply with the proposed specifications are not expected to substantially increase the initial first cost of MBEJs.

4.2 SUGGESTED RESEARCH

The following items are recommended for additional research.

- Additional fatigue testing should be conducted at stress ranges near the CAFL to better define the fatigue threshold for MBEJ details. As opposed to typical fatigue tests for MBEJ subassemblies, these tests will each last longer than 10 million cycles, which corresponds to about 40 days of continuous test time. Additional fatigue test data on various splices, equidistant spring attachments, stainless steel cover plates, and stirrup details should be acquired.
- Perform additional fatigue testing to investigate the phenomenon of slow crack growth in full-penetration welded connections.
- Review the adequacy of construction and installation specifications and prepare additional guidelines, including a training course or videotape if necessary. Prepare guidelines, a training course, or a videotape on inspection, maintenance, and repair of MBEJs in service.
- Determine the best solution to avoid reflective cracking in the concrete deck directly above support boxes, considering the relative flexibility of the top plates of the support boxes, concrete cover, transverse reinforcement over the support boxes, and slump of the concrete mixture.
- Develop a general test method that will simulate environmental exposure as well as truck loading to qualify elastomeric parts and function of MBEJs and other expansion joints.
- Review the adequacy of the material specifications for the elastomeric parts and prepare additional material specifications, test methods, and requirements if neces-

sary. Further develop the proposed fatigue test method for elastomeric bearings.

- Determine under which limited circumstances strength may control the design, and eliminate the necessity to check strength provided that fatigue strength requirements are met in all other circumstances.
- Expand the current work to develop design and test specifications for other deck elements including other types of expansion joints, grid decks, steel and aluminum orthotropic decks, and floor beams, including calculation of wheel load patch size and distribution of wheel loads to these elements and dynamic impact factors.

REFERENCES

1. Burke, M. P., Jr., "Bridge Deck Joints." *NCHRP Report 141*, Transportation Research Board, Washington, DC (1989).
2. Burke, M. P. , Jr., "Generalized Evaluations for Bridge Deck Joints." 5th Int. Bridge Conf., Pittsburgh, PA, Proc. (1988).
3. Demers, C. E., and Fisher, J.W., *Fatigue Cracking of Steel Bridge Structures, Vol 1: A Survey of Localized Cracking in Steel Bridges—1981 to 1988*. FHWA-RD-89-166. FHWA, U.S. Department of Transportation, McLean, VA (1990).
4. Bush, G. A., and Watson, R. J., "Finger Joints: A Historical Review of Design and Performance." 3rd Int. Bridge Conf., Pittsburgh, PA, Proc. (1986).
5. Bush, G. A., and Watson, R. J., "Finger Joints: A Further Evaluation Utilizing the Results of a Field Condition Survey." 4th Int. Bridge Conf., Pittsburgh, PA, Proc. (1987).
6. "Bridge Deck Joint Sealing Systems: Evaluation and Performance Specification." *NCHRP Report 204*, Transportation Research Board, Washington, DC (1979).
7. Parikh, J., and Munjal, S., *Field Evaluation of Bridge Expansion Joints*. Report FHWA/MD-84/04. Maryland Department of Transportation, (June 1989).
8. Maeda, K., Machida, F.,Tomizawa, K., Ikebe, T., and Miyazaki, S., "Durability of Bridge Expansion Joints." *IABSE Symposium*, (Sept. 1989).
9. Romack, G. P., *Performance of Bridge Deck Expansion Joints*. Summary Report FHWA-SA-91-010. FHWA, U.S. Department of Transportation, (Oct. 1990).
10. Romack, G. P., *Performance of Bridge Joint Systems Designed for Large Movements*. Research Report. FHWA, U.S. Department of Transportation, (Jan. 1992).
11. Koster, W., "Experiences and Tests with Elastomeric Seals and Springs for Modular Expansion Joints." 6th Int. Bridge Conf., Pittsburgh, PA, Proc. (1989).
12. American Association of State Highway and Transportation Officials. *Standard Specification for Highway Bridges—LRFD*. 1st Ed. Washington, DC (1994).
13. Washington State Department of Transportation, "Bridge Modular Expansion Joint System Specification." Olympia (June 1993).
14. Van Lund, J. A., "Improving the Quality and Durability of Modular Bridge Expansion Joints." *Transportation Research Record 1393*, Transportation Research Board, Washington, DC (Dec. 1993).
15. Tschemmernegg, F., and Pattis, A., "Using the Concept of Fatigue Test to Design a Modular Expansion Joint." Presented at 73rd Annual Meeting of the Transportation Research Board, Washington, DC (Jan. 1994).
16. Poellot, W. N., "Design Recommendations for Sealed Modular Bridge Expansion Joints." 8th Int. Bridge Conf., Pittsburgh, PA, Proc. (1991).
17. Roeder, C. W., *Fatigue Cracking in Modular Bridge Expansion Joints*. Research Report WA-RD 306.1, Washington State Transportation Center, Seattle, WA (June 1993).
18. Roeder, C. W., Hildahl, M., and Van Lund, J. A., "Fatigue Cracking in Modular Bridge Expansion Joints." Presented at 73rd Annual Meeting of the Transportation Research Board, Washington, DC (Jan. 1994).
19. Mayrbaurl, R. M., "Analysis of the Manhattan Bridge Modular Expansion Joints." Presented at 73rd Annual Meeting of the Transportation Research Board, Washington, DC (Jan. 1994).
20. Kaczinski, M. R., Dexter, R. J., and Connor, R. J., "Fatigue Criteria for Modular Bridge Expansion Joints." *NCHRP Interim Report, Project 12-40*, Transportation Research Board, Washington, DC (unpublished, March 1995).
21. Dahir, S. H., and Mellott, D. B., *Bridge Expansion Joints*. Research Project Report 83-37, Pennsylvania Department of Transportation, Washington, DC (Dec. 1985).
22. Rajan, S. D., and Zaniewski, J. P., *Bridge Expansion Joints and Joint Guard Angles*. State of the Art Final Report, FHWA, U.S. Department of Transportation, Washington, DC (June 1989).
23. Babaei, K., and Hawkins, N. M., *Development of Durable Anchorage Systems for Bridge Expansion Joints*. Final Report, FHWA, U.S. Department of Transportation, Washington, DC (June 1989).
24. Anlage zu Erlazz Zl., *Ubergangskonstruktionen (Grade Crossing Construction)*. Austrian Code, 800.040/32-VI/A/7/93.
25. Eurocode 3. *Design of Steel Structures, Section 9—Fatigue*. (April 1992).
26. Keating, P. B. and Fisher, J. W., "Evaluation of Fatigue Tests and Design Criteria on Welded Details." *NCHRP Report 286*, Transportation Research Board, Washington, DC (1986).
27. Pattis, A., "Dynamische Bemessung Von Wasserdichten Fahrbahnubergangen—Modulsysteme (Dynamic Design of Waterproof Modular Expansion Joints)." Ph.D. dissertation. Department of Civil Engineering and Architecture, University of Innsbruck, Austria (Dec. 1993).
28. Kluibenschedl, A., "Fatigue Design of Modular Bridge Expansion Joints According to American Codes." Diploma thesis. Department of Civil Engineering and Architecture, University of Innsbruck, Austria (1993).
29. Fisher, J. W., Nussbaumer, A., Keating, P. B., and Yen, B. T., "Resistance of Welded Details under Variable Amplitude Long-Life Fatigue Loading." *NCHRP Report 354*, Transportation Research Board, Washington, DC (1993).
30. Kaczinski, M. R., Dexter, R. J., and Van Dien, J. P., "Fatigue-Resistant Design of Cantilevered Signal Sign and Light Supports." Final Report NCHRP Project 10-38, Washington, DC (July 1996) (to be published as an NCHRP Report, 1997).
31. Tschemmernegg, F., "The Design of Modular Expansion Joints." 3rd World Congr. on Joint Sealing and Bearing Systems for Concrete Structures, Toronto, Proc. (1991).
32. Van Lund, J. A., Kaczinski, M. R., and Dexter, R. J., "Modular Bridge Expansion Joints for the Lacey V. Murrow Floating Bridge," Presented at 76th Annual Meeting of the Transportation Research Board, Washington, DC (Jan. 1997).
33. Moses, F., Schilling, C. G., and Raju, K. S., "Fatigue Evaluation Procedures for Steel Bridges." *NCHRP Report 299*, Transportation Research Board, Washington, DC (1987).

34. American Association of State Highway and Transportation Officials, *Guide Specifications for Fatigue Design of Steel Bridges*, 1st Ed., Washington, DC (1989).
35. Schilling, C. G., *Variable Amplitude Load Fatigue, Task A—Literature Review: Volume I—Traffic Loading and Bridge Response*. Publication FHWA-RD-87-059, FHWA, U.S. Department of Transportation, Washington, DC (July 1990).
36. Nowak, A. S., and Laman, J. A., "Monitoring Bridge Load Spectra." IABSE Symposium, *Extending the Lifespan of Structures*, San Francisco (1995).
37. Connor, R. J., "Fatigue Criteria for Modular Expansion Joints." M.S. thesis. Department of Civil and Environmental Engineering, Lehigh University, Bethlehem, PA (1996).
38. Tschemmernegg, F., "Messung Von Vertikal- und Horizontallasten Beim Anfahren, Bremsen und Uberrollen Von Fahrzeugen auf Einem Fahrbahnubergang (Measurement of Vertical and Horizontal Loads due to Accelerating, Braking, and Rolling Vehicles on an Expansion Joint)." *Der Bauingenieur*, Vol. 48 (1973).
39. Ostermann, M., "Stresses in Elastically Supported Modular Expansion Joints under Wheel Impact Load." *Der Bauingenieur*, Vol. 66 (1991).
40. Tschemmernegg, F., and Pattis, A., *Bericht Uber die Messungen am Fahrbahnubergang der Nettetalbrucke der Autobahn Bab 61 (Report on Measurements on Expansion Joint of Nettetal-Bridge Highway Bab 61)*. Institute of Steel and Timber Structures, Faculty of Civil Engineering and Architecture, University of Innsbruck, Austria, and the Firm Maurer Sohne, Munich, Germany (March 1991).
41. Agarwal, A. C., "Static and Dynamic Testing of a Modular Expansion Joint in the Burlington Skyway." 3rd World Congr. on Joint Sealing and Bearing Systems for Concrete Structures, Toronto, Proc. (1991).
42. Roeder, C. W., "Field Measurements of Dynamic Wheel Loads on Modular Expansion Joints." *Final Research Report Project T9233, Task 46*, Washington State Transportation Center (April 1995).
43. Tschemmernegg, F., and Pattis, A., *Fatigue Testing and Design of Modular Expansion Joints*. Report Prepared for D. S. Brown Co., New Baltimore, Ohio (March 1992).
44. Dexter, R. J., Kaczinski, M. R., and Fisher, J. W., "Fatigue Testing of Modular Expansion Joints for Bridges." IABSE Symposium, *Extending the Lifespan of Structures*, San Francisco, Vol. 73, No. 2 (1995) pp. 1091–1096.
45. Lwin, M. M., "The Lacey V. Murrow Floating Bridge, USA." *Structural Engineering International*, Vol. 3, No. 3 (1993) pp. 145–148.

APPENDIX A

PROPOSED FATIGUE DESIGN SPECIFICATION AND COMMENTARY

Section 14.5.7 Special Requirements for Modular Joints

14.5.7.1 GENERAL

Modular bridge expansion joints are structural systems which permit both translation and rotation between adjacent bridge elements. The joints are located in the plane of the bridge deck and are parallel to the centerline of bearings for a structure. This section of the specification addresses the fatigue design and strength design of modular bridge expansion joints (MBEJ). The functional design of MBEJ is not addressed.

The specification was developed primarily for the two common types of modular expansion joints, multiple and single support bar systems, including swivel-joist systems. The provisions of this section are not necessarily applicable to the design of other expansion joint systems.

The structural components, connections, and attachments of MBEJ meeting the requirements of this section of the specification should be fatigue resistant and have sufficient strength. Alternate methods of design that have been shown to achieve approximately equal or greater reliability level for fatigue resistance and strength may be used if approved by the engineer.

Multiple-Support-Bar MBEJ System

Multiple-support-bar MBEJ have transverse centerbeams which are rigidly connected to longitudinal support bars. Each support bar supports only one centerbeam. The support bars span across the joint opening and slide between elastomeric springs and bearings in support boxes to accommodate the thermal expansion and contraction of the bridge superstructure. The support boxes are cast into the concrete on both sides of the joint. For the multiple-support-bar system, a support box will hold as many support bars as there are centerbeams.

Single-Support-Bar MBEJ System

Single-support-bar MBEJ have transverse centerbeams which are attached to support bars using steel yokes and elastomeric springs and bearings. Each support bar supports all the centerbeams. The support bars span across the joint opening and slide between elastomeric springs and bearings in support boxes. The support boxes are cast into the concrete on both sides of the joint. One special type of single-support-bar MBEJ system is the swivel-joist system, in which the SB swivels as well as slides in the support boxes.

14.5.7.2 DESIGN AXLE LOADS AND IMPACT FACTORS

The centerbeams, support bars, bearings, and other structural components shall be designed for the simultaneous application of vertical and horizontal loads from a tandem axle. The tandem axle shall consist of a pair of axles spaced 1.2 m (4 ft.) apart with vertical and horizontal loads specified in Articles 14.5.7.2.1 to 14.5.7.2.3. The distribution of the wheel load among centerbeams is given in Article 14.5.7.3.

14.5.7.2.1 Vertical Axle Load for Fatigue Design

The vertical load range for fatigue design is the largest axle load from the three-axle design truck specified in Article 3.6.1.2.2. For fatigue design of modular expansion joints, this axle load shall be considered as the total load on a tandem, i.e. the total load shall be split into two axle loads spaced 1.2 m (4 ft.) apart. Only one of these tandem axles must be considered in the design, unless the joint opening exceeds 1.2 m (4 ft.). The load range shall be increased by the dynamic load allowance (Impact Factor) of 75% specified for Deck Joints in Table 3.6.2-1.

14.5.7.2.2 Vertical Axle Load for Strength Design

The vertical load for strength design shall be the design tandem axles specified in Article 3.6.1.2.3. This load shall be increased by the dynamic load allowance (Impact Factor) of 75% specified for Deck Joints in Table 3.6.2-1.

14.5.7.2.3 Horizontal Load for Fatigue Design and Strength Design

The horizontal load range for fatigue design and the horizontal load for strength design shall be 20 percent of the amplified vertical axle load (LL + IM) specified in Article 14.5.7.2.1 or 14.5.7.2.2. For MBEJ to be installed at locations where significant braking and/or acceleration forces are expected (i.e., adjacent to toll booths, traffic signals, etc.), the horizontal load range for fatigue design shall be 50 percent of the amplified vertical axle load.

For MBEJ installed on vertical grades in excess of 5 percent, the additional horizontal component due to grade shall be added to the horizontal axle load described above.

14.5.7.3 DISTRIBUTION OF WHEEL LOADS

Table 1 specifies the centerbeam distribution factor which is the percentage of the design vertical axle load and the horizontal load which shall be applied to an individual centerbeam for the design of that centerbeam and associated support bars. Distribution factors shall be interpolated for centerbeam top flange widths not given in the table, but in no case shall the distribution factor be taken as less than 50%. The remainder of the load shall be divided equally and applied to the two adjacent centerbeams or edge beams.

Table 14.5.7.3-1 - Centerbeam Distribution Factors

Width of Centerbeam Top Flange	Distribution Factor
64 mm (or less)	50%
80 mm	60%
100 mm	70%
120mm	80%

14.5.7.4 FATIGUE LIMIT STATE DESIGN REQUIREMENTS

14.5.7.4.1 General

MBEJ structural members, connections (bolted and welded), splices, and attachments shall be designed to resist the load combination for the fatigue limit state which is specified in Table 3.4.1-1 for the simultaneous application of vertical and horizontal axle loads specified in Article 14.5.7.2. Loads shall be distributed as specified in Article 14.5.7.3.

14.5.7.4.2 Design Stress Range

The nominal stress ranges (Δf) at all fatigue critical details shall be obtained from a structural analysis of the modular joint system applying the design vertical and horizontal axle loads specified in Article 14.5.7.2, distributed as specified in Article 14.5.7.3. The MBEJ shall be analyzed with a gap opening at least as large as the midrange configuration (at least half of maximum gap opening). The design axle load shall be applied as two wheel loads with transverse widths of 510 mm (20 in.) spaced in accordance with Article 3.6.1.2.2. For each detail under consideration, the wheel loads shall be positioned transversely on a centerbeam to achieve the maximum nominal stress range at that detail. The vertical and horizontal wheel loads shall be applied as line loads to the top of the centerbeams and along the centerlines of the centerbeams. The design stress range in the centerbeam/support bar connection shall be calculated according to 14.5.7.4.2a or 14.5.7.4.2b. The design nominal stress ranges (Δf) shall be used for fatigue design as specified in Article 14.5.7.4.3.

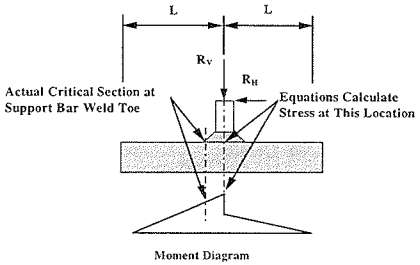

Figure 14.5.7.4.2-1

14.5.7.4.2a Welded or Bolted Single-Support-Bar Systems

Centerbeam

The nominal stress range (Δf) in the centerbeam at a welded or bolted stirrup shall be the sum of the longitudinal stress ranges in the centerbeam resulting from horizontal and vertical bending at the critical section. The effects of stresses in any load-bearing attachments such as the stirrup or yoke shall not be considered when calculating the longitudinal stress range in the centerbeam. For bolted single-support-bar systems, stress ranges shall be calculated on the net section.

Stirrup

The nominal stress range (Δf) in the stirrup or yoke shall be calculated without considering the effects of stresses in the centerbeam. The stress range shall be calculated by assuming a load range in the stirrup which is equal to 30% of the total vertical reaction force between the centerbeam and support bar. The effects of horizontal loads may be neglected in the design of the stirrup.

14.5.7.4.2b Welded Multiple-Support-Bar Systems

The equations below may be used to calculate the nominal stress range (Δf). The reduced moment on a critical cross section or the moment at the centerline of the connection may be used in these equations, as shown in Figure 14.5.7.4.1-1 for the case of the support bar.

Centerbeam Weld Toe Cracking (Type A Cracking)

Type A cracking is driven by a combination of vertical and horizontal bending stress ranges in the centerbeam (S_{RB}) and the vertical stress ranges in the weld throat (S_{RZ}) (See Figure A at the end of this section.) These two stress components shall be taken as:

$$S_{RB} = \frac{M_V}{S_{Xcb}} + \frac{M_Y}{S_{Ycb}} \qquad \textbf{(14.5.7.4.2b-1)}$$

and

$$S_{RZ} = \frac{M_{OT}}{S_{Wtop}} + \frac{R_V}{A_{Wtop}} \qquad \textbf{(14.5.7.4.2b-2)}$$

Where $M_{OT}=R_H d_{cb}$

Support Bar Weld Toe Cracking (Type B Cracking)

Type B cracking is driven by a combination of horizontal and vertical stress ranges in the connection. (See Figure B at the end of this section.)
The stress range in the support bar shall be taken as:

$$S_{RB} = \frac{M_V}{S_{Xsb}} + \frac{1}{2}\frac{R_H(d_{cb} + h_W + \frac{1}{2}d_{sb})}{S_{Xsb}} \qquad (14.5.7.4.2b\text{-}3)$$

The vertical stress range in the weld shall be taken as:

$$S_{RZ} = \frac{R_H(d_{cb} + h_W)}{S_{Wbot}} + \frac{R_V}{A_{wbot}} \qquad (14.5.7.4.2b\text{-}4)$$

Type C Cracking

The stress range driving Type C weld throat cracking (See Figure C at the end of this section.) shall be taken as:

$$S_{RZ} = \frac{R_V}{A_{Wmid}} + \frac{R_H(d_{cb} + \frac{1}{2}h_W)}{S_{Wmid}} \qquad (14.5.7.4.2b\text{-}5)$$

In the above equations:

R_V= Vertical reaction in the connection.
R_H= Horizontal reaction in the connection.
M_V= Horizontal bending moment in the centerbeam or the bending moment in the support bar due to vertical forces .
M_H= Horizontal bending moment in the centerbeam and the bending moment in the support bar due to the applied horizontal force.
S_{Xcb}, S_{Ycb}, and S_{Xsb}= Section modulus of the bottom of the centerbeam or of the support bar.
A_{Wtop}, A_{Wbot}, and A_{wbot}= Area of weld at the top, middle, and bottom of the connection, respectively.
S_{Wtop}, S_{Wbot}, and S_{Wbot}= Section modulus of the weld at the top, middle, and bottom of the connection, respectively.
h_w= Height of the weld.
d_{cb} and d_{sb}= Depth of the centerbeam and support bar respectively

The nominal stress range (Δf) at welded multiple-support-bar connection details shall be calculated for each case from the following:

$$\Delta f = \sqrt{S^2_{RB} + S^2_{RZ}} \qquad (14.5.7.4.2b\text{-}6)$$

Where:

S_{RB}= Combined bending stress range in the centerbeam or support bar, from above.
S_{RZ}= Vertical stress range in the centerbeam to support bar weld from the reaction of the support beam. Components of this stress range include the vertical load and overturning moment.

14.5.7.4.3 Design Criteria

To ensure an infinite fatigue life, all modular expansion joint structural steel members, connections (bolted and welded), splices, and attachments shall satisfy the following:

$$\Delta f \le \frac{F_{TH}}{2} \qquad (14.5.7.4.3\text{-}1)$$

where:

Δf = The nominal stress range as specified in Article 14.5.7.4.2.
F_{TH}= The fatigue threshold as specified in Article 14.5.7.5.

14.5.7.5 FATIGUE RESISTANCE

The fatigue resistance of details shall be characterized in terms of the fatigue categories described in Table 6.6.1.2.5-1. Many details used on MBEJ may be clearly associated with the structural details illustrated in Figure 6.6.1.2.3-1. In these cases, the fatigue categories for these details given in Table 6.6.1.2.3-1 may be used for design. In cases where the details do not clearly resemble the structural details illustrated in Figure 6.6.1.2.3-1, fatigue testing shall be conducted to establish the appropriate fatigue threshold.

14.5.7.6 STRENGTH-I LIMIT STATE DESIGN REQUIREMENTS

Modular expansion joint structural steel members and connections (bolted and welded) shall be designed to resist the load combination for the Strength-I limit state which is specified in Table 3.4.1-1 for the simultaneous application of vertical and horizontal axle loads specified in Article 14.5.7.2, distributed as specified in Article 14.5.7.3.

14.5.7.7 DETAILING CONSIDERATIONS

The design and detailing of the bridge to accommodate MBEJ systems shall include:

- Providing access to the underside of the joint system to ensure that inspection and maintenance activities are possible.
- Providing adequate concrete cover, providing adequate stiffness of the support box top plate, and installing reinforcement in the deck slab to minimize concrete cracking above support boxes.
- Careful detailing of the joint system and deck reinforcement to ensure that proper concrete consolidation can be achieved under the support boxes.

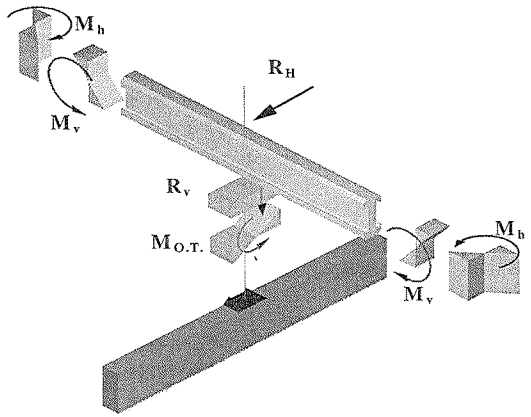

Figure A - Stresses and Forces Associated with Type A Cracking

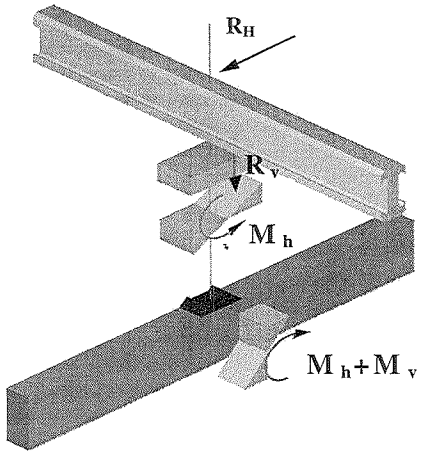

Figure B - Stresses and Forces Associated with Type B Cracking

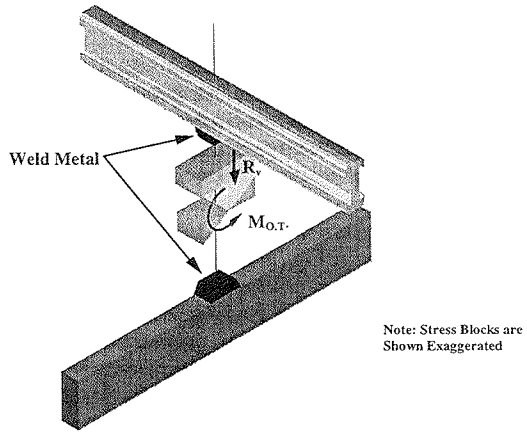

Figure-C Stresses and Forces Associated with Type C Cracking

Commentary to the Design specification

Commentary to Article 14.5.7.1:

These MBEJ design specifications provide a rational and conservative method for the design of the main load carrying steel components of MBEJ. The design of the MBEJ will typically be governed by the stress range at critical details for fatigue. Static strength must also be checked, but will typically not govern the design. Alternate design methods and criteria may be used if such methods can be shown (through testing and/or analysis) to yield fatigue-resistant and safe designs. The target reliability level for fatigue is 97.5 percent probability of no fatigue cracks over the lifetime of the MBEJ.

These specifications do not specifically address the functional design of MBEJ or the design of the elastomeric parts. These specifications are based on research performed as part of NCHRP project 12-40. The final report from this project contains extensive discussion of the loads and measured dynamic response of MBEJ, the fatigue resistance of common MBEJ details, as well as the durability of the elastomeric parts. Fatigue test procedures were developed for the structural details as well as the elastomeric bearings.

The four main types of elastomeric MBEJ parts are the seals, bearings, springs, and equidistant devices. The MBEJ manufacturers have learned which materials give good durability, and consequently the service performance of the springs and equidistance devices in most recent MBEJ is adequate. There is some concern about bearings, which can fatigue and wear and eventually fall out. The loss of a bearing causes the loss of support of a support bar and essentially doubling of the centerbeam span and the fatigue stress ranges.

The ASTM specifications for the seal material are believed to be sufficient to assure adequate durability under normal wear and tear and environmental exposure. Watertightness is sometimes tested after installation. Improvements in the design and adhesive are believed to have addressed the problem of detachment from centerbeams. Some agencies do not allow the seal to be installed in the field because of the potential for detachment. However, if the joint is placed in stages as it often is in rehabilitation of existing bridges, a field splice will be required in the seal if the seal is installed in the shop. Field splices of the seals should be avoided. Therefore, at least in the case of staged construction, field installed seals should be allowed to achieve one continuous seal without a splice; after both parts of the MBEJ are installed. Consideration should be given to the possibility of buckling of the seal in bridges with significant skew.

Another common problem is that the seals fill with debris. Traffic passing over the joint can work the seal from its anchorage by "pushing " on this debris. MBEJ systems are supposed to be self-cleaning because as the joint approaches full open and closed positions, debris is expelled from the joint. However, many designers conservatively oversize the MBEJ thus preventing the joint from being self-cleaning.

Commentary to Article 14.5.7.2:

The vertical axle load for fatigue design is one-half the 142 kN (32 kip) HS20 axle load or 71 kN (16 kip). This reduction recognizes that the main axles of the HS20 truck are a simplification of actual tandem axles. The simplification is not satisfactory for MBEJ and other expansion joints because expansion joints experience a separate stress cycle for each individual axle.

For strength design, there are two load combinations that could be considered. However, recognizing that each main axle of the HS20 vehicle should actually be treated as 142 kN (32 kip) tandems, it is clear the 222 kN (50 kip) tandem (which is not used for fatigue design) will govern for strength design.

Although horizontal loads of 20% of the total vertical load plus impact are specified for both fatigue and strength design, the percentages represent different types of loading for each limit state. For fatigue design, the 20% horizontal load represents a *load range* (i.e., 10% forward and 10% backward). However, for strength design, peak loads, not load ranges, are of interest. Thus, when strength is considered, the 20% horizontal load requirement corresponds to a peak load of 20% applied in the braking direction.

The 20 % horizontal load is greater than the expected loading from traffic at steady speeds, including the effect of acceleration and routine braking. However, horizontal force effects resulting from extreme braking can be much greater than at steady speeds. These large braking forces can occur if the MBEJ is located near a traffic light, stop sign, or toll facility. Large bridge structures which typically use MBEJ also experience high traffic volume. As a result, these highways are frequently susceptible to congested traffic in which all vehicles are constantly stopping and starting while crossing the MBEJ. In these situations, the horizontal load range for fatigue should be 50% of the total vertical load.

The larger horizontal load of 50% of the total vertical load is greater than the expected loading from extreme braking at most locations. However, it is known that at a large swivel-type single-support-bar MBEJ with unusually wide centerbeams the maximum horizontal response due to braking was 65% of the vertical response. These types of large MBEJ should be specially designed for an even greater horizontal load, as deemed necessary by the engineer.

The impact factor specified for deck joints in the LRFD code of 75 percent was developed from field testing of MBEJ conducted in Europe and was confirmed in recent field tests of MBEJ which showed that the maximum downward amplification of the response is 32 percent, with about 31 percent rebound in the upward direction. Field measurements were taken at a variety of locations, so typical truck excitations should be reflected in the impact factor. However, a joint located on a structure with significant settlement or deterioration of the approach roadway may be exposed to higher than expected impact forces due to dynamic excitation of the trucks. MBEJ with centerbeam spans less than 1220 mm (4.0 ft) are reported to have lower dynamic effects.

At sites with a tight horizontal curve (less than 150 m (490 ft.) radius) the vertical moments could be about 20 percent higher than would be expected. An increase in the impact factor for cases where there is a tight horizontal curve is not considered necessary if the speed of trucks on these curves is limited. In this case, the dynamic impact will be less than for trucks at full speed and the decreased dynamic impact will approximately

offset the increased vertical load due to the horizontal curve.

The same impact factor is used for strength design, although this implies that the downward part only is amplified by the 1.75, since strength design deals with the peak load and not the load range. The impact factor is overconservative for strength design, since the maximum measured downward vertical moment was only 1.32 times the static moment. However, strength rarely governs the design.

Commentary to Article 14.5.7.3:

The distribution factor, i.e. the fraction of the design wheel load range assigned to a single centerbeam, is a function of applied load, tire pressure, gap width, and centerbeam height mismatch. Unfortunately, many of the factors affecting the distribution factor are difficult to quantify individually and even more difficult to incorporate in an equation or graph. Existing methods to estimate the distribution factor do not incorporate all of these variables and consequently can be susceptible to error when used outside the originally intended range. In view of this uncertainty, a simplified tabular method is proposed to estimate the distribution factor.

Wheel load distribution factors shown in Table 1 are based on field and laboratory testing recently conducted as part of NCHRP Project 12-40 - *Fatigue Criteria for Modular Bridge Expansion Joints* and have been found to be in acceptable agreement with the findings of other researchers. These distribution factors are based on the worst-case assumption of maximum joint opening (maximum gap width). Calculating the stress ranges at maximum gap opening may be very conservative for fatigue. However, this conservatism compensates for a perceived lack of conservatism in the AASHTO fatigue design truck. Even though maximum gap opening occurs only rarely, it is an appropriate assumption for checking the Strength-I limit state, however.
Another advantage of using the higher distribution factors is that it may compensate for ignoring the effect of centerbeam height mismatch. Laboratory studies show that height mismatch of 3 mm resulted in a 24 percent increase in the measured distribution factor.

Commentary to Article 14.5.7.4:

Although the design axle load and distribution factors represent a "worst case", it was decided that the structural analysis for fatigue design need not represent conditions worse than average. Therefore, for fatigue loading, the assumed gap can be equal to or greater than the midrange of the gap (typically 38mm or 1.5in), which is probably close to the mean or average opening. The gap primarily affects the support bar span.

However, when considering the Strength-I limit state, the gap between centerbeams shall be assumed to be at the fully-opened position (typically 76 mm or 3 in).

Analyzing the centerbeam as a continuous beam over rigid supports has been found to give good agreement with measured strains for loads in the vertical direction. For loads in the horizontal direction, the continuous beam model is conservative. For the loads in the horizontal direction, more accurate results can be achieved by treating the centerbeams and support bars as a coplanar frame pinned at the ends of the support bars.

Maximum centerbeam stress ranges in interior spans are typically generated with one of the wheel loads centered in the span. However, if the span lengths are the same, the exterior spans (first from the curb) will typically govern the design. In an optimum

design, this exterior span should be about ten percent less than typical interior spans. The vertical and horizontal wheel loads are idealized as line loads along the centerlines of the centerbeams, i.e. it is not necessary to take into account eccentricity of the forces on the centerbeam. The maximum reaction of the centerbeam against the support bar is generated when the wheel load is centered over the support bar. This situation may govern for cracking through the throat of the centerbeam/support bar weld, for design of the stirrup of a single-support-bar system, or for cracking of the support bar.

MBEJ installed on skewed structures may require special attention in the design process. Skew is measured relative to the longitudinal axis of travel, therefore a joint transverse to the longitudinal axis is considered to have 90 degrees skew. On structures with joint skews less than 76 degrees, it can be shown that the wheels at either end of an axle will not roll over a particular centerbeam simultaneously. This asymmetric loading could significantly affect the stress range at fatigue sensitive details, either favorably or adversely. Nevertheless, a skewed centerbeam span is subjected to a range of moments which includes the negative moment from the wheel in the adjoining span, followed or preceded by the positive moment from the wheel in the span.

For all details except the welded-multiple-support-bar centerbeam to support bar connection, the design stress range can be calculated using the nominal moment at the location of interest. Special equations for calculating the stress range are provided for welded multiple-support-bar MBEJ These special equations are based on cracking described in Article 14.5.7.4.2b which has been observed in fatigue testing of welded multiple-support-bar MBEJ. For the case of welded multiple-support bar centerbeam to support bar connections, the nominal stress range is obtained by taking the square root of the sum of the squares of the horizontal stress ranges in the centerbeam or support bar and vertical stress ranges in the weld. Note this method of combining the stresses ignores the contribution of shear stresses in the region. Shear stresses are ignored in this procedure since they are typically small and very difficult to determine accurately. More details are provided in the final report for NCHRP Project-*12-40 Fatigue Criteria for Modular Bridge Expansion Joints*.

The designer must also anticipate any other fatigue critical details and check these for fatigue also. See the Commentary for Article 14.5.7.5 below.

The support bar bending stress range is a result of the sum of the bending moment created by the applied centerbeam reaction and the additional bending moment developed by the horizontal force applied at the top of the centerbeam.

Provisions are not included for a finite life fatigue design. Typically, most structures which require a modular expansion joint carry enough truck traffic to justify an infinite-life fatigue design approach. Furthermore, uncertainty regarding the number of axles per truck and the number of fatigue cycles per axle would make a finite life design approach difficult. For example, assuming an MBEJ with a 25 year life and a category C CB/SR (CAFL=10ksi), it can be shown that the maximum permissible ADTT is about 100 trucks/day if the CAFL is just slightly exceeded. With such a low limit on ADTT, a finite life calculation is not of much use. Furthermore, little cost is added to the MBEJ by designing for infinite fatigue life.

Division of the constant-amplitude fatigue limit (CAFL) by two is consistent with the fatigue provisions in Article 6.6.1.2.5. This reduction recognizes that, because of the

shape of typical truck weight spectra, the fatigue design axle load is approximately one half of the limit-state fatigue axle load and as such should be compared to one-half the CAFL. The intent of this procedure is to assure that the stress range from the fatigue limit-state load range is less than the CAFL and thereby ensuring essentially an infinite fatigue life.

Commentary to Article 14.5.7.5:

The fatigue design procedure for long-life variable-amplitude loading is based on the fatigue threshold. For most details, few tests have been conducted with the stress range near the fatigue threshold. Therefore, the emphasis in fatigue testing of details should be on defining the fatigue threshold, which requires more expensive long-term testing at stress ranges close to service stress ranges. Acceptable procedures for conducting fatigue tests are included in the Final Report for NCHRP Project 12-40 - *Fatigue Criteria for Modular Bridge Expansion Joints.*

The fatigue strength of particular details in aluminum are approximately one-third the fatigue strength of the same details in steel and therefore aluminum is typically not used in MBEJ.

Material properties (strength and fracture toughness) and weld quality have not been noted as particular problems for MBEJ.

Fatigue-critical MBEJ details include: 1) the connection between the centerbeams and the support bars; 2) connection of any attachments to the centerbeams (e.g. horizontal stabilizers or outriggers); and, 3) shop and/or field splices in the centerbeams. MBEJ details can in many cases be clearly associated with analogous details in the bridge design specifications. In other cases, the association is not clear and must be demonstrated through full-scale fatigue testing.

The detail of primary concern is the connection between the centerbeams and the support bars. A typical full-penetration welded connection, which was shown previously, can be associated with Category C. Fillet welded connections have very poor fatigue resistance and should not be allowed.

According to AASHTO bridge specifications, bolted connections should be classified as a Category D detail, with respect to the bending stress range in the centerbeam. As in any construction, more than one bolt must be used in bolted connections.

The bolted connections in single-support-bar MBEJ usually involve a yoke or stirrup through which the support bar slides and/or swivels. It is difficult to determine what fraction of the vertical reaction force range at the support bar is carried by the stirrup and what fraction passes directly through the bearing, but it is clear that the stirrup must take part of the load range, especially the uplift portion. However, there have been no particular problems noted with these stirrups.

Field-welded splices of the centerbeams and edgebeams are also prone to fatigue. In new construction, it may be possible to make a full-penetration welded splice in the field before the joint is lowered into the blockout. However, in reconstruction work, the joint is often installed in several sections at a time to maintain traffic. In these cases, the splice must be made after the joint is installed. Because of the difficulty in access and position, obtaining a full-penetration butt weld in the field after the joint is installed may

be impossible, especially if there is more than one centerbeam. Partial-penetration splice joints have inherently poor fatigue resistance and should not be allowed.

Other splice details have been proposed which add attachments to increase the moment of inertia of the centerbeam in the location of the splice in an attempt to reduce the stress range at this detail. The ends of these attachments, if welded, are often a very severe detail and therefore may create a worse condition than the field splice itself.

Bolted splices have been used and no cracking of these bolted splice details has been reported. The bolted splice plates behave like a hinge, i.e. they do not take bending moments. As a result, such details are subjected only to small shear stress ranges and need not be explicitly designed for fatigue. However, the hinge in the span creates greater bending moments at the support bar connection, therefore the span with the field splice must be much smaller than the typical spans to reduce the applied stress ranges at the support bar connection.

Thin stainless-steel slider plates are often welded like coverplates on the support bars. In the AASHTO bridge design specifications, the fatigue strength of the ends of coverplates is Category E. However, there have not been any reports of fatigue cracks at these slider plate details in MBEJ. The lack of problems may be because the support bar bending stress range is much lower at the location of the slider plate ends than at the centerbeam connection, which is the detail that typically governs the fatigue design of the support bar. Also, it is possible that the fatigue strength is greater than that of conventional cover plates, perhaps because of the thinness of the slider plate. Some manufacturers have proposed bonding the slider plates with adhesives for economical reasons. The adhesive joint would not affect the fatigue strength of the support bar and therefore could potentially be better than a welded detail. However, at least one manufacturer has had problems with the long term performance of the adhesives. As a result, many agencies require these stainless steel plates to be welded to the support bar.

Welded attachments on the sides of support bars to react against the horizontal equidistant springs are of little concern with respect to the bending stress range in the support bar because the stress range at these details is very small. In addition to checking the equidistant spring attachments with respect to the stress range in the support bar, there is also some bending load in the attachment itself. The equidistant springs take part of the horizontal load, especially in single-support bar systems. The horizontal load is also transferred through friction in the bearings and springs of the centerbeam connection. However, since this transfer is influenced by the dynamic behavior of the MBEJ, it is very difficult to quantify the load in the attachments. Since there have been no reported problems with cracking of these equidistant attachments or wear of the springs, it is recommended that they need not be explicitly designed as a loaded attachment for fatigue.

Welds for temporary attachments to the centerbeams or support bars for erection purposes must be removed and the surface ground smooth.

Commentary to Article 14.5.7.7:

Refer to the AASHTO LRFD Bridge Construction Specifications for additional fabrication and installation considerations/requirements. Many MBEJ durability problems are a result of poor detailing and/or poor construction techniques. Construction problems include poor consolidation of concrete under the support boxes, concrete in the

offset the increased vertical load due to the horizontal curve.

The same impact factor is used for strength design, although this implies that the downward part only is amplified by the 1.75, since strength design deals with the peak load and not the load range. The impact factor is overconservative for strength design, since the maximum measured downward vertical moment was only 1.32 times the static moment. However, strength rarely governs the design.

Commentary to Article 14.5.7.3:

The distribution factor, i.e. the fraction of the design wheel load range assigned to a single centerbeam, is a function of applied load, tire pressure, gap width, and centerbeam height mismatch. Unfortunately, many of the factors affecting the distribution factor are difficult to quantify individually and even more difficult to incorporate in an equation or graph. Existing methods to estimate the distribution factor do not incorporate all of these variables and consequently can be susceptible to error when used outside the originally intended range. In view of this uncertainty, a simplified tabular method is proposed to estimate the distribution factor.

Wheel load distribution factors shown in Table 1 are based on field and laboratory testing recently conducted as part of NCHRP Project 12-40 - *Fatigue Criteria for Modular Bridge Expansion Joints* and have been found to be in acceptable agreement with the findings of other researchers. These distribution factors are based on the worst-case assumption of maximum joint opening (maximum gap width). Calculating the stress ranges at maximum gap opening may be very conservative for fatigue. However, this conservatism compensates for a perceived lack of conservatism in the AASHTO fatigue design truck. Even though maximum gap opening occurs only rarely, it is an appropriate assumption for checking the Strength-I limit state, however.

Another advantage of using the higher distribution factors is that it may compensate for ignoring the effect of centerbeam height mismatch. Laboratory studies show that height mismatch of 3 mm resulted in a 24 percent increase in the measured distribution factor.

Commentary to Article 14.5.7.4:

Although the design axle load and distribution factors represent a "worst case", it was decided that the structural analysis for fatigue design need not represent conditions worse than average. Therefore, for fatigue loading, the assumed gap can be equal to or greater than the midrange of the gap (typically 38mm or 1.5in), which is probably close to the mean or average opening. The gap primarily affects the support bar span.

However, when considering the Strength-I limit state, the gap between centerbeams shall be assumed to be at the fully-opened position (typically 76 mm or 3 in).

Analyzing the centerbeam as a continuous beam over rigid supports has been found to give good agreement with measured strains for loads in the vertical direction. For loads in the horizontal direction, the continuous beam model is conservative. For the loads in the horizontal direction, more accurate results can be achieved by treating the centerbeams and support bars as a coplanar frame pinned at the ends of the support bars.

Maximum centerbeam stress ranges in interior spans are typically generated with one of the wheel loads centered in the span. However, if the span lengths are the same, the exterior spans (first from the curb) will typically govern the design. In an optimum

design, this exterior span should be about ten percent less than typical interior spans. The vertical and horizontal wheel loads are idealized as line loads along the centerlines of the centerbeams, i.e. it is not necessary to take into account eccentricity of the forces on the centerbeam. The maximum reaction of the centerbeam against the support bar is generated when the wheel load is centered over the support bar. This situation may govern for cracking through the throat of the centerbeam/support bar weld, for design of the stirrup of a single-support-bar system, or for cracking of the support bar.

MBEJ installed on skewed structures may require special attention in the design process. Skew is measured relative to the longitudinal axis of travel, therefore a joint transverse to the longitudinal axis is considered to have 90 degrees skew. On structures with joint skews less than 76 degrees, it can be shown that the wheels at either end of an axle will not roll over a particular centerbeam simultaneously. This asymmetric loading could significantly affect the stress range at fatigue sensitive details, either favorably or adversely. Nevertheless, a skewed centerbeam span is subjected to a range of moments which includes the negative moment from the wheel in the adjoining span, followed or preceded by the positive moment from the wheel in the span.

For all details except the welded-multiple-support-bar centerbeam to support bar connection, the design stress range can be calculated using the nominal moment at the location of interest. Special equations for calculating the stress range are provided for welded multiple-support-bar MBEJ These special equations are based on cracking described in Article 14.5.7.4.2b which has been observed in fatigue testing of welded multiple-support-bar MBEJ. For the case of welded multiple-support bar centerbeam to support bar connections, the nominal stress range is obtained by taking the square root of the sum of the squares of the horizontal stress ranges in the centerbeam or support bar and vertical stress ranges in the weld. Note this method of combining the stresses ignores the contribution of shear stresses in the region. Shear stresses are ignored in this procedure since they are typically small and very difficult to determine accurately. More details are provided in the final report for NCHRP Project-*12-40 Fatigue Criteria for Modular Bridge Expansion Joints.*

The designer must also anticipate any other fatigue critical details and check these for fatigue also. See the Commentary for Article 14.5.7.5 below.

The support bar bending stress range is a result of the sum of the bending moment created by the applied centerbeam reaction and the additional bending moment developed by the horizontal force applied at the top of the centerbeam.

Provisions are not included for a finite life fatigue design. Typically, most structures which require a modular expansion joint carry enough truck traffic to justify an infinite-life fatigue design approach. Furthermore, uncertainty regarding the number of axles per truck and the number of fatigue cycles per axle would make a finite life design approach difficult. For example, assuming an MBEJ with a 25 year life and a category C CB/SB (CAFL=10ksi), it can be shown that the maximum permissible ADTT is about 100 trucks/day if the CAFL is just slightly exceeded. With such a low limit on ADTT, a finite life calculation is not of much use. Furthermore, little cost is added to the MBEJ by designing for infinite fatigue life.

Division of the constant-amplitude fatigue limit (CAFL) by two is consistent with the fatigue provisions in Article 6.6.1.2.5. This reduction recognizes that, because of the

support boxes, and improper placement of reinforcement steel near the joint. In extreme cases, voids under a support box could lead to movement of the support box. If a support box is not well supported, it is ineffective and the span of the centerbeams is essentially doubled. Concrete should be placed on one side of the support bar box and vibrated so that it appears on the opposite side prior to placing concrete on that side.

Problems with poor detail design include improper detailing of superstructure elements and reinforcement steel, reflective cracking in the concrete cover directly above support boxes, and lack of access to the underside of the MBEJ for inspection and maintenance. Reflective cracking in the concrete deck directly above support boxes has been noted at almost every MBEJ. These cracks permit water intrusion which may eventually cause delamination of the concrete cover over the support bar boxes. Reflective cracking is most significant in a region of the deck which has transverse negative moment causing transverse tension stress in the top of the deck, i.e. where the deck is continuous over a girder in a direction transverse to the longitudinal axis of the bridge. Among the factors believed to affect reflective cracking are: 1) the discontinuity in the slab thickness caused by the support box; 2) the relative flexibility of the thin plates used to construct the top of the support boxes; and 3) slump of the concrete mixture. In either case, it seems that the solution may be to provide adequate concrete cover and transverse reinforcement over the support boxes to minimize the crack widths.

Blockouts are used for modular joints to facilitate placement and adjustment. The blockout must be designed to support the weight of the joint, particularly on deck overhangs. Sometimes the ends of steel girders are notched to accommodate the joint. The possible fatigue problem at these notches should be considered. Careful installation of the joint and placement of blockout concrete are critical to ensure a durable joint.

Close cooperation is required between the designer, contractor, and joint manufacturer to ensure a quality joint installation. For example, designers should work with the manufacturers when detailing blockout reinforcement. By working together, experienced designers, typically more familiar with reinforcement needs or details of the adjacent structural elements and manufacturers, often more familiar with installation problems and factors affecting MBEJ durability, will likely develop good details that reduce placement problems during construction. Unfortunately, it is difficult to anticipate reinforcement requirements during design because the joint system and manufacturer are not known until after contract award.

MBEJ should be accessible so that they may be inspected or repaired from below.

APPENDIX B

PROPOSED FATIGUE TEST SPECIFICATION AND COMMENTARY

Fatigue Test Specification for Modular Bridge Expansion Joints
NCHRP Project 12-40

1.0 General

1.1 Scope

This specification describes a test procedure for the primary load-carrying metal components of modular bridge expansion joints (MBEJ). This test procedure is applicable to welded or bolted single-support-bar and multiple-support-bar MBEJ systems. The testing procedure described here does not pertain to other expansion joint systems (i.e., strip seal joints, finger joints, etc.) used in bridge structures.

Appendix A of this specification presents a minimum performance criterion and fatigue test method for elastomeric bearings for MBEJ.

1.2 Summary

This test procedure can be used to establish the fatigue resistance of the centerbeam to support bar connection (CB/SB connection) in MBEJ. Data reported includes the applied nominal-stress range (S_r) and the number of cycles (N) at a predetermined extent of crack propagation (defined as failure) or test termination. Ten reportable fatigue cracks (data) must be acquired for each detail. Reportable data should be in the very long life range, i.e. as close to the threshold as practical, but in no case less than 200,000 cycles. The lower bound to the data determines which AASHTO category is appropriate for design.

1.3 Approach

The nominal stress range must be calculated at the location where a crack is anticipated to initiate. The nominal stress is determined from standard equations for bending and axial load which are essentially the same as the equations used in strength design. The stress concentration effect of the weld, bolt hole, or other local features are not taken into account in the nominal stress.

The cycles to failure (N) and the applied constant-amplitude nominal stress range (S_r). data are plotted on a log-log scale together with several standard S-N curves. The data are associated with the greatest S-N curve which represents a lower bound to the data. The equation for the standard S-N curves are as follows:

$$N = (A)/(S_{r_{eff}})^3 \qquad (1)$$

Where : N = Number of cycles
$S_{r_{eff}}$ = Nominal effective stress range at the detail under consideration
A = Detail Constant (See Table 1)

Detail Category	Constant A
B	$120.0\ 10^8$
C	$44.0\ 10^8$
D	$22.0\ 10^8$
E	$11.0\ 10^8$

Table 1 Detail Category Constant 'A'

Alternatively, the data may be associated with the greatest constant amplitude fatigue limit (CAFL) The CAFL must be selected from among the CAFL for the seven AASHTO fatigue categories, corresponding to the CAFL that is just below the lowest stress range that resulted in crack.). In this case, all the data used to infer the CAFL must be within 4 ksi of the CAFL

2.0 Specimens

2.1 Metal Components - General

Specimens shall be full-scale centerbeam/support bar assemblies representative of those to be used in the field applications. Each specimen shall consist of three continuous centerbeam spans over four equally spaced support bars. Spans between centerbeams shall be a minimum of 0.91m (3'-0") and a maximum of 1.35m (4'-6") (See Figure 1). Support bar spans shall be a minimum of 0.91m (3'-0") and a maximum of 1.12m (3'-8") (See Figure 2). The centerbeam/support bar connection shall be located at midspan of each support bar. Figure 3 illustrates a typical welded multiple-support-bar subassembly specimen.

Any welded or bolted attachments used to secure equidistant springs to a support bar, centerbeam, or stirrup shall be included on the specimen (see Figure 3). A load path (rigid support fixed to the test frame or floor) shall be provided to resist any horizontal forces or displacements which are normally resisted through these attachments. Any miscellaneous welded or bolted attachments, e.g. the welded attachments used to secure the elastomeric seals to the centerbeam, shall also be included on the subassembly specimens.

Support bars of subassembly specimens that are components of a single-support-bar swivel-joist type MBEJ, shall be orientated perpendicular to the longitudinal axis of the centerbeam.

Prior to testing, specimens shall be visually inspected for any flaws, defects, loose fasteners, etc., that could possibly affect the fatigue resistance of the detail under consideration. Defects and flaws shall be defined as per the appropriate governing specification (e.g.,. contract specifications, ASTM A-6, AWS D1.5, etc.). Data obtained from specimens containing defects shall not be excluded from the data set except as permitted in Section 5.1. Any observed defect shall also be reported with the data.

2.2 Instrumentation

Each specimen shall be sufficiently instrumented to measure static nominal strain ranges in the specimen for a specific interval of loading. Best results can usually be obtained when the loading interval for the static calibration tests does not pass through zero load. Strain measurements shall be made at locations not influenced by local effects (i.e., away from weld toes or bolt holes). As a minimum, specimens shall be instrumented as illustrated in Figures 4a and 4b.

The structural analysis model shall be considered verified when predicted strain ranges are within ±25% of the measured strain ranges at every location. Upon verification, the results from the structural analysis model shall be used in preference to the measurements to determine the nominal stress ranges at the details of interest for reporting results.

3.0 Fixtures

3.1 Fixture Details

Fixtures capable of adequately supporting and securing the specimen during the test shall be provided. The fixture shall be fabricated to sufficient tolerance so that additional stresses are not generated in the specimen as a result of fixture misalignment. In addition, any fabrication

errors in the specimen shall be corrected or compensated for using non-mechanical means (i.e., shimming). It is not permitted to "force" a specimen into the fixture.

Typical elastomeric springs and bearings used to transfer vertical loads from the support bar to the support box can be replaced with steel bearings in the test fixture. This will permit the fatigue test to be conducted at load ranges greater than those found in service.

4.0 Test Procedure

4.1 General

A minimum of ten (10) data are required to establish the fatigue resistance for each detail under consideration. The entire CB/SB connection shall be considered as a single detail.

Several data may be obtained from a single subassembly by repairing the cracked portions of the specimen and resuming the test. However, the repair must have minimal effects on the proportion and orientation of stress ranges at unfailed details still under consideration. If a detail that has been repaired cracks again, this shall not be included as additional data.

4.2 Loads

Loads shall be applied through hydraulic actuators or other similar loading devices. The magnitude of the vertical load range (ΔP_v) shall be maintained throughout the entire test (i.e., "load control"). Load ranges shall be monitored continuously throughout the test to ensure that the desired load range is maintained. Both vertical and horizontal load ranges shall be applied to the test specimen simultaneously in the following proportions:

Vertical Load Range = ΔP_v

Horizontal Load Range = $.2(\Delta P_v)$

The proportions of horizontal and vertical load ranges given above may be obtained by inclining the specimen 11.3° off of the horizontal plane and applying load through actuators oriented in the vertical plane.

Multiple Support Bar Systems

The direction of loading shall be either all tension or all compression and shall be applied at a constant amplitude at any desired frequency. The applied load range shall be in a direction such that the reaction force between the centerbeam and support bar is tensile. The load range shall not pass through the zero load position and a minimum preload shall be maintained throughout the test.

Single Support Bar Systems

Single support bar systems may be loaded using the same procedures as specified above for multiple support bar systems.. In the event that premature failure of the stirrup occurs, a load range may be used which is 70% downward and 30% uplift.

4.2.1 Application of Load

Load shall be applied through two 250mm(10") long patches, typically steel plates with hard rubber bearing pads, placed in contact with the bottom portion of the centerbeam as shown in Figure 5. Each patch shall be located in the center of each outer span. Note that the specimen is shown upside down in Figure 5.

4.2.2 Static Calibration Test

A static calibration test shall be conducted in order obtain strain range measurements required to verify the structural analysis model. In order to assure sufficient seating of the

specimen in the fixture, a minimum of 45kN (10kips) shall be applied at each patch load. (This requirement shall be waived for tests of single support bar systems conducted with load reversal.) Once this load is applied, all strain measuring devices shall be rebalanced to zero strain while the preload is maintained. An additional load which is approximately equal to the desired load range shall be applied. Strain ranges shall be measured for the load range from 45kN (10 kip) to the peak load. Each static calibration test shall be repeated three times while still maintaining a minimum 45 kN (10kip) load at each load patch throughout each. The measured strain ranges from each repetition should vary by no more than 25% from the mean value. In the event the strain ranges are not repeatable, appropriate modifications to the fixture shall be made until the strain ranges are repeatable. Once it is established that the data are repeatable, the measured strain range shall be compared to the strain range calculated using the structural analysis model.

4.2.3 Magnitude of Fatigue Load Ranges

The load ranges used in the test shall not be so large as to alter the observed failure mode from that which would be observed under service conditions. Under no circumstance shall applied stresses exceed the yield stress of the material in any portion of the specimen. Testing shall be performed at a minimum of two different load (stress) ranges.

If the purpose of the test is to identify the CAFL (fatigue threshold), the first load range should be chosen so that the applied stress range is just above the postulated CAFL. The load range in the subsequent test is increased or decreased according to whether the test was a runout or failed, respectively. A suggested increment in load is such that the stress range is increased or decreased by 14 MPa (2 ksi). The CAFL must be selected from among the CAFL for the seven AASHTO fatigue categories, corresponding to the CAFL that is just below the lowest stress range that resulted in crack.

4.3 Definition of Failure

The following criteria shall be used to define failure of a given centerbeam support bar connection.

4.3.1 Welded Centerbeam Support Bar Connections

Occurrence of fatigue cracks or fractures specified below shall be considered as sufficient reason to declare a connection as failed

Type A Cracking

Type A cracking originates at or near the centerbeam weld toe, propagates up into the centerbeam at some angle and grows back over the connection. Typically, Type A cracks grow at an angle of about 45°. A specimen shall be considered as failed due to Type A cracking when a crack has grown on any vertical face a length of d/2 from point of origin. Where 'd' is the depth of the centerbeam. The limits of type A of cracking are illustrated in Figure 6.

Type B Cracking

Type B cracking originates at or near the support bar weld toe, propagates down into the support bar and grows back under the connection at some angle, typically about an angle of 45°. A specimen shall be considered as failed due to Type B cracking when a crack has reached a length of d/2 from point of origin on any vertical support bar face, where 'd' is the depth of the support bar. Type B of cracking and the associated limits are illustrated in Figure 6.

Type C Cracking

Type C cracking originates in the weld throat and typically grows in a plane parallel to the longitudinal axis of the support bar at about mid-depth of the weld throat (see Figure 6.). A

specimen shall be considered as failed due to Type C cracking when a complete fracture of the weld throat has occurred.

Type C cracks have been observed to turn down into the support bar, but only after significant growth. In such instances, the criteria for type B cracking shall be applied.

4.3.2 Welded Stirrup Connections

The following criteria shall be used to define failure of a given CB/SB connection that utilizes welded stirrups.

1. Fatigue cracks which result in complete fracture of any leg of a stirrup.
2. Fatigue cracks originating at or near a stirrup weld toe that have grown a distance of d/2 into the centerbeam on any face, where 'd' is the depth of the centerbeam.

4.3.3 Bolted Centerbeam Support Bar Connections

The following criteria shall be used to define failure of a given bolted centerbeam support bar connection.

1. Fatigue cracks which have grown out of a bolt hole resulting in complete fracture of the tension flange in the centerbeam.
2. Fatigue cracks growing out of a bolt hole and extending a distance of $\frac{d}{2} - t_f$ into the centerbeam web on any face, where 'd' is the depth of the centerbeam and 't_f' is the flange thickness.
3. Complete fracture of any portion of a stirrup.
4. Complete fracture of any single bolt.

4.3.4 Alternate Criteria for Termination of a Fatigue Test-Optional

A test may also be terminated when, for a given stress range, the specimen has survived the number of cycles required to plot the data above a particular fatigue resistance curve, or the maximum permitted in Section 4.5. For example, if the applied stress range is 117Mpa (17ksi) and the desired fatigue resistance curve is category C, then using equation 1 and Table 1, the test may be terminated after application of about 900,000 cycles, provided of course, the specimen has not failed based on the criteria described above.

4.4 Nominal-Stress Range Calculation

4.4.1 Welded MBEJ

Type A Cracking

The nominal-stress range for Type A cracking is obtained by taking the square root of the sum of the squares of the horizontal bending stress ranges in the centerbeam and vertical stress ranges in the weld. Figure 7 illustrates the location and orientation of the force components leading to Type A cracks.

Type B Cracking

The nominal stress range for Type B cracking is calculated from a square root of the sum of squares of the longitudinal bending stress range in the support bar and the vertical stress ranges in the weld. The axial load component in the support bar due to the horizontal load is relatively small and may be ignored. Figure 8 illustrates the location and orientation of the force components leading to Type B cracks.

Type C Cracking

The stress range driving Type C cracking is the vertical stress range in the throat of the weld Figure 9 illustrates the location and orientation of the force components leading to Type C cracks.

Welded Stirrup Connections

The nominal stress range in the centerbeam at a welded stirrup shall be taken as the summation of the longitudinal stress ranges in the centerbeam resulting from horizontal and vertical bending. The entire load range should be used in this calculation, even if the loading is partly in compression. The effects of stresses generated in the stirrup itself shall not be considered in the centerbeam stress ranges.

The load range in the stirrup itself shall be taken as 30% of the total vertical load range carried through the connection. The effect of the horizontal forces may be neglected.

4.4.2 Bolted MBEJ

Centerbeam Connections

The nominal stress range in the centerbeam shall be taken as the sum of the longitudinal stress ranges in the centerbeam resulting from horizontal and vertical bending. Stress ranges shall be calculated on the net section. The effects of stresses generated in the stirrup itself shall not be considered when calculating the stress range in the centerbeam.

Stirrup Connections

The load range in the bolt group and stirrup assembly shall be taken as 30% of the total vertical load range carried through the connection. The effect of the horizontal forces may be neglected.

4.5 Maximum Fatigue Resistance The data may be used to obtain an S-N curve which represents a lower bound to the data. In this case, the maximum fatigue resistance of any detail shall not exceed that prescribed in Table 2. Alternatively, the data may be used to obtain the greatest constant amplitude fatigue limit (CAFL). A unique CAFL (different from the CAFL associated in the AASHTO Bridge Design Specifications with the detail category) may be established if ten data are generated within 4 ksi of the unique CAFL.

Type of Detail	Maximum Permitted Category[3]
Welded Multiple CB/SB Connections	C
Welded Stirrup Attachments for SSB Systems	B
Bolted Stirrup Attachments for SSB Systems	D
Groove-Welded Centerbeam Splices[1]	C
Miscellaneous Welded Connections[2]	C
Miscellaneous Bolted Connections	D

Table 2 - Maximum Permitted Fatigue Category for MBEJ Details

Notes:
1. Groove-welded full-penetration splices may be increased to category B if weld soundness is established by NDT.
2. Miscellaneous connections include attachments for equidistant devices.
3. The maximum permitted category applies only to the S-N curve at stress ranges above the CAFL. A CAFL that is higher than the CAFL associated with these categories may be used if the CAFL is established with a minimum of ten test data.

5.0 Results

5.1 Interpretation of Results

(Note, this section does not apply to tests that are conducted to establish the CAFL (fatigue

threshold) of a given detail. In such instances it is not permitted to discard any data obtained. Therefore proceed directly to Section 6)

The data obtained from the fatigue testing shall be plotted with the AASHTO fatigue resistance curves as shown in Figure 10. The detail category shall be the greatest AASHTO S-N curve that is less than all ten data, except as limited in Table 2. For example, for the data plotted in Figure 10, category D would be selected as the appropriate fatigue resistance curve to be used for design.

In the event that all but one data point fall above a given desired fatigue curve, that one data point may be discarded and replaced by three new data obtained through additional testing. The additional testing shall be conducted at the same stress range that the discarded data point was obtained. These three additional data shall be plotted along with the remaining nine data. The detail category shall be the greatest AASHTO S-N curve that is less than all twelve of these data, except as limited in Table 2. For any detail, one and only one data may be discarded and subsequently replaced with three additional data for any set of ten original data. None of the additional data, if acquired, shall be discarded.

5.1.1 Welded Stirrup Details

The fatigue resistance in the finite life regime for stirrups welded to a centerbeam flange shall not be taken greater than that defined using AASHTO fatigue details. The fatigue resistance of the centerbeam is analogous to and shall be considered as a *"Longitudinally Loaded Groove-Welded Attachment"* or a *"Longitudinally Loaded Fillet-Welded Attachment"*, depending on the type of connection used. The fatigue resistance of the stirrup is analogous to and shall be considered as a *"Transversely Loaded Groove-Welded Attachment"* or a *"Transversely Loaded Fillet-Welded Attachment"*, depending on the type of connection used.

6.0 Reporting of Data

6.1 Fatigue Test Results and Observations

Data shall be reported in the typical S-N format (log(S) vs. log(N)) with the log of the stress range plotted as the ordinate (y axis). In addition, the data shall also be reported in tabular format. The table shall contain the following information:

- Nominal stress range at detail of interest ($S_{r\,eff}$).
- Applied load range for each patch.
- Number of cycles at first observation of a crack (for report purpose only, not to be used in the S-N data).
- Number of cycles at failure or termination of the test (N). The reason for stopping the test shall also be noted (i.e., failure or termination).
- Type of crack as described in section 4.3.1. If the observed crack does not resemble any of the crack types described in section 4.3.1, then a detailed description of the fatigue crack shall be provided.

6.2 Miscellaneous Required Information

The following additional information shall also be reported.

- Joint type and manufacturer.
- A drawing showing shape, size, and dimensions of the specimen. Drawings shall also present details of the fixture including specimen orientation.
- Section properties and detail dimensions of the centerbeam and support bars.

- For welded MBEJ, the weld procedures specification shall be attached. For bolted MBEJ, the bolt size, material specification, location, and method of tightening shall be reported.

APPENDIX A

Guidelines for Durability Testing of Springs and Bearings for MBEJ
NCHRP Project 12-40

A1.0 General

A1.1 Scope

The procedures contained in this appendix are guidelines for durability testing of the elastomeric bearings typically used in modular bridge expansion joints (MBEJs). In addition, some minimum performance criteria are prescribed. The requirements presented herein for these components are not sufficient to ensure durability in service. Additional specifications for environmental durability should also be considered. These guidelines do not necessarily apply to springs, equidistant springs, or other elastomeric parts.

A1.2 Summary

A minimum performance criterion is provided for MBEJ bearings. The test is carried out dynamically on individual bearings. Data to be reported include the applied nominal-strain range and the number of cycles at failure or test termination

A1.3 Approach

The fatigue life will be determined by the displacement range applied to the specimen rather than the load or stress range.

A2.0 Specimens General

Specimens shall be full-scale bearing components representative of those to be used in the field applications. Teflon sliding surfaces, or materials typically bonded to the bearing shall be included on the specimen.

Prior to testing, specimens shall be visually inspected for any flaws or defects that could possibly affect the fatigue resistance of the specimen. Defects and flaws shall be defined as per the appropriate governing specification (e.g., contract specifications). Data obtained from specimens containing defects shall not be excluded from the data set. Any observed defect shall be reported with the data.

A3.0 Fixtures

A3.1 Fixture Details

Fixtures capable of adequately supporting and securing the specimen during the test shall be provided. The fixture shall be fabricated to sufficient tolerance so that additional stresses are not generated in the specimen as a result of fixture misalignment.

A4.0 Test Procedure

A4.1 General

A minimum of three fatigue tests are required to establish the durability of each type of bearing.

A4.2 Loads

Loads shall be applied through hydraulic actuators or other similar loading devices. The

magnitude of the *displacement* shall be maintained throughout the entire test (i.e., "displacement control"). Displacement and load ranges shall be monitored continuously throughout the test to ensure that the desired displacement range and a minimum preload are maintained.

A4.3 Application of Load

Load shall be applied to the specimen through flat steel plates that are smooth and free of rust. The plates shall be sufficiently thick so as to ensure even load distribution to the specimen.

A4.4 Dynamic Stiffness Test

Dynamic stiffness testing of the spring or bearing, a dynamic load test shall be conducted. The dynamic stiffness shall be obtained for at least three different loading frequencies, the maximum being the expected in service loading frequency. The maximum service loading frequency shall be estimated assuming a vehicle travel speed of 96kmh (60mph).

$$f = \frac{V}{2 \cdot (g + b)} \qquad (2)$$

Where:
f = Loading frequency
V = Vehicle speed (assume 96kmh (60mph))
b = Centerbeam width
g = Centerbeam gap (assume mid-opening position)

The load range applied during the dynamic stiffness of the specimen shall be that obtained from structural analysis using fatigue wheel loads and wheel load distribution factors specified in the governing design specification. Each dynamic test shall be repeated three times and the data compared to assure the results are consistent.

A4.5 Fatigue Test

The fatigue test shall be conducted under displacement control. The displacement (strain) range shall be applied at any desired frequency less than or equal to the service loading frequency using a sine or other smooth waveform. Throughout the test, a minimum precompression strain shall be maintained (see Section A4.2.2). The minimum cyclic strain applied to the specimen shall be equal to the precompression strain.

The minimum and maximum dynamic load shall be recorded at the beginning of the test. Throughout the test, the minimum and maximum dynamic load shall be monitored and periodically recorded.

At the end of each complete cycle, the displacement shall be held (i.e., a dwell time) at the precompression position for no less than one half of the period of loading to help promote heat dissipation. In addition, it is acceptable to use a fan to aid in heat dissipation. Excessive heat generation will have negative effects on fatigue life.

A4.5.1 Amplitude of Displacement

The fatigue test shall be run using displacement control. The magnitude of the displacement amplitude to be used during the fatigue test (Δ) shall be determined using equation (3) below:

$$\Delta = \frac{Rv}{K} \qquad (3)$$

Where:

Rv = Vertical reaction force at the bearing obtained from analysis

K = Dynamic stiffness of spring or bearing determined in Section 4.3

A4.5.2 Minimum Precompression

A minimum precompression strain equal to that which is generated in a spring or bearing after it is installed in a support box or stirrup shall be applied to the specimen. The minimum cyclic strain applied to the specimen shall be equal to the precompression strain.

A4.6 Performance Criteria

A4.6.1 Criteria for Failure

The following criteria shall be used to define failure and to terminate a test.

1. Excessive deterioration or cracking of the elastomeric material.
2. The measured minimum dynamic load falls to 30% of the initial value recorded at the beginning of the test.
3. The measured maximum dynamic load range decreases to half of the initial dynamic load range recorded at the beginning of the test.

A4.6.2 Criteria for Acceptance

A test may be terminated and the specimen will be considered as having satisfied the requirements of the fatigue test after successfully withstanding 2 million cycles.

A5.0 Reporting of Data

A5.1 Test Results and Observations

Data shall be reported in tabular format. The table shall contain the following information:

- Minimum (i.e., precompression strain) and maximum strain, displacement and load at beginning of test.
- Nature of the forcing function (i.e., sin, ramp, etc.).
- Number of cycles at first observation of a distress (for report purpose only, not to be used in the data).
- Number of cycles at failure.
- A description of the mode of failure.

5.2 Miscellaneous Required Information

The following additional information shall also be reported.

- Bearing or spring type and manufacturer.
- A drawing showing shape, size, and dimensions of the specimen. Drawings shall also present details of the fixture including specimen orientation.

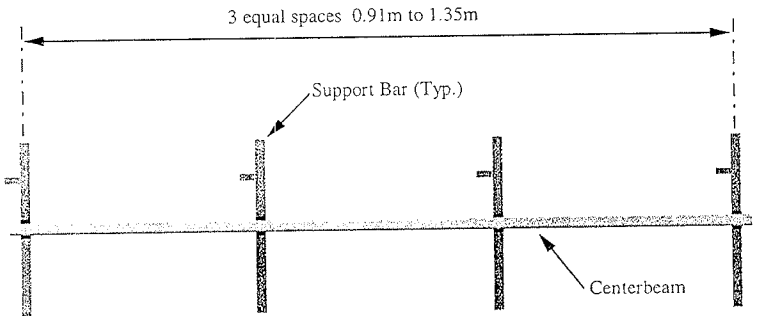

Figure 1-Acceptable Centerbeam Spans

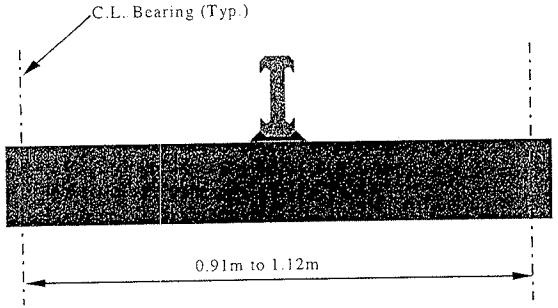

Figure 2-Acceptable Support Bar Spans

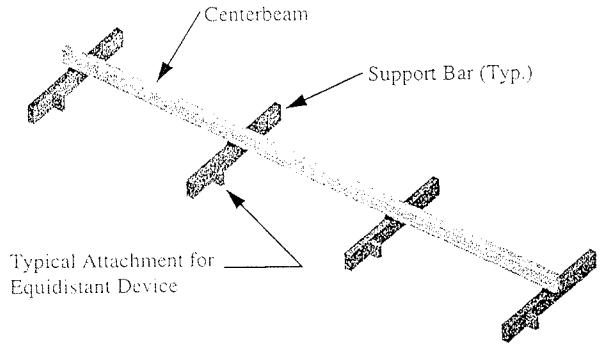

Figure 3 - Typical Subassembly Specimen

(Welded Multiple Support Bar Subassembly Shown)

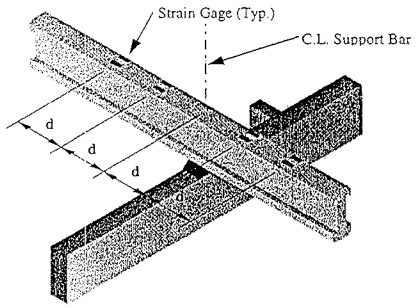

Figure 4a - Strain Gage Layout at Interior Centerbeam/Support Bar Connection (Exterior Connection Similar)

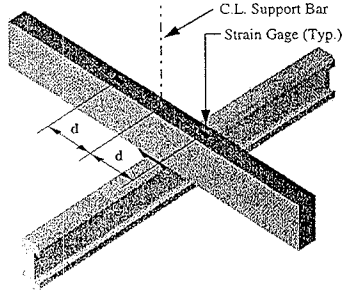

Figure 4b - Typical Support Bar Strain Gage Layout (Bottom View)

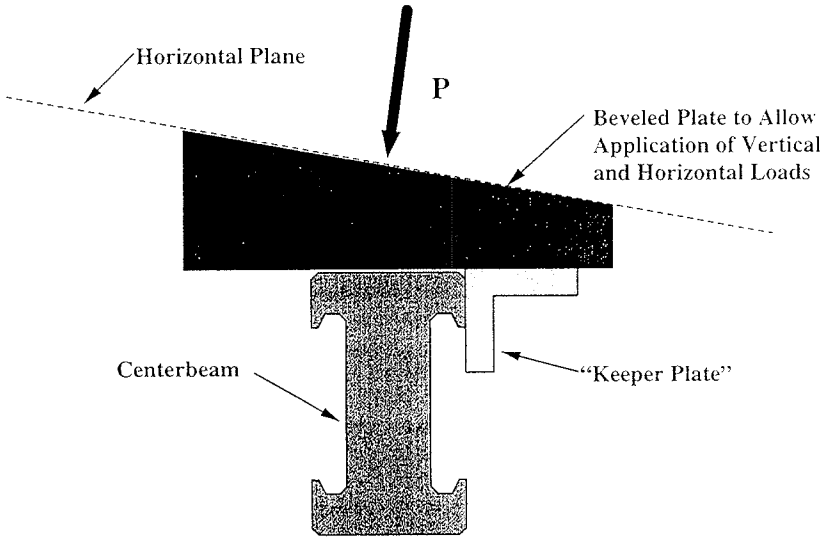

Figure 5 Typical Fixture Used to Apply Load to Centerbeam

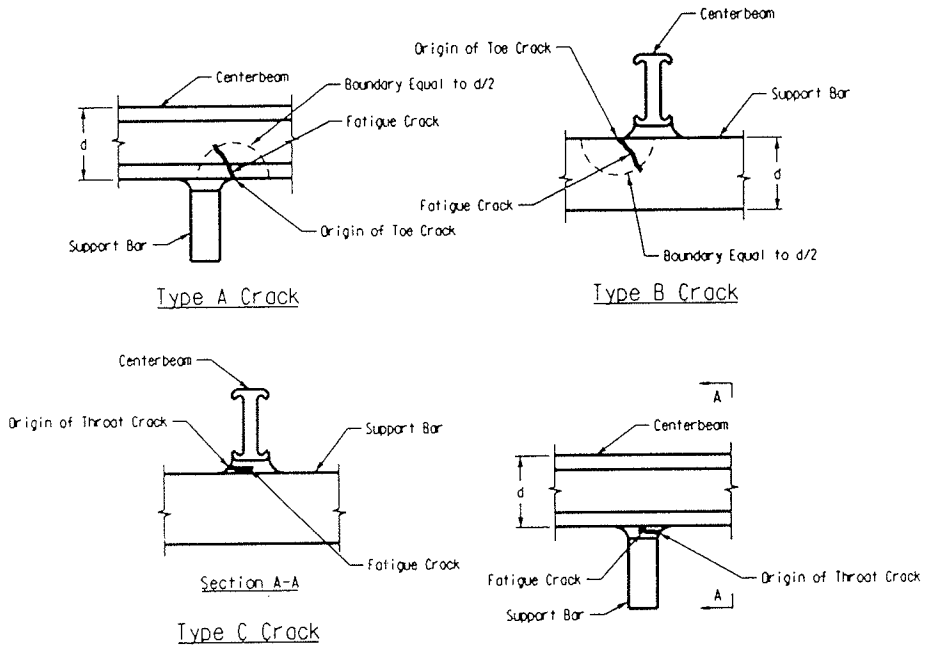

Figure 6 - Sketches of Different Types of Cracks Observed in Welded Multiple Support Bar MBEJ fatigue Tests

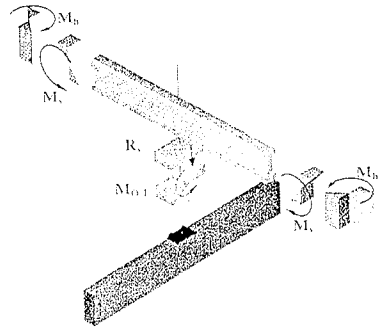

Figure 7 - Stresses and Forces Associated with Type A Cracking

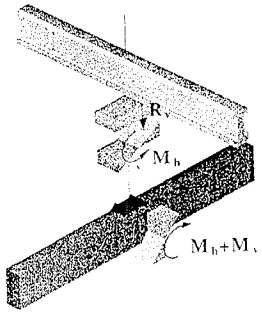

Figure 8 - Stresses and Forces Associated with Type B Cracking

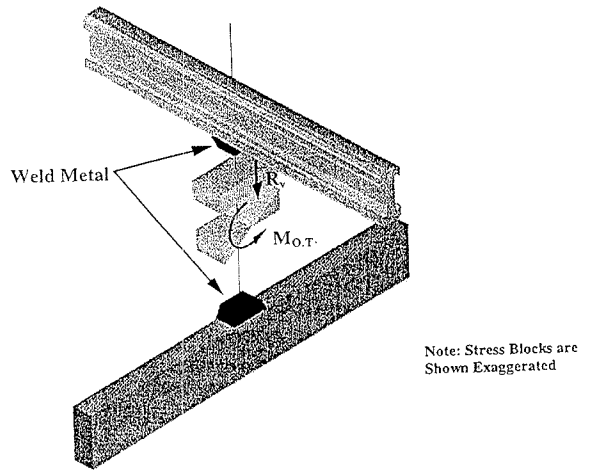

Figure-9 Stresses and Forces Associated with Type C Cracking

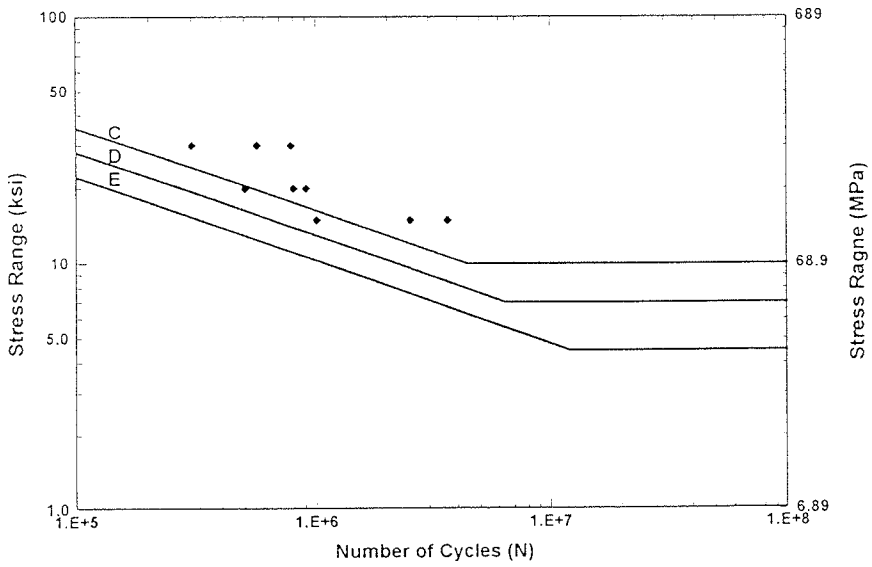

Commentary to the Fatigue Testing Acceptance Procedures for Modular Bridge Expansion Joints

NCHRP Project 12-40

Commentary to Article 1.1 Scope

Modular expansion joints are structural systems which permit both translation and rotation between adjacent bridge elements. Such joints are located in the plane of the bridge deck and are parallel to the centerline of bearings for most structures.

Commentary to Article 1.2 Summary

Fatigue resistance of the metal components used in MBEJs can be established through this standard. The procedure is based on the nominal-stress S-N-curve approach and is consistent with current AASHTO fatigue design provisions. Full scale testing of representative details is required. The test results are used to establish the appropriate AASHTO fatigue category of various MBEJ details used in design. The procedure can also be used to establish the fatigue resistance in terms of any other nominal-stress based S-N curves, such as those included in Eurocode 3. It is required that ten data be acquired for each detail in order to determine which AASHTO category is appropriate for design. Data reported includes the applied nominal-stress range and the number of cycles at failure or test termination. The fatigue design procedure for MBEJ is based on the fatigue threshold (i.e. the constant-amplitude fatigue limit or CAFL). Therefore, the emphasis in this fatigue test procedure is on defining the CAFL, which requires more expensive long-term testing at stress ranges close to service stress ranges.

The centerbeam to support bar connection (CB/SB connection) is the primary focus of this standard. However, if there are any other details which are more susceptible to fatigue, this procedure will yield data for the fatigue resistance of these details as well. If there are other details which crack prior to cracking of the CB/SB connection, these details may have to be modified in order to obtain data on the CB/SB connection. Typically, the MBEJ is not efficiently designed if details other than the CB/SB connection are governing the fatigue life.

Commentary to Article 1.3 Approach

The detail category accounts for stress concentrations, weld quality, and other parameters that are highly variable and difficult to quantify

Commentary to Article 2.2 Instrumentation

The measured static strain ranges obtained during a calibration test shall be used to estimate the nominal moment and strain distribution in the specimen and used to verify structural analysis models. Details of the calibration test are discussed in Section 4.2.2. (For guidance on modeling techniques for MBEJ, the reader is referred to the final report for NCHRP Project 12-40 Fatigue Criteria For Modular Bridge Expansion Joints). The structural analysis model shall be considered verified when predicted strain ranges are within ±25% of the measured strain ranges. Experience with these tests suggests that this is about the best agreement that is practical to obtain. Considering that the strain at every location in the MBEJ must be within this tolerance, the strain at most locations is in much better agreement than this maximum tolerance. The structural

analysis model will present less variation than the measurements, therefore the results from the structural analysis model shall be used in preference to the measurements to determine the nominal stress ranges at the details of interest for reporting results

Commentary to Article 4.1 General

For welded or bolted MBEJ specimens, the entire CB/SB connection shall be considered as a single detail. For example, cracks occurring at a welded centerbeam/support bar connection may occur either 1) at the centerbeam weld toe, 2) support bar weld toe or, 3) through the weld throat. In any case, this cracking defines failure of the SB/CB connection (i.e., detail)

Commentary to Article 4.2 Loads

Multiple Support Bar Systems

The applied load range shall be in a direction such that the reaction force between the centerbeam and support bar is tensile. In the configuration with the centerbeams on top, this loading would be considered uplift. An alternative method is to test the specimen upside down, and apply the loads entirely in compression. The specified loading is entirely uplift to avoid long crack propagation lives which result in greater variability.

Single Support Bar Systems

Single support bar systems may be loaded using entirely uplift loading as for multiple support bar systems. However, it is recognized that the above procedure results in an unrealistic severe loading of the stirrups which may result in premature failure of the stirrup. In the event this occurs, a load range may be used which is 70% downward and 30% uplift. Fatigue testing in which the loading passes through zero load (i.e. load reversal) is typically much more difficult and costly to conduct.

Commentary to Article 4.2.2 Magnitude of Fatigue Load Ranges

Fatigue tests are typically conducted at load ranges (ΔP) which are much higher than the expected service load ranges. However, the load ranges shall not be so large as to alter the observed failure mode from that which would be observed under service conditions.

Commentary to Article 4.3.1 Welded Centerbeam Support Bar Connection

Type C cracks have been observed to turn down into the support bar, but only after significant growth. This change in propagation direction is attributed to the changing orientation of the plane of principal stress with crack growth. In such instances, the criteria for type B cracking shall be applied.

Commentary to Article 4.4.1 Welded MBEJ

Type A Cracking

Type A cracking is driven by a combination of horizontal bending stress ranges in the centerbeam and the vertical stress ranges in the weld throat at this location. The vertical component is generated by the following two forces: 1) the vertical reaction at the support and 2) the overturning moment resulting from horizontal forces applied to the centerbeam.

The nominal-stress range is obtained by taking the square root of the sum of the squares of the horizontal stress ranges in the centerbeam and vertical stress ranges in the weld. The vertical stress range in the throat of the weld is generated by the following two components: 1) the vertical reaction at the support and 2) the overturning moment resulting form horizontal. Note this method of combining the stresses ignores the contribution of shear stresses in the region. Shear stresses are ignored in this procedure since they are typically small and very difficult to determine accurately. Figure 7 illustrates the location and orientation of the force components leading to Type A cracks.

Type B Cracking

Type B cracking is driven by a combination of horizontal and vertical stress ranges in this location. The vertical component is generated by the same two forces discussed for Type A cracking: i.e., 1) the vertical reaction at the support and 2) the overturning moment resulting from horizontal force. In the case of Type B cracking, however, the horizontal component is a result of longitudinal support bar bending stress range. The support bar bending moment is the sum of the moment created by the applied centerbeam reaction and the additional bending moment developed by the horizontal force applied at the top of the centerbeam.

The nominal stress range is calculated from a square root of the sum of squares of the longitudinal support bar stress ranges and the vertical stress ranges in the weld. Figure 8 illustrates the location and orientation of the force components leading to Type B cracks.

Type C Cracking

The stress range driving Type C cracking is the vertical stress range in the throat of the weld generated by the following two components: 1) the vertical reaction at the support and 2) the overturning moment resulting form horizontal. Figure 9 illustrates the location and orientation of the force components leading to Type C cracks

Commentary to Article 4.5 Maximum Fatigue Resistance

Based on the results of previous fatigue testing, the upper bound of the fatigue strength for typical details has been well characterized for the finite life regime. Therefore, the maximum fatigue resistance of any detail shall not exceed that prescribed in Table 2 if the testing is conducted in the finite life regime. However, testing may be conducted with the purpose of determining the CAFL (fatigue threshold) of the detail, a unique CAFL may be established. In such a case, all ten data must be used to establish the CAFL.

Commentary to Article 5.1 Interpretation of Results

It is noted that the acquisition of three additional data may result in selection of a fatigue category that is lower than would have originally been selected based on the original ten data. Such a situation may arise if the newly obtained data demonstrates an unusually poor fatigue resistance.

Commentary to APPENDIX A

Guidelines for Durability Testing of Springs and Bearings for MBEJ

Commentary on Article A1.1 Scope

These guidelines do not necessarily apply to springs, equidistant springs, or other elastomeric parts. However, these other elastomeric parts are not subjected to the significant load ranges that bearings are subjected to. Consequently, few problems have been encountered with the durability of these other elastomeric parts.

Commentary to Article A1.2 Summary

A minimum performance criterion is provided for MBEJ bearings. This performance criterion is relatively arbitrary, but it is known that present bearings can in most cases meet this criterion.

Commentary to Article A1.3 Approach

While fatigue is typically assessed in terms of the stress range applied to a member, in nonlinear materials it can be shown that the strain range, rather than the stress range, is actually the parameter which should be considered. In addition, for nonlinear, viscoelastic materials such as neoprene, the stiffness of the component varies with the strain rate. Therefore, the fatigue life will be determined by the displacement range applied to the specimen and would not vary significantly if the strain rate (and hence the load range) were varied.

APPENDIX C

FATIGUE DESIGN EXAMPLES

Design Example #1

1.0 General

These example fatigue design calculations are applicable to a typical welded multiple-support-bar modular bridge expansion joint system. The movement classification of this MBEJ is assumed to be 9 in. The system consists of 2 in. × 4.75 in. support bars spaced at 3′-3″. The MBEJ is not located near a traffic metering device or toll facility. The geometry and section properties of the centerbeam and centerbeam/support bar weld are given below.

Centerbeam:

S_{Xcb} = 9.68 in^3 (Strong axis section modulus at the bottom of the centerbeam)
S_{Ycb} = 3.38 in^3 (Weak axis section modulus at the bottom of the centerbeam)
d_{cb} = 5 in (Depth of the centerbeam)

Support Bar

t = 2 in. (Thickness of the support bar)
d_{sb} = 4.75 in (Depth of the support bar)
S_{Xsb} = 7.5 in^3 (Strong axis section modulus of the support bar)

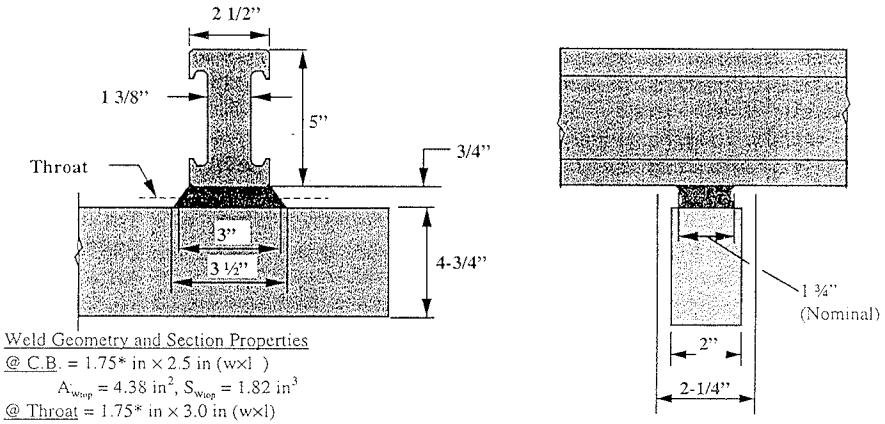

Weld Geometry and Section Properties

@ C.B. = 1.75* in × 2.5 in (w×l)
A_{Wtop} = 4.38 in^2, S_{Wtop} = 1.82 in^3
@ Throat = 1.75* in × 3.0 in (w×l)
A_{Wmid} = 5.25 in^2, S_{Wmid} = 2.63 in^3
@ S.B. = 1.75* in × 3.5 in (w×l)
A_{Wbot} = 6.12 in^2, S_{Wbot} = 3.6 in^3
h_w = 0.75 in (height of the weld)
*Nominal Width

w = width parallel to the longitudinal axis of the C.B.
l = length perpendicular to the longitudinal axis of the C.B.
A_{Wtop}, A_{Wmid}, and A_{Wbot} = Area of weld at the top, middle, and bottom of the connection, respectively.
S_{Wtop}, S_{Wmid}, and S_{Wbot} = Section modulus of the weld at the top, middle, and bottom of the connection, respectively for bending perpendicular to the longitudinal axis of the centerbeam.

1.1 Fatigue Design Methodology

The following design will conform to the recommendations for fatigue design of MBEJ as given in Article 14.5.7 of the proposed specification. In this method, stress ranges (Δf) generated by the fatigue truck must be kept less than one half the CAFL ($\Delta F_{TH}/2$). Theoretically, if this condition is satisfied infinite life is ensured.

1.2 Fatigue Design

1.2.1 Loads

As per Article 14.5.7.2, the MBEJ system shall be designed to resist the simultaneous application of vertical and horizontal loads from a tandem axle. As specified in Article 14.5.7.2.1, the appropriate axle for fatigue design is the largest axle load from the three-axle design truck specified in Article 3.6.1.2.2. This axle has a gross weight of 32 kips. However, as per 14.5.7.2.1, this axle shall be considered as the total load on a tandem. Therefore, the actual design load consists of two 16 kip axles spaced at 4′-0″. Since the joint opening is less than 4′-0″, only one of the axles in the tandem shall be considered (Article 14.5.7.2.1). The dynamic amplification factor is specified as 75% in Table 3.6.2-1. and Article 14.5.7.2.1. A load factor of 0.75, as specified in Table 3.4.1-1, shall be applied for the fatigue limit state.

Fatigue Load Ranges

Static Vertical Axle Load = F_{VS} = 16 kip/axle (Note this is half of the 32 kip tandem)

Amplified Vertical Axle Load Range = ΔF_{VAmp} = (16 kip/axle)(1+.75) = 28.0 kip/axle

As per Article 14.5.7.2.3, the horizontal load range (ΔF_H) for fatigue design shall be taken as 20% of the amplified vertical axle load range. (Had the MBEJ been located at a signal or other metering device, the horizontal load range would be taken as 50% of the amplified vertical axle load range.)

$\Delta F_H = (0.2)(\Delta F_{VAmp}) = (0.2)(28 \text{ kip/axle}) = 5.6$ kip/axle

As per Article 14.5.7.3, the percentage of the design vertical axle load and horizontal load that shall be distributed to a centerbeam and associated support bars is specified in Table 14.5.7.3-1. The top width of the centerbeam is given as 2.5 in. Thus, from Table 14.5.7.3-1, the centerbeam distribution factor shall be taken as 50%.

D.F. = 0.50

1.3 Check Centerbeam Support Bar Connection

The nominal stress ranges shall be obtained from structural analysis as specified in Article 14.5.7.4.2. For fatigue design, the MBEJ shall be assumed to be at the midrange opening. The design stress range at an interior connection shall be checked for fatigue in this example. Though not shown here, an exterior span should also be checked using the same methods.

Since this is a welded multiple-support-bar MBEJ, stresses shall be calculated as specified in Article 14.5.7.2b. Three separate checks are required for the centerbeam to support bar connection in welded multiple-support-bar systems.

Check Centerbeam Weld Toe Cracking (Type A Cracking)

Type A cracking is driven by a combination of horizontal and vertical stress ranges in the connection (see Figure A at the end of this example).

Through trial and error, the axle was positioned to maximize the stress range at the centerbeam weld toe. The final position is shown below in Figure 1.3-1. These loads are to be applied to the top of the centerbeams and along the centerlines of the centerbeams. The vertical line loads are calculated below:

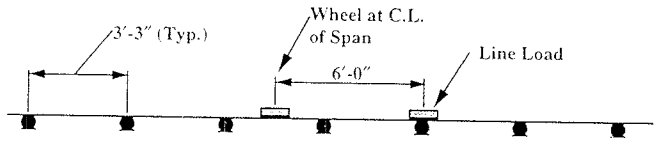

Figure 1.3-1

Vertical Load Range (Line Load)

$$w_V = 0.50 \times 0.75 \times \frac{28\text{kip/axle}}{(20\text{in} \times 2\text{wheel/axle})} = (0.263\text{kip/in})/\text{wheel}$$

Horizontal Load Range (Line Load)

$$w_H = 0.50 \times 0.75 \times \frac{5.6\text{kip/axle}}{(20\text{in} \times 2\text{wheel/axle})} = (0.053\text{kip/in})/\text{wheel}$$

Note: The above equations incorporate the distribution factor (DF) of 0.50 as specified in Table 14.5.7.3-1 and the load factor (LF) of 0.75 as specified in Table 3.4.1-1.

From structural analysis, the following information was obtained:

R_V = 3.3 kip $\quad$ M_V = 15.9 k-in

R_H = 0.66 kip (i.e., 20% of R_V) $\quad$ M_H = 3.2 k-in (i.e., 20% of M_V)

Where

R_V= Vertical reaction in the connection.

R_H= Horizontal reaction in the connection.

M_V= Horizontal bending moment in the centerbeam due to the applied vertical forces.

M_H= Horizontal bending moment in the centerbeam due to the applied horizontal forces.

$$S_{RB} = \frac{M_V}{S_{Xcb}} + \frac{M_H}{S_{Ycb}} \qquad (14.5.7.4.2b\text{-}1)$$

$$S_{RB} = \frac{15.9\text{k-in}}{9.68\text{in}^3} + \frac{3.2\text{k-in}}{3.38\text{in}^3} = 2.6\text{ksi}$$

$$S_{RZ} = \frac{R_H d_{cb}}{S_{Wtop}} + \frac{R_V}{A_{Wtop}} \qquad (14.5.7.4.2b\text{-}2)$$

$$S_{RZ} = \frac{.66\text{k} \times 5\text{in}}{1.82\text{in}^3} + \frac{3.3\text{k}}{4.38\text{in}^2} = 2.6\text{ksi}$$

Where:

S_{Xcb} and S_{Ycb} =Section modulus of the centerbeam

A_{Wtop} = Area of weld at the top of the connection.

S_{Wtop}, = Section modulus of the weld at the top of the connection.

d_{cb} = Depth of the centerbeam.

Calculate Δf as specified in 14.5.7.4.2b to check centerbeam weld toe cracking.

$$\Delta f = \sqrt{S^2_{RB} + S^2_{RZ}} \qquad (14.5.7.4.2b\text{-}6)$$

$$\Delta f = \sqrt{2.6^2\text{ksi} + 2.6^2\text{ksi}} = 3.7\text{ksi}$$

Where:

S_{RB}= Combined bending stress range in the centerbeam or support bar.

S_{RZ}= Vertical stress range in the centerbeam to support bar weld from the reaction of the support beam. Components of this stress range include the vertical load and overturning moment.

Check Article 14.5.7.4.3
To ensure an infinite fatigue life the connections shall satisfy the following:

$$\Delta f \le \frac{F_{TH}}{2} \qquad (14.5.7.4.3\text{-}1)$$

Where:

Δf = The nominal stress range as specified in Article 14.5.7.4.2.
F_{TH} = The fatigue threshold as specified in Article 14.5.7.5.

For this MBEJ, the fatigue resistance of the centerbeam to support connection was established through testing to be Category C. For a Category C detail, F_{TH} = 10ksi as specified in Table 6.6.1.2.5-3.

$$3.6\text{ksi} \le \frac{10\text{ksi}}{2} \qquad \textbf{O.K.!}$$

Equation 14.5.7.4.3-1 is satisfied and centerbeam weld toe cracking will not occur.

Support Bar Weld Toe Cracking (Type B Cracking)

Through trial and error, the axle was positioned to maximize the stress range at support bar weld toe. The final position of the axle is shown below in Figure 1.3-2. These loads are to be applied to the top of the centerbeams and along the centerlines of the centerbeams. The vertical line loads calculated above should be applied here as well:

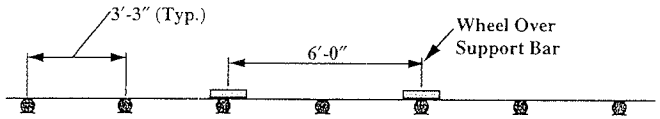

Figure 1.3-2

From structural analysis of the above system, the following information was obtained:

R_V = 4.8 kip
R_H = 1.0 kip (i.e., 20% of R_V)
M_V = 20.5 k-ft (see below)

Where:

R_V = Vertical reaction in the connection.
R_H = Horizontal reaction in the connection.
M_V = Bending moment in the support bar due to vertical and horizontal forces.

Type B cracking is driven by a combination of horizontal and vertical stress ranges in the connection (see Figure B at the end of this example). The moment in the support bar results from the vertical and horizontal reactions as shown in Figure 1.3-3. Since the centerbeam is located at midspan (see Figure 1.3-3), the maximum moment in the support bar occurs at the center of the span. The total length of the span is 17.1 inches (i.e., 2L).

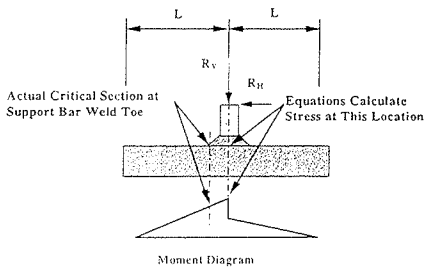

Figure 1.3-3

The moment in the support bar (M_V) due to the vertical reaction force (R_V) must be calculated. Note that (M_V) is a result of the vertical reaction only, the additional moment from the horizontal force is calculated by the second half of equation 14.5.7.4.2b-3 shown below.

$$M_V = \frac{1}{2}(R_V) \times L = \frac{1}{2}(4.8\text{kip}) \times 8.55\text{in} = 20.5\text{k} - \text{in}$$

Note

$$8.55\text{in} = \frac{17.1\text{in}}{2} = L$$

The stress range in the support bar (S_{RB}) is calculated using Eq. 14.5.7.4.2b-3:

$$S_{RB} = \frac{M_V}{S_{Vsb}} + \frac{1}{2}\frac{R_H(d_{cb} + h_W + \frac{1}{2}d_{sb})}{S_{Vsb}} \qquad (14.5.7.4.2b\text{-}3)$$

$$S_{RB} = \frac{20.5\text{k} - \text{in}}{7.5\text{in}^3} + \frac{1}{2}\frac{1.0\text{k}(5\text{in} + 0.75\text{in} + \frac{1}{2}(4.75\text{in}))}{7.5\text{in}^3} = 3.3\text{ksi}$$

Where,

R_H = Horizontal reaction in the connection.
M_V = Bending moment in the support bar due to vertical forces.
S_{Vsb} = Section modulus of the support bar.
L = Distance from C.L. of bearing to C.L. of connection.

The vertical stress range in the weld (S_{RZ}) is calculated using Eq. 14.5.7.4.2b-4

$$S_{RZ} = \frac{R_H(d_{cb} + h_W)}{S_{Wbot}} + \frac{R_V}{A_{wbot}} \qquad (14.5.7.4.2b\text{-}4)$$

$$S_{RZ} = \frac{1.0\text{k}(5.0\text{in} + 0.75\text{in})}{3.6\text{in}^3} + \frac{4.8\text{k}}{6.12\text{in}^2} = 2.4\text{ksi}$$

Where:

R_V = Vertical reaction in the connection.
R_H = Horizontal reaction in the connection.
A_{wbot} = Area of weld at the bottom of the connection.
S_{wbot} = Section modulus of the weld at the bottom of the connection.
h_w = Height of the weld.

Calculate Δf as specified in 14.5.7.4.2b to check for support bar weld toe cracking.

$$\Delta f = \sqrt{S^2_{RB} + S^2_{RZ}} \qquad (14.5.7.4.2b\text{-}6)$$

$$\Delta f = \sqrt{3.3^2\text{ksi} + 2.4^2\text{ksi}} = 4.1\text{ksi}$$

Where:

S_{RB} = Combined bending stress range in the support bar.
S_{RZ} = Vertical stress range in the centerbeam to support bar weld from the reaction of the support beam. Components of this stress range include the vertical load and overturning moment.

Check Article 14.5.7.4.3

To ensure an infinite fatigue life the connections shall satisfy the following:

$$\Delta f \le \frac{F_{TH}}{2} \qquad (14.5.7.4.3\text{-}1)$$

Where:

Δf= The nominal stress range as specified in Article 14.5.7.4.2.
F_{TH}= The fatigue threshold as specified in Article 14.5.7.5.

For this MBEJ, the fatigue resistance of the centerbeam to support connection was established through testing to be Category C. For a Category C detail, F_{TH} = 10ksi as specified in Table 6.6.1.2.5-3.

$$4.1\text{ksi} \le \frac{10\text{ksi}}{2} \qquad \textbf{O.K.!}$$

Since equation 14.5.7.4.3-1 is satisfied, support bar weld toe cracking will not occur. Had the stress range been too high (i.e., greater than 5ksi), the calculations could account for the moment gradient and the stress range at the actual critical section could have been calculated (see Figure 1.3-3). Since the result is acceptable as is, the design is conservative.

Weld Throat Cracking (Type C Cracking)

Type C cracking is driven by a combination of horizontal and vertical stress ranges in the connection (see Figure C at the end of this example).

The axle position which maximizes the stress range in the weld throat is shown in Figure 1.3-2. The wheel loads shown are to be applied to the top of the centerbeams and along the centerlines of the centerbeams. The vertical line loads calculated above should be applied here as well. From above:

$R_V = 4.8$ kip
$R_H = 1.0$ kip (i.e., 20% of R_V)

Where:

R_V = Vertical reaction in the connection.
R_H = Horizontal reaction in the connection.

The stress range driving Type C weld throat cracking shall be calculated using Eq. 14.5.7.4.2b-5:

$$S_{RZ} = \frac{R_V}{A_{Wmid}} + \frac{R_H(d_{cb} + \frac{1}{2}h_W)}{S_{Wmid}} \qquad (14.5.7.4.2b\text{-}5)$$

$$S_{RZ} = \frac{4.8k}{5.25in^2} + \frac{1.0k(5in + \frac{1}{2}(0.75in))}{2.63in^3} = 3.0ksi$$

Where:

A_{Wmid} = Area of the weld at the middle of the connection.
S_{Wmid} = Section modulus of the weld at the middle of the connection.
h_w = Height of the weld.

Check Article 14.5.7.4.3

To ensure an infinite fatigue life, the connections shall satisfy the following:

$$\Delta f \le \frac{F_{TH}}{2} \qquad (14.5.7.4.3\text{-}1)$$

where:

Δf= The nominal stress range as specified in Article 14.5.7.4.2.
F_{TH}= The fatigue threshold as specified in Article 14.5.7.5.

For this MBEJ, the fatigue resistance of the centerbeam to support connection was established through testing to be Category C. For a Category C detail, F_{TH} = 10ksi as specified in Table 6.6.1.2.5-3.

$$3.0ksi \le \frac{10ksi}{2} \qquad \textbf{O.K.!}$$

Since equation 14.5.7.4.3-1 is satisfied, weld throat cracking will not occur.

1.4 Check Centerbeam Shop Splice

The centerbeam shop splice is located in the center of one of the spans. The splice is a full-penetration groove weld. The welds have been inspected and all required grinding was done in the direction of applied stress. The fatigue strength of this detail is given in Table 6.6.1.2.3-1 and is illustrated in Figure 6.6.1.2.3-1 as Example 10. The detail category for this connection is Category B. For a Category B detail, F_{TH} = 16ksi as specified in Table 6.6.1.2.5-3.

From structural analysis, the amplified vertical moment range (ΔM_V) at this location was found to be:

$\Delta M_V = 35.0$ k-in

As per Article 14.5.7.2.3, the horizontal load range (ΔF_H) for fatigue design shall be taken as 20% of the amplified vertical axle load range. In this case, the horizontal moment range (ΔM_H) for fatigue design shall be taken as 20% of the amplified vertical moment range.

$$\Delta M_H = 0.2 \times \Delta M_V = 0.2 \times 35.0k - in = 7.0k - in$$

Stress range the detail can be calculated with Eq. 14.5.7.4.2b-1:

$$S_{RB} = \frac{M_V}{S_{Xcb}} + \frac{M_H}{S_{Ycb}} \qquad (14.5.7.4.2b\text{-}1)$$

$$S_{RB} = \frac{35.0k - ft}{9.68in^3} + \frac{7.0k - ft}{3.38in^3} = 5.7ksi$$

In this case, $\Delta f = S_{RB}$

Check Article 14.5.7.4.3

To ensure an infinite fatigue life, the connections shall satisfy the following:

$$\Delta f \le \frac{F_{TH}}{2} \qquad (14.5.7.4.3\text{-}1)$$

where:

Δf= The nominal stress range as specified in Article 14.5.7.4.2.
F_{TH}= The fatigue threshold as specified in Article 14.5.7.5.

For this MBEJ, the fatigue resistance of the centerbeam field splice is Category B. For a Category B detail, F_{TH} = 16 ksi as specified in Table 6.6.1.2.5-3.

$$5.7\text{ksi} \le \frac{16\text{ksi}}{2} \qquad \textbf{O.K.!}$$

Since equation 14.5.7.4.3-1 is satisfied, the shop splice is adequately designed for fatigue.

1.5 Check a Typical Attachment for an Equidistant Spring.

This attachment consists of a 0.5 inch thick plate that is 3 inches square fillet welded to the side of the support bar. The fatigue strength of this detail is given in Table 6.6.1.2.3-1 and illustrated in Figure 6.6.1.2.3-1 as Example 6. The detail is analogous to a web stiffener of a plate girder. Therefore the detail category for this connection is Category C or Category C′. Conservatively assuming Category C detail, F_{TH} = 10ksi as specified in Table 6.6.1.2.5-3.

The detail is located approximately 3 inches from the centerline of bearing for the support bar. The stress ranges near the support will be considerably smaller than those at the CB/SB connection, which is also a Category C detail. Therefore, by inspection it can be concluded that the detail will satisfy Equation 14.5.7.4.3-1.

1.6 Check Attachment for Stainless Steel Slider Plate.

This attachment consists of a 0.125 inch thick plate that is tack welded to the side of the support bar. The fatigue strength of this detail can be conservatively considered as a coverplate end detail. The fatigue strength of such a detail is given in Table 6.6.1.2.3-1 and illustrated in Figure 6.6.1.2.3-1 as Example 7. Because the plate is very thin (0.125 inches), the detail category will be taken as Category E with F_{TH} = 4.5ksi as specified in Table 6.6.1.2.5-3.

The end of the detail is located approximately 4 inches from the centerline of bearing for the support bar. From the previous check for support bar weld toe cracking, the maximum stress range in the support bar at midspan was found to be 3.3ksi. Using interpolation, the stress range (Δf) at the end of the plate can be calculated as:

$$\Delta f = 3.3\text{ksi} \times \frac{4\text{in}}{8.55\text{in}} = 1.54\text{ksi}$$

Check Article 14.5.7.4.3

To ensure an infinite fatigue life, the connections shall satisfy the following:

$$\Delta f \le \frac{F_{TH}}{2} \qquad (14.5.7.4.3\text{-}1)$$

where:

Δf= The nominal stress range as specified in Article 14.5.7.4.2.
F_{TH}= The fatigue threshold as specified in Article 14.5.7.5.

For this MBEJ, the fatigue resistance of the centerbeam field splice is Category E. For a Category E detail, F_{TH} = 4.5 ksi as specified in Table 6.6.1.2.5-3.

$$1.5\text{ksi} \le \frac{4.5\text{ksi}}{2} \qquad \textbf{O.K.!}$$

Since equation 14.5.7.4.3-1 is satisfied, the stainless steel slider plates are adequately designed for fatigue.

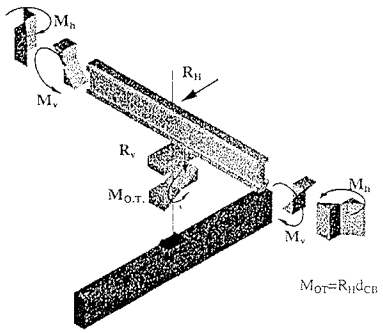

Figure A - Stresses and Forces Associated with Type A Cracking

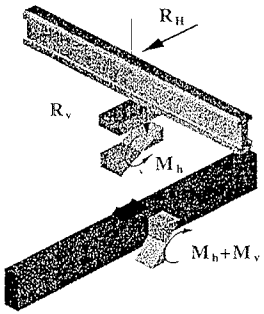

Figure B - Stresses and Forces Associated with Type B Cracking

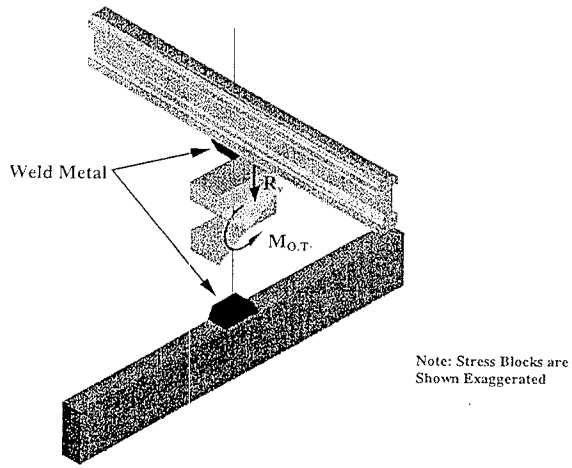

Figure-C Stresses and Forces Associated with Type C Cracking

Design Example #2

1.0 General

These example fatigue design calculations are applicable to a typical bolted-single-support bar modular bridge expansion joint system. The movement classification of this MBEJ is assumed to be 18 inches. The system consists of 3 in. × 4.75 in. support bars spaced at 3′-3″. The connection is fabricated using a stirrup type connection using four 5/8 in diameter A-325 bolts. The MBEJ is not located near a traffic metering device or toll facility. The geometry and section properties of the centerbeam are given below.

Centerbeam:

$S_{XGcb} = 9.0\ in^3$	(Strong-axis gross-section modulus at the bottom of the centerbeam)
$S_{YGcb} = 3.75\ in^3$	(Weak-axis gross-section modulus at the bottom of the centerbeam)
$S_{XNcb} = 6.1\ in^3$	(Strong-axis net-section modulus at the bottom of the centerbeam)
$S_{YNcb} = 2.1\ in^3$	(Weak-axis net-section modulus at the bottom of the centerbeam)
$d_{cb} = 5$ in	(Depth of the centerbeam)
$B_{cb} = 3.125$ in	(Top width of the centerbeam flange)
$A_{eff\ Bolts} = 0.23 in^2$	(Net area of one bolt)

Support Bar

t = 3 in.	(Thickne s of the support bar)
$d_{sb} = 4.75$ in	(Depth o the support bar)
$S_{Xsb} = 11.3\ in^3$	(Strong : xis section modulus of the support bar)

1.1 Fatigue Design Methodology

The following design will conform to the recommendations for fatigue design of MBEJ as given in Article 14.5.7 of the proposed specification. In this method, stress ranges (Δf) generated by the fatigue truck must be kept less than one half the CAFL ($\Delta F_{TH}/2$). If this condition is satisfied, theoretically infinite life is ensured.

1.2 Fatigue Design

1.2.1 Loads

As per Article 14.5.7.2, the MBEJ system shall be designed to resist the simultaneous application of vertical and horizontal loads from a tandem axle. As specified in Article 14.5.7.2.1, the appropriate axle for fatigue design is the largest axle load from the three-axle design truck specified in Article 3.6.1.2.2. This axle has a gross weight of 32 kips. However, as per 14.5.7.2.1, this axle shall be considered as the total load on a tandem. Therefore, the actual design load consists of two 16 kip axles spaced at 4′-0″. Since the joint opening is less than 4′-0″, only one of the axles in the tandem shall be considered (Article 14.5.7.2.1). The dynamic amplification factor is specified as 75% in Table 3.6.2-1, and Article 14.5.7.2.1. A load factor of 0.75, as specified in Table 3.4.1-1, shall be applied for the fatigue limit state.

Fatigue Load Ranges

Static Vertical Axle Load = F_{Vs} = 16 kip/axle (Note this is half of the 32 kip tandem)

Amplified Vertical Axle Load Range = ΔF_{VAmp} = (16 kip/axle)(1+.75) = 28.0 kip/axle

As per Article 14.5.7.2.3, the horizontal load range (ΔF_H) for fatigue design shall be taken as 20% of the amplified vertical axle load range. (Had the MBEJ been located at a signal or other metering device, the horizontal load range would be taken as 50% of the amplified vertical axle load range.)

$\Delta F_H = (0.2)(\Delta F_{VAmp}) = (0.2)(28\ kip/axle) = 5.6\ kip/axle$

As per Article 14.5.7.3, the percentage of the design vertical axle load and horizontal load that shall be distributed to a centerbeam and associated support bars is specified in Table 14.5.7.3-1. The top width of the centerbeam is given as 3.125 in. Thus, from Table 14.5.7.3-1, the centerbeam distribution factor shall be taken as 60%.

D.F. = 0.60

1.3 Check Centerbeam Support Bar Connection

The nominal stress ranges shall be obtained from structural analysis as specified in Article 14.5.7.4.2. For fatigue design, the MBEJ shall be assumed to be at the midrange opening. The design stress range at an interior connection shall be checked for fatigue in this example. Though not shown here, an exterior span should also be checked using the same methods.

Since this is a bolted single-support-bar MBEJ, stresses shall be calculated as specified in Article 14.5.7.2a. Also as specified in Article 14.5.7.2a, the effects of stresses generated in the stirrup itself shall not be considered when calculating the longitudinal stress range in the centerbeam.

Check Centerbeam

Through trial and error, the axle was positioned to maximize the stress range in the centerbeam. The final position is shown below in Figure 1.3-1. These loads are to be applied to the top of the centerbeams and along the centerlines of the centerbeams. The vertical line loads are calculated below:

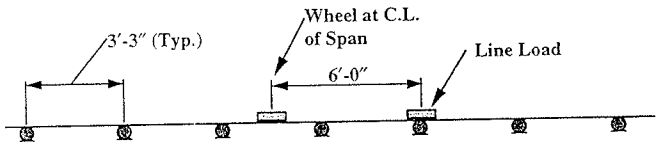

Figure 1.3-1

Vertical Load Range (Line Load)

$$w_V = 0.60 \times 0.75 \times \frac{28\text{kip/axle}}{(20\text{in} \times 2\text{wheel/axle})} = (0.315\text{kip/in})/\text{wheel}$$

Horizontal Load Range (Line Load)

$$w_H = 0.60 \times 0.75 \times \frac{5.6\text{kip/axle}}{(20\text{in} \times 2\text{wheel/axle})} = (0.063\text{kip/in})/\text{wheel}$$

Note: The above equations incorporate the distribution factor (DF) of 0.60 as specified in Table 14.5.7.3-1 and the load factor (LF) of 0.75 as specified in Table 3.4.1-1.

From structural analysis, the following information was obtained:

M_V = 19.1 k-ft
M_H = 3.8 k-ft (i.e., 20% of M_V)

Where:

M_V = Horizontal bending moment in the centerbeam due to the applied vertical forces.
M_H = Horizontal bending moment in the centerbeam due to the applied horizontal force.

$$S_{RB} = \frac{M_V}{S_{XNcb}} + \frac{M_H}{S_{YNcb}} \qquad (14.5.7.4.2b\text{-}1)$$

$$S_{RB} = \frac{19.1\text{k-ft}}{6.1\text{in}^3} + \frac{3.8\text{k-ft}}{2.7\text{in}^3} = 4.5\text{ksi}$$

Where:

S_{XNcb} and S_{YNcb} = Vertical and horizontal net section modulus of the centerbeam, respectively.
S_{RB} = Combined bending stress range in the centerbeam.

For the case of a bolted single-support-bar MBEJ

$\Delta f = S_{RB} = 4.5\text{ksi}$

The stress range (4.5ksi) is calculated at the centerline of the connection between the centerbeam and the support bar on the net section.. However, in reality, the bolt holes are located about 4 inches away from where the moment is calculated. It can be shown that due to the moment gradient the stress range at the bolt holes is about 70% of this value or about 3.2ksi.

Therefore, $\Delta f = (0.70)4.5\text{ksi} = 3.2\text{ksi}$

Check Article 14.5.7.4.3
To ensure an infinite fatigue life the connections shall satisfy the following:

$$\Delta f \le \frac{F_{TH}}{2} \qquad (14.5.7.4.3\text{-}1)$$

Where:

Δf= The nominal stress range as specified in Article 14.5.7.4.2.
F_{TH}= The fatigue threshold as specified in Article 14.5.7.5.

For this MBEJ, the fatigue resistance of the centerbeam with drilled holes was established through testing to be Category D. For a Category D detail, F_{TH} = 7ksi as specified in Table 6.6.1.2.5-3.

$$3.2\text{ksi} \le \frac{7\text{ksi}}{2} \qquad \textbf{O.K.}$$

Since equation 14.5.7.4.3-1 is satisfied and net section fatigue cracking of the centerbeam will not occur.

Check Stirrup for Fatigue

Through trial and error, the axle was positioned to maximize the stress range in the stirrup. The final position is shown below in Figure 1.3-2. These loads are to be applied to the top of the centerbeams and along the centerlines of the centerbeams. The vertical line loads calculated above should be applied here as well:

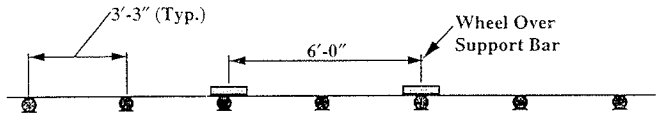

Figure 1.3-2

The only information required to check the stirrup for fatigue, is the vertical reaction range at the stirrup. From structural analysis of the above system, the following information was obtained.

R_v = 5.8 kip

Where:

R_v= Vertical reaction in the connection.

As specified in Article 14.5.7.2a, the vertical stress range in the stirrup shall be calculated by assuming and load range in the stirrup equal to 30% of the total vertical reaction force between the centerbeam and the support bar.

The load range in the stirrup is:

$$R_{SV} = 0.30 \times R_V = 0.30 \times 5.8k = 1.7k$$

It will be assumed that the bolts share equally in the load. Therefore the load per bolt can be calculated as:

$$R_{SVBolt} = \frac{RSV}{4Bolts} = \frac{1.7k}{4Bolts} = 0.43k / Bolt$$

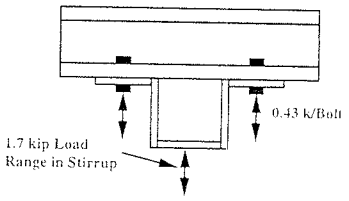

Stirrup Forces

Calculate the stress range in one bolt. From the information given, the net area of the bolt is $0.23in^2$. Thus the stress range in each bolt is:

$$S_{KBolt} = \frac{R_{SVBolt}}{A_{effNet}} = \frac{0.43k / Bolt}{0.23in^2} = 1.9ksi$$

Where:

S_{VBolt} = Load in each bolt
S_{KBolt} = Stress range in each bolt

Check Article 14.5.7.4.3
To ensure an infinite fatigue life, the connections shall satisfy the following:

$$\Delta f \le \frac{F_{TH}}{2} \qquad (14.5.7.4.3\text{-}1)$$

Where

Δf= The nominal stress range as specified in Article 14.5.7.4.2.
F_{TH}= The fatigue threshold as specified in Article 14.5.7.5.

For this MBEJ, the fatigue resistance of a threaded fastener has been established through testing to be Category D. For a Category D detail, F_{TH} = 7ksi as specified in Table 6.6.1.2.5-3.

$$1.9ksi \le \frac{7ksi}{2} \qquad \textbf{O.K.}$$

Since equation 14.5.7.4.3-1 is satisfied, the stirrup bolts are adequately sized for fatigue. However, the stirrup itself must also be checked in the same manner as the bolts. This can be done by checking the nominal stress range in the stirrup welds and comparing the appropriate fatigue category (typically Category E). However, the nominal stress in the stirrup will be small because it has a very large area (i.e., compared to the four bolts). Therefore, by inspection it will not control.

1.4 Calculate the Maximum Moment in the Support Bar

The moment in the support bar (M_v) due to the vertical reaction force (R_v) must be calculated. Note that (M_v) is a result of the vertical reaction only, and the effects of horizontal forces need not be considered. For this single-support-bar MBEJ, the support bar carries all the load from the wheel. This wheel load is distributed to a maximum of three centerbeams as specified in Article14.5.7.3 and as shown below.

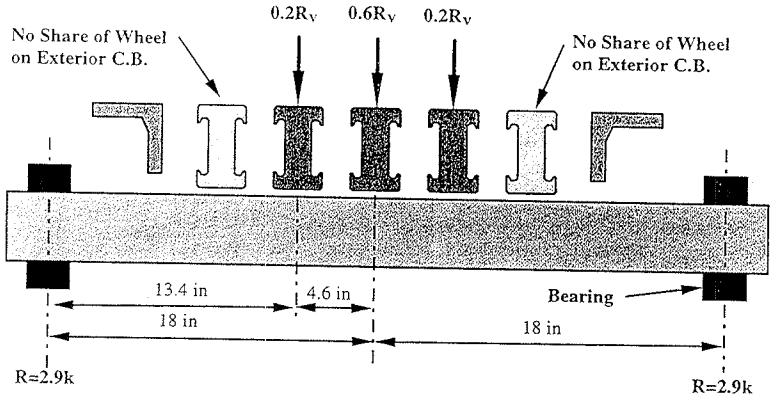

Figure 1.4-3

Note: Stirrups not shown for clarity.

Based on the loading shown (R_v=5.8k) the reactions are equal and are 2.9kip. From the geometry given the maximum moment (M_v) in the support bar can be calculated from the shear diagram.

$$M_V = 13.4in \times 2.9kip + 4.6in \times 1.72kip = 46.8k - in$$

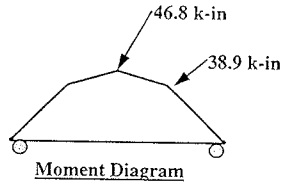

Moment Diagram

The stress range in the support bar can now be calculated.

$$\Delta f = \frac{M_V}{S_{Xsb}} = \frac{46.8k - in}{11.3in^3} = 4.2ksi$$

Check Base Metal of Support Bar .

The base metal of the support bar will be checked for fatigue. As specified in Table 6.6.1.2.3-1 Article and Table 6.6.1.2.5-3, the support bar base metal must be checked as a Category A detail. The maximum stress range in the support bar was found above to be 4.2 ksi.

Check Article 14.5.7.4.3

To ensure an infinite fatigue life, the connections shall satisfy the following:

$$\Delta f \le \frac{F_{TH}}{2} \qquad (14.5.7.4.3\text{-}1)$$

where:

Δf= The nominal stress range as specified in Article 14.5.7.4.2.
F_{TH}= The fatigue threshold as specified in Article 14.5.7.5.

For this MBEJ, the fatigue resistance of the support bar base metal is a Category A detail. For a Category A detail, F_{TH} = 24 ksi as specified in Table 6.6.1.2.5-3.

$$4.2\text{ksi} \le \frac{24\text{ksi}}{2} \qquad \textbf{O.K.}$$

Equation 14.5.7.4.3-1 is satisfied.

Check Attachment for Stainless Steel Slider Plate.

This attachment consists of a 0.125 inch thick plate that is tack welded to the side of the support bar. The fatigue strength of this detail can be conservatively considered as a coverplate end detail. The fatigue strength of such a detail is given in Table 6.6.1.2.3-1 and illustrated in Figure 6.6.1.2.3-1 as Example 7. Because the plate is very thin (0.125 inches), the detail category will be taken as Category E with F_{TH} = 4.5ksi as specified in Table 6.6.1.2.5-3.

Since this is a single support bar system, the detail is continuous from centerline of bearing to centerline of bearing along the support bar. However, the plate is only welded at the ends and the third points. The maximum stress range in the support bar at the welds must be calculated.

Based on the loading shown in Figure 1.4-3 (R_v=5.8k) the reactions are equal and are 2.9kip. From the geometry given the moment (M_v) in the support bar at the third point (i.e. 12 inches) can be calculated.

$$M_V = 12.0\text{in} \times 2.9\text{kip} = 34.8\text{k} - \text{in}$$

The stress range in the support bar cannot be calculated.

$$\Delta f = \frac{M_V}{S_{Xsb}} = \frac{34.8\text{k} - \text{in}}{11.3\text{in}^3} = 3.1\text{ksi}$$

Check Article 14.5.7.4.3

To ensure an infinite fatigue life, the connections shall satisfy the following:

$$\Delta f \le \frac{F_{TH}}{2} \qquad (14.5.7.4.3\text{-}1)$$

where:

Δf= The nominal stress range as specified in Article 14.5.7.4.2.
F_{TH}= The fatigue threshold as specified in Article 14.5.7.5.

For this MBEJ, the fatigue resistance of the centerbeam field splice is Category E. For a Category E detail, F_{TH} = 4.5 ksi as specified in Table 6.6.1.2.5-3.

$$3.1\text{ksi} \le \frac{4.5\text{ksi}}{2} \qquad \textbf{No Good!!}$$

Equation 14.5.7.4.3-1 is not satisfied and a redesign of the support bar is required. The section modulus of the support bar needs to be increased by about 38%. Thus, increasing the width to 4 inches will provide an acceptable decrease in the stress range. Another solution is to decrease the spacing between the support bars.

1.4 Check Centerbeam Shop Splice
Similar to as Example 1.

1.5 Check Attachment of for Equidistant Spring.
Similar to as Example 1.

1.6 Check Attachment for Stainless Steel Slider Plate.
Similar to as Example 1.

Design Example #3

1.0 General

These example fatigue design calculations are applicable to a typical welded multiple-support-bar modular bridge expansion joint system. The movement classification of this MBEJ is assumed to be 305mm. The system consists of 38.1mm. × 95mm. support bars spaced at 1435mm. The MBEJ is not located near a traffic metering device or toll facility. The geometry and section properties of the centerbeam and centerbeam/support bar weld are given below.

Centerbeam:

$S_{x-b} = 115365\ mm^3$ (Strong axis section modulus at the bottom of the centerbeam)
$S_{y-b} = 30808\ mm^3$ (Weak axis section modulus at the bottom of the centerbeam)
$d_{cb} = 127\ mm$ (Depth of the centerbeam)

Support Bar

$t = 38.1\ mm$ (Thickness of the support bar)
$d_{sb} = 95\ mm$ (Depth of the support bar)
$S_{x-b} = 57309\ mm^3$ (Strong axis section modulus of the support bar)

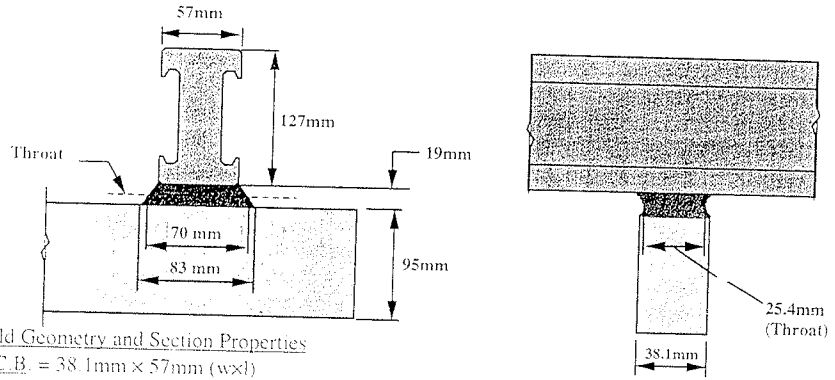

Weld Geometry and Section Properties

@ C.B. = 38.1mm × 57mm (w×l)
$A_{w-t} = 2172mm^2$, $S_{w-t} = 20631mm^3$
@ Throat = 25.4mm × 70mm (w×l)
$A_{w-m} = 1778mm^2$, $S_{w-m} = 20743mm^3$
@ S.B. = 38.1mm × 83mm (w×l)
$A_{w-b} = 3162mm^2$, $S_{w-b} = 43745mm^3$
$h_w = 19mm$ (height of the weld)

w = width parallel to the longitudinal axis of the C.B.
l = length perpendicular to the longitudinal axis of the C.B.
A_{w-t}, A_{w-m}, and A_{w-b} = Area of weld at the top, middle, and bottom of the connection, respectively.
S_{w-t}, S_{w-m}, and S_{w-b} = Section modulus of the weld at the top, middle, and bottom of the connection, respectively, for bending perpendicular to the longitudinal axis of the centerbeam.

1.1 Fatigue Design Methodology

The following design will conform to the recommendations for fatigue design of MBEJ as given in Article 14.5.7 of the proposed specification. In this method, stress ranges (Δf) generated by the fatigue truck must be kept less than one half the CAFL ($\Delta F_{TH}/2$). Theoretically, if this condition is satisfied infinite life is ensured.

1.2 Fatigue Design

1.2.1 Loads

As per Article 14.5.7.2, the MBEJ system shall be designed to resist the simultaneous application of vertical and horizontal loads from a tandem axle. As specified in Article 14.5.7.2.1, the appropriate axle for fatigue design is the largest axle load from the three-axle design truck specified in Article 3.6.1.2.2. This axle has a gross weight of 142kN. However, as per 14.5.7.2.1, this axle shall be considered as the total load on a tandem. Therefore, the actual design load consists of two 71kN axles spaced at 1219mm. Since the joint opening is less than 1219mm, only one of the axles in the tandem shall be considered (Article 14.5.7.2.1). The dynamic amplification factor is specified as 75% in Table 3.6.2-1. and Article 14.5.7.2.1. A load factor of 0.75, as specified in Table 3.4.1-1, shall be applied for the fatigue limit state.

Fatigue Load Ranges

Static Vertical Axle Load = F_{Vs} = 71kN/axle (Note this is half of the 142kN tandem)

Amplified Vertical Axle Load Range = $\Delta F_{VAmp.}$ = (71kN/axle)(1+.75) = 124.3kN/axle

As per Article 14.5.7.2.3, the horizontal load range (ΔF_H) for fatigue design shall be taken as 20% of the amplified vertical axle load range. (Had the MBEJ been located at a signal or other metering device, the horizontal load range would be taken as 50% of the amplified vertical axle load range.)

$\Delta F_H = (0.2)(\Delta F_{VAmp}) = (0.2)(124.3kN/axle) = 24.9kN/axle$

As per Article 14.5.7.3, the percentage of the design vertical axle load and horizontal load that shall be distributed to a centerbeam and associated support bars is specified in Table 14.5.7.3-1. The top width of the centerbeam is given as 57mm. Thus, from Table 14.5.7.3-1, the centerbeam distribution factor shall be taken as 50%.

D.F. = 0.50

1.3 Check Centerbeam Support Bar Connection

The nominal stress ranges shall be obtained from structural analysis as specified in Article 14.5.7.4.2. For fatigue design, the MBEJ shall be assumed to be at the midrange opening. The design stress range at an interior connection shall be checked for fatigue in this example. Though not shown here, an exterior span should also be checked using the same methods.

Since this is a welded multiple-support-bar MBEJ, stresses shall be calculated as specified in Article 14.5.7.2b. Three separate checks are required for the centerbeam to support bar connection in welded multiple-support-bar systems.

Check Centerbeam Weld Toe Cracking (Type A Cracking)

Type A cracking is driven by a combination of horizontal and vertical stress ranges in the connection (see Figure A at the end of example 1).

Through trial and error, the axle was positioned to maximize the stress range at the centerbeam weld toe. The final position is shown below in Figure 1.3-1. These loads are to be applied to the top of the centerbeams and along the centerlines of the centerbeams. The vertical line loads are calculated below:

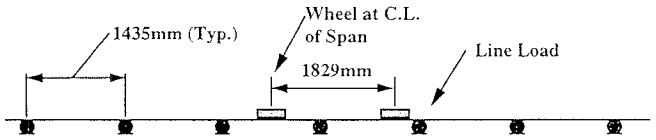

Figure 1.3-1

Vertical Load Range (Line Load)

$$w_V = 0.50 \times 0.75 \times \frac{124.3\text{kN / axle}}{(508\text{mm} \times 2\text{wheel / axle})} = (0.046\text{kN / mm}) / \text{wheel}$$

Horizontal Load Range (Line Load)

$$w_H = 0.50 \times 0.75 \times \frac{24.9\text{kN / axle}}{(508\text{mm} \times 2\text{wheel / axle})} = (0.009\text{kN / mm}) / \text{wheel}$$

Note: The above equations incorporate the distribution factor (DF) of 0.50 as specified in Table 14.5.7.3-1 and the load factor (LF) of 0.75 as specified in Table 3.4.1-1.

From structural analysis, the following information was obtained:

R_V = 19.7kN M_V = 3803kN-mm

R_H = 3.9kN (i.e., 20% of R_V) M_H = 761kN-mm (i.e., 20% of M_V)

Where

R_V = Vertical reaction in the connection.

R_H = Horizontal reaction in the connection.

M_V = Horizontal bending moment in the centerbeam due to the applied vertical forces.

M_H = Horizontal bending moment in the centerbeam due to the applied horizontal forces

$$S_{RB} = \frac{M_V}{S_{Xcb}} + \frac{M_H}{S_{Ycb}} \qquad (14.5.7.4.2b\text{-}1)$$

$$S_{RB} = \frac{3803\text{kN} - \text{mm}}{115365\text{mm}^3} + \frac{761\text{kN} - \text{mm}}{30808\text{mm}^3} = 0.0576\text{kN / mm}^2 = 57.6\text{MPa}$$

$$S_{RZ} = \frac{R_H d_{cb}}{S_{Wtop}} + \frac{R_V}{A_{Wtop}} \qquad (14.5.7.4.2b\text{-}2)$$

$$S_{RZ} = \frac{3.9\text{kN} \times 127\text{mm}}{20631\text{mm}^3} + \frac{19.7\text{kN}}{2172\text{mm}^2} = 0.0331\text{kN / mm}^2 = 33.1\text{MPa}$$

Where:

S_{Xcb} and S_{Ycb} =Section modulus of the centerbeam

A_{Wtop} = Area of weld at the top of the connection.

S_{Wtop} = Section modulus of the weld at the top of the connection.

d_{cb} = Depth of the centerbeam.

Calculate Δf as specified in 14.5.7.4.2b to check centerbeam weld toe cracking.

$$\Delta f = \sqrt{S^2_{RB} + S^2_{RZ}} \qquad (14.5.7.4.2b\text{-}6)$$

$$\Delta f = \sqrt{57.6^2\text{MPa} + 33.1^2\text{MPa}} = 66.4\text{MPa}$$

Where:

S_{RB} = Combined bending stress range in the centerbeam or support bar.

S_{RZ} = Vertical stress range in the centerbeam to support bar weld from the reaction of the support beam. Components of this stress range include the vertical load and overturning moment.

Check Article 14.5.7.4.3
To ensure an infinite fatigue life the connections shall satisfy the following:

$$\Delta f \le \frac{F_{TH}}{2} \qquad (14.5.7.4.3\text{-}1)$$

Where:

Δf = The nominal stress range as specified in Article 14.5.7.4.2.
F_{TH} = The fatigue threshold as specified in Article 14.5.7.5.

For this MBEJ, the fatigue resistance of the centerbeam to support connection was established through testing to be Category C. For a Category C detail, F_{TH} = 68.9 MPa as specified in Table 6.6.1.2.5-3.

$$66.4\text{MPa} > \frac{68.9\text{MPa}}{2} \qquad \text{NO GOOD!}$$

Equation 14.5.7.4.3-1 is not satisfied and centerbeam weld toe cracking can be expected to occur. Thus, modifications to the connection and/or a heavier centerbeam section are required. In addition, the support bar spacing could be reduced thereby decreasing moments in the centerbeam.

Support Bar Weld Toe Cracking (Type B Cracking)

Through trial and error, the axle was positioned to maximize the stress range at support bar weld toe. The final position of the axle is shown below in Figure 1.3-2. These loads are to be applied to the top of the centerbeams and along the centerlines of the centerbeams. The vertical line loads calculated above should be applied here as well:

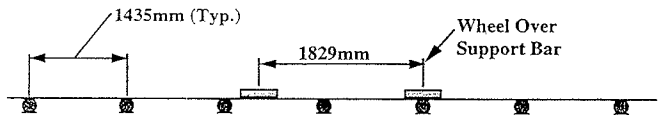

Figure 1.3-2

From structural analysis of the above system, the following information was obtained:

R_V = 20.1kN
R_H = 4.0kN (i.e., 20% of R_V)
M_v = 2535kN-mm (see below)

Where:

R_V = Vertical reaction in the connection.
R_H = Horizontal reaction in the connection.
M_V = Bending moment in the support bar due to vertical and horizontal forces.

Type B cracking is driven by a combination of horizontal and vertical stress ranges in the connection (see Figure B at the end of example 1). The moment in the support bar results from the vertical and horizontal reactions as shown in Figure 1.3-3. Since the centerbeam is located at midspan (see Figure 1.3-3), the maximum moment in the support bar occurs at the center of the span. The total length of the span is 508mm (i.e., 2L).

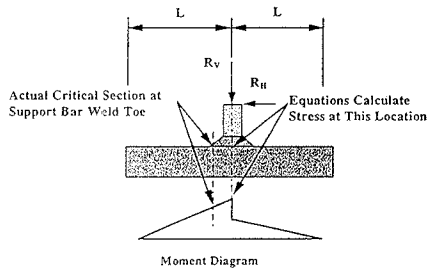

Figure 1.3-3

The moment in the support bar (M_V) due to the vertical reaction force (R_V) must be calculated. Note that (M_V) is a result of the vertical reaction only, the additional moment from the horizontal force is calculated by the second half of equation 14.5.7.4.2b-3 shown below.

$$M_V = \tfrac{1}{2}(R_V) \times L = \tfrac{1}{2}(20.1\text{kN}) \times 254\text{mm} = 2553\text{kN} - \text{mm}$$

Note:

$$254\text{mm} = \frac{508\text{mm}}{2} = L$$

The stress range in the support bar (S_{RB}) is calculated using Eq. 14.5.7.4.2b-3:

$$S_{RB} = \frac{M_V}{S_{Xsb}} + \frac{1}{2}\frac{R_H(d_{cb} + h_W + \frac{1}{2}d_{sb})}{S_{Xsb}} \qquad (14.5.7.4.2b\text{-}3)$$

$$S_{RB} = \frac{2553\text{kN} - \text{mm}}{57309\text{mm}^3} + \frac{1}{2}\frac{4.0\text{kN}(127\text{mm} + 19\text{mm} + \frac{1}{2}(95\text{mm}))}{57309\text{mm}^3} = 0.0512\text{kN/mm}^2 = 51.2\text{MPa}$$

Where;

R_H = Horizontal reaction in the connection.
M_V = Bending moment in the support bar due to vertical forces.
S_{Xsb} = Section modulus of the support bar.
L = Distance from C.L. of bearing to C.L. of connection.

The vertical stress range in the weld (S_{RZ}) is calculated using Eq. 14.5.7.4.2b-4

$$S_{RZ} = \frac{R_H(d_{cb} + h_W)}{S_{Wbot}} + \frac{R_V}{A_{wbot}} \qquad (14.5.7.4.2b\text{-}4)$$

$$S_{RZ} = \frac{4.0\text{kN}(127\text{mm} + 19\text{mm})}{43745\text{mm}^3} + \frac{20.1\text{kN}}{3162\text{mm}^2} = 0.0196\text{kN/mm}^2 = 19.6\text{MPa}$$

Where:

R_V = Vertical reaction in the connection.
R_H = Horizontal reaction in the connection.
A_{Wbot} = Area of weld at the bottom of the connection.
S_{Wbot} = Section modulus of the weld at the bottom of the connection.
h_w = Height of the weld.

Calculate Δf as specified in 14.5.7.4.2b to check for support bar weld toe cracking.

$$\Delta f = \sqrt{S^2_{RB} + S^2_{RZ}} \qquad (14.5.7.4.2b\text{-}6)$$

$$\Delta f = \sqrt{51.2^2\text{MPa} + 19.6^2\text{MPa}} = 54.8\text{MPa}$$

Where:

S_{RB} = Combined bending stress range in the support bar.
S_{RZ} = Vertical stress range in the centerbeam to support bar weld from the reaction of the support beam. Components of this stress range include the vertical load and overturning moment.

Check Article 14.5.7.4.3

To ensure an infinite fatigue life the connections shall satisfy the following:

$$\Delta f \le \frac{F_{TH}}{2} \qquad (14.5.7.4.3\text{-}1)$$

Where:

Δf= The nominal stress range as specified in Article 14.5.7.4.2.
F_{TH}= The fatigue threshold as specified in Article 14.5.7.5.

For this MBEJ, the fatigue resistance of the centerbeam to support connection was established through testing to be Category C. For a Category C detail, F_{TH} = 68.9MPa as specified in Table 6.6.1.2.5-3.

$$54.8\text{MPa} > \frac{68.9\text{MPa}}{2} \qquad \textbf{NO GOOD!}$$

Since equation 14.5.7.4.3-1 is not satisfied, support bar weld toe cracking is expected to occur. Since the stress range is too high (i.e., greater than 34.5MPa), the calculations could account for the moment gradient and the stress range at the actual critical section could have been calculated (see Figure 1.3-3). However, since the calculated stress range is well over the allowable limit, the reduction in stress range that can be realized is not likely to be sufficient. Therefore a redesign of the connection which may include changes to the support bar spacing and geometry are required.

Weld Throat Cracking (Type C Cracking)

Type C cracking is driven by a combination of horizontal and vertical stress ranges in the connection (see Figure C at the end of this example).

The axle position which maximizes the stress range in the weld throat is shown in Figure 1.3-2. The wheel loads shown are to be applied to the top of the centerbeams and along the centerlines of the centerbeams. The vertical line loads calculated above should be applied here as well. From above:

R_V = 20.1kN
R_H = 4.0 kN (i.e., 20% of R_V)

Where:

R_V = Vertical reaction in the connection.
R_H = Horizontal reaction in the connection.

The stress range driving Type C weld throat cracking shall be calculated using Eq. 14.5.7.4.2b-5:

$$S_{RZ} = \frac{R_V}{A_{Wmid}} + \frac{R_H(d_{ch} + \frac{1}{2}h_W)}{S_{Wmid}} \qquad (14.5.7.4.2b\text{-}5)$$

$$S_{RZ} = \frac{20.1\text{kN}}{1778\text{mm}^2} + \frac{4.0\text{kN}(127\text{mm} + \frac{1}{2}(19\text{mm}))}{20743\text{mm}^3} = 0.0373\text{kN/mm}^2 = 37.3\text{MPa}$$

Where

A_{Wmid} = Area of the weld at the middle of the connection.
S_{Wmid} = Section modulus of the weld at the middle of the connection.
h_W = Height of the weld.

Check Article 14.5.7.4.3

To ensure an infinite fatigue life, the connections shall satisfy the following:

$$\Delta f \le \frac{F_{TH}}{2} \qquad (14.5.7.4.3\text{-}1)$$

where

Δf= The nominal stress range as specified in Article 14.5.7.4.2.
F_{TH}= The fatigue threshold as specified in Article 14.5.7.5.

For this MBEJ, the fatigue resistance of the centerbeam to support connection was established through testing to be Category C. For a Category C detail, F_{TH} = 68.9MPa as specified in Table 6.6.1.2.5-3.

$$37.3\text{MPa} > \frac{68.9\text{MPa}}{2} \qquad \text{NO GOOD!}$$

Since equation 14.5.7.4.3-1 is not satisfied, weld throat cracking is expected to occur. Considering the above results, a complete redesign of this MBEJ is required.

1.4 Check Centerbeam Shop Splice

Similar to previous examples.

1.5 Check a Typical Attachment for an Equidistant Spring.

Similar to previous examples.